Functional studies of insecticides and acaricides acting on ligand-gated ion channels

Sofia Iqbal

Thesis submitted to University of Nottingham for the degree of Doctor of Philosophy

December 2018

Declaration

The work presented here is the author's own and has not previously been accepted in substance for any degree.

Signed:

Sofia Iqbal

Abstract

Arthropod pests such as ticks and fleas are important ectoparasites of livestock and companion animals that cause economic losses, spread disease and pose a public health risk. They are most commonly controlled using chemical pesticides, the majority of which have a neurotoxic mode of action. Two important targets within the arthropod nervous system are the GABA receptor (GABAR) and the nicotinic acetylcholine receptor (nAChR). They are targeted by a diverse range of chemical classes, although prolonged use of certain compounds has resulted in the development of resistance. This continues to be an ever-increasing problem for effective pest control and is often caused by simple point mutations within the target that disrupt the high selectivity of the target-ligand interaction at the binding site.

This thesis describes investigations into the mode of action of compounds acting on these targets, their selectivity and the molecular basis of resistance. Bioassay screening of the most common species of flea, *Ctenocephalides felis*, highlighted cross-resistance and decreased efficacy of ethiprole in dieldrin-resistant fleas. This was attributed to a known point mutation (A301S) within the GABAR channel, and was further confirmed by two-electrode voltage clamp electrophysiology of *Xenopus laevis* oocytes expressing the A301S modified GABA receptor. The possible role of a second, novel, amino acid change (M354I), linked to fipronil resistance was also investigated. Interestingly, it was found that rather than conferring resistance, this second substitution instead restored susceptibility to ethiprole and fipronil insensitive A301S modified receptors. This was further verified by expression studies *in vivo*, using transgenic strains of the model organism *Drosophila melanogaster*.

An electrophysiological analysis of the cattle tick, *Rhipicephalus microplus*, nicotinic acetylcholine receptor (α6 subunit) was also carried out to investigate residues thought to be involved in the selective binding of spinosad to these homomeric receptors. Three residues previously identified from a modelling study, F265L, G324A and C329S, were introduced into the *R. microplus* α6 subunit cDNAs and expressed in Xenopus oocytes to form functional acetylcholine-responsive receptors. All three substitutions resulted in a reduced channel efficacy of spinosad, confirming that these residues do play a key role in spinosad binding.

Acknowledgements

This thesis would not have been possible without the help of my wonderful supervisory team. I would like to extend my gratitude to Andreas Turberg for welcoming me at Bayer Animal Health, Lin Field for putting up with my last-minute submissions, Ian Mellor and Emyr Davies for all their support. I would like to particularly thank Martin Williamson; this work would not have been possible without his guidance and open door.

I would also like to thank the whole Insect Molecular Biology group. I am particularly indebted to Mirel Puinean for his informal supervision, for teaching me molecular biology techniques and for his patience whilst I learnt electrophysiology. I would also like to thank Rafael Homem, Ewan Richardson, Heather Angus and Will Garrood for bearing with me in the fly lab.

Thank you to all my friends, particularly Suki Gill and Sam Hussain who have no idea what I do but smile anyway, to Rosie Brian who I met over a plate of biscuits on the first day of my PhD, to Joe Moughan for his long-distance support, to Lucy Hyde and Beth Wallace for endless coffee breaks, and to Aislinn Pearson for always walking by my side.

I am also grateful for my parents for supporting me through thirty years of education, my parents-in-law for their encouragement, my wonderful brothers, sisters and sisters-in-law, and the twelve sprogs for always keeping me smiling. Special thanks to Anj for my weekly therapy sessions, you're the world's best big sister.

Last but not least, thank you to my wonderful husband for his unending support and love, for making me dinner, for sharing my commiserations and celebrations, and taking me on plenty of holidays.

Contents

Contents 5

Abbreviations 11

List of Figures 13

List of Tables 20

1. General introduction 22

1.1. Arthropod pests of domesticated animals 22

1.1.1. Fleas 22

1.1.2. Ticks 25

1.2. Arthropod pest control 28

1.3. Insecticide and Acaricide Targets 34

1.3.1. Cys-Loop receptors 34

1.3.2. The γ-aminobutyric acid (GABA) receptor 35

1.3.3. The glutamate chloride receptor 36

1.3.4. The nicotinic acetylcholine receptor 37

1.4. Resistance to insecticides and acaricides 39

1.4.1. Resistance mechanisms 39

1.4.2. Metabolic resistance 40

1.4.3. Target-site resistance 40

1.4.4. Resistance resulting from changes in the arthropod GABAR 41

1.4.5. Resistance resulting from changes in the arthropod nicotinic acetylcholine receptor 42

1.5. Aims and Objectives 45

2. Methods 46

2.1. Source Material 46

2.1.1. Insect and Acari 46

2.1.2. Media and reagents 46

2.1.3. Genomic DNA extraction 46
2.1.4. RNA extraction 47
2.1.5. cDNA synthesis 48
2.2. Polymerase chain reaction (PCR) 49
2.2.1. Primer Design 49
2.2.2. Standard PCR 49
2.2.3. High-fidelity PCR 49
2.2.4. *Taq*Man PCR of *C. felis* 50
2.2.5. PCR purification 51
2.2.6. Agarose gel electrophoresis 51
2.2.7. Extraction of PCR products form agarose gels 52
2.3. Molecular cloning and transformation 53
2.3.1. PCR cloning 53
2.3.2. Bacterial transformation 54
2.3.3. Colony PCR 55
2.3.4. Plasmid purification 55
2.4. Site-directed mutagenesis 56
2.5. Sequencing and analysis 57
2.6. Two-Electrode voltage clamp electrophysiology 57
2.6.1. *In vitro* cRNA synthesis 57
2.6.2. *X. laevis* oocyte preparation 59
2.6.3. TEVC electrophysiology system 61
2.6.4. TEVC electrophysiology recordings 64
2.6.5. Electrophysiological data analysis 65
3. Bioassays of GABAergic compounds on *C. felis, R. microplus, R. sanguineus* and *I. Ricinus* 67
3.1. Introduction 67

3.2. Methods 70
3.2.1. Acari species 70
3.2.2. Artificial rearing of *C. felis* 71
3.2.3. Coated glass vial contact bioassay 72
3.2.4. *R. microplus* oviposition bioassay 75
3.2.5. The 'artificial dog' bioassay 77
3.2.6. Bioassay data analysis 79
3.3. Results and discussion 80
3.3.1. *C. felis* contact bioassays 81
3.3.2. *I. ricinus* contact bioassays 86
3.3.3. *R. microplus* oviposition bioassays 89
3.3.4. *C. felis* 'artificial dog' bioassays 92
3.3.5. TaqMan sequencing of Georgi C. *felis* 95
3.3.6. Discussion 97
3.4. Conclusions 99
4. Electrophysiology Studies of Antagonists and Agonists of the *C. felis* GABA Receptor 100
4.1. Introduction 100
4.2. Methods 102
4.2.1. Annotation of the *C. felis* GABAR 102
4.2.2. Sub-cloning of the C. felis GABARbd 103
4.2.3. Site-directed mutagenesis and transformation 104
4.2.4. *In Vitro* cRNA synthesis 105
4.2.5. Electrophysiological recordings and analysis 105
4.3. Results and discussion 107
4.3.1. Optimisation of *C. felis* GABARbd expression 107
4.3.2. Antagonists of the *C. felis* GABAR 112

4.3.3. *C. felis* GABARbd mutant functional responses to GABA 115

4.3.4. Characterisation of the interactions of picrotoxin and dieldrin with the *C. felis* GABARbd with the A301S and M354I substitutions 116

4.3.5. Characterisation of the interactions of phenylpyrazoles with the *C. felis* GABARbd with the A301S and M354I Substitutions 120

4.3.6. Recovery of *C. felis* GABARbd after removal of antagonists 124

4.3.7. Characterisation of the A301S and M354I *C. felis* GABARbds receptors with isoxazolines 125

4.4. Discussion 129

4.5. Conclusions 133

5. *In vivo* study of *C. felis* GABAR mutations introduced into *D. melanogaster* 134

5.1. Introduction 134

5.1.1. φC31 integration and the GAL4/UAS systems 134

5.2. Methods.....136

5.2.1. Sub-cloning of the *D. melanogaster* GABAR 136

5.2.2. Site-directed Mutagenesis and Transformation 137

5.2.3. *D. melanogaster* rearing 138

5.2.4. Crossing strategy for *D. melanogaster* injection line ..138

5.2.5. Germline transformation.....140

5.2.6. Larval bioassays 142

5.3. Results 145

5.3.1. Range-finding trials 146

5.3.2. *D. melanogaster* larval bioassays 147

5.4. Discussion 153

5.5. Conclusions 155

6. Functional characterisation of the *R. microplus* nAChRα6 Spinosad binding site 156

6.1. Introduction 156

6.1.2. Human nAChRα7 and the *R. microplus* nAChRα6 sequence alignment 157

6.2. Methods 160

6.2.1. Source material 160

6.2.2. Site-directed mutagenesis 160

6.2.3. *In vitro* cRNA synthesis 162

6.2.4. Electrophysiological recordings 162

6.2.5. Electrophysiological Data Analysis 163

6.3. Results 165

6.3.1. Responses of *R. microplus* nAChRα6 and human nAChRα7 expressed in oocytes to acetylcholine 165

6.3.2. Characterisation of the *R. microplus* nAChRα6 spinosad binding site 167

6.4. Discussion 174

6.5. Conclusions 177

7. General discussion 178

7.1. Cross-resistance between dieldrin and ethiprole or fipronil 178

7.2. Functional studies of a novel mutation in the *C. felis* GABAR 181

7.3. Isoxazolines: the next generation of GABAergic compounds 182

7.4. Spinosad binding to the *R. microplus* nicotinic acetylcholine receptor 183

7.5. Future work 184

8. Appendices.....186
8.1. Appendix 1 186
8.2. Appendix 2 188
8.3. Appendix 3 197
8.4. Appendix 4 199
8.5. Appendix 5 200
8.6. Appendix 6 201
8.7. Appendix 7 202
8.8. Appendix 8 203
9. References.....205

Abbreviations

ACh	Acetylcholine
AChE	Acetylcholinesterase
AMP	Ampicillin
AUC	Area under the curve
BLAST	Basic local alignment search tool
Bp	Base pair(s)
°C	Celsius
Ca^{2+}	Calcium ions
cDNA	Complementary deoxyribonucleic acid
CDS	Coding sequence
CI	Confidence interval
Cl	Chlorine
Cm	Centimetre
cRNA	Complementary ribonucleic acid
DDT	Dichlorodiphenyltrichloroethane
DMSO	Dimethyl-sulphoxide
DNA	Deoxyribonucleic acid
dNTPs	Deoxyribonucleoside triphosphates
dsRNA	Double stranded ribonucleic acid
g	Gram
GABA	Gamma-aminobutyric acid
GluCl	Glutamate-gated chloride channel
GST	Glutathione S transferases
H	Hour
HEPES	4-(2-hydroxyethyl)-1-piperazineethanesulfonic acid
I	Current
IC_{50}	Concentration causing 50% response inhibition
I_{MAX}	Peak current
IPM	Integrated Pest Management
IRAC	Insecticide Resistance Action Committee
Kdr	Knockdown resistance

L	Litre
LB	Lysogeny broth
LC	Lethal concentration
LD	Lethal dose
Log 10	Log to the based 10 of a value
M	Molar
Mg	Milligram
Min	Minute
Mg	Milligram
mL	Millilitre
mM	Millimolar
µg	Microgram
µL	Microliter
µM	Micromolar
n	number of cells in a test group
nAChR	Nicotinic acetylcholine receptor
ng	Nanogram
nm	Nanomolar
PCR	Polymerase chain reaction
RNA	Ribonucleic acid
RR	Resistance ratio
s	Second
SD	Standard deviation
SEM	Standard error of the mean
SNP(s)	Single nucleotide polymorphism(s)
Taq polymerase	*Thermus aquaticus* polymerase
TEVC	Two electrode voltage clamp
Tm	Melting temperature
TM	Transmembrane domain
V	Voltage
WHO	World health organisation

List of Figures

Figure 1.1. *Ctenocephalides felis* life cycle. The time between growth stages shown are for optimal conditions. Open source images of life stages used from Centers for Disease control and Prevention (2018).

Figure 1.2. Generalised life cycle of a hard tick. The time between each life stage varies based on species, temperature, host availability and other factors. Open source images of life stages from the Centers for Disease control and Prevention (2018).

Figure 1.3. Schematic showing the targets of common synthetic pesticides. The cyclodienes, avermectins, phenylpyrazoles and isoxazolines act in the GABA receptor. Nicotine, neonicotinoids and spinosysns act on the nicotinic acetylcholine receptor (nAChR). Organophosphates (OPs) and carbamates target the enzyme acetylcholinesterase(AChE). Dichlorodiphenyltrichloroethane (DDT) and pyrethroids act on the sodium channel. Diagram courtesy of Martin Williamson (Rothamsted Research).

Figure 1.4. The prototypic pentameric chloride cys-loop receptor. A. Five subunits form an ion selective channel. B. Each subunit is made up of four transmembrane (TM) regions, and two extracellular N- and C-terminal domains.

Figure 1.5. Compounds from the three main groups of pesticides targeting the nicotinic acetylcholine receptor. A. Nereistoxins. B. Neonicotinoids. C. Spinosyns.

Figure 2.1. A. TEVC electrophysiology rig contained in a Faraday cage with gravity driven perfusion system using pinch valves and c-flex tubing for even-flowing application of solutions and seamless transitions between perfusates. B. Oocyte workstation. Micromanipulators with current and voltage electrodes positioned above a slotted oocyte chamber (with amplifier) on an adjustable headstage.

Figure 2.2. Schematic showing TEVC setup of electrodes. Oocyte is kept in place using a small dip in the bath and clamped with the current and voltage electrodes. Ligand solution flows over the membrane proteins expressed on the outer surface of the cell (in green).

Figure 3.1. Artificial rearing apparatus for *C. felis*. Adult fleas in the *C. felis* cage fed on bovine blood placed in the feeding reservoir. The eggs and faeces fall through the nylon mesh and are collected to rear and maintain the population.

FIGURE 3.2. COATED GLASS VIAL BIOASSAY ANALYSIS ON A HEATED PLATE. THE *R. SANGUINEUS* UNAFFECTED BY THE DOSAGE OF COMPOUND CLIMB UP THE GLASS VIAL DISPLAYING HEAT AVOIDANCE (ALSO BEHAVIOUR SEEN IN *I. RICINUS*). THOSE TREATED WITH AN EFFECTIVE DOSE REMAIN ON THE BOTTOM OF THE VIAL.

FIGURE 3.3. MULTI-CHAMBERED PLATE WITH INJECTED TICKS IN INDIVIDUAL CHAMBERS WHERE EACH ROW REPRESENTS 5 X REPLICATES OF A COMPOUND DOSE. A. NORMAL OVIPOSITION. B. DESICCATED EGGS C. TICK MELANISATION.

FIGURE 3.4. BIRDS EYE VIEW OF THE 'ARTIFICIAL DOG' BIOASSAY SYSTEM. FEEDING CYLINDERS WERE PLACED IN THE MESH WELLS ALLOWING THE *C. FELIS* TO FEED. THE GRADIENT OF WASTE PRODUCT IS ALSO INDICATIVE OF FLEA SURVIVAL AT LOWER DOSES.

FIGURE 3.5. LOG DOSE RESPONSE CURVES FOR C. FELIS OBTAINED USING COATED GLASS VIAL CONTACT ASSAYS WITH ORGANOCHLORINES, PHENYLPYRAZOLES, BIFENAZATE AND PICROTOXIN. *=SIGNIFICANTLY DIFFERENT TO POSITIVE CONTROL FIPRONIL LC50 WHERE $P<0.05$ IN A TWO-SIDED T-TEST.

FIGURE 3.6. LOG DOSE RESPONSE CURVE FOR *C. FELIS* OBTAINED USING COATED GLASS VIAL CONTACT ASSAYS WITH ISOXAZOLINES AND MACROCYCLIC LACTONES. *=SIGNIFICANTLY DIFFERENT TO POSITIVE CONTROL FIPRONIL LC_{50} WHERE $P<0.05$ IN A TWO-SIDED T-TEST.

FIGURE 3.7. THE CHEMICAL STRUCTURES OF FIPRONIL AND ETHIPROLE, HIGHLIGHTING THE TRIFLUOROMETHYLSULFINYL TO ETHYLSULFINYL SUBSTITUTION

FIGURE 3.8. OVERLAY OF THE CHEMICAL STRUCTURES OF IVERMECTIN, AN AVERMECTIN, AND MOXIDECTIN, A MILBEMYCIN. THE DISACCHARIDE GROUP PRESENT IN IVERMECTIN AND THE METHOXYIMINO GROUP IN MOXIDECTIN ARE HIGHLIGHTED.

FIGURE 3.9. LOG DOSE RESPONSE CURVES FOR *I. RICINUS* COATED GLASS VIAL CONTACT ASSAY FOR ORGANOCHLORINES, PHENYLPYRAZOLES, BIFENAZATE AND PICROTOXIN. *=SIGNIFICANTLY DIFFERENT TO POSITIVE CONTROL FIPRONIL LC_{50} WHERE $P<0.05$ IN A TWO-SIDED T-TEST.

FIGURE 3.10. LOG DOSE RESPONSE CURVES FOR *I. RICINUS* COATED GLASS VIAL CONTACT ASSAY FOR ISOXAZOLINES AND MACROCYCLIC LACTONES. *=SIGNIFICANTLY DIFFERENT TO POSITIVE CONTROL FIPRONIL LC_{50} WHERE $P<0.05$ IN A TWO-SIDED T-TEST.

FIGURE 3.11. LOG DOSE RESPONSE CURVES FOR *R. MICROPLUS* OVIPOSITION BIOASSAY FOR ORGANOCHLORINES, PHENYLPYRAZOLES, BIFENAZATE AND PICROTOXIN. *=SIGNIFICANTLY DIFFERENT TO POSITIVE CONTROL FIPRONIL LC_{50} WHERE $P<0.05$ IN A TWO-SIDED T-TEST

FIGURE 3.12. LOG DOSE RESPONSE CURVES FOR *R. MICROPLUS* OVIPOSITION BIOASSAY FOR ISOXAZOLINES AND MACROCYCLIC LACTONES. *=SIGNIFICANTLY DIFFERENT TO POSITIVE CONTROL FIPRONIL LC_{50} WHERE $P<0.05$ IN A TWO-SIDED T-TEST.

FIGURE 3.13. LOG DOSE RESPONSE CURVES FOR *C. FELIS* 'ARTIFICIAL DOG' BIOASSAY FOR ORGANOCHLORINES, PHENYLPYRAZOLES, BIFENAZATE AND PICROTOXIN. *=SIGNIFICANTLY DIFFERENT TO POSITIVE CONTROL FIPRONIL LC_{50} WHERE $P<0.05$ IN A TWO-SIDED T-TEST.

FIGURE 3.14. LOG DOSE RESPONSE CURVES FOR *C. FELIS* 'ARTIFICIAL DOG' BIOASSAY FOR ISOXAZOLINES AND MACROCYCLIC LACTONES. *=SIGNIFICANTLY DIFFERENT TO POSITIVE CONTROL FIPRONIL LC_{50} WHERE $P<0.05$ IN A TWO-SIDED T-TEST.

FIGURE 3.15. *C. FELIS TAQ*MAN ALLELIC DISCRIMINATION READOUT. G= GEORGI, KA= KIEL ALIVE, KD= KIEL DEAD. GREEN FLUORESCENCE INDICATES HOMOZYGOUS FOR THE WILD TYPE, RED DENOTES HOMOZYGOUS FOR THE MUTATION BEING TESTED FOR (ALANINE TO SERINE OR METHIONINE TO 1 AND BLUE DENOTES HETEROZYGOUS (ONE ALANINE AND ONE SERINE).

FIGURE 4.1. ANNOTATED PROTEIN SEQUENCE OF *C. FELIS* (GABARBD) WITH SIGNAL PEPTIDE, TRANSMEMBRANE REGIONS 1-4 AND EXONS 3 AND 6 HIGHLIGHTED. SPLICE VARIANTS A/B AND C/D MODIFIED AMINO ACIDS UNDERLINED.

FIGURE 4.2. DENATURED *C. FELIS* GABAR CRNA SAMPLES. A. GENERULER 1 KB DNA LADDER, 1. WT, 2. A301S, 3. M354I AND 4. A301S.M354I.

FIGURE 4.3. INWARD CURRENTS EVOKED WHEN A RANGE OF GABA CONCENTRATIONS WERE APPLIED TO *C. FELIS* GABAR EXPRESSED IN *X. LAEVIS* OOCYTES.

FIGURE 4.4. TOP LEFT: CURRENTS FROM 13.2 NL OF 100 NG/ML (1.32 NG) *C. FELIS* GABAR EXPRESSED IN *X. LAEVIS* OVER A 72 HOUR PERIOD. TOP RIGHT: RESPONSE FROM OOCYTE INJECTED WITH 50 NL OF 500 NG/ML (25 NG) AT 24 HOURS.

FIGURE 4.5. CURRENT DATA YIELDED A CONCENTRATION-RESPONSE CURVE FOR THE *C. FELIS* GABAR (EC_{50}=177.5 µM) WHERE R = RESPONSE, I_{MAX} = MAXIMAL GABA RESPONSE AND N=10. POINTS ARE MEAN % OF I_{MAX} ± SEM.

FIGURE 4.6. PEAK RESPONSE CURRENT AMPLITUDES (IN RESPONSE TO 1 MM GABA) FROM *C. FELIS* GABAR OVER A TEN-MINUTE PERIOD DO NOT DECAY AS DEMONSTRATED BY SAMPLE ELECTROPHYSIOLOGICAL TRACES AND A GRAPH OF MEAN CURRENTS. R= RESPONSE, T=0 IS THE PEAK RESPONSE OF THE FIRST APPLICATION OF 1 MM GABA. (N=3 FOR EACH DATA POINT).

FIGURE 4.7. REPRESENTATIVE TRACES PRODUCED FROM ANTAGONIST APPLICATION TO THE *C. FELIS* GABARBD. THE OOCYTE IS BATHED IN INCREASING CONCENTRATIONS OF FIPRONIL FOR 2 MINUTES WITH A 3 SECOND PULSE OF 1 MM GABA TO INVOKE AN INWARD CURRENT BETWEEN CONCENTRATIONS.

FIGURE 4.8. ANTAGONIST CONCENTRATION-INHIBITION CURVES FOR WT *C. FELIS* GABAR EXPRESSED IN *X. LAEVIS* OOCYTES. ANTAGONISTS WERE PERFUSED OVER THE OOCYTE IN INCREASING CONCENTRATIONS AND 1 MM GABA USED TO EVOKE INWARD CURRENTS EVERY 2 MINUTES. R = RESPONSE, I_{MAX} = MAXIMAL GABA RESPONSE. $N\geq3$ FOR EACH CURVE. POINTS ARE MEAN % OF I_{MAX} ± SEM.

FIGURE 4.9. WT *C. FELIS* GABAR RECOVERY AFTER ANTAGONIST INHIBITION. CELLS WERE PRE-INCUBATED WITH 300 NM (DIELDRIN, FIPRONIL, AFOXOLANER, FLURALANER, SAROLANER) OR 3 µM (PICROTOXIN AND ETHIPROLE) COMPOUND FOR 2 MINUTES. 1 MM GABA PULSES

were applied to the cell every 2 minutes up to 10 minutes with ringer wash in between applications of GABA. n=1 per curve. % recovery compared to 1 mM GABA in the absence of antagonists.

Figure 4.10. GABA concentration-response curves for WT, A301S, M354I and A301S.M354I GABAR *C. felis* GABARs expressed in *X. laevis* oocytes. R= response, I_{MAX} = maximal response to 1 mM GABA. Points are mean % of I_{MAX} ± SEM.

Figure 4.11. Above: Picrotoxin (PTX) concentration-inhibition curves for WT and mutated *C. felis* GABAR. R= response, I_{MAX} = maximal response to 1 mM GABA. Below: TEVC traces show GABA EC_{50} current and the inhibited PTX IC_{50} and IC_{95} response. Points are mean % of I_{MAX} ± SEM.

Figure 4.12. Above: Dieldrin (DIEL) concentration-inhibition curves for WT and mutated *C. felis* GABAR. R= response, I_{MAX} = maximal response to 1 mM GABA. Below: TEVC traces show GABA EC_{50} current and the inhibited DIEL IC_{50} and IC_{95} response. Points are mean % of I_{MAX} ± SEM.

Figure 4.13. Above: Fipronil (FIP) concentration-inhibition curves for WT and mutated *C. felis* GABAR. R= response, I_{MAX} = maximal response to 1 mM GABA. Below: TEVC traces show GABA EC_{50} current and the inhibited PTX IC_{50} and IC_{95} response. Points are mean % of I_{MAX} ± SEM.

Figure 4.14. Ethiprole (ETH) concentration-inhibition curves for WT and mutated *C. felis* GABAR. R= response, I_{MAX} = maximal response to 1 mM GABA. Below: TEVC traces show GABA EC_{50} current and the inhibited PTX IC_{50} and IC_{95} response. Points are mean % of I_{MAX} ± SEM.

Figure 4.15. WT and A301S *C. felis* GABAR recovery after FIP, DIEL and ETH inhibition. Cells were pre-incubated with 300 nM FIP/DIEL or 3 µM ETH for 2 minutes, then washed with Ringer's solution. 1 mM GABA pulses were applied to the cell every 2 minutes up to 20 minutes. n=3/curve. % recovery compared to 1 mM GABA in the absence of antagonists. Points are mean % of I_{MAX} ± SEM.

Figure 4.16. Above: Afoxolaner (AFOX) concentration-inhibition curves for WT and mutated *C. felis* GABARs. R= response, I_{MAX} = maximal response to 1 mM GABA. Below: TEVC traces show GABA EC_{50} current and the inhibited AFOX IC_{50} and IC_{95} response. Points are mean % of I_{MAX} ± SEM.

Figure 4.17. Above: Fluralaner (FLU) concentration-inhibition curves for WT and mutated *C. felis* GABARs. R= response, I_{MAX} = maximal response to 0.3 mM GABA. Below: TEVC traces show GABA EC_{50} current and the inhibited FLU IC_{50} and IC_{95} response. Points are mean % of I_{MAX} ± SEM.

Figure 4.18. Above: Sarolaner (SAR) concentration-inhibition curves for WT and mutated *C. felis* GABARs. R= response, I_{MAX} = maximal response to 1 mM GABA.

BELOW: TEVC TRACES SHOW GABA EC_{50} CURRENT AND THE INHIBITED SAR IC_{50} AND IC_{95} RESPONSE. POINTS ARE MEAN % OF I_{MAX} ± SEM.

FIGURE 5.1. CROSSING STRATEGY TO GENERATE GABAR KNOCKOUT LINES WITH AN INTEGRATION SITE AND INTEGRASE ENZYME FOR Φ31 INTEGRASE-MEDIATED TRANSGENESIS. *RFP*=RED FLUORESCENCE PROTEIN, *VAS*=VASA PROMOTER, *INT*=INTEGRASE, *+*=WILD TYPE, *SP*=STERNUM PLURAL, *CY*=CURLY, *SB*=STUBBLE, *TB-HU*=TUBBY HUMERAL.

FIGURE 5.2. FROM LEFT TO RIGHT: *D. MELANOGASTER* WITH HOMOZYGOUS INTEGRATION OF THE GABARBD GENE AT THE ATTP40 LANDING SITE, FLIES WITH, HETEROZYGOUS INTEGRATION AND FLIES WITH NO INTEGRATION.

FIGURE 5.3. CROSSING STRATEGY TO GENERATE GABAR KNOCKOUT *D. MELANOGASTER* WITH POSITIVE INTEGRATION OF THE *GABARBD* (WT, A301S, M354I AND A301S.M354I) AND THE *C747-GAL4* DRIVER, FOR LARVAL BIOASSAYS. *RFP*=RED FLUORESCENCE PROTEIN, *VAS*=VASA PROMOTER, *INT*=INTEGRASE, *+*=WILD TYPE, *SP*=STERNUM PLURAL, *CY*=CURLY, *SB*=STUBBLE, *TB-HU*=TUBBY HUMERAL.

FIGURE 5.4. LOG DOSE RESPONSE CURVES FOR *D. MELANOGASTER* LARVAE HOMOZYGOUS FOR GABAR SUBSTITUTIONS, TREATED WITH DIELDRIN. SCORED BY NUMBERS PUPATING. *=SIGNIFICANTLY DIFFERENT TO WT LC_{50} WHERE $P<0.05$ IN A TWO-SIDED T-TEST.

FIGURE 5.5. LOG DOSE RESPONSE CURVES FOR *D. MELANOGASTER* LARVAE HETEROZYGOUS FOR GABAR SUBSTITUTIONS, TREATED WITH DIELDRIN. SCORED BY NUMBERS ECLOSING. *=SIGNIFICANTLY DIFFERENT TO WT LC_{50} WHERE $P<0.05$ IN A TWO-SIDED T-TEST.

FIGURE 5.6. LOG DOSE RESPONSE CURVES FOR *D. MELANOGASTER* LARVAE HOMOZYGOUS FOR GABAR SUBSTITUTIONS, TREATED WITH ETHIPROLE. SCORED BY NUMBERS PUPATING. *=SIGNIFICANTLY DIFFERENT TO WT LC_{50} WHERE $P<0.05$ IN A TWO-SIDED T-TEST.

FIGURE 5.7. LOG DOSE RESPONSE CURVES FOR *D. MELANOGASTER* LARVAE HETEROZYGOUS FOR GABAR SUBSTITUTIONS, TREATED WITH ETHIPROLE. SCORED BY NUMBERS ECLOSING. *=SIGNIFICANTLY DIFFERENT TO WT LC_{50} WHERE $P<0.05$ IN A TWO-SIDED T-TEST.

FIGURE 5.8. LOG DOSE RESPONSE CURVES FOR *D. MELANOGASTER* LARVAE HOMOZYGOUS FOR GABAR SUBSTITUTIONS, TREATED WITH FIPRONIL. SCORED BY NUMBERS PUPATING. *=SIGNIFICANTLY DIFFERENT TO WT LC_{50} WHERE $P<0.05$ IN A TWO-SIDED T-TEST.

FIGURE 5.9. LOG DOSE RESPONSE CURVES FOR *D. MELANOGASTER* LARVAE HETEROZYGOUS FOR GABAR SUBSTITUTIONS, TREATED WITH FIPRONIL. SCORED BY NUMBERS ECLOSING. *=SIGNIFICANTLY DIFFERENT TO WT LC_{50} WHERE $P<0.05$ IN A TWO-SIDED T-TEST.

FIGURE 6.1. PARTIAL SEQUENCE ALIGNMENT OF THE HUMAN NACHRA7 AND THE R. MICROPLUS NACHRA6 (SPLICE VARIANT 3A). TM1, TM2 AND TM3 OF THE R. MICROPLUS NACHRA6 ARE ANNOTATED. RESIDUES ON THE PRINCIPAL SUBUNIT THAT FORM BINDING CONTACTS WITH SPINOSAD ARE HIGHLIGHTED IN GREEN. THE EQUIVALENT RESIDUES ON THE COMPLEMENTARY SUBUNIT THAT FORM BINDING CONTACTS WITH SPINOSAD ARE

highlighted in yellow. The amino acids differences highlighted in red are not conserved and were taken forward for site-directed mutagenesis.

Figure 6.2. Illustration of the percentage decay analysis where R = the peak response in nA and R_2 is a second value taken 5 seconds after the removal of acetylcholine. Left: *R. microplus* nAChRa6 response to 0.3 mM achetylcholine. Right: *R. microplus* nAChRa6 response to 0.3 mM achetylcholine after 2 minute incubation with 30 µM spinosad.

Figure 6.3. Illustration of the 'area under the curve' analysis where the total AUC of a test trace (right) is normalised to the response to acetylcholine-only (left) (AUC_{MAX}). The hatched red area indicates the total area used for calculations. Left: *R. microplus* nAChRa6 response to 0.3 mM achetylcholine. Right: *R. microplus* nAChRa6 response to 0.3 mM achetylcholine after 2 minute incubation with 30 µM spinosad.

Figure 6.4. Representative traces of the concentration-dependent inward currents in response to acetylcholine in *X. laevis* receptors expressing the Wild Type *R. microplus* nAChRa6 (above) and human nAChRa7 (below).

Figure 6.5. Acetylcholine concentration-response curves for WT and mutated *R. microplus* nAChRa6 and human nAChRa7 expressed in *X. laevis* oocytes. R= response, I_{MAX} = maximal response to 0.3 mM ACh.

Figure 6.6. Sample electrophysiological trace from WT and mutated *R. microplus* nAChRa6 and human nAChRa7. For each current trace, spinosad was pre-applied for 15 seconds, then co-applied with 0.3 mM acetylcholine for a further ~3 seconds, with a 2 minute ringer wash in between increasing concentrations of spinosad.

Figure 6.7. Boxplot of peak responses to 0.3 mM spinosad for *R. microplus* nAChRa6 (*Rma*6) channels with an average inward current of 1126 nA for the WT, 456.8 nA for F265L, 269.3 nA for G324A and 63.88 nA for C329S (n=9 for WT, n=8 per mutated channel).

Figure 6.8. Spinosad agonist dose-response curve for *R. microplus* nAChRa6 Wild Type expressed in *X. laevis* oocytes. R=response, I_{MAX}=maximal response to spinosad. n=9. EC_{50}=31.05 µM (95% CI 25.78-37.39 µM), Hill Slope=4.2 ±11.3).

Figure 6.9. Spinosad percentage decay concentration-response curves for WT and mutated *R. microplus* nAChRa6 and human nAChRa7 expressed in *X. laevis* oocytes. R= peak response to 0.3 mM ACh, R_2 = response 5 seconds after removal of ACh.

Figure 6.10. Spinosad 'Area Under the Curve' (AUC) concentration-response curves for WT and mutated *R. microplus* nAChRa6 and human nAChRa7 expressed in *X.*

LAEVIS OOCYTES. AUC OF THE SPINOSAD-TREATED CURRENT NORMALISED AGAINST THE AUC OF THE 0.3 MM ACHETYLCHOLINE ONLY CURRENT.

List of Tables

TABLE 2.1. COMPONENTS OF THE *TAQ*MAN ASSAY PROBE/PRIMER MIX USED FOR THE DETECTION OF THE A301S AND M354I MUTATION IN THE *C. FELIS* GABAR.

TABLE 2.2. FORMULATION OF CA^{2+} FREE BARTH'S AND CA^{2+} CONTAINING BARTH'S SOLUTION.

TABLE 3.1. FUNCTION, MODE OF ACTION, CHEMICAL GROUP AND STRUCTURE DETAILS OF COMPOUNDS USED IN THIS STUDY. ALL COMPOUNDS ARE GABA AGONISTS OR ANTAGONISTS, EXCLUDING GLUTAMATE AND THE MACROCYCLIC LACTONES, WHICH ACT PRIMARILY ON THE GLUTAMATE-GATED CHLORIDE CHANNEL (GLUCL).

TABLE 3.2. CONCENTRATIONS (PPM) OF CHEMICALS TESTED ON *C. FELIS* AND TICKS IN THE COATED GLASS VIAL BIOASSAY. CHEMICALS WERE DISSOLVED IN ACETONE.

TABLE 3.3. CHEMICALS, NUMBER OF DOSES AND CONCENTRATIONS USED (PPM) FOR *R. MICROPLUS* OVIPOSITION BIOASSAY. ALL CHEMICALS WERE DISSOLVED IN APPROPRIATE SOLUTE.

TABLE 3.4. NUMBER OF DOSES AND CONCENTRATIONS USED (PPM) FOR THE 'ARTIFICIAL DOG'

TABLE 3.5. THE LC_{50} VALUES TAKEN FROM A PROBIT ANALYSIS OF DATA DERIVED FROM THE *C. FELIS* 'ARTIFICIAL DOG' BIOASSAY, THE *R. MICROPLUS* OVIPOSITION BIOASSAY AND THE CONTACT BIOASSAYS ON *C. FELIS* AND *I. RICINUS* FOR A RANGE OF CHEMICAL COMPOUNDS.

TABLE 4.1. OLIGONUCLEOTIDE PRIMERS USED FOR SITE-DIRECTED MUTAGENESIS OF *C. FELIS* GABAR TO INTRODUCE A301S AND M354I SUBSTITUTION AND PRIMERS USED FOR SEQUENCING TO VERIFY THE MUTATION OF THE DNA.

TABLE 4.2. COMPARATIVE GABA EC_{50} VALUES FOR *X. LAEVIS* OOCYTES EXPRESSING FUNCTIONAL GABA RECEPTORS.

TABLE 4.3. PARAMETERS DERIVED FROM ANTAGONIST CONCENTRATION-INHIBITION CURVES FOR WT *C. FELIS* GABAR.

TABLE 4.4. PARAMETERS DERIVED FROM GABA CONCENTRATION-RESPONSE CURVES FOR WT, A301S, M354I AND A301S + M354I *C. FELIS* GABARS.

TABLE 4.5. PARAMETERS DERIVED FROM PICROTOXIN AND DIELDRIN CONCENTRATION-INHIBITION CURVES FOR WT, A301S, M354I AND A301S.M354I *C. FELIS* GABARS.

TABLE 4.6. PARAMETERS DERIVED FROM FIPRONIL AND DIELDRIN CONCENTRATION-INHIBITION CURVES FOR WT, A301S, M354I AND A301S.M354I *C. FELIS* GABARS.

TABLE 4.7. PARAMETERS DERIVED FROM ISOXAZOLINE CONCENTRATION-INHIBITION CURVES FOR WT, A301S, M354I AND A301S.M354I *C. FELIS* GABARS.

TABLE 5.1. OLIGONUCLEOTIDE PRIMERS USED FOR SITE-DIRECTED MUTAGENESIS OF *D. MELANOGASTER* GABARBD TO INTRODUCE A301S AND M354I SUBSTITUTIONS AND PRIMERS USED FOR SEQUENCING TO VERIFY THE MUTATION OF THE DNA.

TABLE 6.1. OLIGONUCLEOTIDE PRIMERS USED FOR SITE-DIRECTED MUTAGENESIS OF THE *R. MICROPLUS* NACHR TO INTRODUCE F265L, G324A AND C329S SUBSTITUTIONS AND PRIMERS USED FOR SEQUENCING TO VERIFY THAT THE CORRECT MUTATIONS WERE PRESENT.

TABLE 6.2. OLIGONUCLEOTIDE PRIMERS USED FOR SITE-DIRECTED MUTAGENESIS OF THE HUMAN NACHR TO INTRODUCE L299F, A358G AND S363C SUBSTITUTIONS AND PRIMERS USED FOR SEQUENCING TO VERIFY THAT THE CORRECT MUTATIONS WERE PRESENT.

TABLE 6.3. PARAMETERS DERIVED FROM ACETYLCHOLINE CONCENTRATION-RESPONSE CURVES FOR *R. MICROPLUS* NACHRA6 (*RM* A6) WT, F265L, G324A, C329S AND HUMAN NACHRA7 (HUMAN A7) WT AND L299F.A358G.S363C.

TABLE 6.4. PARAMETERS DERIVED FROM SPINOSAD PERCENTAGE DECAY CONCENTRATION-RESPONSE CURVES FOR *R. MICROPLUS* NACHRA6 (*RM*A6) WT, F265L, G324A, C329S AND HUMAN NACHRA7 WT AND A955G.S960C.L1235F.

TABLE 6.5. PARAMETERS DERIVED FROM SPINOSAD 'AREA UNDER THE CURVE' CONCENTRATION-RESPONSE CURVES FOR *R. MICROPLUS* NACHRA6 (*RM*A6) WT, F265L, G324A, C329S AND HUMAN NACHRA7 WT AND A955G.S960C.L1235F.

TABLE 6.6. ACETYLCHOLINE EC_{50} VALUES OF INSECT AND ACARI NACHR SUBUNITS CLONED AND EXPRESSED IN *X. LAEVIS* OOCYTES IN COMBINATION WITH A VERTEBRATE SUBUNIT, EXCLUDING THE HOMO-OLIGOMERIC *MYZUS PERSICAE* NACHRA1. N.B. NACHR SUBUNITS CO-EXPRESSED WITH VERTEBRATE SUBUNITS IN CULTURED CELL LINES HAVE BEEN OMITTED BUT INCLUDE *DROSOPHILA MELANOGASTER* NACHRA4, NACHRA6, NACHRA7, NACHRB1, NACHRB2, *CTENOCEPHALIDES FELIS* NACHRA1 AND NACHRA2, *SCHISTOCERA GREGARIA* NACHRA1.

1. General introduction

1.1. Arthropod pests of domesticated animals

Arthropod pests are generally responsible for economic losses, crop devastation and influence both human and animal health around the world. Within the animal health industry, close relationships of domestic animals with humans, increases in transportation, habitat loss and climate change are resulting in increases in arthropod populations and incidences of arthropod-borne zoonotic diseases (Beugnet and Marie, 2009). The control of such pests is worth billions of pounds per year with new products coming onto the market regularly (Groff and Bishop, 2017). This study reports studies on products acting on ligand-gated ion channels of fleas and ticks affecting companion animals and livestock, and this chapter focuses on the pests, their chemical control, the chemical targets and resistance to the treatments.

1.1.1. Fleas

There are over 2500 flea species, of which approximately 15 infest companion animals, with *Ctenocephalides felis* being the most common and important pest of dogs and cats worldwide (Rust, 2017). *C. felis,* or cat fleas, are parasitic insects in the order Siphonaptera and are small flightless and hematophagous. They have a highly specialised metamorphous life cycle made up of four distinct stages, with the time taken between stages being dependent on temperature (Figure 1.1) (Rust, 2017). Within 24-36 hours following a blood meal the adult females lay 30-40 eggs in the host's hair and the eggs then drop into the surrounding environment (usually the hosts' feeding or resting place) and hatch into larvae within two days to two weeks. The larvae then feed on digested blood from the adult flea faeces and molt three times, with the third instar developing into prepupae and forming cocoons. The pupal stage can provide protection in adverse conditions, and there have been instances where pupae have been found to survive many

months in the cocoon ((Metzger and Rust, 1997)). Adult fleas emerge when pressure and heat are detected, and usually die within two weeks if a suitable host is not found. Once on a host reproducing females can live up to 100 days. However host grooming shortens this and the average longevity of fleas on hosts is 7.8 days (Rust, 2017).

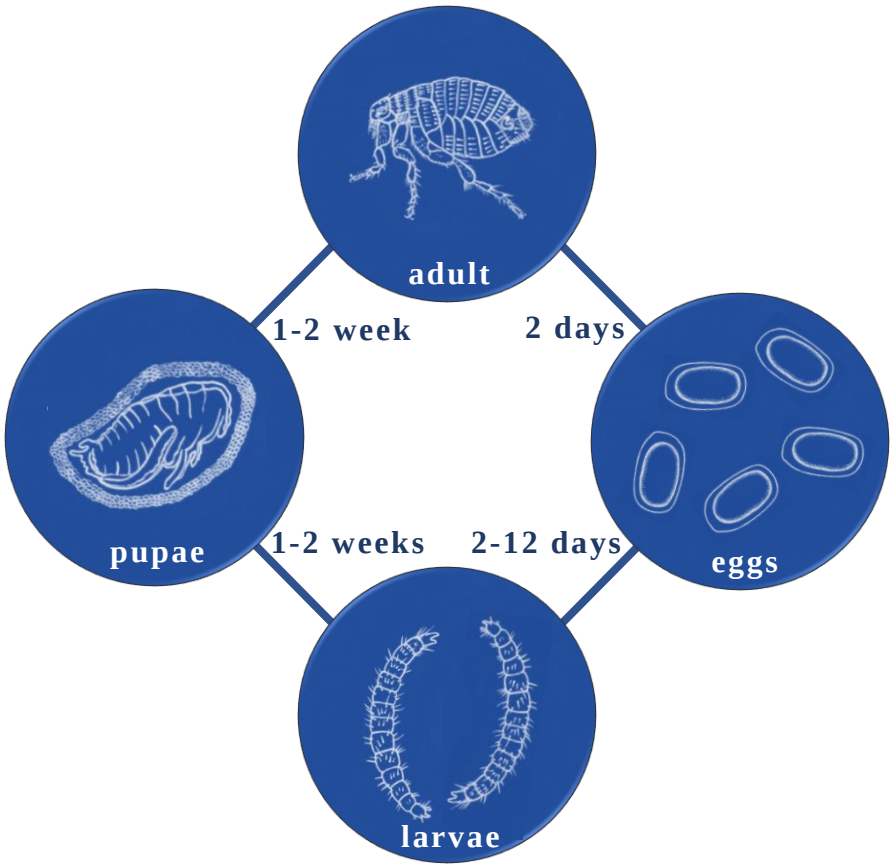


Figure 1.1. *Ctenocephalides felis* life cycle. The time between growth stages shown are for optimal conditions. Open source images of life stages used from Centers for Disease control and Prevention (2018).

Fleas are not only a nuisance to companion animals and their owners, but also have medical and veterinary importance. For example, *C. felis* can act directly on the animal causing a range of problems including anaemia, weight loss and behavioural modification. They also act indirectly as vectors of diseases such as flea allergy dermatitis (FAD) and flea bite dermatitis (FBD), rickettsial diseases, cat scratch disease (CAD) and very importantly they can act as intermediate hosts of other disease such as plague (Rust, 2017, Iannino et al., 2017).

FAD is the one of the most common skin diseases of cats and dogs and is the result of an exaggerated immune response to antigens present in the flea saliva, and FBD is a distinct but similar condition. The most severe infection spread by over 40 flea species is the plague, caused by *Yersinia pestis* (Eisen et al., 2008). Rat fleas have played a crucial historical role in the transmission of a particular form of plague, bubonic plague, however *C. felis* has also been found to be a vector in plague-endemic regions and can infest rodent reservoirs (Stenseth et al., 2008). Rickettsial diseases thought to be transmitted by *C. felis* include murine typhus (*Rickettsia typhi*) and the emerging flea-borne rickettsiosis caused by *Rickettsia felis.* These diseases cause fevers and flu-like symptoms in most cats and dogs, but in more serious cases can lead to an infection of the red blood cells leading to a blood disorder (Blanton and Walker, 2017)

The control of *C. felis* relies primarily on ‘on-animal’ therapies, where a chemical insecticide is applied to the animal’s skin and fur. Considerable advances have been made in the development of such ectoparasiticide products for companion animals, with an increase in the number of available products over the last 25 years. Products are now available for application either directly on the skin, as slow-release collars or administered orally or injected directly into the animal for systemic distribution ((Pfister and Armstrong, 2016)).

1.1.2. Ticks

Ticks are parasitic arachnids (subclass: acari), and are globally distributed hematophagous ectoparasites of wild and domesticated vertebrates (excluding fish) (Nava et al., 2009). There are an estimated 900 species which fall into two major orders; hard ticks (Ixodida) making up the majority at 700 species, and soft ticks (Argasida) making up the remaining 200 (Baneth, 2014). Hard ticks are characterised by a chitin shield on their dorsal surface called a scutum and beak-like feeding appendages, whilst soft ticks have a leathery body and no scutum (Mehlhorn, 2001). Hard ticks have a complex four-stage life cycle; egg, six-legged larvae, eight-legged nymph and adult (Figure 1.2).

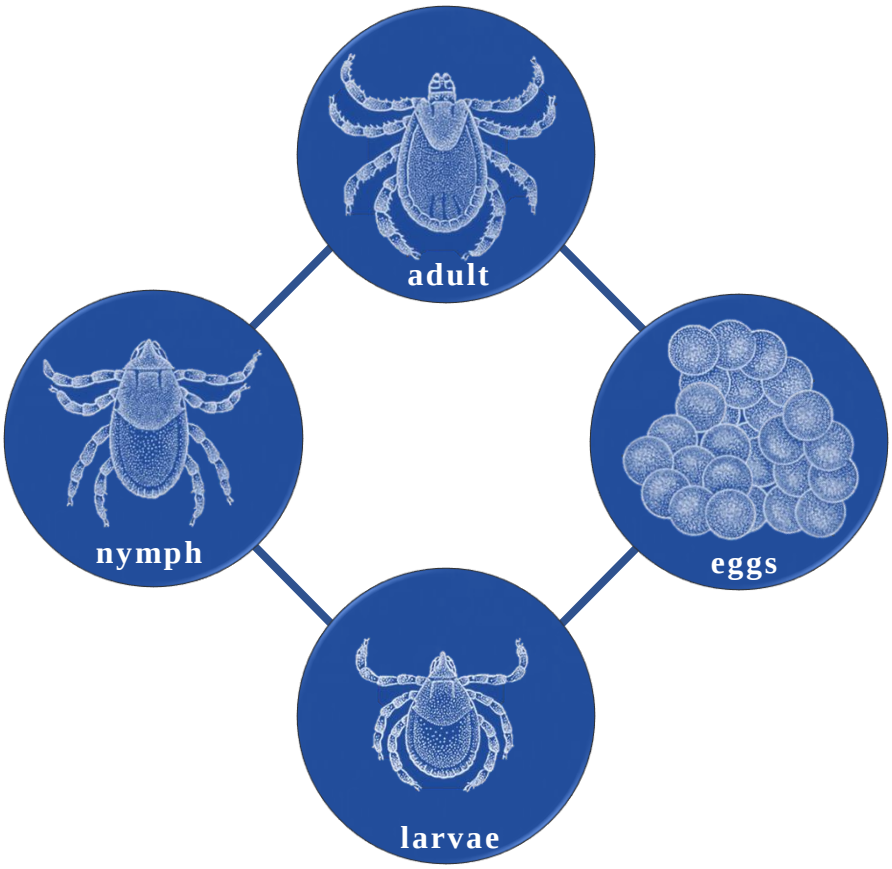


Figure 1.2. Generalised life cycle of a hard tick. The time between each life stage varies based on species, temperature, host availability and other factors. Open source images of life stages from the Centers for Disease control and Prevention (2018).

The larvae feed on the host animal, taking a blood meal and then molt and develop into a nymph, which continues to feed and molts again into the adult. This cycle can last up to three years particularly for species that require a number of different hosts (Fivaz et al., 2012). Most ticks use an 'ambush' strategy to find hosts, climbing onto weeds, grass and leafy vegetation and waiting until a host comes along, which is recognised by the tick's Haller organ, detecting humidity, temperature and carbon dioxide (Blagburn and Dryden, 2009). Adult females take one blood meal before mating on-host and laying a large batch of thousands of eggs, and then dying. Many ticks adopt a 3-host cycle with a different animal at each feeding stage (larvae, nymph and adult).

As with fleas, ticks can cause a number of public health problems for their hosts, including anaemia and weight loss as a result of blood loss. However, the main cause of mortality in their hosts is by the transmission of diseases, helminths and protozoa (Mehlhorn, 2001). The lifestyle of the tick, including blood feeding, secretion of saliva and movement between hosts makes them well suited to the spread of disease. Only a minority of the 900 species of ticks are responsible for the transmission of diseases but these include important human illnesses such as tick-borne encephalitis (TBE), Lyme disease, Crimean-Congo haemorrhagic fever, tick-borne fever, rickettsial disease, babesiosis and anaplasmosis in companion animals (Online: European Centre for Disease Prevention and Control (2018)).

TBE is caused by a virus transmitted by the saliva of *Ixodes ricinus* (the castor bean tick) and *Ixodes persulcatus* (the taiga tick), with over 10,000 reported cases each year (Lindquist and Vapalahti, 2008). Clinical symptoms can vary often starting with flu-like symptoms and escalating to meningitis-like symptoms such as drowsiness, loss of senses and even paralysis (Beugnet and Marie, 2009). TBE has also been found to affect dogs and horses as well as humans but to a lesser extent. Lyme disease, caused by the bacteria *Borrelia burgdorferi*, is primarily vectored by *I. ricinus*, and is characterised by a bulls-eye rash on the bitten skin and flu-like symptoms. If untreated, more serious nervous,

cardiovascular and muscular complications can occur (Alao and Decker, 2012). The Crimean-Congo haemorrhagic fever, primarily transmitted by ticks from the *Hyalomma* genus, is a viral infection increasing in incidence, particularly across Europe, and is a severe disease causing haemorrhagic fever in humans with a high fatality rate (Online: European Centre for Disease Prevention and Control (2018)). The *Hyalomma marginatum* tick is the main vector for the disease, and infection in animal hosts is symptomless, posing a severe threat to people who work with the animals and livestock.

In livestock, ticks can cause considerable economic losses by direct damage to the skin/coat of animals and causing lower meat and milk production (Stafford et al., 2017). In addition, tick-borne disease cause substantial losses with estimates that 80% of cattle populations carry disease (Marcelino et al., 2012). Some of the key disease-carrying ticks that affect domesticated animals and livestock are the hard ticks *Dermacentor variabilis* (American dog tick), *Dermacentor andersoni* (Rocky Mountain wood tick), *Dermacentor occidentalis* (Pacific Coast tick), *Dermacentor albipictus* (the winter tick), *Rhipicephalus sanguineus* (brown dog tick), *Rhipicephalus* (*Boophilus*) *microplus* (cattle tick), *Rhipicephalus appendiculatus* (brown ear tick), *Ixodes scapularis* (deer tick), *I. ricinus* (castor bean tick), *Amblyomma maculatum* (Gulf Coast tick), *Amblyomma americanum* (Lone Star tick), and *Amblyomma hebraeum* (tropical bont tick).

The most common tick-borne diseases of animals are babesiosis and anaplasmosis. Babesiosis is a malaria-like disease caused by protozoan parasites affecting companion animals (particularly dogs), small ruminants and cattle. The main vectors of babesiosis pathogens are *I. ricinus* and *I. scapularis* (Rahlenbeck et al., 2016). Anaplasmosis is caused by bacteria in the genus *Anaplasma*, such as *Anaplasma ovis* and *Anaplasma phagocytophilum* which cause a tick-borne fever affecting sheep and cattle causing considerable losses in productivity. In addition to the ruminant hosts, anaplasmosis has also been found in horses, small rodents, cats and dogs (Tozon et al., 2003). *I. ricinus* is the main vector

of *A. phagocytophilum*, although *Ixodes pacificus* has been implicated in spreading the disease in the US (Beugnet and Marie, 2009). *A. ovis* is transmitted by a wider range of species including ticks from the genus Dermacentor, Amblyomma, Hyalomma and Rhipicephalus (Marcelino et al., 2012).

Tropical theileriosis, known as East Coast fever, is caused by *Theileria annulate* and is transmitted to ruminants (particularly cattle) by ticks of the Hyalomma genus (Rahlenbeck et al., 2016). Symptoms include enlargement of lymph nodes, fevers and haemorrhages (Gill et al., 1977).

Rickesttsial diseases are of world-wide importance and are caused by bacteria from the *Rickettsia* genus, vectored by a wide variety of ticks and varying in intensity depending on the bacterial species responsible. Symptoms can vary from being undetectable to muscle-ache, rashes and flu-like symptoms, and can be potentially fatal (Online: European Centre for Disease Prevention and Control (2018)). Some of the most prominent diseases of this class are the spotted fever group (Rocky Mountain spotted fever caused by *Rickettsia rickettsii* and Mediterranean spotted fever caused by *Rickettsia conorii*) and the typhus group (*Rickettsia prowazekii* and *Rickettsia typhi*) (Beugnet and Marie, 2009).

1.2. Arthropod pest control

Limiting the damaging effects of arthropod pests on domesticated animals and humans can be achieved in many ways including avoidance, adequate physical protection (i.e. full-coverage clothing), environmental modification, improved sanitation, biological control, vaccinations and chemical insecticides and acaricides. (Online: European Centre for Disease Prevention and Control (2018)). However, by far the most popular and effective method of control is selective chemistries tailored to damage the pests and leave the host unharmed (Petney, 1997), used in combination with the other strategies.

1.2.1. Environmental modification, control and sanitation

Environmental modifications can be used to treat and/or prevent infestations of pests. For example, measures which limit the interaction of wild animals (which act as reservoirs of disease), with livestock in agricultural premises, paddocks and pasturage, or with companion animals in residential premises. These methods are largely directed at ticks, many of which live outside in grass, brush and wooded areas for part of their life cycle. Strategic fencing to restrict access by stray wildlife, removal of leaf litter, maintaining vegetation-free borders and maintenance of grass are all recommended methods for management of agricultural and residential land (Stafford et al., 2017). However, in many cases these methods are only one expensive component of an integrated pest management (IPM) strategy (Bloemer et al., 1990, Stafford et al., 2017).

Environmental control and sanitation advice for regulating ticks and fleas is generally used in households with a companion animal. Vacuuming has been found to greatly reduce the number of flea and tick eggs in carpets and soft furnishings, with estimates of 40-60% control (Beck and Pfister, 2004). Steam cleaning has also been found to be effective on all stages of the life cycle of both fleas and ticks (Lappin, 2005). There are also a variety of flea combs on the market which can be used to detect the presence of the ticks and fleas and mechanically remove all life stages from the animal hair. Other methods combine environmental controls with chemical sprays which can be applied around the home and outside areas. However, these are limited in their popularity because of concerns of spraying chemicals around the home (Stafford et al., 2017) and have largely been replaced by the development and advancement of on-animal therapies.

1.2.2. Biological control

Biological control using the natural enemies of pests to control the population has been of only limited use for ticks. Exceptions include the use of the fungus *Metarhizium anisopliae* and the guineafowl bird (Duffy et al., 1992) to reduce to tick populations and control Lyme disease (Tiago et al., 2014). Two fungi (*M. anisopliae* and *Beauveria Bassiana*) were also used in the field to reduce the tick burden in livestock in Kenya (Maranga et al., 2005) and Brazil (Bittencourt, 2000), with both studies producing promising results particularly in cattle. Despite preliminary successes biocontrol is not currently a viable alternative to chemical control in reducing tick abundance (Ostfeld et al., 2006). The biocontrol options are even fewer for fleas of companion animals, where predators of fleas such as ants and beetles haven't been used in a therapeutic manner (Rust, 2017).

1.2.3. Vaccination

In some cases vaccines can be used to control human arthropod-borne diseases by reducing vector populations and/or reducing the vectors capacity for disease transmission (Merino et al., 2013). For example there is an effective preventative vaccine against TBE which is targeted to people in areas of high risk and is the only vaccine to be administered to humans against tick-borne diseases (Smit, 2012). Previously, a vaccine against Lyme disease was in use but this was withdrawn in 2002 mainly due to high costs and low sales (Hanson and Edelman, 2003).

In livestock and companion animals, vaccines are available against the vector-borne Rickettsial disease, babesiosis, canine leishmaniosis, tropical theileriosis and Lyme disease (Marcelino et al., 2012, Otranto, 2018). However, success varies and whilst they reduce the clinical signs, their efficacy in preventing infection is low and therefore they can only form part of a pest management strategy (Otranto, 2018, Lee and Opdebeeck, 1999, Marcelino et al., 2012).

Vaccines targeting the flea or tick directly have great potential, but progress has been limited by the lack of suitable protective antigens (Otranto, 2018). There is a large-scale vaccination programme targeting cattle ticks (*R. microplus, R. annulatus and R. decoloratus*) based on the gut antigen Bm86, which triggers production of antibodies that are then ingested by the feeding ticks (Kiss et al., 2012). However even within this commercialised vaccination programme, there is a high degree of variation in efficacy (Otranto, 2018). The identification of suitable antigens targeting fleas has also made similar slow progress (Otranto, 2018). Historically, vaccinations against livestock arthropod pests has been of commercial value, but this has reduced as more importance has been placed on companion animal vaccinations by the scientific community and the general public (Otranto and Wall, 2008).

1.2.4. Chemical control

Chemical control of fleas and ticks is the most effective method and often a key component of any integrated pest management (IPM) strategy. They act by either repelling or killing the pest, or in the case of ticks, disrupting attachment. Insecticides and acaricides, with a neurotoxic mode of action are responsible for direct kill and constitute over 70% of the world insecticide market (Nauen, 2002). Pesticides targeting the invertebrate nervous system, or nerve poisons, have been used ever since dichlorodiphenyltrichloroethane (DDT) and various polychlorocycloalkanes (PCCAs) were introduced in the 1940s. This was followed by organophosphates in the 1950s, methylcarbamates in the 1960s, pyrethroids in the 1970s, neonicotinoids in the 1990s, the diamides in the 2000s and the isoxazolines in the 2010s (Casida and Durkin, 2013). The nervous system has at least 11 targets for neuroactive insecticides and acaricides, many of them very sensitive sites where even a small disruption can ultimately prove to be lethal (Casida and Durkin, 2013). Some of the main groups of compounds and their neurotoxic targets are shown in Figure 1.3.

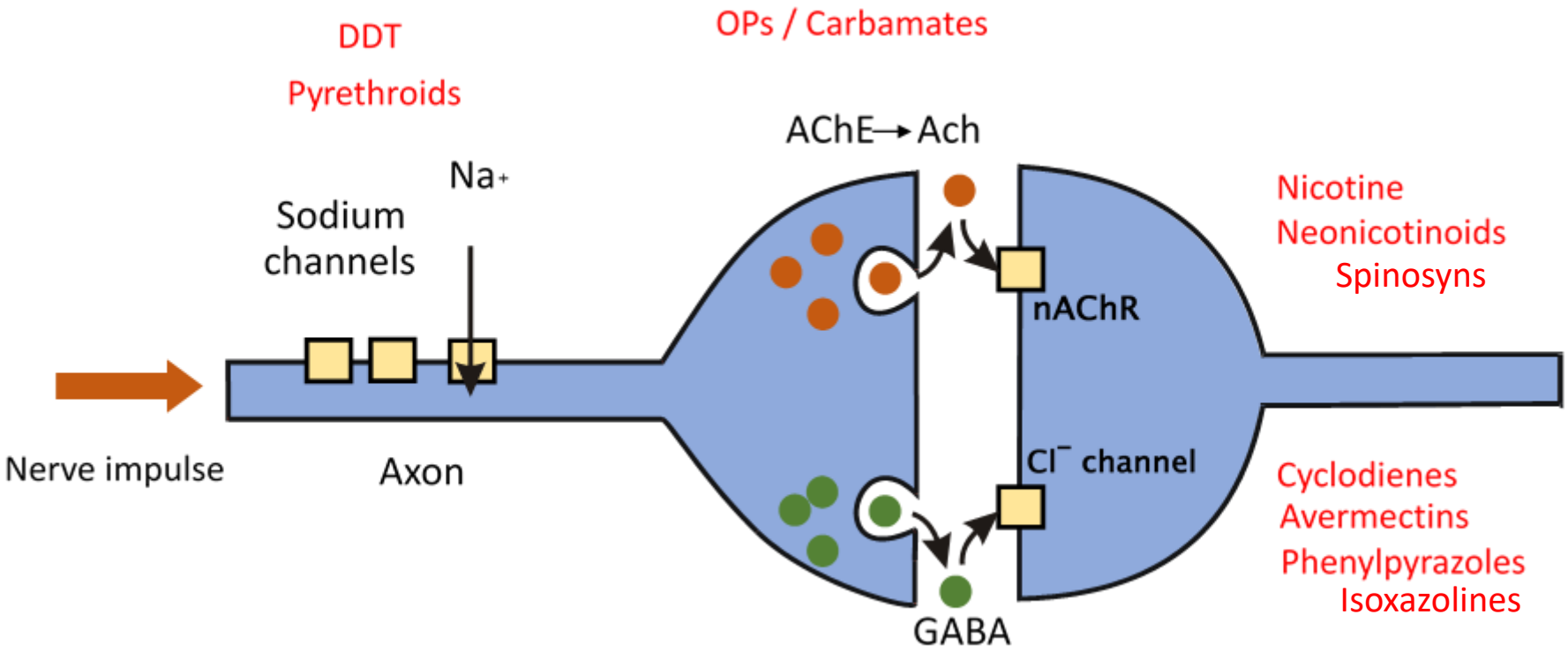


Figure 1.3. Schematic showing the targets of common synthetic pesticides. The cyclodienes, avermectins, phenylpyrazoles and isoxazolines act in the GABA receptor. Nicotine, neonicotinoids and spinosysns act on the nicotinic acetylcholine receptor (nAChR). Organophosphates (OPs) and carbamates target the enzyme acetylcholinesterase(AChE). Dichlorodiphenyltrichloroethane (DDT) and pyrethroids act on the sodium channel. Diagram courtesy of Martin Williamson (Rothamsted Research).

1.2.5. Chemical control modes of action

Insecticides and acaricides can act as blockers, agonists, antagonists, modulators and allosteric antagonists of their targets (reviewed in depth in Sparks and Nauen (2015)). Briefly, channel blockers enter and are trapped in the pore of the receptor, blocking ion flow through the channel. Agonists bind to and mimic the action of the neurotransmitter at the orthosteric binding site, whilst antagonists also bind to the neurotransmitter site but hinder activation of the ion channel. Modulators are compounds that bind to a modulatory site and modify the normal function of the channel by activating the channel and keeping it open longer than normal or prevent the channel from opening at all. Allosteric antagonists bind the modulatory site of the receptor in the closed state and prevent channel opening by agonists.

1.3. Insecticide and acaricide targets

1.3.1. Cys-Loop receptors

Many of the binding sites for insecticides and acaricides acting on the neuromuscular system are within ligand-gated ion channels. These transmembrane channels have a typical structure composed of heteromeric or homomeric subunits arranged around a central pore, and contain N-terminal and C-terminal extracellular domains. The cys-loop receptors, so named due to the characteristic loop formed by a disulphide bond at the N-terminal domain, include the γ-aminobutyric acid receptor (GABAR), the glutamate chloride receptor (gluCl), the cation selective nicotinic acetylcholine receptor (nAChR), the glycine receptor (GlyR) and 5-hydroxytryptamine (5-HT_3) receptor (Figure 1.4).

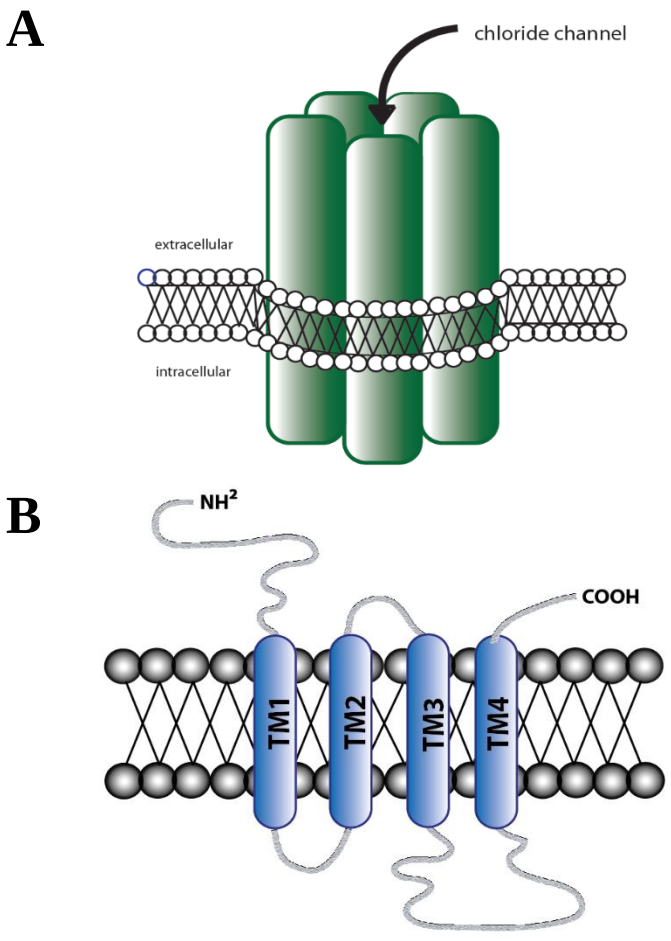


Figure 1.4. The prototypic pentameric chloride cys-loop receptor. A. Five subunits form an ion selective channel. B. Each subunit is made up of four transmembrane (TM) regions, and two extracellular N- and C-terminal domains.

1.3.2. The γ-aminobutyric acid (GABA) receptor

GABA is the primary inhibitory neurotransmitter in invertebrates, and the receptor has been well characterised at the genomic and protein levels (Asahi et al., 2015). The subunit composition is homomeric, with one gene encoding the subunit that assembles to form the GABAR. Highly conserved GABAR genes have been identified in several insect orders, with transcripts identified in *D. melanogaster* (RDL, GRD and LCCH3) which have been heterologously expressed and assessed functionally (Buckingham et al., 2005). The insect GABAR subunit-encoding the *RDL (Resistance to Dieldrin)* gene was first isolated from a naturally occurring strain of *D. melanogaster* and termed RDL (Ffrench-Constant et al., 1993). Their expression patterns suggest roles in fast synaptic transmission, as well as learning and visual and olfactory processing (Buckingham et al., 2005). Skeletal muscles of insect and acari have been shown to be considerable diverse depending on their function (Wicher et al., 2001). RDL subunits are distributed throughout the adult and embryonic nervous systems of *D. melanogaster*, however immunocytochemical studies have shown the protein products of the *RDL* gene are not present in the musculature of *D. melanogaster* (Harrison et al., 1996, Hosie et al., 1997). With regards to other insect and acari species, there is evidence of the presence and functional conductance of the GABAR in locust muscle and in the muscle fibres of the tick *Amblyomma hebraeum* (Duce et al., 1995).

The GABAR is the target for many insecticides, acaricides and anthelmintics of widely varied structures (Kaji et al., 2015), including the organochlorides, lindane and dieldrin (which were later banned because of their environmental persistence (Garcia-Reynaga et al., 2013)), cyclodienes, avermectins, phenylpyrazoles and isoxazolines. Data obtained using site-directed mutagenesis, radio-ligand binding and electrophysiology suggest that the binding sites of insecticides targeting GABARs, are within the channel pore, (Asahi et al., 2015). Recently, homology modelling of the GABAR has suggested there are four distinct but overlapping and coupled targets of pesticide action

with little or no cross-resistance between classes of insecticides interacting with the different sites (Casida and Durkin, 2015).

The GABAR has three binding sites for non-competitive antagonists (channel blockers) with pesticide action. These are contained in the pore formed by two transmembrane regions of the receptor. The avermectin site (AVE) is a target for allosteric modulators of the chloride channel in the macrocyclic lactone (ML) group. The primary targets for these compounds is the gluCl however they have been found to also act on the GABAR (Ozoe, 2013). The other two non-competitive antagonist sites overlap, with one site for the cyclodienes and phenylpyrazoles, and the other for newer compounds such as isoxazolines and meta-diamides (Casida and Durkin, 2015).

The recently discovered isoxazolines are broad spectrum pesticides with high efficacy against fleas and ticks, as well as a number of other insect targets. They are non-competitive GABAR antagonists and have a high selectivity for arthropod GABARs with little effect against mammalian GABARs (Casida and Durkin, 2015). They have a systemic mode of action and block the transmission of neural signals to paralyse and kill pests.

1.3.3. The glutamate chloride receptor

GluCl receptors are homomeric ionotropic chloride channels closely related to the GABAR. They are responsible for the mediation of inhibitory synaptic transmission of neuronal cells, and have a number of key roles in invertebrates including memory, learning and communication (Traynelis et al., 2010). Insect GluCls are present extrasynaptically on muscles (Gration et al., 1979). Their key role in invertebrates, and the lack of gluCls in mammals, make the receptor a good target for selective pesticidal compounds.

The arthropod gluCl is the major target for MLs, a group of pesticides which modulate the receptor. The effect of these compounds on the *C.*

elegans gluCl has been studied using two-electrode voltage clamp electrophysiology in *Xenopus laevis* oocytes expressing the receptor, showing the MLs successfully activated the channel keeping it open (Wolstenholme, 2012). Furthermore, the ML avermectin has been shown to have a pharmacological effect on locust skeletal muscle (Duce et al., 1995) which was attributed to the estimates of 100 channels per μM^2 in locust muscle (Dudel et al., 1989). Interestingly, within the phylum arthropoda, tick muscles have been found to be unresponsive to ivermectin suggesting the absence of the GluCl channel, whereas locusts have been found to have GluCl channels and are responsive to ivermectin (Duce et al., 1995). GluCls are also blocked by the phenylpyrazole fipronil, which has the GABAR as its main target (Narahashi et al., 2010).

1.3.4. The nicotinic acetylcholine receptor

The nAChR is a heteromeric, cation permeable, ligand-gated ion channel that plays a central role in the mediation of rapid excitatory neurotransmission in the insect nervous system. Most nAChRs are composed of α and non-α subunits, with the α subunits providing loops A, B and C, while the non-α subunits provide loops D, E and F. The neonicotinoid orthosteric binding site is localised at the α and non-α interface, however, another binding site at the α-α interface has been identified (Shimomura et al., 2006).

Acetylcholine is the endogenous agonist released from the presynaptic membrane, which interacts with the nAChR extracellular binding site, leading to a conformational change and the subsequent opening of the channel pore (Jeschke and Nauen, 2008). Pesticides targeting nAChRs are now the most important class of insecticides in the global market since the synthetic pyrethroids (Bass et al., 2015), and are used for control of insect pests on major crops as well as livestock and companion animal pests. Three distinct classes of insecticides and acaricides selectively target nAChRs and disrupt the normal functioning of the receptors (Crossthwaite et al., 2014) (Figure 1.5).

The first group, the nereistoxin analogues (e.g. cartap) bind at the non-competitive blocker site of insect nAChRs (Lee et al., 2003). The second are five- and six-membered ring systems (as well as non-cyclic structures) derived from the lead structure nithiazine (e.g. imidacloprid), which act as nAChR agonists and are collectively referred to as the neonicotinoids. Finally, the fermentation derived spinosyns are a family of macrocyclic lactones (e.g. spinosad) acting on nAChRs by exciting motor neurons and causing involuntary muscle contractions, leading to paralysis and death (Kirst, 2010).

Neonicotinoids have a wide target pest spectrum and multiple application methods (Longhurst et al., 2013). Of the three classes, they are by far the most commercially successful, with annual global sales in excess of $3.7 billion in 2014, accounting for over 25% of the global market (Crossthwaite et al., 2014). However in 2013, wide-spread controversy over their off-target effects has led to their ban as seed treatments on crops that flower in Europe (Gross, 2013). Further bans have followed in agriculture, but these have not extended to veterinary use of the compounds.

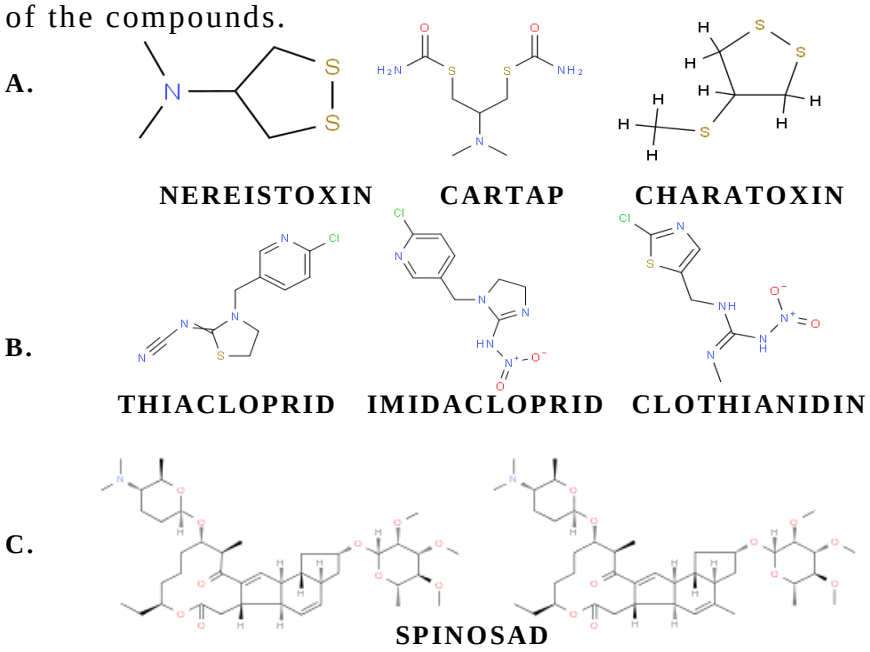


Figure 1.5. Compounds from the three main groups of pesticides targeting the nicotinic acetylcholine receptor. A. Nereistoxins. B. Neonicotinoids. C. Spinosyns.

1.4. Resistance to insecticides and acaricides

Pesticide resistance has become a major factor influencing insect control and pest management for more than half a century, with estimates suggesting that over 600 arthropod species (insect, ticks and mites) exhibit resistance to pesticides (Sparks and Nauen, 2015, Bass and Field, 2011). The widespread and intensive repeated use of these compounds has led to the rapid rise of resistance in many insect and acari species around the world. Since the introduction of synthetic organic insecticides such as DDT, cyclodienes and organophosphorus insecticides in the 1940s, important crop pests, parasites of livestock, common urban pests and disease vectors have developed resistance, some to increasingly challenging levels (Van Leeuwen et al., 2010, Sparks and Nauen, 2015).

1.4.1. Resistance mechanisms

The development of insecticide resistance is influenced by many factors, including biology and ecology, genetics and pest management strategies. It is driven by individual diversity in populations, i.e. genetic differences, producing phenotypic differences that give enhanced survival and are therefore passed on to the next generation (Perry et al., 2011, Dryden, 2014). There are many mechanisms of resistance including reduced penetration, where the cuticle has reduced uptake of xenobiotic compounds, and behavioural resistance where the arthropods detect danger and avoid the toxin (Casida and Durkin, 2013). However, by far the most important mechanisms are increased metabolism and target site changes (Van Leeuwen et al., 2010). Metabolic resistance results from the elevated activity of enzymes that break down toxic chemicals like pesticides. Target site resistance occurs when the site of binding of the pesticide becomes modified to reduce or prevent the effect of the chemical.

1.4.2. Metabolic resistance

Metabolic resistance is caused by the overexpression of several types of enzymes, mainly the cytochrome P450 monooxygenases (P450s), the carboxylesterases (CCEs) and the glutathione S-transferases (GSTs) (Li et al., 2007). The increased abundance of the enzymes can result from gene amplification, changes in gene expression by regulatory cis- and trans-elements or mutations that make the enzymes more efficient (Bass and Field, 2011). Increased metabolism means that xenobiotic compounds do not reach their target, resulting in a reduced susceptibility to the pesticide.

1.4.3. Target-site resistance

Target-site resistance can be characterised as changes to the target site protein which prevent or reduce binding of the pesticides. The target protein, normally within the nervous system, is altered by mutations in the coding sequence resulting in a changed conformation of the pesticide target site. Cys-loop receptors and transmembrane proteins are the most documented group detailing this mode of resistance, however it can also occur in nervous system enzymes (Casida and Durkin, 2013). There have been instances of widespread target-site resistance mutations present in many groups of arthropods. Some of the most prominent include knockdown resistance (*kdr*) to pyrethroids, caused by a leucine to phenylalanine substitution at position 1014 in the sodium channel, resistance to neonicotinoids, caused by an arginine to threonine substitution at position 81 in the nAChR and organochloride resistance resulting from an alanine to serine mutation at position 301 in the GABAR. The latter two are discussed further below.

1.4.4. Resistance resulting from changes in the arthropod GABAR

The GABAR is the target site for cyclodiene pesticides, and reports of resistance at this site to these compounds has been widely reported in a range of arthropod pests (Ffrench-Constant, 1994). This type of resistance was first characterised in *D. melanogaster* and found to result from a single point mutation in the M2 transmembrane region of the channel leading to the substitution of the highly conserved alanine by serine at position 301 and conferring 4000-fold resistance to the cyclodiene, dieldrin (Ffrench-Constant et al., 1993). Electrophysiology on channels expressed in cells showed that this amino acid substitution in the M2 pore domain leads to conformational change and decreases the binding affinity (Ffrench-Constant et al., 1993, Perry et al., 2011). Although dieldrin has been out of use for many years, the A301S substitution persists in many insects including mosquitoes, gnats and houseflies (Dermauw et al., 2012, Dryden, 2014).

A similar A301S substitution also occurs in the target-site region for phenylpyrazoles, and some low-level cross-resistance has been found for fipronil in houseflies that contain this change (Cole et al., 1995). Thus, although the cyclodienes and phenylpyrazoles have slightly different GABAR binding sites, they must be close enough for cross-resistance to occur (Comitani et al., 2014, Remnant et al., 2014). Remnant and colleagues (2014) used a candidate gene approach and explored natural variation at the *GABAR* locus in inbred strains of *D. melanogaster* to identify a gene duplication, and lines containing the substitutions A301S, A301G and T350M. A *D. simulans* strain with two changes, A301G and T350M, shows 20,000-fold resistance to fipronil (Le Goff et al., 2005) and an A301N change occurs in a fipronil-resistance strain of *Laodelphax striatellus* (Nakao et al., 2011).This suggest that the A residue in the GABAR is important for binding. This is supported by homology modelling based on the mutagenesis studies carried out by Remnant et al. (2014) The existence of these resistance mutations does not appear to affect the binding of isoxazolines, which

are proposed to have a separate binding site (Casida and Durkin, 2015, Ffrench-Constant et al., 2016).

For *C. felis*, monitoring of control efficacy and potential resistance problems is largely done by exposing the fleas to treated filter paper according to the World Health Organisation's (WHO) recommended methods, although other methods such as topical larval spot application have been shown to be more effective allowing individuals to be tested (Rust et al., 2015). For ticks, the WHO-recommended larval packet test (LPT) assay is used to measure susceptibility to acaricides. Resistance to DDT was first reported in *C. felis* in 1952, followed by reports of resistance to benzene hexachloride (BHC), dieldrin in 1956 and subsequently carbamates, pyrethroids and pyrethrins, and fipronil (Busvine, 1963, Dryden, 2014, Rust et al., 2015). Resistance is widespread and cross resistance to fipronil is suggested, as the target site for both compounds is predicted to be similar (Casida, 2015).

Resistance to BHC, cyclodienes and organophosphates has been found in *A. americanum*, *D. variabilis*, *R. sanguineus.* and *R. microplus*, with the latter having been studied at length, and there are an estimated 562 cases of resistance reported to 50 different compounds with a simple search of the Arthropod Pesticide Resistance Database (2018).

1.4.5. Resistance resulting from changes in the arthropod nicotinic acetylcholine receptor

Insecticides and acaricides targeting the nAChR are widely used and very effective, with resistance to neonicotinoids being relatively slow to develop and where it has occurred, being the result of metabolic detoxification enzyme, rather than target site changes (Crossthwaite et al., 2014). Resistance to spinosyns, particularly spinosad, has been documented in several insect species both in the lab and field (Sparks et al., 2012).

In the cases where underlying mechanisms have been studied, two-thirds are associated with target-site resistance. Studies in spinosad-selected *D. melanogaster* identified a mechanism of target-site resistance, in Loop D of the α6 nAChR subunit (Perry et al., 2007). Likewise, spinosad resistance in a strain of *Plutella xylostella* was unaffected by synergists, showed no cross-resistance to any other insecticides, and was found to be a recessive, autosomal trait suggesting a target site-based mechanism (Zhao et al., 2002). This was recently confirmed when changes to the *P. xylostella* nAChRα6 were found to be associated with spinosad resistance (Baxter et al., 2010). Studies with field strains of *Spodoptera exigua* (beet armyworm) from the USA (Arizona) and Thailand demonstrated reduced susceptibility to spinosad compared to a the control susceptible strain (Moulton et al., 2000).

In general, the underlying mechanisms associated with emerging spinosyn resistance have yet to be determined, but Loop D of the nAChR is increasingly implicated, involving either a nAChR α6 knockout (causing a missense mutation) or a single point mutation (G257E) found in *Thrips palmi* (melon thrips), *Tuta absoluta* (tomato leafminer) and *Frankliniella occidentalis* (western flower thrips) (Puinean et al., 2013b, Silva et al., 2016, Bao et al., 2014).

Target site resistance to the neonicotinoid imidacloprid has been confirmed in a small number of hemipteran species, such as *Nilaparvata lugens* (brown planthopper), *Myzus persicae* (peach-potato aphid) and *Aphis gossypii* (cotton-melon aphid) (Bass et al., 2015). A field resistant strain of *M. persicae* collected in 2009 demonstrated high levels of resistance to neonicotinoids (Bass et al., 2014), and although metabolic resistance was implicated, a point mutation in the loop D region of the β1 subunit was identified. The mutation causes an arginine to threonine substitution (R81T) in the binding site of neonicotinoids that is a primary determinant of the selective toxicity of neonicotinoids to invertebrates (Bass et al., 2015). The R81T mutation has also been implicated in target-site resistance to neonicotinoids in *A. gossypii* samples collected from six sites in South Korea in 2012 that gave

maximum resistance of 1500-fold to imidacloprid, 2600-fold to acetamiprid and 14,000-fold to clothianidin (Hirata et al., 2017).

N. lugens is the most serious pest of rice crops, and imidacloprid was first used against this pest in the 1990s. Imidacloprid originally had excellent efficacy and was largely unaffected by resistance, however after decades of use, resistance is now widespread with reports of 600-800 fold resistance from across Asia (Bass et al., 2015) and reduced susceptibility to imidacloprid from strains originating from different countries (Garrood et al., 2015). The first mechanism of resistance reported was a tyrosine to serine substitution at position 151 of the nAChR α1 and α3 subunit conferring 250-fold resistance however this mutation has yet to be identified in any field populations (Bao et al., 2014, Liu et al., 2005, Bass et al., 2015).

1.5. Aims and objectives

The monitoring of pesticide use, the detection of resistance and the elucidation of the molecular basis of the incidences of resistance are all important aspects for the success of integrated pest management in arthropod pests of animals. In this thesis, data relevant to the control of ticks and fleas were obtained and the main objectives were:

- Chapter 2: to monitor and assess the effect of pesticides on fleas and ticks using bioassays with a range of compounds

- Chapter 3: to assess the effects of known and novel mutations in the *C. felis* GABAR sequence on the functioning of the channel using two-electrode voltage clamp electrophysiology on channels expressed in *Xenopus laevis* oocytes

- Chapter 4: to assess the effects of known and novel mutations in the *C. felis* GABAR sequence by introducing the mutations into *D. melanogaster* and assessing the effect on the phenotype of the of the flies

- Chapter 5: to assess the effects of known and novel mutations in the *R. microplus* nAChR sequence on the functioning of the receptor using two-electrode voltage clamp electrophysiology on channels expressed *Xenopus laevis* oocytes

2. Methods

2.1. Source material

2.1.1. Insect and acari

Artificially reared *C. felis* (Georgi strain), *C. felis* reared on cat (Kiel strain) and *R. microplus* reared on cattle (Parkhurst strain) were provided by Bayer Animal Health Breeding Lab (Monheim, Germany). *I. ricinus* and *R. sanguineous* were obtained by Bayer Animal Health from Insect Services, Berlin and EL LABS, California respectively. The HH (Hemel Hempstead) *C. felis* samples were provided by B. Troczka, Rothamsted Research, UK.

For RNA analyses, samples were snap-frozen in liquid nitrogen and shipped on dry ice to Rothamsted Research or sent immersed in QIAGEN RNALater Stabilisation reagent. For DNA analyses, samples were sent on ice.

2.1.2. Media and reagents

Lysogeny Broth (LB) was prepared from 5 g tryptone, 2.5 g yeast extract and 2.5 g NaCl made up to 500 mL in the equivalent volume Duran bottle and autoclaved. For plates, agar was added (7.5 g Bacto-agar per 500 mL) and the solution was re-autoclaved before pouring into the plates. For Ampicillin and Kanamycin plates, 250 µL of 50 mg/mL stock antibiotic was added to the LB agar when it was at a temperature of 60°C.

2.1.3. Genomic DNA extraction

DNA was extracted from *C. felis* adults (stored at -20°C or dried after storage in ethanol) using the QIAGEN DNeasy Blood and Tissue kit according to the manufacturers protocol. Briefly, individuals or pooled samples (up to 25 mg) were placed in 1.5 mL Eppendorf tubes and 180

µL of Lysis Buffer ATL was added and the sample was homogenised with a sterile pestle. 20 µL of proteinase K was added and the sample vortexed and incubated at 56 °C until the cells were completely lysed (approximately 1 hour but up to overnight with no adverse effect). 4 µL of RNase A was added, mixed and incubated for 2 minutes to remove any RNA. 200 µL each of Buffer AL and 100% ethanol were added and the sample was vortexed until homogeneous. The solution was then pipetted onto the DNeasy mini spin column over a collection tube and centrifuged at 8000 x g for 1 minute to bind the DNA to the membrane. The membrane with bound DNA was washed with 500 µL of Buffer AW1, which was added to the tube and then centrifuged for 1 minute. The flow-through was discarded and 500 µL of Buffer AW2 was applied to the spin column and centrifuged at 16,000 x g for 3 minutes to remove the wash buffer and dry the column avoiding any ethanol contamination. The column was then placed in a fresh 1.5 mL Eppendorf and 20- 100 µL Buffer AE (dependent on initial tissue volume) added, incubated for 1 minute to elute the DNA and then centrifuged at 8000 x g for 1 minute. For individual/small insects in small volumes of buffer, the elution step was repeated and the samples were pooled.

2.1.4. RNA extraction

Total RNA was extracted from *C. felis* adults stored at -80°C using Bioline Isolate RNA Minikit according to the manufacturers protocol. Individuals were placed in 1.5 mL Eppendorf tubes and flash frozen in liquid nitrogen then ground to a fine powder with a chilled sterile pestle. 350 µL of lysis buffer was added and further homogenised to ensure cell lysis. The homogenate was then centrifuged at 16,000 x g for 1 minute to pellet insect debris. The clear lysate was then filtered through an isolate II filter over a fresh 1.5 mL Eppendorf and centrifuged for 1 minute. The filter was discarded and the filtrate combined with an equal volume of 70% ethanol (approximately 250 µL) and vortexed. The RNA was then bound to an RNA Mini Column over a 2 mL collection tube by applying the mixture to the membrane and centrifuging at 11,000 x g

for 1 minute. The membrane with bound RNA was then desalted using 350 µL buffer and centrifuging at 11,000 g for 1 minute. A solution of DNase I and Reaction Buffer for DNase I (1 in 10) was then applied to the centre of the membrane and incubated at room temperature for 15 minutes to digest any remaining genomic DNA. The membrane was then washed once with Wash Buffer 1 and twice with Wash Buffer 2. The column was then centrifuged for a further 2 minutes at 11,000 x g to remove any residual wash solution and dry the membrane. The RNA was eluted in 30 µL of RNase-free water, after incubation for 5 minutes at room temperature (the 1 minute incubation recommended by the protocol resulted in a lower yield). The quantity of the RNA was determined using a ThermoScientific Nanodrop spectrophotometer. Extracted RNA was stored at -80°C.

If required, the quality of the RNA was determined by denaturing a 1 in 5 RNA dilution in a 2X formamide RNA loading buffer at 65°C for 5 minutes and running on a 1.5% agarose electrophoresis gel.

2.1.5. cDNA synthesis

Total RNA was used for cDNA synthesis using the ThermoScientific SuperScript III First-strand cDNA synthesis kit. 0.5-5 µg of template RNA (typically 3 µg) was mixed with 1 µL of oligo$(dT)_{20}$, 1 µL of 10 mM dNTP mix (10 mM each of dATP, dGTP, dCTP, dTTP at neutral pH) and nuclease-free water up to 13 µL in a 1.5 mL Eppendorf tube. The mixture was incubated at 65°C for 5 minutes and then placed on ice for 1 minute. 4 µL of 5X First-Strand buffer, 1 µL of 0.1 M DTT, 1 µL of RNaseOUT Recombinant RNase Inhibitor and 1 µL of SuperScript III were added and mixed by gently pipetting up and down. The final 20 µL mixture was incubated at 50°C for 1 hour. The reaction was inactivated by heating to 70°C for 15 minutes. cDNA was stored at -20°C.

2.2. Polymerase chain reaction (PCR)

2.2.1. Primer Design

Primers were designed to have the correct melting temperature, molecular weight, % GC content and restriction sites. OligoCalc was used to ensure optimal parameters (Kibbe, 2007). They were usually 20-30 nucleotides in length with a GC content of 40-60% and a melting temperature (T_m) of 50-60 °C. All were synthesised by Sigma Aldrich.

2.2.2. Standard PCR

Standard PCR reactions were done in 0.5 mL thin-walled PCR tubes using 12.5 µL of ThermoScientific 2X DreamTaq with Taq polymerase, 1 µL of dNTP mix, 1 µL of 10 µM forward primer, 1 µL of 10 µM reverse primer, 1-2 µL of DNA and sterile water up to 25 µL. The cycling conditions varied depending on the primers and the length of the amplicon. Initial denaturation was carried out at 95°C for 1-2 minutes. This was followed by 25-35 cycles of denaturation (95°C for 30 seconds), annealing (55-65°C for 30 seconds) and extension (72°C for 1 minute/Kb). The final elongation was carried out at 72°C for 5 minutes.

2.2.3. High-fidelity PCR

High-fidelity PCR with BioLabs Phusion DNA Polymerase was used for long amplicons or when very accurate amplification of the DNA sequence was needed. The reactions were done in 0.5 mL thin-walled PCR tubes and contained 4 µL of 5X Phusion Buffer, 0.4 µL of dNTP mix, 1 µL of 10 µM forward primer, 1 µL of 10 µM reverse primer, up to 250 ng genomic template DNA or 10 ng plasmid DNA, 0.2 µL Phusion DNA Polymerase and sterile water up to 20 µL. Initial denaturation was at 98°C for 30 seconds followed by 30 cycles of denaturation (98°C for 10 seconds), annealing (45-72°C for 30 seconds) and extension (72°C for 30 seconds/Kb) with a final elongation at 72°C for 10 minutes.

2.2.4. *Taq*Man PCR of *C. felis*

A ThermoScientific real time PCR *Taq*Man assay designed and set up by Martin Williamson (Rothamsted Research) was used for high throughput identification of the presence of the A301S mutation in *C. felis*. Insects were kept in ethanol until use and blotted onto tissue paper before sucrose DNA extraction. To prepare DNA for the *Taq*Man assay, individual fleas were placed in an Eppendorf tube, snap-frozen in liquid nitrogen and homogenised with a sterile pestle. 40 µL of a 300 mM sucrose solution was added to each tube and the solution transferred to individual wells of a 96-well PCR plate. The plate was covered with ThermoScientific Adhesive PCR Plate seal and placed in a gently boiling shallow water bath (~100 °C) for 10 minutes. The plate was then centrifuged at 3500 rpm, room temperature for 2 minutes followed by 5 minutes on ice. Taking care, the supernatant was transferred to a fresh plate.

The probes and primers for the probe/primer mix for detection of the A301S mutation were designed by M. S. Williamson (Table 2.1). The VIC fluorescent dye labelled probes detected the Wild Type susceptible amino acid (alanine for A301S). The FAM fluorescent dye labelled probes detected the mutated serine amino acid.

Table 2.1. Components of the *Taq*Man assay Probe/Primer mix used for the detection of the A301S and M354I mutation in the *C. felis* GABAR.

Primer/Probe	Sequence
Cf_ A301S_VIC probe	TCGAGTCGCTCTCG
Cf_ A301S_FAM probe	CTCGAGTCTCTCTCG
Cf_ A301S_F primer	GTTTTGGCTGAATCGTAATGCTACA
Cf_ A301S_R primer	CATGGTCAACACAGTGGTCACT
	Primers designed by M. S. Williamson

13.5 µL of a *Taq*man mastermix consisting of 0.375 µL of the probe/primer mix (containing 800 nM of each primer and 200 nM of

each probe), 7.5 µL of Sensifast and 5.625 µL of sterile water was placed into each well of a ThermoScientific 96-well Nunc PCR plate. From each well of the DNA extraction, 1.5 µL of supernatant was transferred into the corresponding well on the Nunc plate. An allelic discrimination analysis was done on the plate using the ABI 7900 Sequence Detection System.

2.2.5. PCR purification

PCR products were purified from the PCR reaction mixes by adding 1 volume of 4M NH_4OAc (20 µL) and 100 µL ethanol (both at room temperature) to the 20 µL PCR reaction. The mixture was vortexed and centrifuged at 16,000 x g for 20 minutes at room temperature (21°C). The supernatant was removed and the resulting pellet washed with 100 µL of chilled 75% ethanol (from -20°C freezer). The ethanol was removed and the sample spun in a SpeedVac to remove and dry any residual ethanol. The pellet was then dissolved in 20 µL sterile water and the concentration measured using a ThermoScientific Nanodrop spectrophotometer.

Alternatively, a Qiagen MiniElute PCR purification kit was used by adding five volumes of Buffer PB, mixing and applying to the QIAquick spin column and centrifuged for 1 minute at 10,000 x g. The DNA bound to the column was then washed with 750 µL of Buffer PE and centrifuged. A further 1 minute in the centrifuge ensured the removal of wash buffer. To elute the DNA, 30 µL of Buffer EB or nuclease-free water was added directly to the centre of the membrane and incubated for 1 minute. The column was then centrifuged to elute the DNA and the resulting sample concentration measured using a ThermoScientific Nanodrop spectrophotometer.

2.2.6. Agarose gel electrophoresis

The size and quality of the PCR products were assessed by agarose gel electrophoresis. The gels were made by diluting ThermoScientific

agarose in 1X TAE (Tris-Acetate-EDTA) buffer. 50 x TAE buffer was made with 121 g Tris base, 28.5 mL acetic acid and 50 mL 0.5 M EDTA made up to 500 mL with sterile water and adjusted to pH 7.4 with acetic acid. 1X TAE buffer was made with 20 mL of the 50 x TAE buffer stock and diluted in 1 L triple distilled sterile water. The percentage agarose was dependent of the size of PCR product being visualised- typically <1% for larger fragments (>3Kb) and >1% for smaller fragments (<1Kb). The mixture was heated to an elevated temperature to dissolve the agarose and allowed to cool slightly before the addition of ethidium bromide to a final concentration of 0.4 µg/mL (2.5 µL in 50 mL gels and 5 µL in 100 mL gels). The gel was set using combs to introduce wells for the nucleic acid samples. Samples were mixed with bromophenol blue dye (2 µL of 6X loading dye, 2 µL PCR product and 8 µL sterile water) and run alongside ThermoScientific GeneRuler 1 Kb DNA ladder (1 µL of ladder with 1 µL of 6X loading dye and 4 µL of sterile water). Standard voltage settings were between 70-100 mV, the current was set at 100 mA and the gel run time was approximately 1 hour or until sufficient band separation. The resulting bands were visualised on a Gene Genius Bio-Imaging System using the Syngene UV transilluminator.

2.2.7. Extraction of PCR products form agarose gels

Gel extraction and purification of PCR products was done using the Qiagen QIAquick Gel Extraction Kit. The gel was placed on a UV light source and the DNA fragments were excised from the gel using a clean, sharp scalpel, with a minimum amount of gel. The gel fragment was then weighed in a 1.5 mL Eppendorf tube and 3 volumes of preheated Buffer QG were added (where 1 mg equates to 1 mL) and incubated at 50 °C for 10 minutes, with vortexing every 2 minutes to help the gel to dissolve fully. 1 volume isopropanol (corresponding to the weight of the original gel slice) was added. The sample was pipetted onto the QIAquick spin column and centrifuged at 16,000 x g for 1 minute. The flow-through was discarded and a further 500 µL of preheated buffer

QG was added to remove any remaining gel. To wash the sample, 750 µL of Buffer PE was applied to the membrane and centrifuged for 1 minute. The sample was then centrifuged for a further 1 minute to remove any remaining wash buffer. 30-50 µL of Buffer EB or nuclease-free water was added to the column and incubated for 5 minutes before centrifugation for 1 minute to elute the DNA. The concentration of the purified DNA was measured using a spectrophotometer.

2.3. Molecular cloning and transformation

Molecular cloning allows the replication of recombinant DNA molecules by transformation into a host organism. The DNA fragment of interest is inserted into a vector or plasmid which contains all the elements necessary for replication of the DNA, which can then be analysed.

2.3.1. PCR cloning

DNA fragments, amplified by PCR and gel purified, were ligated into plasmids, chosen according to the subsequent use of the plasmid, the size of the insert (Kb) and presence of restriction sites. The vector and PCR fragments were linearised and a ligated plasmid created by digestion with an appropriate restriction enzyme using the ThermoScientific FastDigest system. For plasmid DNA, up to 1 µg was combined with 1 µL of FastDigest enzyme, 2 µL of FastDigest Green Buffer, made up to 20 µL with sterile water and incubated at 37°C for 30 minutes. For PCR products, up to 0.2 µg of DNA was combined with 1 µL of FastDigest enzyme, 2 µL of FastDigest Green Buffer, made up to 30 µL with sterile water and incubated at 37°C for 5 minutes. If required, the enzyme was inactivated by heating for 5 minutes at 80°C. The linearisation was checked by running on an agarose gel alongside untreated samples.

The samples were briefly centrifuged and a ligation reaction set up containing vector and insert at a 3:1 molar ratio combined with 1 µL T4 DNA ligase, 1 µL T4 ligase Buffer and made up to 20 µL with sterile water. The reaction was incubated at 4°C overnight and ligation confirmed by doing a standard PCR.

2.3.2. Bacterial transformation

The plasmids containing inserts were transformed into bacterial hosts using either ThermoScientific One Shot TOP10 Chemically Competent *E. coli* or Agilent Technologies XL10-Gold Ultracompetent Cells for cloning of larger plasmids.

In preparation for the transformation, Super Optimal Broth with Catabolite Repression (S.O.C) was warmed to 37°C. S.O.C was prepared by adding 20 g tryptone, 5 g yeast extract, 0.6 g NaCl and 250 mL KCl to 950 mL triple distilled sterile water and adjusted to pH7 with 5 M NaOH. The volume was made up to 1 L and autoclaved. Once cooled, 5 mL of 2 M $MgCl_2$ and 20 mL filter sterilised 20% glucose solution was added. The S.O.C was aliquoted and kept at -20°C.

One 50 µL vial of TOP10 Ultracompetent cells was thawed on ice and 2 µL of the ligation reaction was added, mixed gently by inverting and incubated on ice for 30 minutes. The cells were then heat shocked in a 42°C water bath for 30 seconds and placed directly on ice for 2 minutes. 250 µL of preheated S.O.C medium was added and the tube incubated horizontally at 37°C for 1 hour Agar plates containing either ampicillin or kanamycin (depending on the selector in the plasmid) were prewarmed and two plates per transformant were spread with 20 µL and 50 µL of the cell mix, to ensure well-spaced colonies. The plates were incubated at 30°C overnight.

For larger plasmids, XL10-Gold Ultracompetent Cells were used. 1 round-bottomed 14 mL falcon tube per transformation was pre-chilled on ice. The XL10-Gold cells were thawed on ice, and 25 µL aliquoted into each falcon tube. 1 µL of β-Mercaptoethanol was added to each

tube and swirled gently. The cells were incubated for 10 minutes, mixing gently every 2 minutes. 2 µL of ligation mixture was added to the tube and incubated on ice for a further 30 minutes. The tubes were then heat shocked in a 42°C water bath for 30 seconds and placed directly on ice for 2 minutes. 250 µL of preheated S.O.C medium was added and incubated at 37°C for 1 hour with shaking at 225-250 rpm. Two plates were spread (as for the TOP10 transformation) and incubated at 30°C overnight.

2.3.3. Colony PCR

A colony PCR was done on the colonies if sufficient growth had occurred overnight. Using autoclaved 2 µL pipette tips, cells from single colonies were picked from the plate and streaked onto a new plate, which was incubated at 37°C overnight and stored at -4°C. The tip was then placed into a PCR tube containing a PCR mastermix with appropriate primers. Typically, 4-8 colonies were picked for each transformation. The colony PCR cycle conditions were an initial denaturation (95°C for 2 minutes), then 35 cycles of denaturation (94°C for 20 seconds), annealing (60°C for 30 seconds) and extension (72°C for 1 minute/Kb) with a final 72°C for 10 minutes. The PCR products were analysed alongside untransformed plasmid DNA on agarose gels.

2.3.4. Plasmid purification

Colonies identified as successful transformants were propagated in liquid culture prior to being purified. Cells were transferred with a 2 µL pipette tip, by placing the tip in a 14 mL falcon tube containing 4 mL LB broth and 2 µL 50 mg/mL antibiotic. The tubes were then incubated overnight (or >18 hours) at 37°C in a shaking incubator at 225-250 rpm.

To isolate plasmids of high-purity, the QIAGEN QIAprep Spin Miniprep Kit was used. After incubation, the bacterial overnight culture was pelleted by centrifuging in the falcon tube at 4000 x g for 20 minutes at

10°C. The supernatant was discarded and the pellet resuspended in 250 µL Resuspension Buffer P1, vortexed thoroughly until the pellet was dissolved and transferred to a 1.5 mL Eppendorf tube. Cell lysis was completed using 250 µL Lysis Buffer P2 and inverting the tube 4-6 times until the solution became clear and homogenous. The lysis reaction was for 5 minutes and was terminated by the addition of 350 µL of Neutralisation Buffer N3, inverting the tube 4-6 times. The solution was then centrifuged at 16,000 x g for 10 minutes and the supernatant decanted onto a QIAprep spin column and centrifuged for 1 minute to bind the DNA. The column was then washed with 500 µL of Buffer PB and centrifuging for 1 minute, and an additional wash with 750 µL of Buffer PE. The column was then centrifuged for a further 1 minute at 11,000 x g to remove any residual wash solution and dry the membrane. To elute the plasmid DNA, the column was placed in a 1.5 mL Eppendorf tube and 50 µL EB Buffer was applied to the membrane and incubated for 1 minute at room temperature and then centrifuged for 1 minute to elute DNA. The quantity of the plasmid DNA was determined using a spectrophotometer and the plasmid was stored at -20°C.

2.4. Site-directed mutagenesis

For the introduction of single and multiple mutations within a DNA sequence, Agilent Site-Directed Mutagenesis QuikChange kits were used. Primers were designed manually according to the Agilent guidelines and were 25-45 bases in length, with the base to be changed in the middle and terminating in C or G. OligoCalc was used to avoid self-complementary sequences, to ensure GC content was at least 40% and the Tm was as close to 80˚C as possible whilst staying within the above parameters.

PCR reactions were done in thin-walled PCR tubes with 5 µL of 10X Buffer, 100 ng double-stranded DNA template, 1.25 µL each of forward and reverse primer (10 µM), 1 µL of dNTP mix made up to 50 µL with

sterile water. The mixture was then briefly vortexed and centrifuged before the addition of 1 µL *PfuUltra* DNA polymerase. The initial denaturation step was 95°C for 1 minute, followed by 18 cycles of denaturation (95°C for 50 seconds), annealing (60°C for 50 seconds) and extension (68°C for 1 minute/Kb) with for a final extension of 68°C for 7 minutes. For each reaction, the average T_m of the two primers was typically between 65-75°C. Following the PCR reaction, the plasmids were digested with *Dpn1* using 1 µL/reaction at 37°C for 1 hour. This removed any parental, non-mutated, supercoiled dsDNA.

Transformation of the plasmid DNAs with the mutation were carried out in XL10-Gold Ultracompetent cells following methods given in 2.3.2.

2.5. Sequencing and analysis

All sequencing was outsourced to Eurofins Genomics TubeSeq sequencing service. Samples were submitted premixed with the appropriate primer in a 1.5 mL safelock Eppendorf tube. For PCR products up to 1000 bp, 15 µL of 5 ng/ µL was premixed with 2 µL of 10 µM primer. For PCR products over 1000 bp, 15 µL of 10 ng/ µL of was premixed with 2 µL of 10 µM primer. Analyses of the sequences was done using Geneious, the bioinformatics software platform supplied by Biomatters Limited.

2.6. Two-Electrode voltage clamp electrophysiology

The structure/function of ligand-gated ion channels was studied by expressing the cRNAs into functional proteins in *X. laevis* oocytes and doing electrophysiology.

2.6.1. *In vitro* cRNA synthesis

DNA fragments encoding the required cRNAs for electrophysiological experiments were cloned into pGEM vectors purchased from Promega, which have high efficiency ligation, contain several restriction sites and

have a SP6/T3/T7 RNA polymerase transcription site for cRNA production. After cloning the insert and the insertion site were sequenced to check that the orientation of insertion was correct and that it was inserted downstream of the required promotor (SP6, T7 or the T3). Plasmid DNA with the correct inserts were then linearised with the appropriate restriction enzyme using the FastDigest system for at least 30 minutes at -20°C. The reactions were terminated by the addition of 1 µL of (0.5 M) EDTA and 2 µL of (3 M) NaOAc and the DNA was pelleted by centrifugation at 13,000 x g for 20 minutes at 4°C, washed with 70% ethanol, air dried and resuspended in 6 µL of nuclease-free water. *In vitro* transcription was designed to give 5′-capped cRNAs using the Ambion mMESSAGE mMACHINE SP6/T7/T3 transcription kit. Reactions contained 10 µL 2X NTP/CAP (a buffered solution containing 15 mM ATP, CTP, GTP, UTP and 5' RNA cap analog), 2 µL 10X Reaction buffer, 1 µg dsDNA template, 2 µL enzyme mix and made up to a final volume of 20 µL with sterile water. The reactions were incubated for 2 hours at 37 °C and then 1 µL of TURBO DNase was added and the reaction incubated at 37 °C for 15 minutes to remove template DNA. cRNA transcripts were recovered and purified by phenol/chloroform extraction. 115 µL sterile water and 15 µL ammonium acetate were added to the samples and mixed thoroughly. Then 75 µL each of phenol and chloroform were added and mixed well and left at room temperature, before centrifugation at 16,000 x g for 5 minutes. The tubes were then left for 5 minutes to allow the two distinct aqueous and organic phases to separate. The aqueous phase containing the cRNA, was pipetted off avoiding disruption of the organic phase containing the phenol, chloroform and any proteins/lipids. An isopropanol precipitation was done by adding the aqueous phase to an equal volume of isopropanol (approximately 150 µL) and leaving on ice for 30 minutes. The sample was centrifuged at 16,000 x g for 20 minutes at 4°C and the supernatant removed and the resulting cRNA dried and resuspended in 10-20 µL of sterile water depending on the size of the pellet.

A 1 µL aliquot of cRNA was diluted in 4 µL sterile water and 1 µL used to determine the sample concentration using a spectrophotometer. The quality of the cRNA was determined by adding 3 µL of the cRNA to 6 µL of ThermoScientific 2X RNA gel loading buffer and 3 µL of sterile water, denaturing by heating to 70°C for 10 minutes, transferring onto ice for 2 minutes and then running on a 1.5% agarose gel at 80V for 1 hour (2.2.6). The remaining cRNA was dissolved in nuclease-free water at a final concentration of 100-500 ng/µL and stored at −80°C. The frozen stocks were never subjected to more than 5 freeze-thaw cycles, to ensure that the cRNA was not degraded.

2.6.2. *X. laevis* oocyte preparation

Calcium-free Barth's and calcium containing Barth's solutions for use in preparing oocytes were made according to Table 2.2 and filtered with ThermoScientific Nalgene Rapid-Flow Sterile Disposable Filter Units using a vacuum system.

Table 2.2. Formulation of Ca^{2+} free Barth's and Ca^{2+} containing Barth's solution.

Solution	**Ca^{2+} free Barth's**	**Ca^{2+} containing Barth's**
10X NaCl (880 mM)	25 mL	25 mL
100X Tris (1.5 M)	2.5 mL	2.5 mL
100X $NaHCO_3$ (0.24 M)	2.5 mL	2.5 mL
100X $MgCl_2$ x $6H_20$	2.5 mL	2.5 mL
100X KCl (0.1M)	2.5 mL	2.5 mL
100X $CaCl_2$ x $2H_20$ (7.7 mM)	-	2.5 mL
Penicillin + Streptomycin	-	2.5 mL
Kanamycin (50 mg/mL)	-	20 µL
Tetracycline (50 mg/mL	-	250 µL
Distilled H_20	to 250 mL	to 250 mL
	pH 7.5 with HCl (5 M)	
	Filter and store at 4°C.	

Ovarian tissue from *X. laevis* was purchased from the University of Portsmouth European Xenopus Resource Centre and delivered in modified Barth's solution on ice. The oocytes were separated from the ovarian lobes in clumps of 10-20 oocytes and the connective tissue was softened and dissolved using 'collagenisation'. The oocytes were placed in a 30 Mm petri dish containing collagenase (2 mg/mL from *Clostridium histolyticum* supplied by Sigma Aldrich) dissolved in 5 mL of Ca^{2+} free Barth's solution and incubated for approximately 30 minutes at room temperature with slow shaking on a table top orbital shaker. Oocyte were drawn-up into a wide-bore plastic pipette (trimmed Pasteur pipette) to facilitate collagenisation. Once collagenised, the oocytes were washed four times Ca^{2+} free Barth's solution, with 5 -10 minutes slow shaking after each wash. This ensured removal of any residual collagenase and helped to prevent degradation of the oocytes. Healthy stage IV-V oocytes were selected based on the presence of clear animal/vegetal pole divisions and being without spots or markings on the surface. The selected cells were manually defolliculated with forceps to facilitate injection and because the electrically coupled cells in the follicular layer can interfere with TEVC recordings.

cRNA was injected into the oocytes using a Drummond Scientific Nanoject II with the specific concentration and volume having been determined in optimisation experiments. Injection tips were 'pulled' into shape on a Stoelting App-1 52500 All Purpose Puller using Alpha Laboratories 3.5" borosilicate glass capillaries. The ends of the pulled capillaries were trimmed to form a 10 µM opening and filled with mineral oil using the Nanoinject fill mechanism for aspiration. Transcript cRNA diluted to the appropriate concentration was then placed on sterile Parafilm and gradually drawn into the injection needle avoiding any air bubbles, this was done quickly to avoid degradation of cRNA. Prepared oocytes were submerged in a ridged bath containing Ca^{2+} free Barth's solution. The Nanoinject was set at a 45-degree angle to the cells and the tip of the needle inserted on the vegetal hemisphere close to the barrier between the two halves which facilitates successful

cytoplasmic injection (Au et al., 2010). Injected oocytes were stored in Ca2+ containing Barth's in a VWR 24-Well Flat-Bottomed TC-treated plate with no more than 3 cells per well. The plate was placed in a Ztopia Reptile Egg Incubator for the optimised incubation time at 17 °C.

2.6.3. TEVC electrophysiology system

The electrophysiology experiments used a gravity fed conventional TEVC rig (Figure 2.1). Glass voltage and current microelectrodes were pulled from Harvard Apparatus 75 mM borosilicate capillaries with filament using the Stoelting App-1 52500 All Purpose Puller to a resistance of 4 MΩ, required for sufficient current to pass and fast clamping of the oocyte. Capillaries were filled one third with 1 M KCl and connected to the oocyte amplifier with a Teflon-coated silver wire with chlorided tip immersed in the KCl. The wire was chlorided by immersing the stripped silver wire into bleach (containing chlorine) until a light grey colour formed on the silver-silver chloride electrode. These electrodes were connected to Märzhäuser Wetzlar manipulators. A 3% agar bridge in I M KCl was made by heating the agar and allowing it to set around another chlorided electrode in the agar bridge well contained in the oocyte chamber. This connected ground electrodes to the bath.

Ligand solutions to be tested were dissolved in Ringer's solution (100 mL HEPES (0.2 M), 92 mL NaCl (2.5 M), 3.6 mL $CaCl^2$ (1 M) and 1.6 mL KCl (3 M)) to the concentrations indicated in the experimental chapters, and all solutions were added to Becton Dickinson 50 mL syringes. The Warner Instruments Eight Channel Perfusion Valve Control System (VC-8) using CR-TEC pinch valves (with C-Flex tubing) for seamless application of individual and multiple solutions was used. An adjustable suction tube with a 2 L collection flask was attached to a vacuum and used to maintain the flow and to remove solutions from the bath at a rate of 10 mL/minute.

Individual oocytes were placed in the narrow-slotted bath in the Warner Instruments Slotted Bath Oocyte Recording Chamber (RC-3Z) containing Ringer's solution using a Pasteur pipette. The system uses LED lighting and an Olympus 10X stereo microscope (SZ-STB1) to allow viewing and injection of the oocytes. The cells were perfused or bathed continuously with Ringer's solution to avoid drying out.

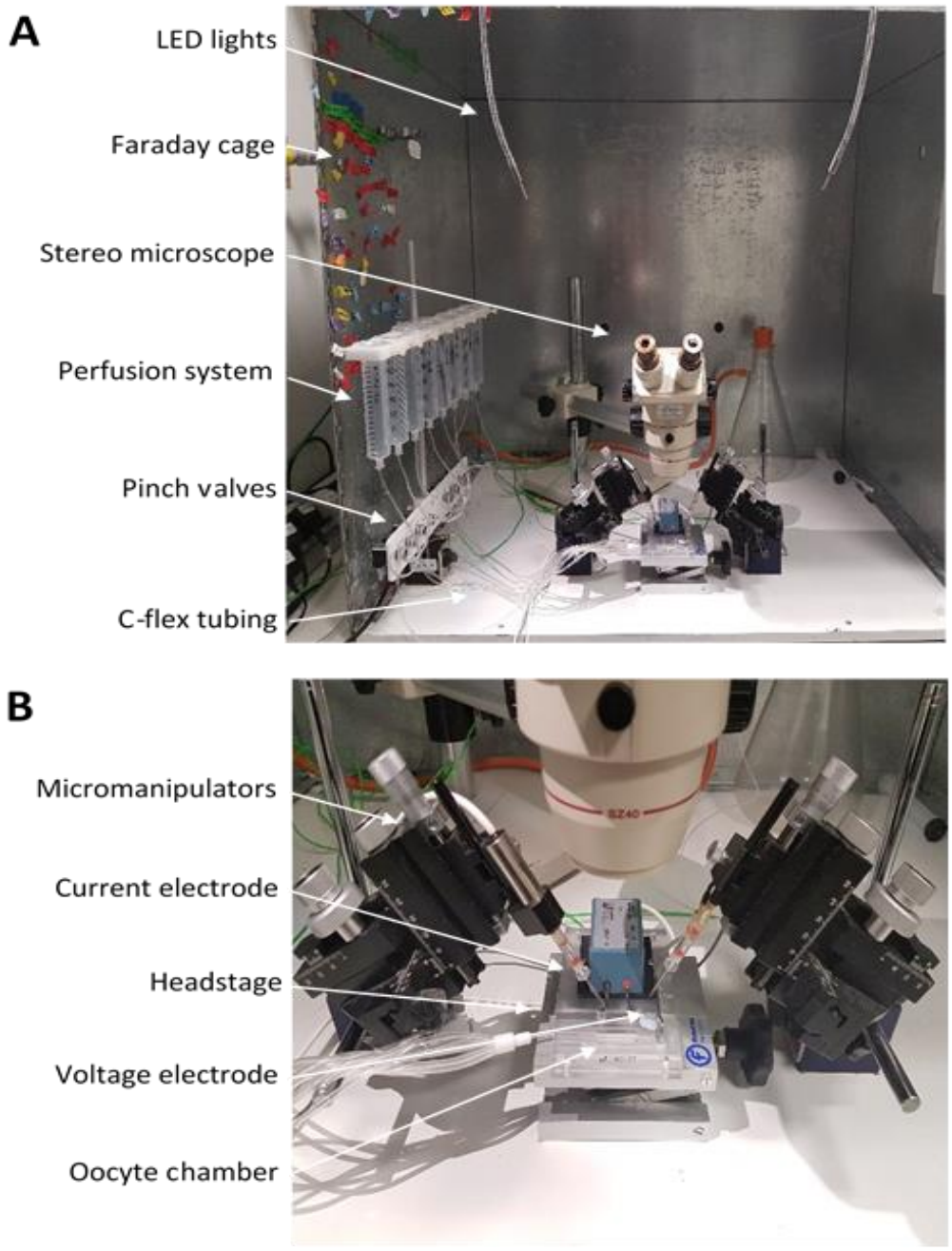


Figure 2.1. A. TEVC electrophysiology rig contained in a Faraday cage with gravity driven perfusion system using pinch valves and c-flex tubing for even-flowing application of solutions and seamless transitions between perfusates. B. Oocyte workstation. Micromanipulators with current and voltage electrodes positioned above a slotted oocyte chamber (with amplifier) on an adjustable headstage.

2.6.4. TEVC electrophysiology recordings

The *X. laevis* oocyte expression combined with TEVC electrophysiology, allows the measurement of changes in current from ion flow across the membrane, depending on the type of channel present in the oocyte membrane (as shown in Figure 2.2). The conductance of the membrane is directly proportional to the ion channel activity and by clamping and holding the membrane voltage of the oocyte constant at -60 mV, the current changes can be measured. These measurements were recorded with an iWorx IX-408 Data Acquisition Recorder from the Warner Instruments OC-725C Oocyte Clamp Amplifier which recorded the analogue signal then converted it to a digital output onto a PC running LabScribe2 software.

To start the readings, the electrodes were placed on the surface of the oocyte until dimpled and the manipulators were gently tapped until the electrodes had penetrated the membrane. The resting potential of the cell was measured with an ideal of -15 to -30 mV and current leakage of no more than -200 nA. The cell was then perfused with Ringer's solution and clamped to -60 mV. The ion channel of interest and ligands used dictated the perfusate application protocol, described in the experimental chapters. Data analysis used Prism 8 provided by GraphPad Software.

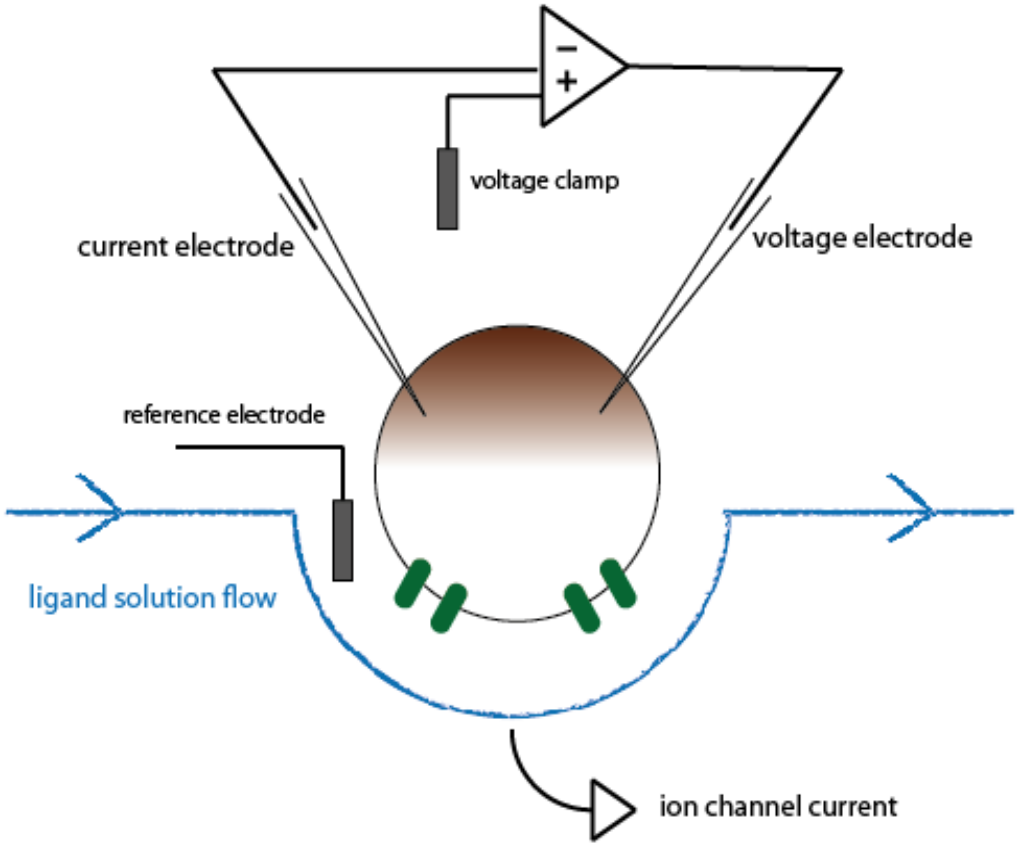


Figure 2.2. Schematic showing TEVC setup of electrodes. Oocyte is kept in place using a small dip in the bath and clamped with the current and voltage electrodes. Ligand solution flows over the membrane proteins expressed on the outer surface of the cell (in green).

2.6.5. Electrophysiological data analysis

Un-injected oocytes were clamped and all agonists and antagonists tested for any endogenous responses. Functionally expressing receptors were also tested for background noise by perfusing with Ringer alone to determine baseline responses.

LabScribe2 Software was used for data acquisition. From the traces produced by the software, peak current responses (R) to agonists were measured in nA and normalised to the maximal current (I_{MAX}) on Excel for Windows. Normalised, concentration-dependent data were fitted to the four-parameter logistic equation (4PL) in GraphPad Prism. The 4PL parameters are top plateau, bottom plateau, middle ($logIC_{50}$) and Hill

slope giving the equation Y=Bottom+(Top-Bottom)/(1+10^((LogIC_{50}-X)*HillSlope)). EC_{50} and IC_{50} values were calculated from the midpoint of the sigmoidal, normalised, concentration-response curve ideally obtained from multiple oocytes from multiple batches.

The Hill Slope was used as an interaction coefficient to measure co-operativity in the binding of a chemical to the receptor. For inhibition studies, a slope coefficient of -1 was considered standard and indicated independent binding. Steeper curves have values ≤ -1 (usually -2 and lower), indicative of positive co-operativity where one ligand facilitates the binding of subsequent ligands. A hill slop ≥ -1 (usually 0 and higher), associated with a shallow curve, indicates negative co-operativity with binding of subsequent ligands being impeded.

Statistical significance in relation to receptor variant EC_{50} and IC_{50} values was determined pairwise, using the extra sum-of-squares F-test. This method compares the goodness of fit of individual curves to a curve fit to all data sets. Threshold values of $P<0.05$ and $P<0.0001$ were used to determine significance.

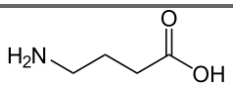
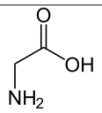
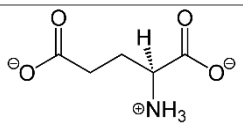
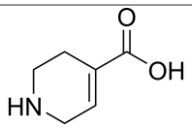
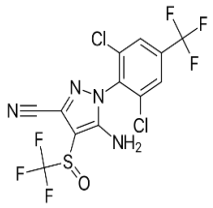
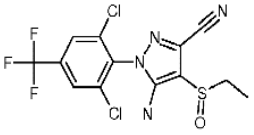
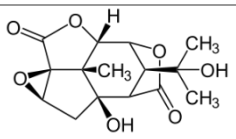
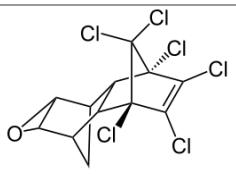
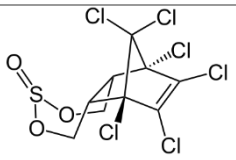
3. Bioassays of GABAergic compounds on *C. felis, R. microplus, R. sanguineus* and *I. Ricinus*

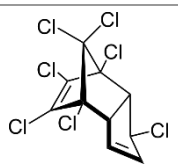
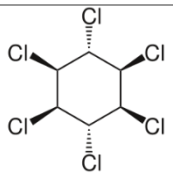
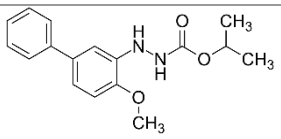
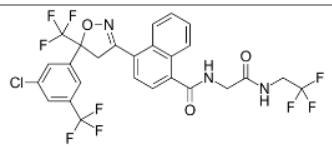
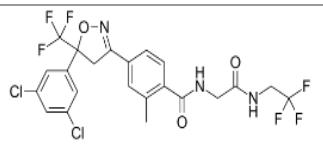
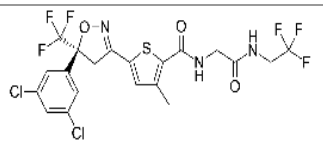
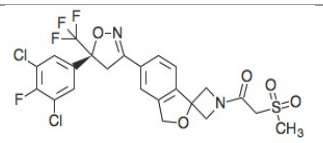
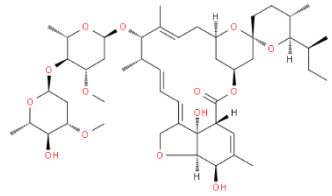
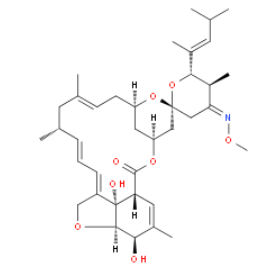
3.1. Introduction

The efficacy of GABAergic compounds in controlling insects and acari varies depending on the target pest, its ability to metabolise compounds, the chemical structure of the compound and the binding affinity of the chemical to the specific GABA chloride-gated channel. The efficacy can be tested directly using laboratory bioassays to generate toxicity data and this can give a better understanding of the whole insect and acari interactions with the chemicals used for control and therefore conclusions can be made on the mode of action of the pesticide.

This chapter reports comparative studies of the activity of GABAergic compounds on the insect *C. felis* and the acari species *R. microplus, R. sanguineus* and *I. ricinus.* Compounds from a variety of different chemical classes (Table 3.1) were tested using a range of bioassay methods.

Table 3.1. Function, mode of action, chemical group and structure details of compounds used in this study. All compounds are GABA agonists or antagonists, excluding glutamate and the macrocyclic lactones, which act primarily on the glutamate-gated chloride channel (GluCl).

Chemical	Function/Chemical Group	Structure
Gaba **$C_4H_9NO_2$**	Orthosteric agonist Inhibitory neurotransmitter	
Glycine **$C_2H_5NO_2$**	Orthosteric agonist Inhibitory neurotransmitter	
Glutamate **$C_5H_8NO_4$**	Orthosteric agonist	
Isoguvacine **$C_6H_9NO_2$**	Orthosteric agonist	
Fipronil **$C_{12}H_4Cl_2F_6N_4OS$**	Non-competitive antagonist Phenylpyrazole	
Ethiprole **$C_{13}H_9Cl_2F_3N_4OS$**	Non-competitive antagonist Phenylpyrazole	
Picrotoxin **$C_{30}H_{34}O_{13}$**	Non-competitive antagonist Plant derived toxin	
Dieldrin **$C_{12}H_8Cl_6O$**	Non-competitive antagonist Organochlorine	
Endosulfan **$C_9H_6Cl_6O_3S$**	Non-competitive antagonist Organochlorine	

Heptachlor **$C_{10}H_5Cl_7$**	Non-competitive antagonist Organochlorine	
Lindane **$C_6H_6Cl_6$**	Non-competitive antagonist Organochlorine	
Bifenazate **$C_{17}H_{20}N_2O_3$**	Weak allosteric modulator Carbazate	
Afoxolaner **$C_{26}H_{17}ClF_9N_3O_3$**	Non-competitive antagonist Isoxazoline	
Fluralaner **$C_{22}H_{17}Cl_2F_6N_3O_3$**	Non-competitive antagonist Isoxazoline	
Lotilaner **$C_{20}H_{14}Cl_3F_6N_3O_3S$**	Non-competitive antagonist Isoxazoline	
Sarolaner **$C_{23}H_{18}Cl_2F_4N_2O_5S$**	Non-competitive antagonist Isoxazoline	
Ivermectin **$C_{48}H_{74}O_{14}$**	Primary target is GluCl Positive allosteric modulator Macrocyclic lactone Avermectin	
Moxidectin **$C_{37}H_{53}NO_8$**	Primary target is GluCl Positive allosteric modulator Macrocyclic lactone Avermectin	

3.2. Methods

All bioassays were done at Bayer Animal Health, Monheim, Germany. The contact, tick oviposition and 'artificial dog' assays are optimised and established methods used by Bayer for toxicology experiments. Using these methods, bioassay testing with the compounds in Table 3.1 was carried out by the author on site as per the company protocols. The animals used as hosts for rearing the tick species were healthy and looked after according to international standards and legislation. The health status of the animals was routinely checked by a veterinarian.

3.2.1. Acari species

The acari species used for bioassays were *R. microplus* (cattle tick), *R. sanguineus* (brown dog tick) and *I. ricinus* (castor bean tick). The cattle ticks were the Parkhurst strain as used by the Bayer Animal Health Breeding lab. Engorged ticks which had fallen off the host animal were collected from the cattle the day of use. Due to their slow movement, there was no need to constrain the cattle ticks to set up the bioassays. *R. microplus* larvae were collected on the day of use and provided in vials for bioassays by Bayer Animal Health. The castor bean and brown dog ticks used for bioassays were from stocks provided by Bayer Animal Health and kept at room temperature and 90% humidity. A heated frame (80 °C) was used to contain the castor bean and brown dog ticks when sorting for bioassays.

3.2.2. Artificial rearing of *C. felis*

The 'Georgi' strain of *Ctenocephalides felis Bouché* was reared according to the method of Wade and Georgi (1988). This method negates the need for an animal host and decreases costs. Briefly, this involved a cylindrical apparatus that contained the fleas with a fine gauze mesh that allowed faeces and eggs to pass through and also allows the fleas close access to a Parafilm membrane through which they feed on 20 mL of citrated bovine blood (Figure 3.1).

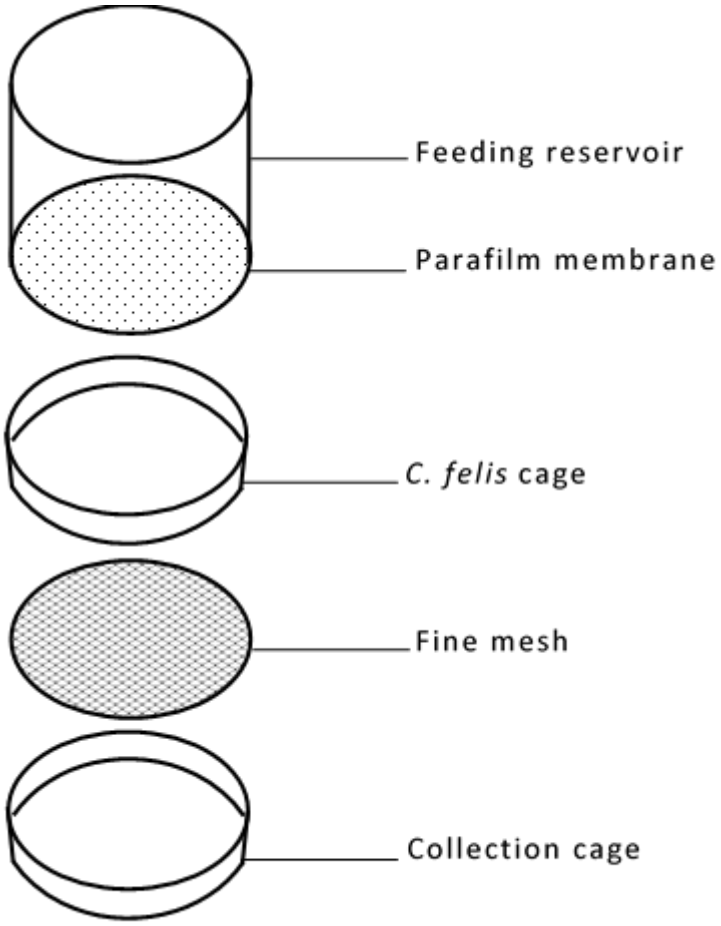


Figure 3.1. Artificial rearing apparatus for *C. felis*. Adult fleas in the *C. felis* cage fed on bovine blood placed in the feeding reservoir. The eggs and faeces fall through the nylon mesh and are collected to rear and maintain the population.

The bovine blood used as the feed was mixed with 20% sodium citrate, kept at 4°C and the feeding reservoir in the apparatus was replaced weekly. The *C. felis* were kept at 28 °C, 80% humidity and under a 12 hour light/dark cycle. To slow reproduction if required, the *C. felis* were kept in permanent darkness at 27 °C and 65% humidity. The waste and any eggs laid in the apparatus pass through the fine mesh keeping the adults separate. New stocks were produced by placing eggs/larvae and waste mix from the collection cage into a dry blend of 2 parts haemoglobin blood meal, 2 parts fine silica, 1 part powdered 'mice and rat' feed and 1 part brewer's yeast. For the bioassays, adults were anaesthetised with CO_2 for 5 seconds and then collected into a small container using a suction based aspirator that deterred jumping and they were kept at room temperature for no more than 5 days prior to use.

3.2.3. Coated glass vial contact bioassay

The efficacy of GABAergic compounds on *C. felis* and tick species was tested using a coated glass vial bioassay based on Campanhola and Plapp (1989). The compounds were prepared as stocks of 900 ppm (equivalent to 500 g/Ha) dissolved in acetone and then serial dilutions were made. with acetone. Five-fold dilutions were prepared by mixing 200 µL of stock solution with 800 µL of acetone and then diluting a further 1 in 5 to get the number of dilutions needed (Table 3.2).

Table 3.2. Concentrations (ppm) of chemicals tested on *C. felis* and ticks in the coated glass vial bioassay. Chemicals were dissolved in acetone.

Chemical	Concentrations used (ppm)
Gaba, Glycine, Glutamate, Isoguvacine	900, 180, 36
Dieldrin, Picrotoxin, Lindane, Heptachlor, Bifenazate, Ivermectin, Moxidectin	900, 180, 36, 7.2
Ethiprole, Endosulfan, Afoxolaner, Lotilaner, Sarolaner	900, 180, 36, 7.2, 1.44
Fipronil, Fluralaner	900, 180, 36, 7.2, 1.44, 0.288

250 µL of each concentration was placed in a Fisherbrand 25 mL Snap Cap Glass Vial. Due to the high vapour pressure of acetone, the pipette was primed by pipetting and aspirating 3 times before transferring the accurate amount of solution. The vials were then placed on the Labinco Rock'n Roller bench top roller in a fume hood and rotated at 10 rpm for 2 hours to allow an even coating of the vials. An acetone only vial was also prepared as a control (alongside a vial with no treatment). The vials were then sealed with Fisherbrand Natural Polythene Snap-on caps with small perforations. Considering the surface area of the vial (minus the lid which was not coated), this gave a concentration of approximately 5 µg per cm^2 at 900 ppm.

Approximately 20 *R. microplus* larvae were transferred into the coated glass vials using a thin paintbrush. 5 unfed female ticks of *R. sanguineus* or *I. ricinus* (identified by their size and colouring) were transferred into the coated glass vials and the vials were stored horizontally (to promote maximum contact) in the dark at room temperature and toxicity scored after 24 and 48 hours. This was done by tapping the vile to get the ticks to the bottom, and then transferring the vials onto a 50 °C heated plate which stimulated the ticks to move up the glass to avoid the elevated temperature (Figure 3.2). They were kept on the heated plate no longer than 10 minutes. The ticks exhibiting normal movement up the vial were considered as healthy and the toxicity of the compound was assumed to be zero. Those with limited/unusual movement and/or convulsions were considered as exhibiting a 'knockdown effect' and any unmoving ticks were considered dead.

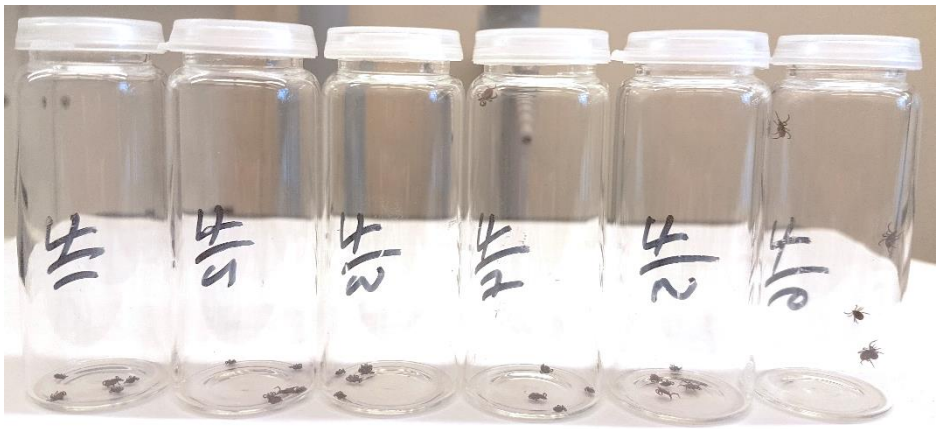


Figure 3.2. Coated glass vial bioassay analysis on a heated plate. The *R. sanguineus* unaffected by the dosage of compound climb up the glass vial displaying heat avoidance (also behaviour seen in *I. ricinus*). Those treated with an effective dose remain on the bottom of the vial.

For *C. felis,* 10-15 fleas were transferred to the treated vials and stored as above. Flea activity was monitored by tapping the vials to promote movement. Those that did not move were considered dead, those showing upright body position and occasional jumps were evaluated as healthy and those showing limited movement and/or convulsing and twitching were considered as 'knockdown' fleas.

Any 'knockdown' ticks or fleas were considered dead for analysis. Ticks and fleas placed in untreated and acetone-treated vials were used as the negative control; the positive control was a pre-established range of concentrations of Fipronil giving complete kill to no effect. The bioassays were done in duplicate for each compound/concentration for all species tested.

3.2.4. *R. microplus* oviposition bioassay

The acaricidal efficacy of GABAergic compounds was tested on *R. microplus* by injecting the compound and assessing oviposition. The protocol was modified from (Booth, 1989). The compounds were dissolved in either water for GABA, glycine, glutamate and isoguvacine or DMSO for the others to give stock solutions of 100,000, 20,000 and 4000 ppm (based on potency) and the purity was accounted for with the final volume of solute. Serial dilutions were then done in DMSO as shown in Table 3.3. A sonicator was used to agitate and disperse the particles and allow them to dissolve. Five-fold dilutions were then prepared by mixing 45 µL of stock solution with 180 µL of DMSO to give a range of concentrations as shown in Table 3.3.

The injections used a 5 mL Hamilton Microliter Autosampler Syringe fitted with a 26s gauge ultra-fine needle. The syringe was back filled with 5 µL of test solution and 1 µL injected into 5 replicate ticks per dose. The ticks were engorged and selected on their size, colour and health (dark with no ruptures). They were injected with the test compounds by inserting the needle 1/3 into the body via the scutum on the posterior end, avoiding damage to the anterior end.

Table 3.3. Chemicals, number of doses and concentrations used (ppm) for *R. microplus* oviposition bioassay. All chemicals were dissolved in appropriate solute.

Chemical	Concentrations used (ppm)
Gaba, Glycine, Glutamate, Isoguvacine	100000, 20000, 4000
Dieldrin, Lindane, Endosulfan, Heptachlor	20000, 4000, 800, 160, 32
Fipronil, Ethiprole. Picrotoxin	20000, 4000, 800, 160, 32, 6.4, 1.28
Bifenazate, Afoxolaner, Fluralaner, Lotilaner, Sarolaner, Ivermectin, Moxidectin	4000, 800, 160, 32, 6.4, 1.28, 0.256

Injections were done from low to high concentrations and the needle and syringe were thoroughly cleaned in between each chemical with at least 5 DMSO rinses. After injection the ticks were incubated 1 per chamber (4 x 2 cm) in a 25-chamber flat bottomed multi-dish at 28 °C and 80% humidity for 7 days. For every repetition, 5 un-injected and 5 DMSO injected ticks served as negative controls whilst a range of fipronil doses (Table 3.3) was used as the positive control. The bioassay was scored after 7 days by analysing the effect on oviposition i.e. if a normal egg cluster was produced treatment was scored as zero effect. No oviposition, tick death, tick melanisation and production of desiccated eggs was scored as an effective dose (Figure 3.3). At least 3-4 replicates for each chemical/concentration were done.

Data from experiments where more than 20% of the combined negative controls were not ovipositing was discarded.

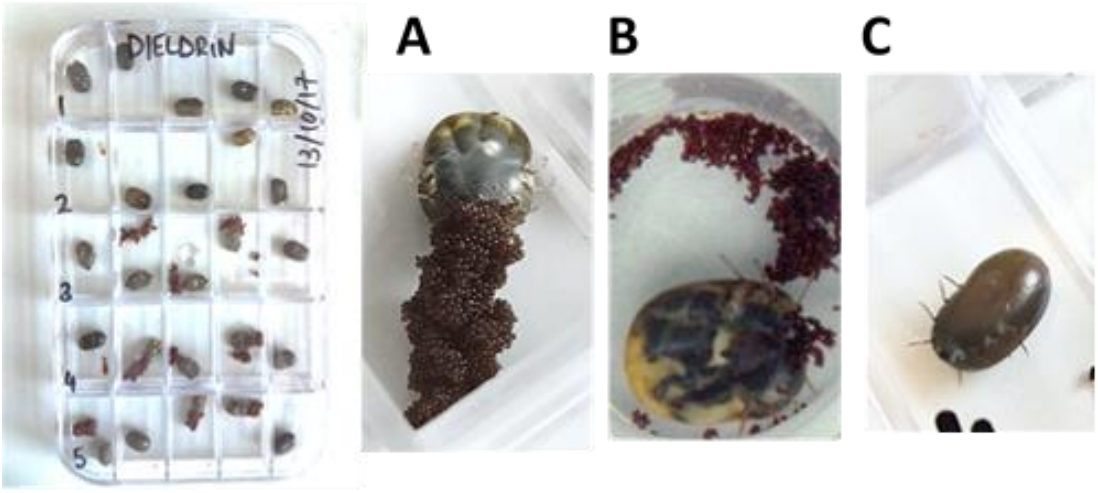


Figure 3.3. Multi-chambered plate with injected ticks in individual chambers where each row represents 5 x replicates of a compound dose. A. Normal oviposition. B. Desiccated eggs C. Tick melanisation.

3.2.5. The ‘artificial dog’ bioassay

The ‘artificial dog’ bioassay used to test the activities of GABAergic compounds was based on a breeding system developed by Wade and Georgi (1988) as described in 3.2.2. The chemicals and the dilutions were the same as described for the *R. microplus* oviposition bioassay (Table 3.3) giving a series of five-fold dilutions. 10-15 adult fleas were anesthetised and placed in small round circular flea cages, sealed with a mesh screen, the proportions of which were designed for placement of a feeding cylinder and the cages placed in a large plexiglass frame as shown in Figure 3.4.

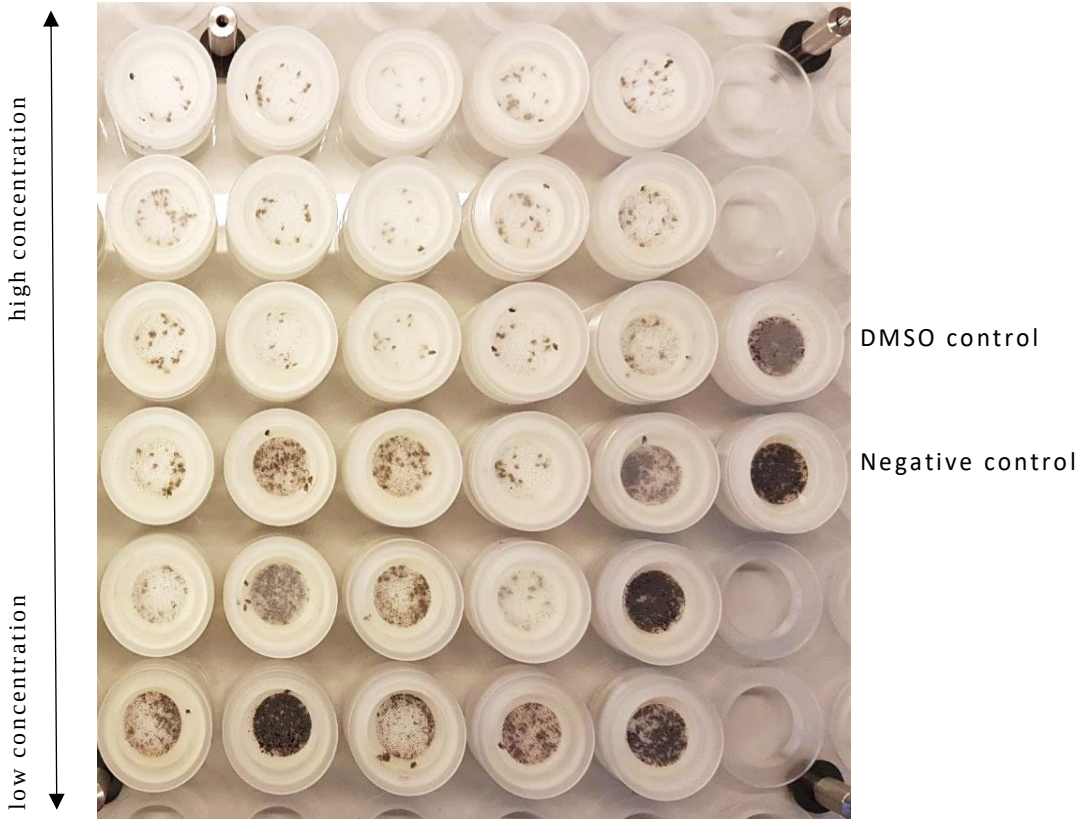


Figure 3.4. Birds eye view of the ‘artificial dog’ bioassay system. Feeding cylinders were placed in the mesh wells allowing the *C. felis* to feed. The gradient of waste product is also indicative of flea survival at lower doses.

The sterile metal cylinders were covered with a taut membrane comprising 2 sheets of parafilm. Using an auto-pipette, 1.5 mL of citrated bovine blood was aliquoted into each cylinder, 15 µL of each dose of compound was pipetted into the blood and a further 1.5 mL of

blood was added. This gave the final concentrations shown in Table 3.4. Negative controls were either blood only or blood plus DMSO, whilst the positive controls were the pre-determined range of concentrations of fipronil.

The feeding reservoirs were gently placed in the dip of the flea cage, ensuring the integrity of the parafilm membrane, and the top of the cylinder was capped. The entire plexiglass frame was then placed in an incubator where the upper region (with the feeding cylinders) was warmed to 37 °C and the lower portion, with the suspended flea cages, was kept at room temperature. A tray with water and detergent mix was placed below the artificial feeding system to contain any escapees.

For scoring, the plexiglass frame was removed from the incubator and the feeding cylinders were lifted from the flea cages. The percentage efficacy of a dose on *C. felis* was noted according to the same criteria used for the coated glass vial contact bioassay (3.2.3). The amount of waste product was also taken into consideration when scoring the bioassay as the quantity of detritus is correlated to the health of fleas (using the positive controls for comparison) (Figure 3.4). Scoring was done at 24 hour and 48 hours, with the same feeding cylinders being removed and replaced in-between the analyses. The experiment was carried out in duplicate.

Table 3.4. Number of doses and concentrations used (ppm) for the 'artificial dog'

Chemical	Concentrations used (ppm)
Gaba, Glycine, Glutamate, Isoguvacine	500, 100, 20
Fipronil	4, 0.8, 0.16, 0.032, 0.0064, 0.00128
Dieldrin, Ethiprole, Lindane, Endosulfan, Heptachlor, Bifenazate	100, 20, 4, 0.8, 0.16, 0.032
Afoxolaner, Fluralaner, Lotilaner, Sarolaner, Ivermectin, Moxidectin	20, 4, 0.8, 0.16, 0.032, 0.0064

3.2.6. Bioassay data analysis

The data were analysed using the Probit model of regression (Bliss, 1934), whereby mortality was considered the binary outcome of the treatment . In the Probit model, the assumption is that the tolerance to chemicals follows a normal Gaussian distribution after transforming data to log doses. The assumption of this 'normality' was checked by confirming a bell-shape histogram, assuming constant variance. The over dispersion of the model was also checked and a value of close to 1 required for the residual. Analysis was performed with GenStat (Windows 18th edition) using the built in generalised linear model probit analysis. This generated LC_{50} values (lethal concentration for 50%), by fitting a nonlinear function to the sigmoidal data and running a regression. Mortality in the absence of any dose was adjusted based on the control where appropriate. The LC_{50} and LC_{95} as well as lower and upper 95% confidence intervals (95% CI) were calculated, back-transformed to the raw dose scale and used comparatively. Where there was a large variation in the data, the 95% CI was not calculated (nc). Dose response curves were produced using a coding script detailed in Appendix 1.

A Student's paired t-test was used to distinguish if the difference between a chemical treatment and the positive control, fipronil, was statistically significant. Fipronil was used as the positive control as it had continued high efficacy against all the insects and ticks used in the established bioassays here. The test was carried out in GenStat using the coding script detailed in Appendix 1. The critical value, determined by the t distribution, was used to estimate if the difference in LC_{50} would fall into the region of the distribution where the null hypothesis could be rejected. A p value threshold of <0.05 was used to indicate the probability that the t value statistic was more extreme than the critical value.

Resistance ratios (RR) were calculated by dividing the LC_{50} of the compound of interest by the LC_{50} of fipronil (susceptible).

3.3. Results and discussion

As would be expected, the GABA agonist compounds tested (GABA, glycine, glutamate and isoguvacine) showed no toxicity towards any of the species across all three bioassays. The results for these compounds are given in Appendix 2 but are not considered further.

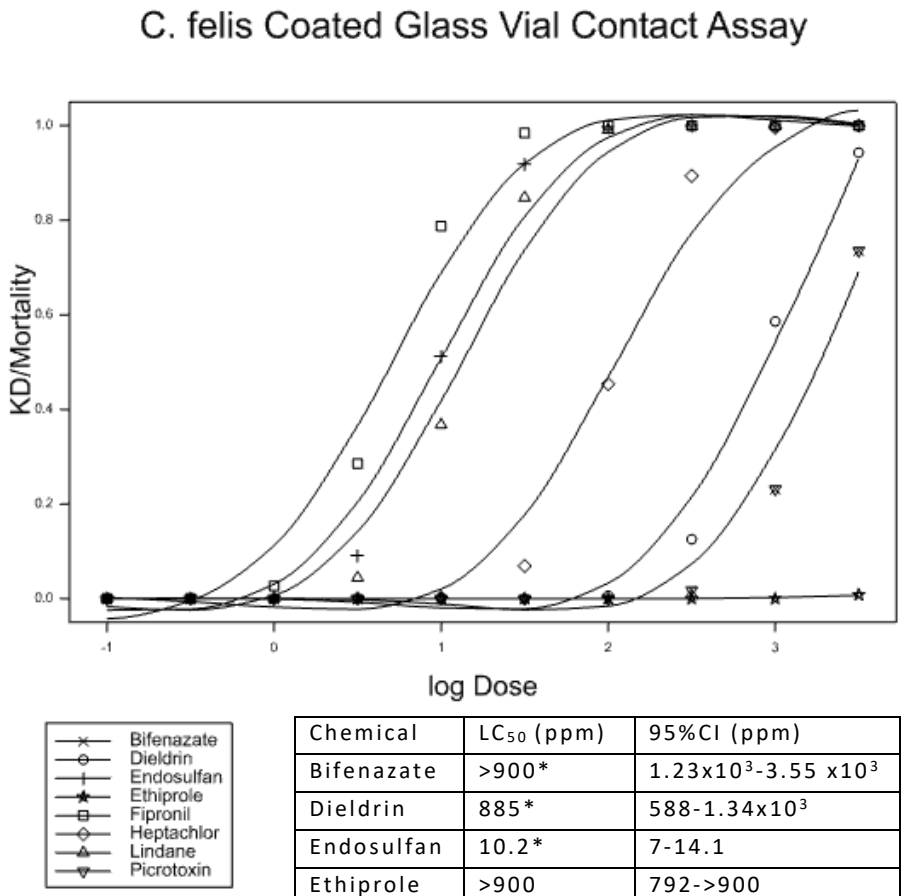
For the contact bioassays done on *R. microplus* larvae, the small size of the larvae meant the doses used caused skewed data and the results showed that they did not fit a normal distribution, with 100% mortality for some of the compounds tested, so these were discarded.

There was a high rate of control mortality for the contact bioassays with *R. sanguineus* due to the age and poor quality of the ticks. The data analysis, given in Appendix 3, yielded no statistically significant results and the results are not considered further.

For the coated glass vial contact assays and the 'artificial dog' assays data from previous bioassays (carried out at Bayer) and protocols already in place were used to decide on the range of concentrations tested. However, for the *R. microplus* oviposition bioassays, the concentrations were determined by range finding trials.

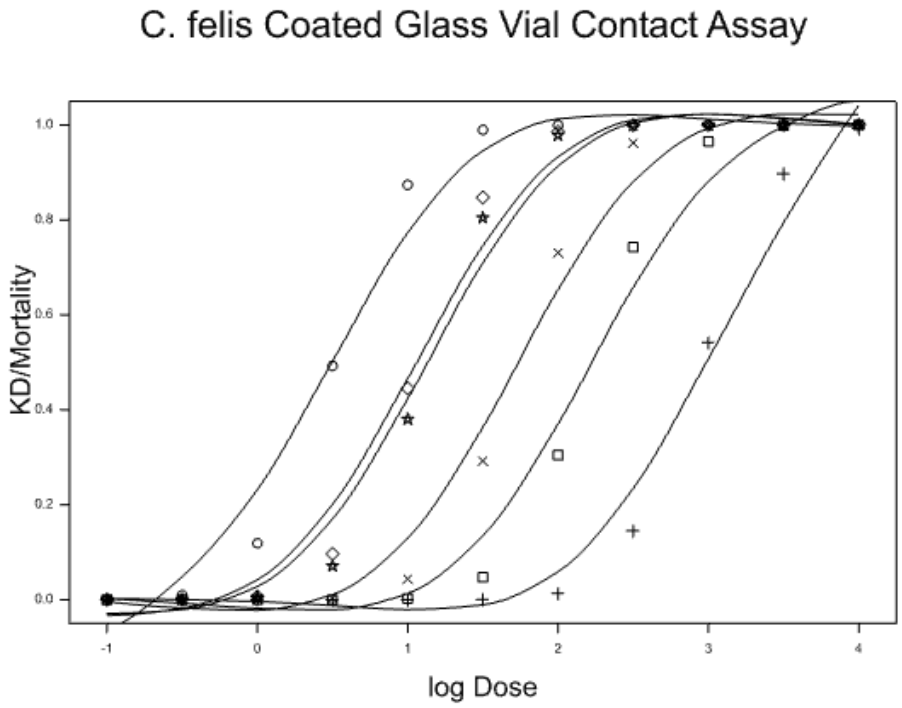
3.3.1. *C. felis* contact bioassays

The results of contact bioassays on *C. felis*, using organochlorines (dieldrin, endosulfan, heptachlor and lindane), phenylpyrazoles (fipronil and ethiprole), bifenazate, picrotoxin, isoxazolines (afoxolaner, fluralaner, lotilaner and sarolaner) and macrocyclic lactones (ivermectin and moxidectin) are shown on Figure 3.5 and Figure 3.6.



Chemical	LC_{50} (ppm)	95%CI (ppm)
Bifenazate	>900*	$1.23x10^3$-$3.55\ x10^3$
Dieldrin	885*	588-$1.34x10^3$
Endosulfan	10.2*	7-14.1
Ethiprole	>900	792->900
Fipronil	5.01	4-7.4
Heptachlor	111*	77-160
Lindane	13.4*	9-19.2
Picrotoxin	>900*	$1.23x10^3$-$3.55x10^3$

Figure 3.5. Log dose response curves for C. felis obtained using coated glass vial contact assays with organochlorines, phenylpyrazoles, bifenazate and picrotoxin. *=significantly different to positive control Fipronil LC50 where P<0.05 in a two-sided t-test.



Chemical	LC_{50} (ppm)	95%CI (ppm)
Afoxolaner	54.1*	37-78.1
Fluralaner	3.67*	2-4.65
Ivermectin	885*	588-1.34x10^3
Lotilaner	14.5*	9-19.5
Moxidectin	167*	110-241
Sarolaner	11.4*	8-16

Figure 3.6. Log dose response curve for *C. felis* obtained using coated glass vial contact assays with isoxazolines and macrocyclic lactones. *=significantly different to positive control Fipronil LC_{50} where P<0.05 in a two-sided t-test.

The LC_{50} values ranged from 3 to over 2000 ppm. Bifenazate is used primarily as a miticide and therefore would be expected gave a low efficacy against *C. felis*, as did picrotoxin both with LC_{50} values of >900 ppm.

For the organchlorines, both endosulfan and lindane were the most toxic with low LC_{50} values comparable to the positive control. Both heptachlor and dieldrin gave much higher LC_{50} values (22-fold and 177-fold differences respectively when compared to fipronil). The lack of

toxicity of heptachlor and dieldrin might be due to the fleas having a resistance mutation. Although the majority of organochlorines are no longer in use worldwide, an A301S substitution in the GABA receptor conferring resistance to cyclodienes has been shown to persist in insect and acari populations (Dryden, 2014). Furthermore, this mutation has been shown in a number of field and lab strains of *C. felis* (Bass et al., 2004). A *Taq*man assay (methods according to section 2.2.4) on the Georgi strain of *C. felis* used for the bioassays confirmed the presence of the A301S substitution. Thus, the decreased toxicity of the organochlorines, particularly for dieldrin, can be attributed to the A301S resistance mutation.

Another interesting finding is the lack of efficacy of ethiprole on *C. felis*. In comparison to the positive fipronil control, there is a high level of resistance (RR= 7513) to ethiprole. This is unexpected given that these two phenylpyrazoles are highly similar in structure only differing in one moiety; an ethylsulfinyl substituent for ethiprole or a trifluoromethylsulfinyl substituent for fipronil (Figure 3.7).

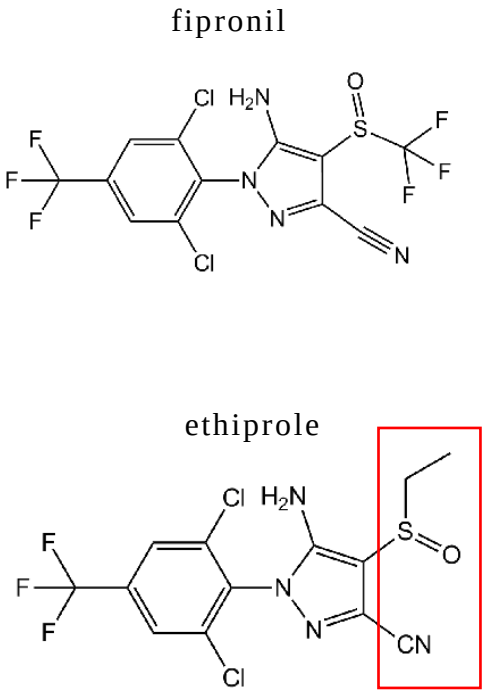


Figure 3.7. The chemical structures of fipronil and ethiprole, highlighting the trifluoromethylsulfinyl to ethylsulfinyl substitution

This difference in structure will influence the lipophilic properties of the compounds, with ethiprole being considerably less lipophilic, however the potency has been found previously to be similar (Caboni et al., 2003). There is evidence of resistance to ethiprole in *N. lugens* where the A301S mutation was present in the binding site of the GABA receptor (Garrood et al., 2017), further supporting the hypothesis that the A301S mutation is implicated in the lack of efficacy of ethiprole and dieldrin in the *C. felis* tested here.

The four isoxazolines tested all had LC_{50} values in the range of 3- 54 ppm, with fluralaner as the most efficacious and afoxolaner the least. These compounds are the primary active ingredient in insecticide and acaricides with high therapeutic efficacy against fleas and ticks. They are administered in a similar range in dogs treated for *C. felis;* i.e. ~2.5 mg/kg per month for afoxolaner (Beugnet et al., 2014), ~25 mg/kg every 3 months for fluralaner (Walther et al., 2014), ~20 mg/kg per month for lotilaner (Karadzovska et al., 2017) and ~2 mg/kg per month for sarolaner (Becskei et al., 2016). 1 mg/kg is equivalent to 1 ppm, therefore the LC_{50} values for the contact bioassay are marginally higher than the therapeutic dose, however these compounds have a systemic mode of action rather than a contact. The results presented here confirm the similar efficacy of all 4 of the new range of isoxazolines used for *C. felis*.

The macrocyclic lactones primarily target the GluCl, and are used as anthelmintic compounds. In the experiments reported here, ivermectin was not very effective against *C. felis* with an LC_{50} of 885 ppm, which is a much higher dose than when it is used as the active ingredient in de-worming treatments in companion animals (~1 mg/kg) (Magalhaes et al., 2016). Similarly, moxidectin showed very little effect in the contact assay with a LC_{50} of 167 ppm, as shown in previous toxicity studies on *C. felis* with both of these compounds (Zakson-Aiken et al., 2001).

Although ivermectin and moxidectin are structurally related and both contain a core macrocyclic lactone ring, there are key substituent differences including the absence of a disaccharide group and the addition of methoxyimino for moxidectin (Figure 3.8). The two compounds also differ in terms of physicochemical properties, pharmacodynamics and kinetics and a comprehensive review has found significant differences across the literature indicating overlapping but a non-identical binding site (Prichard et al., 2012).

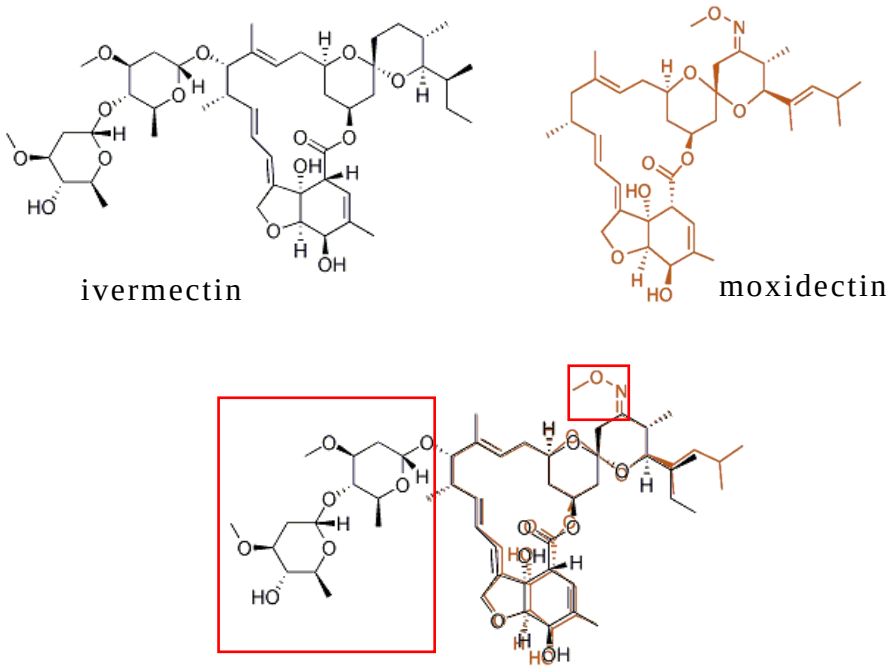
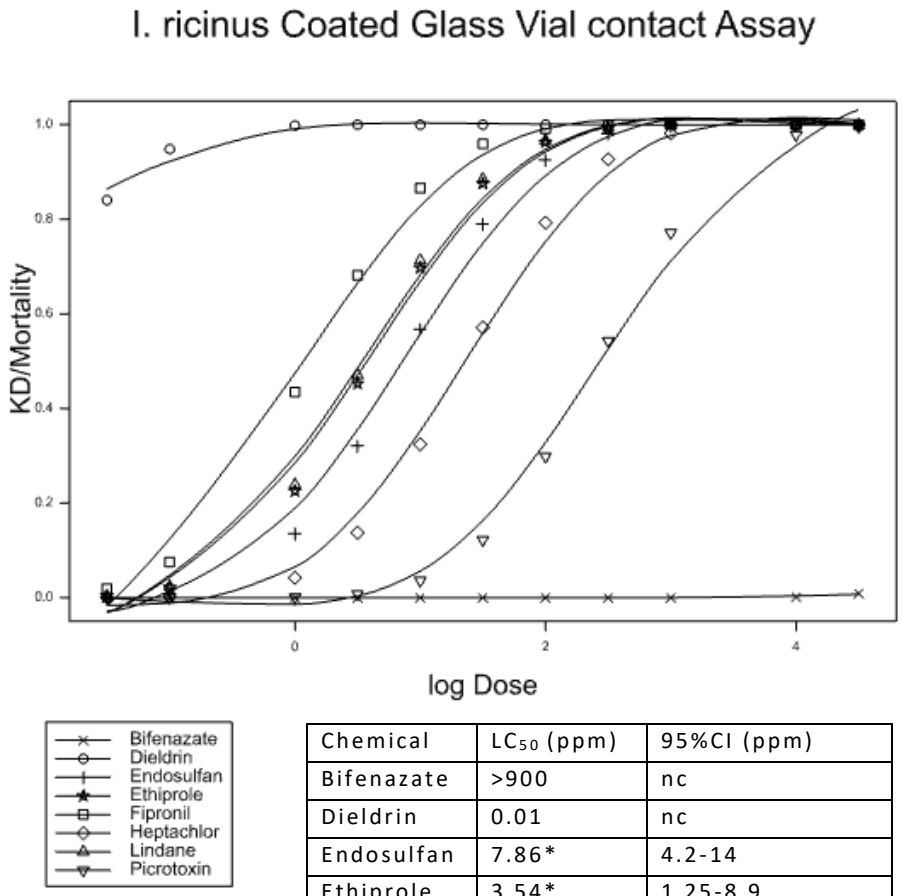


Figure 3.8. Overlay of the chemical structures of ivermectin, an avermectin, and moxidectin, a milbemycin. The disaccharide group present in ivermectin and the methoxyimino group in moxidectin are highlighted.

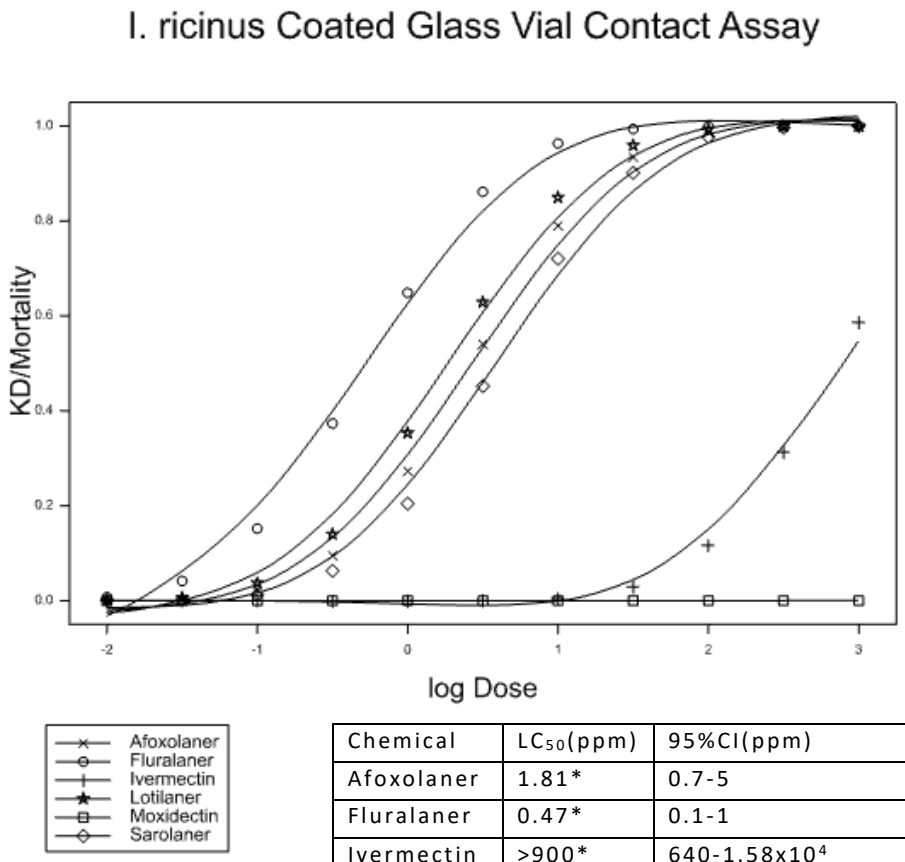
3.3.2. *I. ricinus* contact bioassays

The results of contact bioassays on *I. ricinus*, using organochlorines (dieldrin, endosulfan, heptachlor and lindane), phenylpyrazoles (fipronil and ethiprole), bifenazate, picrotoxin, isoxazolines (afoxolaner, fluralaner, lotilaner and sarolaner) and macrocyclic lactones (ivermectin and moxidectin) are shown in Figure 3.9 and Figure 3.10.



Chemical	LC_{50} (ppm)	95%CI (ppm)
Bifenazate	>900	nc
Dieldrin	0.01	nc
Endosulfan	7.86*	4.2-14
Ethiprole	3.54*	1.25-8.9
Fipronil	1.24	0.47-3
Heptachlor	24.3*	12.6-45
Lindane	4.32*	1.8-9
Picrotoxin	458*	167-1.88x10^3

Figure 3.9. Log dose response curves for *I. ricinus* coated glass vial contact assay for organochlorines, phenylpyrazoles, bifenazate and picrotoxin. *=significantly different to positive control Fipronil LC_{50} where P<0.05 in a two-sided t-test.



Chemical	LC_{50}(ppm)	95%CI(ppm)
Afoxolaner	1.81*	0.7-5
Fluralaner	0.47*	0.1-1
Ivermectin	>900*	640-$1.58x10^4$
Lotilaner	1.11*	0.4-3
Moxidectin	>900	nc
Sarolaner	2.91*	1.1-7

Figure 3.10. Log dose response curves for *I. ricinus* coated glass vial contact assay for isoxazolines and macrocyclic lactones. *=significantly different to positive control Fipronil LC_{50} where P<0.05 in a two-sided t-test.

These demonstrated a range of efficacy, ranging from no effect for bifenazate to high toxicity for dieldrin (0.01 ppm). Dieldrin was 124 times more potent than the positive fipronil control, although this is not statistically significant and the lack on 95% CI undermines the reliability of the LC_{50}. The values established for the other 3 organochlorines were in a similar range to one another with lindane being more potent than endosulfan and heptachlor. Ethiprole was effective with an LC_{50} of 3.54 ppm, which was statistically significant from the LC_{50} to fipronil at 1.24 ppm, however the range is small.

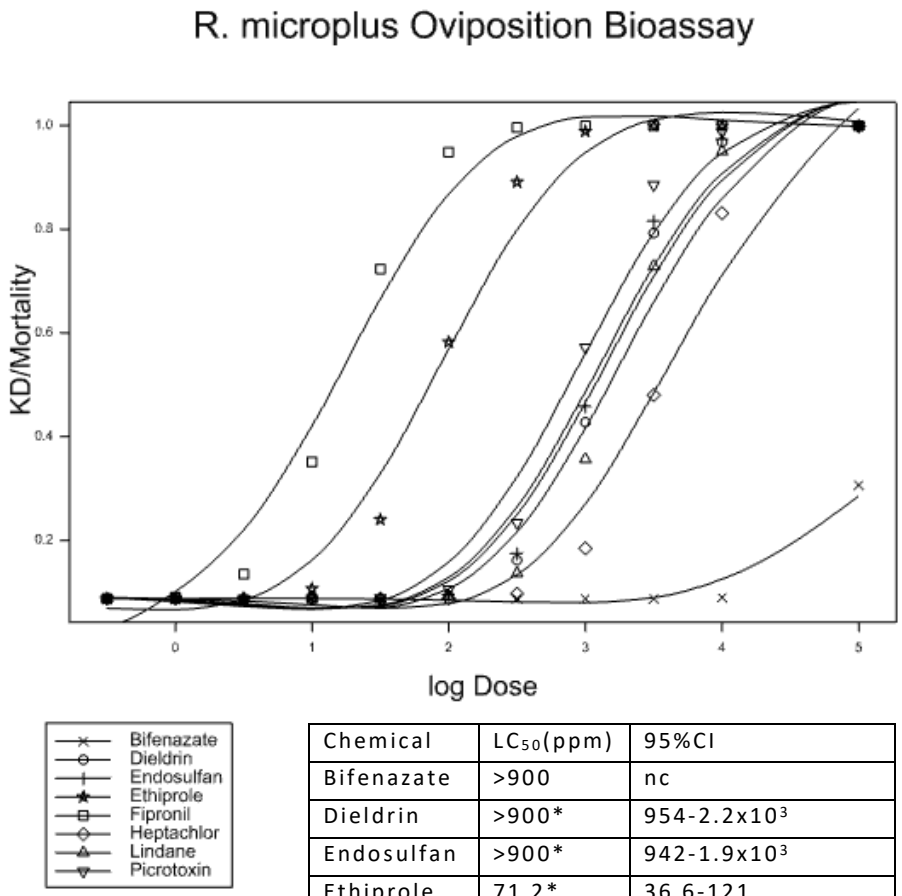
The four isoxazolines showed high levels of acaricidal activity against *I. ricinus*, in agreement with previous studies where all four compounds were reported to be efficacious against *I. ricinus* in dogs, at ~20 mg/kg for lotilaner and fluralaner, and at ~2 mg/kg for afoxolaner and sarolaner (Dumont et al., 2014, Murphy et al., 2017, Wengenmayer et al., 2014, Six et al., 2016b).

I. ricinus showed low levels of sensitivity to both of the macrocyclic lactones. Ivermectin has previously been demonstrated to have no effect on adult female *I. ricinus* in an ingestion experiment on cattle, however treatment with the compound had a marked effect on oviposition and larvae produced, with the treated ticks producing only 3% of larvae compared to the control group (Taylor and Kenny, 1990). A later study found that it took 9 days post ingestion of ivermectin to get 100% cumulative mortality (Krober and Guerin, 2007). This was also seen in the bioassays reported here with the LC_{50} values for ivermectin being much higher at 48 hours than at 24 hours (Appendix 2). This same increase in toxicity with time was not seen for moxidectin.

This could indicate ivermectin has a low speed of kill and therefore longer incubation could prove ivermectin more effective against *I. ricinus* than the results suggest. Krober and Guerin (2007) tested the *in vitro* feeding effect of ivermectin on the tick, it could be hypothesised that the innate insensitivity seen here could be attributed to the contact nature of the bioassay as opposed to direct ingestion.

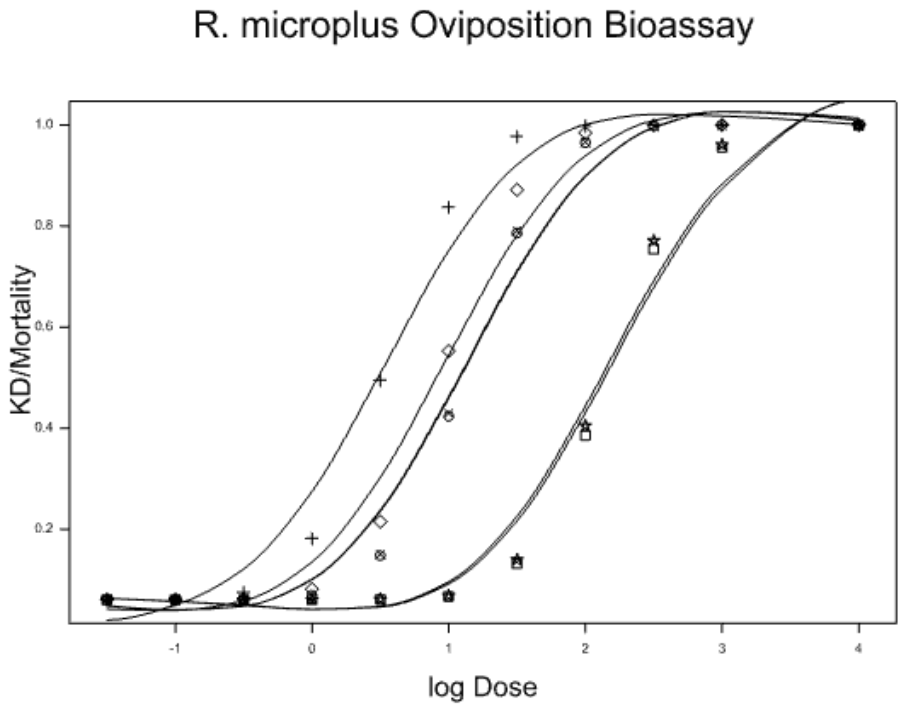
3.3.3. *R. microplus* oviposition bioassays

The results of the oviposition bioassays on *R. microplus*, using organochlorines (dieldrin, endosulfan, heptachlor and lindane), phenylpyrazoles (fipronil and ethiprole), bifenazate, picrotoxin, isoxazolines (afoxolaner, fluralaner, lotilaner and sarolaner) and macrocyclic lactones (ivermectin and moxidectin) are shown in Figure 3.11 and Figure 3.12.



Chemical	LC_{50}(ppm)	95%CI
Bifenazate	>900	nc
Dieldrin	>900*	954-2.2x10^3
Endosulfan	>900*	942-1.9x10^3
Ethiprole	71.2*	36.6-121
Fipronil	16.5	7.8-31.3
Heptachlor	>900*	2.5x10^3-2.3x10^4
Lindane	>900*	1.1x10^3-2.7x10^3
Picrotoxin	820*	489-1.35x10^3

Figure 3.11. Log dose response curves for *R. microplus* oviposition bioassay for organochlorines, phenylpyrazoles, bifenazate and picrotoxin. *=significantly different to positive control Fipronil LC_{50} where P<0.05 in a two-sided t-test



Chemical	LC_{50}(ppm)	95%CI(ppm)
Afoxolaner	13.0*	7.2-22.6
Fluralaner	12.3*	7.3-19.3
Ivermectin	5.71*	4.2-7.8
Lotilaner	142*	80.2-243
Moxidectin	197*	115-592
Sarolaner	9.12*	5-15.96-9

Figure 3.12. Log dose response curves for *R. microplus* oviposition bioassay for isoxazolines and macrocyclic lactones. *=significantly different to positive control Fipronil LC_{50} where P<0.05 in a two-sided t-test.

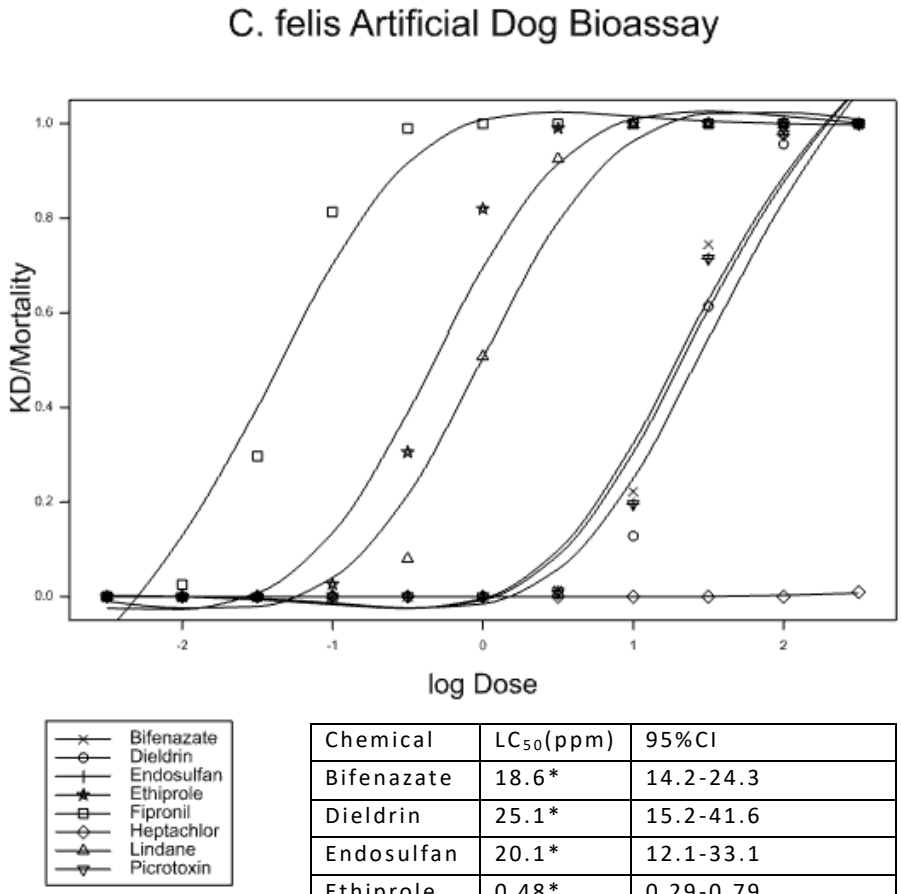
As with the *I. ricinus* contact assays, the oviposition bioassay here showed bifenazate had no effect indicating that this compound has little or no toxicity against the tick species tested here, despite it being effective against mites (particularly spider mites). All four of the organochlorines tested had very little effect on *R. microplus* with LC_{50} values of >900ppm. Many organochlorines have been used for the control of *R. microplus* since the 1940's and this has led to target site modifications and elevated levels of detoxifying metabolites (Rosario-Cruz et al., 2009). The A301S substitution has been found to persist in

R. microplus populations (Hope et al., 2010), and therefore could be present in the Parkhurst strain, explaining the results reported here. In contrast, both phenylpyrazoles were effective with fipronil being ~5 times more potent than ethiprole.

Ivermectin and moxidectin were also effective at 5.7 ppm and 197 ppm respectively. Although macrocyclic lactones are primarily used as anthelmintic compounds, both of these compounds have been found to be effective against *R. microplus* and used as injectables (Pegram and Lemche, 1985, Baker et al., 2014, Lanusse et al., 1997). These compounds have been used widely to overcome organophosphate resistance in *R. microplus* (Sibson, 1994, Cramer et al., 1988) but there have been reports of resistance emerging in South America (Perez-Cogollo et al., 2010, Martins and Furlong, 2001, Klafke et al., 2010) therefore the effectiveness of the isoxazolines could be of commercial importance. Both fluralaner and afoxolaner were as effective as the positive control at 12.3 ppm and 13 ppm, and sarolaner was more potent at 9 ppm. Lotilaner was approximately 10 times less effective than the other three isoxazolines with an LC_{50} of 142 ppm.

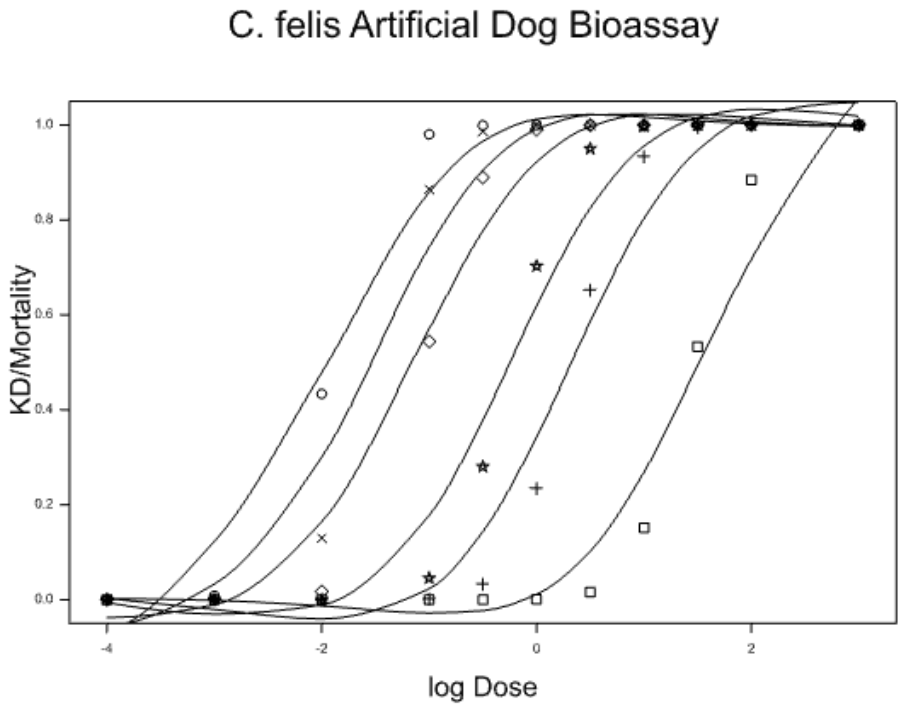
3.3.4. *C. felis* 'artificial dog' bioassays

The results of 'artificial dog' bioassay on *C. felis*, using organochlorines (dieldrin, endosulfan, heptachlor and lindane), phenylpyrazoles (fipronil and ethiprole), bifenazate, picrotoxin, isoxazolines (afoxolaner, fluralaner, lotilaner and sarolaner) and macrocyclic lactones (ivermectin and moxidectin) are shown in Figure 3.13 and Figure 3.14.



Chemical	LC_{50}(ppm)	95%CI
Bifenazate	18.6*	14.2-24.3
Dieldrin	25.1*	15.2-41.6
Endosulfan	20.1*	12.1-33.1
Ethiprole	0.48*	0.29-0.79
Fipronil	0.05	0.03-0.07
Heptachlor	>900	$0.66\text{-}1.77 \times 10^3$
Lindane	0.98*	0.59-1.61
Picrotoxin	20.1*	15.3-26.1

Figure 3.13. Log dose response curves for *C. felis* 'artificial dog' bioassay for organochlorines, phenylpyrazoles, bifenazate and picrotoxin. *=significantly different to positive control Fipronil LC_{50} where P<0.05 in a two-sided t-test.



Chemical	LC_{50}(ppm)	95%CI(ppm)
Afoxolaner	0.03*	0.01-0.06
Fluralaner	0.01*	1.73-2.56
Ivermectin	2.11*	4.2-7.8
Lotilaner	0.58*	0.29-1.18
Moxidectin	25.6*	20.5-32.6
Sarolaner	0.09*	0.05-0.16

Figure 3.14. Log dose response curves for *C. felis* 'artificial dog' bioassay for isoxazolines and macrocyclic lactones. *=significantly different to positive control Fipronil LC_{50} where P<0.05 in a two-sided t-test.

The 'artificial dog' bioassays were an interesting comparison with the contact assays, as the compounds tested are active ingredients (in insecticides) targeting *C. felis*, that are applied either topically with a contact mode of action or for oral treatments with a systemic mode of action. The effective dose was higher for almost all compounds tested in the contact assay with the exception of heptachlor and endosulfan.

However, unlike the contact assay, ethiprole was effective against *C. felis* in the 'artificial dog' bioassays. There was still a ~10-fold difference between the two phenylpyrazoles with fipronil proving to be a more potent insecticide with an LC_{50} of 0.05 ppm. This data suggests that the difference in the hydrophobicity of ethiprole could reduce penetration in comparison to the closely related fipronil

Of the organochlorines, lindane was the most effective with an LC_{50} of 1 ppm, followed by bifenazate (18.6 ppm) and dieldrin (25.1 ppm). Heptachlor proved the least effective with an LC_{50} of >3000 ppm (RR=66,480).

All four of the isoxazolines were effective against *C. felis* with fluralaner being the best and lotilaner being the worst. As discussed in 3.3.1, all four isoxazolines have been found to be very effective against flea infestations in animal experiments and are active ingredients in commercially available pesticide treatments. Since they are used in oral treatments and have a systemic mode of action, it is unsurprising they are so effective in the 'artificial dog' bioassay.

Ivermectin also proved more effective against *C. felis* in the 'artificial dog' bioassays with an LC_{50} of 2.11 ppm compared to 25.6 ppm for moxidectin (RR=12.1) and in contrast to the *C. felis* contact assay results as shown in Table 3.5.

3.3.5. TaqMan sequencing of Georgi C. *felis*

Following the *C. felis* contact and 'artificial dog' bioassays, sampled of fleas were tested for the presence of the A301S mutation by the author using a *Taq*Man assay set up by Martin Williamson (Rothamsted Research) as per the methods in section 2.2.4.

Samples of the Georgi strain of fleas were collected from Bayer and kept on ice. A second strain of fleas, Kiel, were routinely screened with fipronil by Bayer Animal Health and samples that survived 180 ppm fipronil (Kiel alive (KA)) were provided for testing alongside the Georgi strain for the A301S mutation. Kiel strain fleas that died in response to 180 ppm fipronil were used as a control.

A second mutation, M354I, was discovered in fipronil-resistant fleas from Australia, the U.S and the UK, and this mutation resulted from one of two different codon changes (ATA and ATT) (M. S. Williamson personal communication). The Georgi, KA and KD DNA was also tested for the presence of this second mutation.

As shown in Figure 3.15, 100% of the Georgi and Kiel strains that reported a result had the A301S mutation. The M354I ATA and ATT allelic forms were not present in Georgi. ~50% of the KD were homozygous for the M354I mutation and a higher proportion of approximately ~70% of the KA insects carried M354I.

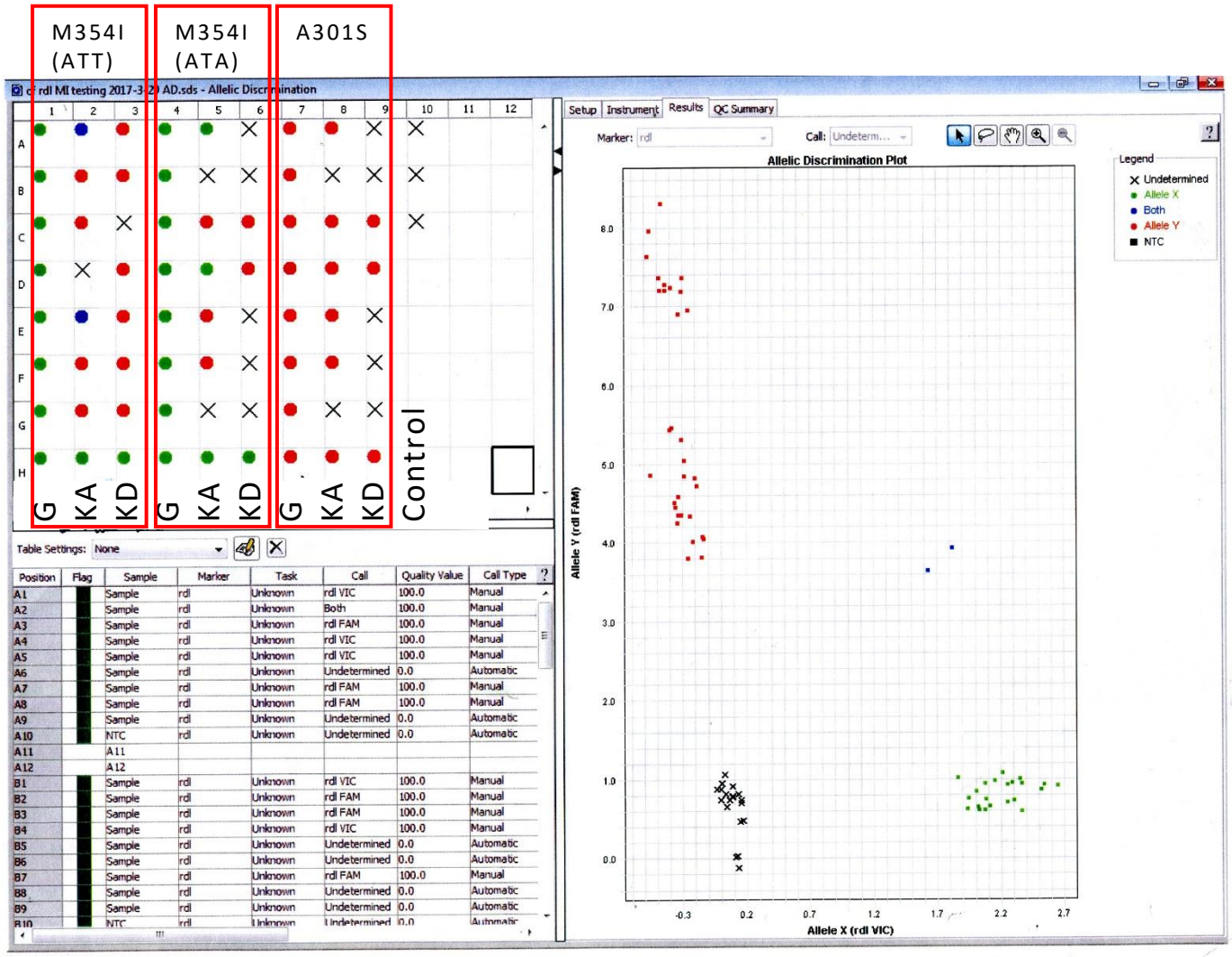


Figure 3.15. *C. felis Taq*Man allelic discrimination readout. G= Georgi, KA= Kiel Alive, KD= Kiel Dead. Green fluorescence indicates homozygous for the Wild Type, red denotes homozygous for the mutation being tested for (alanine to serine or methionine to 1 and blue denotes heterozygous (one alanine and one serine).

3.3.6. Discussion

A comparison across all the bioassays and chemical compounds tested is listed in Table 3.5.

Table 3.5. The LC_{50} values taken from a probit analysis of data derived from the *C. felis* 'artificial dog' bioassay, the *R. microplus* oviposition bioassay and the contact bioassays on *C. felis* and *I. ricinus* for a range of chemical compounds.

Chemical	*C. felis* contact bioassay LC_{50} (ppm)	*I. ricinus* contact bioassay LC_{50} (ppm)	*R. microplus* oviposition bioassay LC_{50} (ppm)	*C. felis* 'artificial dog' bioassay LC_{50} (ppm)
Fipronil	5.01	1.2.1	16.5	0.05
Ethiprole	>900	3.54	71.2	0.48
Picrotoxin	>900	458	820	20.1
Dieldrin	885	0.01	>900	25.1
Endosulfan	10.2	7.86	>900	20.7
Heptachlor	111	24.3	>900	>900
Lindane	13.4	4.32	>900	0.98
Bifenazate	>900	>900	>900	18.6
Afoxolaner	54.1	1.81	13.0	0.03
Fluralaner	3.67	0.47	12.3	0.01
Lotilaner	14.5	1.11	142	0.58
Sarolaner	11.4	2.91	9.12	0.09
Ivermectin	885	>900	5.71	2.11
Moxidectin	167	>900	197	25.6

The pesticidal effectiveness of the compounds varied across the arthropod pests and LC_{50} values showed high levels of sensitivity as low as 0.01 ppm for the isoxazoline fluralaner on the *C. felis* in the 'artificial dog', to very low levels of sensitivity to the organochlorines tested on *R. microplus* in the oviposition bioassay. The variance of the data highlights the importance of monitoring pesticide efficacy using a

range of bioassays that consider the route of administration. For example, ethiprole and bifenazate have a high level of efficacy on *C. felis* when the compound is directly ingested compared to the complete lack of efficacy in the contact bioassay.

Bifenazate is only effective in the 'artificial dog' bioassay. It is unlikely this is due to the mode of application as the *R. microplus* oviposition bioassay also tests the compound in a systemic way, but could be down to the difference in chemical structure compared to the other organochlorines tested (Table 3.1). The high levels of resistance to dieldrin, endosulfan, heptachlor and lindane tested here imply there is organochlorine resistance in the Parkhurst strain of *R. microplus*, however they seem to be effective against *I. ricinus* suggestive of a target-site mutation in the *R. microplus* GABAR that is not present in *I. ricinus*. Further sequencing could verify this hypothesis.

The effectiveness of the isoxazolines as both acaricides and insecticides in all the bioassays signal that this emerging group of compounds are likely to grow in use, particularly due to their additional efficacy against other pests of companion animals such as mites as well as their primary targets (Six et al., 2016a). In a wider context, the exemplary safety profile of these compounds as well as their high efficacy on a variety of insects and acari has led to their proposed use for control of insect vectors carrying human disease, by administrating them as a drug to humans and acting as a systemic insecticide against vectors such as mosquitoes carrying the zika virus (Miglianico et al., 2018).

3.4. Conclusions

This chapter has investigated the *in vivo* toxicity of several GABAergic compounds and some key animal health pests.

The organochlorines tested showed a range of effective doses, with some bioassays highlighting the presence of resistance to the compounds. Although this is interesting, the current ban on the use of organochlorines in many circumstances and the resulting lack of use in commercial markets lessens the importance of further experimentation with these compounds.

The differences between ivermectin and moxidectin across all the bioassays was unsurprising as the differences in chemical structure, pharmacokinetics and pest interactions have been reported previously.

The most notable observation from the contact assays was the lack of efficacy of ethiprole on *C. felis*. This compound is structurally very similar to fipronil, which was effective. The resistance to dieldrin seen here also suggested that there could be target-site resistance and the persistence of the A301S mutation in the populations. A *Taq*Man assay confirmed the hypothesis with the A301S mutation present at 100% across the Georgi *C. felis* strain. This mutation has not previously been implicated in ethiprole resistance in the *C. felis* although this has been found in *N. lugens* (Garrood et al., 2017).

Understanding the mechanisms behind resistance is a key part of animal health pest control, particularly for the GABA receptor which continues to be a primary target for neurotoxic pesticides. Using *in vitro* studies on the GABAR, the effects of the mutations on the functionality of the receptor were tested.

4. Electrophysiology studies of antagonists and agonists of the *C. felis* GABA receptor

4.1. Introduction

In the previous chapter, bioassays showed that the Georgi strain of the cat flea *C. felis* was resistant to ethiprole and a *Taq*Man assay showed that this was possibly linked to an A301S substitution in the M2 transmembrane region of the GABA receptor (GABAR). In addition, sequencing and *Taq*Man assays of fipronil-resistant *C. felis* samples from Australia, Germany and the UK, and from samples tested in section 3.3.5, showed that a M354I substitution, mapping to the transmembrane region three and four in the same receptor, was consistently found in fipronil-resistant populations, and that this resulted from one of two different codon changes (ATA and ATT) (M. S. Williamson personal communication).

Fipronil is a second-generation phenylpyrazole inhibiting GABARs, and is an established pesticide marketed as Frontline® with high efficacy against *C. felis* (Payne et al., 2001, Postal et al., 1995). Colloquial complaints of resistance to fipronil products has been reported via online sites and from veterinary operatives, although the extent and underlying cause of this resistance is unknown. There are reports in the literature, of moderate to low levels of resistance in inbred *Drosophila melanogaster* involving changes to the GABAR, including an A301S substitution (Remnant et al., 2014). However, to date there have been no reports of M354I being involved in fipronil resistance. Therefore, the aim of this chapter was to test the effects of A301S, M354I and A301S in combination with M354I on the properties of the GABAR using electrophysiology.

Electrophysiology is one of the primary methods used to identify the effects of compounds on ion channels. GABARs are cys-loop chloride channels that play a key role in the inhibition of the invertebrate nervous system. GABA is an inhibitory neurotransmitter that mediates

rapid transmission by binding to the ionotropic receptor which results in rapid gating of the GABAR. When GABA binds the receptor, the influx of anions into the post-synaptic neuron results in hyperpolarisation, which mediates inhibition as an action potential is not generated (Staley et al., 1995). Antagonists of the GABAR prevent the activation of, or block the channel and the inhibition necessary for normal function cannot occur. Two-electrode voltage clamp (TEVC) electrophysiology allows artificial control of the membrane potential to study the properties of the GABAR membrane proteins exogenously expressed in *X. laevis* oocytes.

In the present study the optimal parameters for the functional expression of the *C. felis* GABAR channel in oocytes were identified and TEVC was used to assess the pharmacological activity of key insecticides that target this receptor, using the wild type channel and channels with the M354I and A301S substitutions, to evaluate their possible role in conferring resistance to phenylpyrazole and isoxazolines. The invertebrate GABAR is encoded by nine exons, where exon 3 and exon 6 are alternative splice variants and correspond to the extracellular loops D and F, close to the agonist binding site of all cys-loop receptors and therefore are a likely region where alterations could reduce agonist binding affinity or gating efficacy (Hosie et al., 1997). The *D. melanogaster* GABAR encodes four distinct polypeptides due to this alternative splicing, all of which are expressed in *D. melanogaster* (Ffrenchconstant and Rocheleau, 1993), and have been cloned and functionally expressed in *X. laevis* oocytes (GABARac, GABARbc, GABARbd, GABARab) (Hosie and Sattelle, 1996, Jones et al., 2009). Hosie and Sattelle's study (1996) demonstrated differences in agonist potencies amongst the three cloned splice variants, with GABA EC_{50} values of 9-30 µM for GABARac, 56-60 µM for GABARad and 100-150 µM for GABARbd. Thus, GABARbd had the highest EC_{50}, indicating GABA acts with less potency on this isoform. However, GABARbd is the most abundant isoform (Jones et al., 2009) and was therefore the isoform chosen for the studies reported here.

4.2. Methods

4.2.1. Annotation of the *C. felis* GABAR

The *D. melanogaster* GABAR sequence was used in a basic local alignment search tool (BLAST-NCBI) to search for related sequences for *C. felis*. A full length *C. felis* GABAR cDNA sequence was identified (GenBank accession: KF881790.1) (Heska Corporation, 2002). Sequence analysis was then done using Biomatters Geneious software and the resulting sequences for the signal peptide, transmembrane regions 1-4 and exons 3 and 6 of the *C. felis* GABARbd are shown in Figure 4.1.



Exon 3

A: GPPVEVGVTMYVLSISSVSEVLMDTFLDFYF[110]
B: GPPVEVGVTMYVLSISSLSEVKMDTFLDFYF[110]

Exon 6

C: RDIRYFWRDGLSSVGMSSEVELPQFRVLGHRQRATEINLT[250]
D: RDIRYKWNEGPNSVGVSSEVSLPQFKVLGHRQRAMEISLT[250]

Figure 4.1. Annotated protein sequence of *C. felis* (GABARbd) with signal peptide, transmembrane regions 1-4 and exons 3 and 6 highlighted. Splice variants A/B and C/D modified amino acids underlined.

4.2.2. Sub-cloning of the C. felis GABARbd

The DNA sequence encoding the *C. felis* GABARbd shown in Figure 4.1 (1545 bp) was synthesised by GeneArt (Invitrogen) in pMA-T vector (2456 bp) with an ampicillin resistance marker and an added Kozak consensus sequence (GCCACC) immediately upstream of the start codon to improve translation efficiency. *Not*I restriction sites were incorporated at the 5' and 3'-end of the gene and the sequence codon optimised for expression in *X. laevis* oocytes. The full sequence can be found in Appendix 4.

The lyophilised DNA (5 µg) was centrifuged, resuspended in 50 µL of nuclease-free water to give a 100 ng/µL and 10 µL was used in a restriction digest using *Not*I FastDigest Enzyme and run on a gel. The GABARbd insert, seen as the smaller of the two bands was cut out of the gel and purified (see section 2.2).

The GABARbd DNA was then sub-cloned into an *X. laevis* expression vector, PGEM-HE (3015 bp), digested and linearised with *Not*I. A T4 ligation reaction with ~25 ng of the GABARbd DNA and ~75 ng PGEM was carried out overnight and ligation confirmed with gel electrophoresis (~4.5 Kb band). The ligated plasmid DNA was transformed with ThermoScientific One Shot TOP10 Chemically Competent *E. coli*, propagated in media and purified.

The orientation of the gene insert was checked by doing a standard PCR with a T7 forward primer (TAATACGACTCACTATAGGG) and a reverse primer (GGACAGCGAACTGATGGAGAGGACG) in the middle of the *C. felis* GABARbd. A ~750 bp band visualised with gel electrophoresis of the PCR product confirmed that the *C. felis* GABAR coding sequence was downstream of the T7 promoter.

4.2.3. Site-directed mutagenesis and transformation

Primers for site directed mutagenesis of the *C. felis* GABARbd were designed according to Agilent QuikChange II XL Site-Directed Mutagenesis guidelines and purchased from Sigma-Aldrich. This introduced the A301S, M354I and the double A301S and M354I (A301S.M354I) substitutions into the *C. felis* GABARbd (Table 4.1).

Table 4.1. Oligonucleotide primers used for site-directed mutagenesis of *C. felis* GABAR to introduce A301S and M354I substitution and primers used for sequencing to verify the mutation of the DNA.

	Forward Primer (5'-> 3')	**Reverse Primer (5'-> 3')**
A301S primers	CCAGCTCG*AGT*CAGTCTCGG AGTGACC	GGTCACTCCGAGACTG*ACT*C GAGCTGG
M354I primers	GCCACTGTTGGCTAC*ATT*GC TAAGCGCATCC	GGATGCGCTTAGC*AAT*GTAG CCAACAGTGGC
Sequencing primers	TCGCCTGGCGTGCGAGATT CA	GCGAACCTTGAACCGCACC TC
	Red italicised bases deviate from WT sequence	

The reactions and PCRs were done according to the manufacturer's protocol. The *C. felis* GABARbd sequences with the desired mutations were then transformed using Agilent Technologies XL10-Gold Ultracompetent Cells and the resulting transformants plated out on ampicillin agar plates and incubated overnight at 37°C. 4-8 colonies were picked from each plate and used for a colony PCR using the sequencing primers (Table 4.1). DNA sequencing of the colony PCR products confirmed the introduction of the desired mutations into the *C. felis* GABARbd sequence. Positive colonies were propagated in liquid culture and their plasmids were purified with the QIAGEN QIAprep Spin Miniprep Kit.

4.2.4. *In Vitro* cRNA synthesis

The Ambion mMESSAGE mMACHINE T7 transcription kit was used to generate cRNA from the PGEM + *C. felis* GABARbd plasmids (1. Wild Type, 2. A301S, 3. M354I and 4. A301S.M354I). Plasmid DNA was linearised with *Not*I and agarose gel electrophoresis used to confirm complete cleavage. Any uncleaved circular plasmid templates would give long heterogeneous RNA transcripts. The cRNA synthesis was done according to the manufacturer's protocol and a denatured sample loaded onto a further agarose gel to confirm the quality of the cRNA (Figure 4.2).

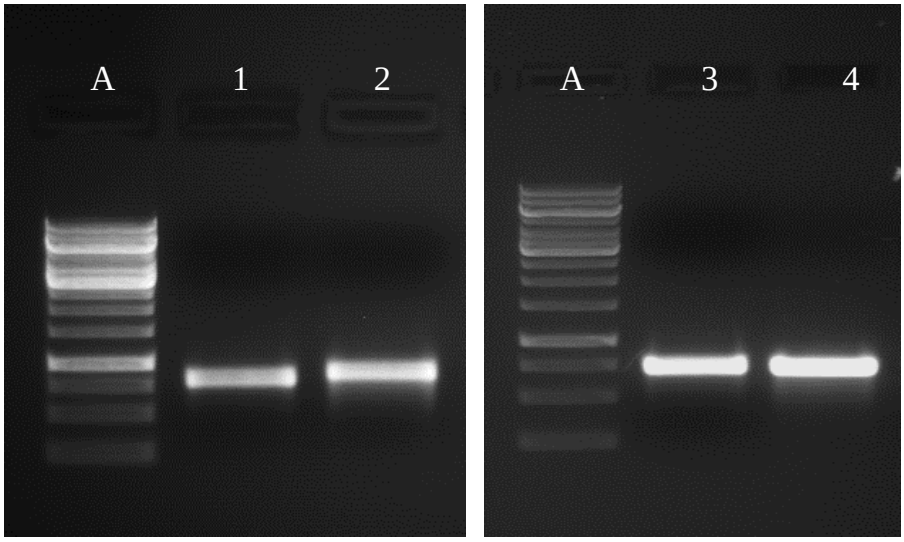


Figure 4.2. Denatured *C. felis* GABAR cRNA samples. A. GeneRuler 1 Kb DNA ladder, 1. WT, 2. A301S, 3. M354I and 4. A301S.M354I.

4.2.5. Electrophysiological recordings and analysis

X. laevis oocytes were prepared and injected as described in 2.6.2. The process was optimised for concentration and quantity of cRNA to be injected into the cells and the incubation time. GABA, picrotoxin, fipronil, ethiprole and dieldrin were purchased from Sigma Aldrich and the isoxazolines (afoxolaner, fluralaner and sarolaner) were supplied by Bayer Animal Health. The chemicals were diluted in DMSO to a 0.1 M stock and stored at 4°C, except for GABA which was a 1 M stock. Serial

dilutions were carried out with fresh Ringer's solution on the day of testing.

GABA was applied to the cells for a ~3 second pulse in increasing concentrations with a 2 minute Ringer solution wash in between applications to minimise desensitisation. To investigate the activity of the test compounds, a bath application protocol was used by pre-incubating the oocytes for 2 minutes with increasing concentrations of the test compound before pulsing with GABA to invoke an inward current. Co-application of antagonists with GABA for short ~5 second pulses showed a negligible blocking effect on the receptor, indicating that the antagonists bind preferentially to open-state GABA-activated receptors. A bath protocol was therefore used to expose the GABA-activated membrane proteins to the test compounds. Initially, a predominantly closed state drug application method was used as it was deemed more physiologically relevant, however, the pulsing of GABA in-between increasing concentrations meant that the open-state receptor was exposed to the compounds being tested for a brief time, and demonstrated effective blocking of the channel.

Recovery experiment protocols involved pre-incubating oocytes with approximate IC_{95} concentrations of the antagonists tested here for 2 minutes. 1 mM GABA pulses were applied to the cell every 2 minutes up to 10 minutes with ringer wash in between applications of GABA.

Control experiments were performed with un-injected and water-only injected oocytes. Data were analysed for agonist and antagonist concentration-response curves according to 2.6.5.

4.3. Results and discussion

4.3.1. Optimisation of *C. felis* GABARbd expression

Application of GABA to oocytes expressing *C. felis* WT GABARbd gave concentration-dependent reversible inward currents (Figure 4.3). Desensitisation was not significant when GABA was applied in 3-5 second pulses successively from low to high concentrations to the oocyte. The receptor recovered quickly following withdrawal of the GABA agonist and replacement with recording Ringer solution (usually within the 30 second recording time frame).

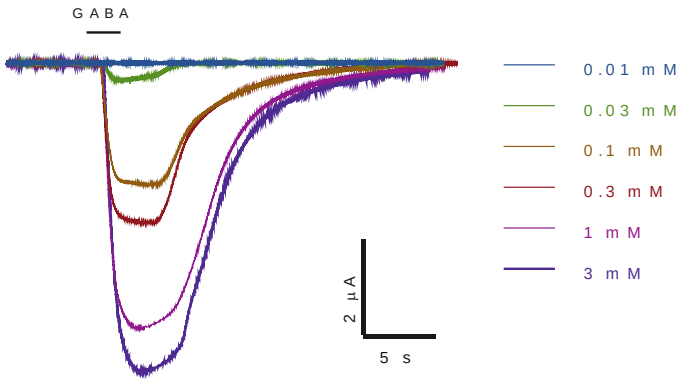


Figure 4.3. Inward currents evoked when a range of GABA concentrations were applied to *C. felis* GABAR expressed in *X. laevis* oocytes.

The incubation time (at 17 °C) required for optimal expression of the *C. felis* GABARbd was determined by measuring the currents evoked by 1 mM GABA at key intervals over a 96-hour period post-cRNA injection. 1 mM GABA was chosen to evoke currents, which equates to the approximate EC_{95} of the *D. melanogaster* GABARbd from a previous TEVC study of this isoform (Hosie et al., 2001). Initially, a 50 nL injection of 500 ng/µL cRNA per oocyte was used, however, a GABA pulse yielded inward currents too high in amplitude for the Warner Instruments apparatus, which has a range of 10 to -10 µA (Figure 4.4, top right). By reducing the concentration to 100 ng/µL and injecting 13.2 nL of cRNA, stable recordable responses to 1 mM GABA were seen (Figure 4.4, top left).

The inward currents increased up to 72 hours incubation and subsequently declined. The responses at 72 hours were high but inconsistent and close to the maximum recording value of the equipment, therefore a 48 hour incubation period was deemed optimal (Figure 4.4, bottom).

The amount of cRNA injected was 1.32 ng, which is lower than reported in some of the literature; for example 50 ng of *D. melanogaster* GABAR (Jones et al., 2009) and 50 ng of *N. lugens* GABAR (Zhang et al., 2016). However, a lower amount (3.5 ng of plasmid DNA) was used for *A. gambiae* GABAR expression (Taylor-Wells et al., 2015). It is likely that the increased efficiency of expression is because *C. felis* GABARbd had been codon optimised for expression in oocytes.

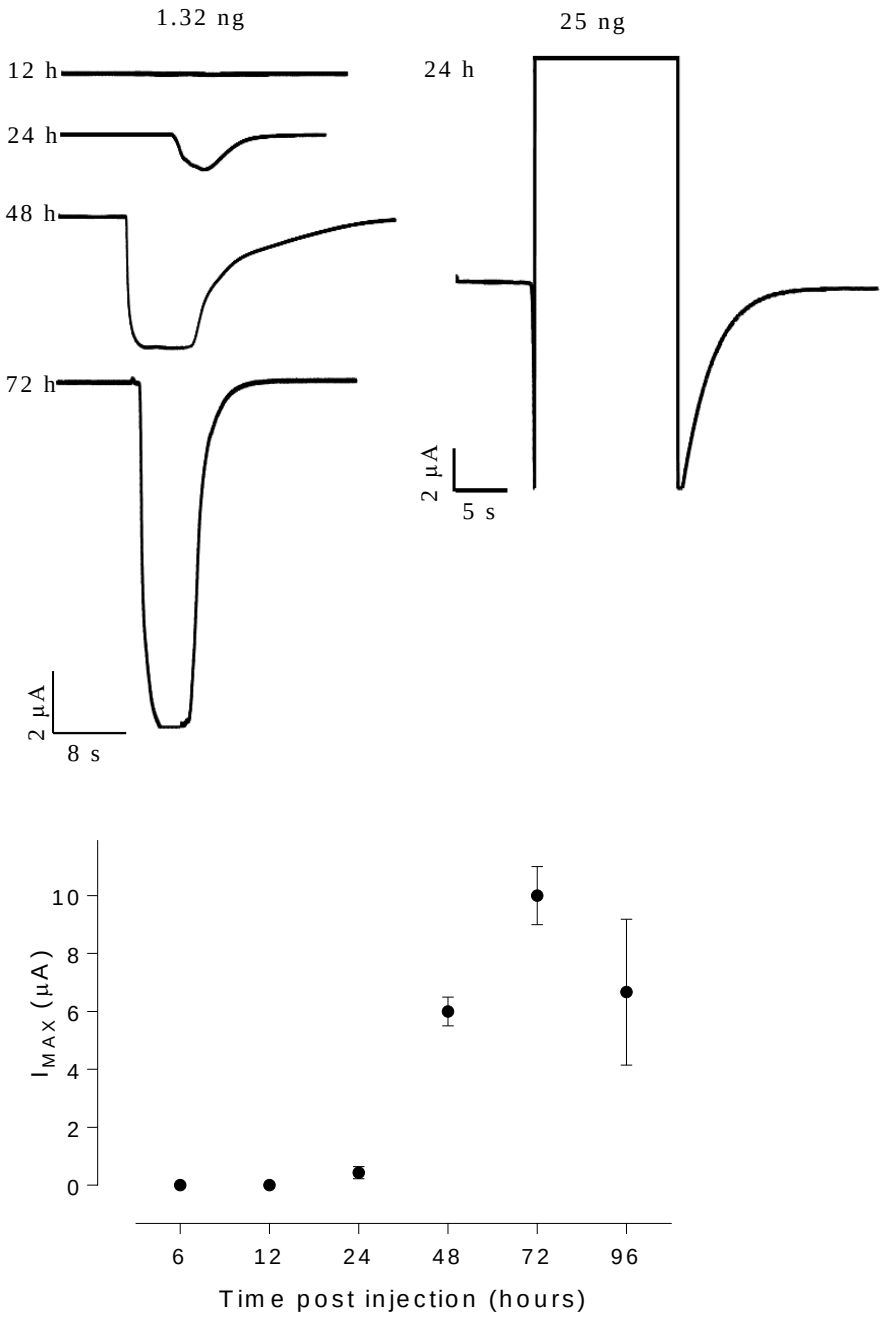


Figure 4.4. Top left: Currents from 13.2 nL of 100 ng/µL (1.32 ng) *C. felis* GABAR expressed in *X. laevis* over a 72 hour period. Top right: Response from oocyte injected with 50 nL of 500 ng/µL (25 ng) at 24 hours.

Below: Peak current responses generated from oocytes over 96 hours (n=3/time point). All responses to 1 mM GABA.

Plotting current amplitude against a range of GABA concentrations from multiple oocytes from different batches gave the *C. felis* GABARbd an EC_{50} value of 177.5 µM and an EC_{95} of 746.9 µM (Figure 4.5) which is in a similar range to previous results (see Table 4.2).

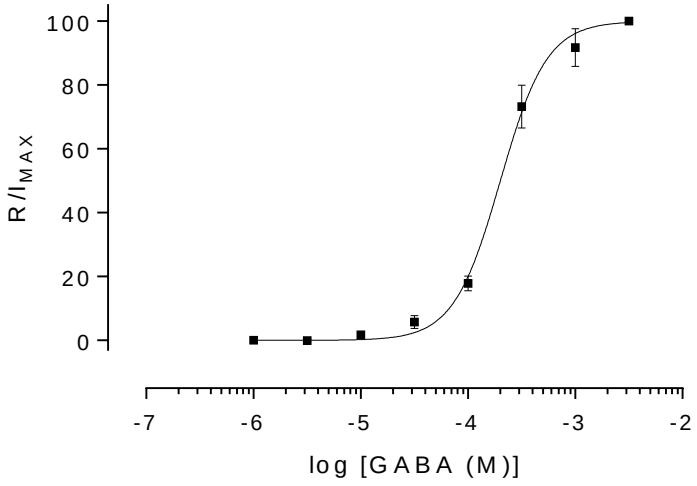


Figure 4.5. Current data yielded a concentration-response curve for the *C. felis* GABAR (EC_{50}=177.5 µM) where R = response, I_{MAX} = maximal GABA response and n=10. Points are mean % of I_{MAX} ± SEM.

Table 4.2. Comparative GABA EC_{50} values for *X. laevis* oocytes expressing functional GABA receptors.

Receptor	EC_{50} (µM)	Reference
Human $GABA_{\alpha 3\beta\gamma 2L}$	102	(Belelli et al., 1996)
***D. melanogaster* GABAR**	152	(Belelli et al., 1996)
***D. melanogaster* GABARac**	27	(Jones et al., 2009)
***D. melanogaster* GABARbd**	152	(Jones et al., 2009)
***A. gambiae* GABAR**	95	(Taylor-Wells et al., 2015)
***N. lugens* GABAR**	38	(Zhang et al., 2016)
***C. felis* GABARbd**	177.5	this study

To determine the stability of receptor recovery and to detect if any decay of current amplitude had occurred, currents were measured over a ten-minute period (a timescale typical of testing on a single oocyte). No decrease in amplitude was detected confirming stable expression (Figure 4.6).

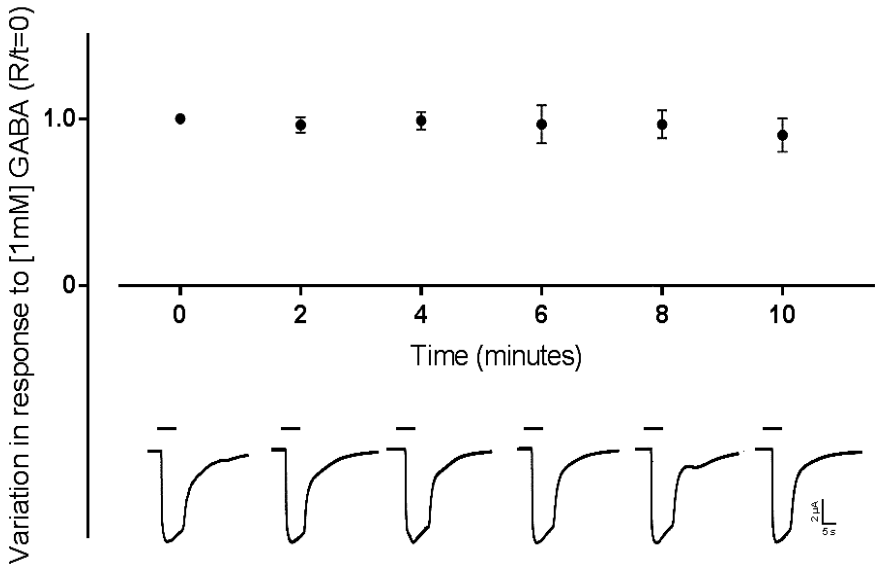


Figure 4.6. Peak response current amplitudes (in response to 1 mM GABA) from *C. felis* GABAR over a ten-minute period do not decay as demonstrated by sample electrophysiological traces and a graph of mean currents. R= response, t=0 is the peak response of the first application of 1 mM GABA. (n=3 for each data point).

For optimal and stable expression of *C. felis* GABARbd in *X. laevis* oocytes, an incubation time of 48 hours was used with an injection of 1.32 ng of cRNA (13.2 nL of 100 ng/μL), generating large currents of ~6 μA and stable expression with an EC_{50} of 177.5 μM. The EC_{50} value generated by concentration-response curves of the WT receptor were used to evaluate the comparative response of mutagenised *C. felis* GABARs to GABA as well as determining a baseline for antagonist studies.

4.3.2. Antagonists of the *C. felis* GABAR

Antagonist application to the *X. laevis* oocytes expressing the *C. felis* GABARbd was done as per the bath protocol described in section 4.2.5. Increasing concentrations of antagonists applied to the oocyte resulted in diminishing currents as represented in the traces in Figure 4.7, showing the effect of fipronil on the *C. felis* GABARbd GABA responses.

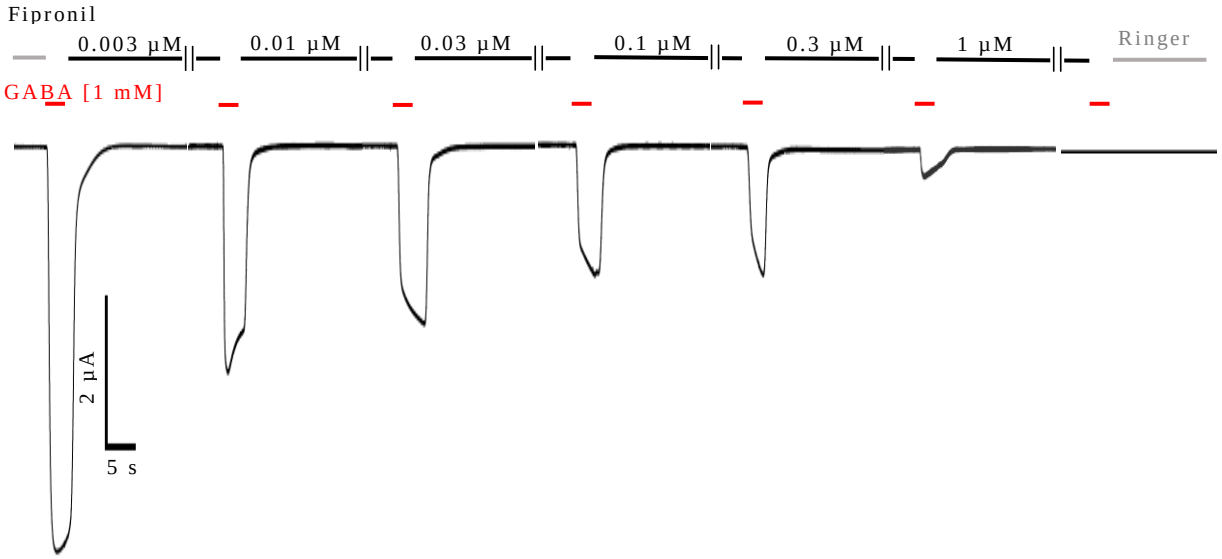


Figure 4.7. Representative traces produced from antagonist application to the *C. felis* GABARbd. The oocyte is bathed in increasing concentrations of fipronil for 2 minutes with a 3 second pulse of 1 mM GABA to invoke an inward current between concentrations.

For the WT *C. felis* GABARbd, treatment of the oocytes with the GABAR antagonists picrotoxin, dieldrin, fipronil, ethiprole, afoxolaner, fluralaner and sarolaner all resulted in subsequent GABA responses being diminished (Figure 4.8, Table 4.3). The results showed a marked difference of potency between picrotoxin and ethiprole in comparison to the other compounds, up to a factor of 200.

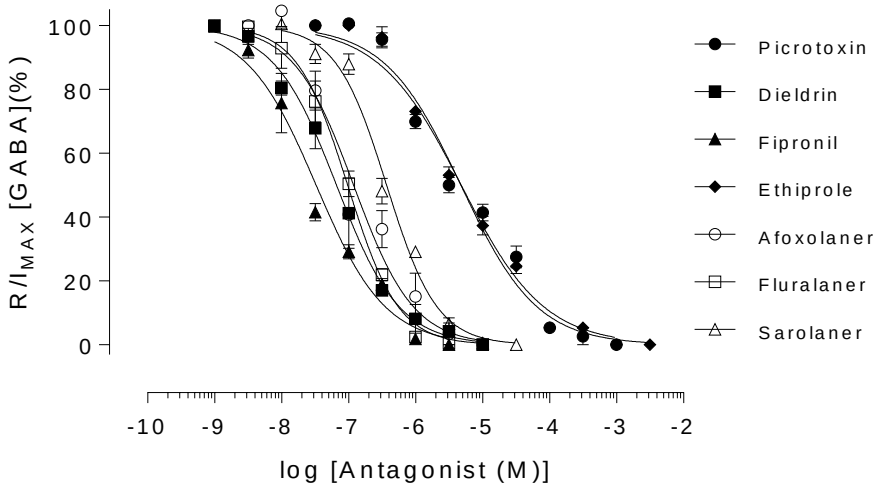


Figure 4.8. Antagonist concentration-inhibition curves for WT *C. felis* GABAR expressed in *X. laevis* oocytes. Antagonists were perfused over the oocyte in increasing concentrations and 1 mM GABA used to evoke inward currents every 2 minutes. R = response, I_{MAX} = maximal GABA response. n≥3 for each curve. Points are mean % of I_{MAX} ± SEM.

Table 4.3. Parameters derived from antagonist concentration-inhibition curves for WT *C. felis* GABAR.

Antagonist	IC_{50} (nM)	95% CI (µM)	Slope (± SD)	n
Picrotoxin	2699	0.92-6.51	-0.5 ± 0.13	3
Dieldrin	63.11	33.48-108.0	-0.9 ± 0.21	5
Fipronil	21.44	3.72-39.75	-0.6 ± 0.15	9
Ethiprole	4084	2.17-8.07	-0.5 ± 0.09	10
Afoxolaner	72.04	22.05-109.7	-0.8 ± 0.24	4
Fluralaner	99.59	72.41-133	-1.1 ± 0.15	4
Sarolaner	366.8	261.8-516.6	-1.1 ± 0.17	3

Following the application of antagonists to the GABAR, the receptor showed some recovery in GABA response following a period of Ringer application once the antagonists were removed (Figure 4.9). This suggests the inhibition caused by antagonists on the *C. felis* GABARbd was slow but reversible, with very little recovery to isoxazolines and fipronil. Pre-antagonist GABA response currents were not restored after 20 minutes of washing, as determined by pulse application of 1 mM GABA every 2 minutes in between washes.

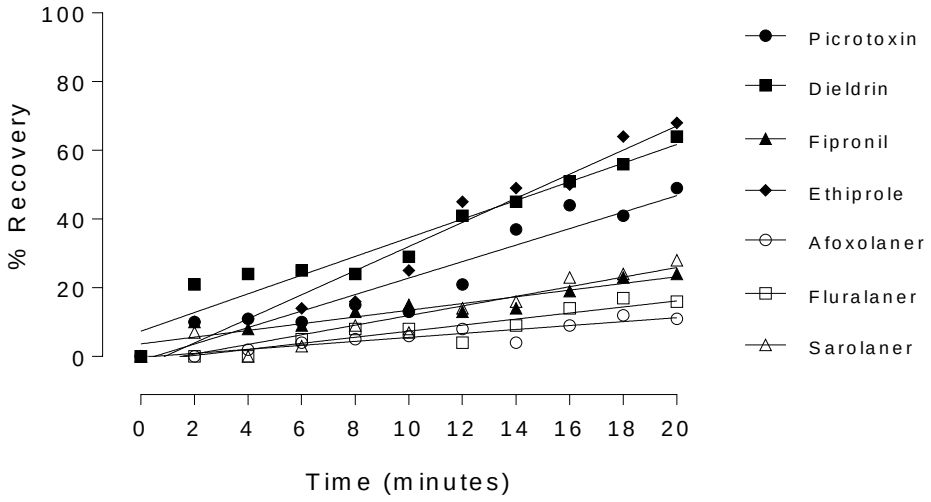


Figure 4.9. WT *C. felis* GABAR recovery after antagonist inhibition. Cells were pre-incubated with 300 nM (dieldrin, fipronil, afoxolaner, fluralaner, sarolaner) or 3 µM (picrotoxin and ethiprole) compound for 2 minutes. 1 mM GABA pulses were applied to the cell every 2 minutes up to 10 minutes with ringer wash in between applications of GABA. n=1 per curve. % recovery compared to 1 mM GABA in the absence of antagonists.

4.3.3. *C. felis* GABARbd mutant functional responses to GABA

For the *C. felis* mutant GABARs A301S, M354I and A301S + M354I, all formed functional receptors with EC_{50} values 143.1 µM, 75.57 µM and 406.2 µM respectively (Figure 4.10). The double mutant was 2-fold less sensitive to GABA in comparison to the WT whilst the M354I was 2-fold more responsive ($P<0.05$) (Table 4.4).

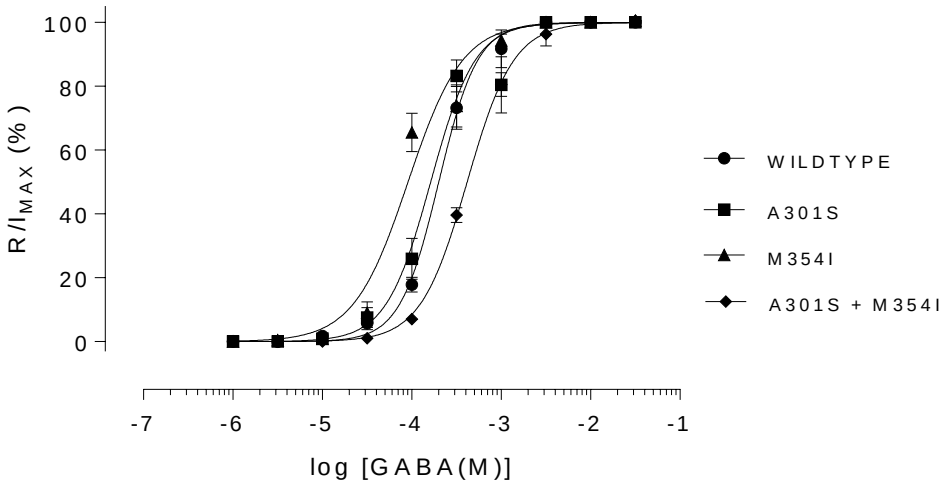


Figure 4.10. GABA concentration-response curves for WT, A301S, M354I and A301S.M354I GABAR *C. felis* GABARs expressed in *X. laevis* oocytes. R= response, I_{MAX} = maximal response to 1 mM GABA. Points are mean % of I_{MAX} ± SEM.

Table 4.4. Parameters derived from GABA concentration-response curves for WT, A301S, M354I and A301S + M354I *C. felis* GABARs.

GABA	EC_{50} (µM)	95% CI (µM)	Slope (± SD)	n
WT	177.5	165.8-204.5	2.2 ± 0.30	10
A301S	143.1	112.6-191	2.5 ± 0.57	10
M354I	75.57^{+}	59.01-101.5	1.7 ± 0.32	10
A301S + M354I	406.2^{+}	364.4-462	1.7 ± 0.14	9
**=significantly different to WT where P<0.05 in a two-sided F-test.*				
+=significantly different to WT where P<0.0001 in a two-sided F-test.				

4.3.4. Characterisation of the interactions of picrotoxin and dieldrin with the *C. felis* GABARbd with the A301S and M354I substitutions

Picrotoxin (PTX) is a polycyclic compound and a typical non-competitive antagonist of GABA receptors (Olsen, 2006). It is known to prevent ion flow through GABA chloride channels and was used here as a control for inhibition of the receptor expressed in oocytes. All four *C. felis* GABARs were inhibited by PTX (Figure 4.11) and the WT had an IC_{50} of 2.7 µM which is in the region of other published values for TEVC of GABARs, including those of *D. melanogaster* and *Varroa destructor* (Zhang et al., 1995, Price and Lummis, 2014, Lees et al., 2014b). The *C. felis* A301S channel was highly resistant to PTX (RR=226 with an IC_{50} of 611.4 µM). However, the M354I channel had an IC_{50} which was very similar to the WT (3.027 µM and 2.699 µM respectively) and statistically not significantly different. Unexpectedly, the A301S.M354I double mutant showed that the presence of the M354I substitution restored the receptor susceptibility in the A301S to PTX, reducing the RR from highly resistant to an RR of 2.4 (Table 4.5).

Dieldrin (DIEL) was used as a positive control because the A301S substitution in the GABAR has been found to cause insensitivity to DIEL in previous TEVC studies (Ffrench-Constant et al., 1993, Remnant et al., 2014). The *C. felis* GABARbd with A301S was completely resistant with an IC_{50} of >300 µM whilst the remaining three channels were inhibited (Figure 4.12). Once again, the M354I GABAR showed a similar sensitivity to the WT (IC_{50} 65.69 nM and 63.11 nM respectively) and the addition of the M354I restored the sensitivity in the double mutant, although it was still ~2.5-fold less sensitive than the WT (Table 4.5).

Interestingly, the data show that the recovery of the receptor from the little inhibition caused by DIEL was quicker in GABARs with the A301S substitution compared to the WT (Figure 4.11 and Figure 4.12). Slower recovery was reinstated with the introduction of the M354I

substitution. The Hill slope values for both antagonists fall within a normal range of 0 to -2 (Table 4.5).

Table 4.5. Parameters derived from picrotoxin and dieldrin concentration-inhibition curves for WT, A301S, M354I and A301S.M354I *C. felis* GABARs.

Picrotoxin	**IC_{50} (µM)**	**95% CI (µM)**	**Slope (± SD)**	**n**
WT	2.699	0.92-6.51	-0.5 ± 0.13	3
A301S	611.4+	318.8-1147	-0.5 ± 0.11	3
M354I	3.027	2.12-4.31	-0.6 ± 0.08	4
A301S.M354I	6.588*	0.85-15.37	-0.5 ± 0.14	3
Dieldrin	**IC_{50} (nM)**	**95% CI (µM)**	**Slope (± SD)**	**n**
WT	63.11	33.48-108.0	-0.9 ± 0.21	5
A301S	Ambiguous+	0-13.96x10^8	-1.5 ± 1.4	6
M354I	65.69	51.24-83.34	-1.3 ± 0.17	5
A301S.M354I	166.2*	131.6-209.8	-1.4 ± 0.19	5

**=significantly different to WT where P<0.05 in a two-sided F-test.*

+=significantly different to WT where P<0.0001 in a two-sided F-test.

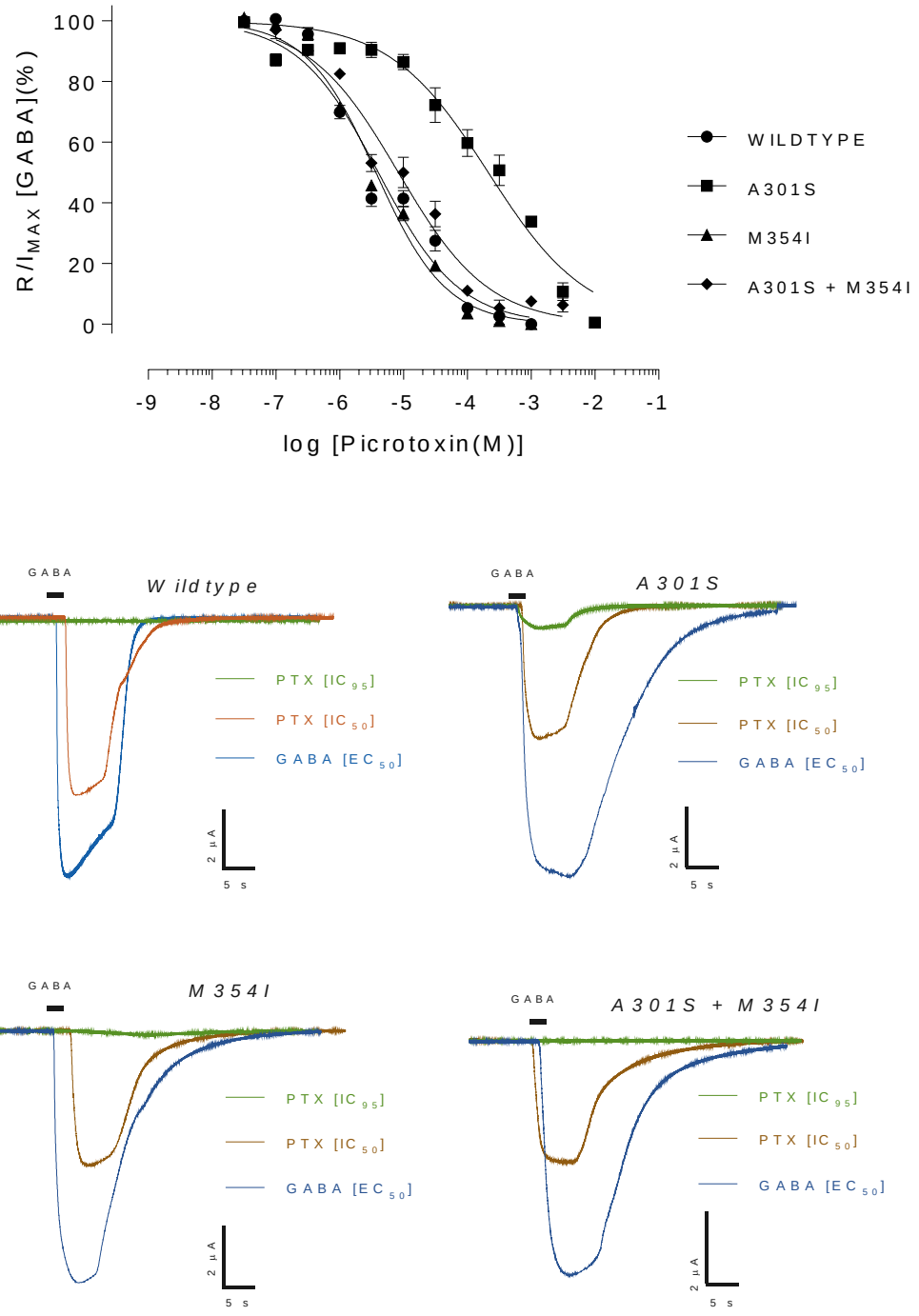


Figure 4.11. Above: Picrotoxin (PTX) concentration-inhibition curves for WT and mutated *C. felis* GABAR. R= response, I_{MAX} = maximal response to 1 mM GABA. Below: TEVC traces show GABA EC_{50} current and the inhibited PTX IC_{50} and IC_{95} response. Points are mean % of I_{MAX} ± SEM.

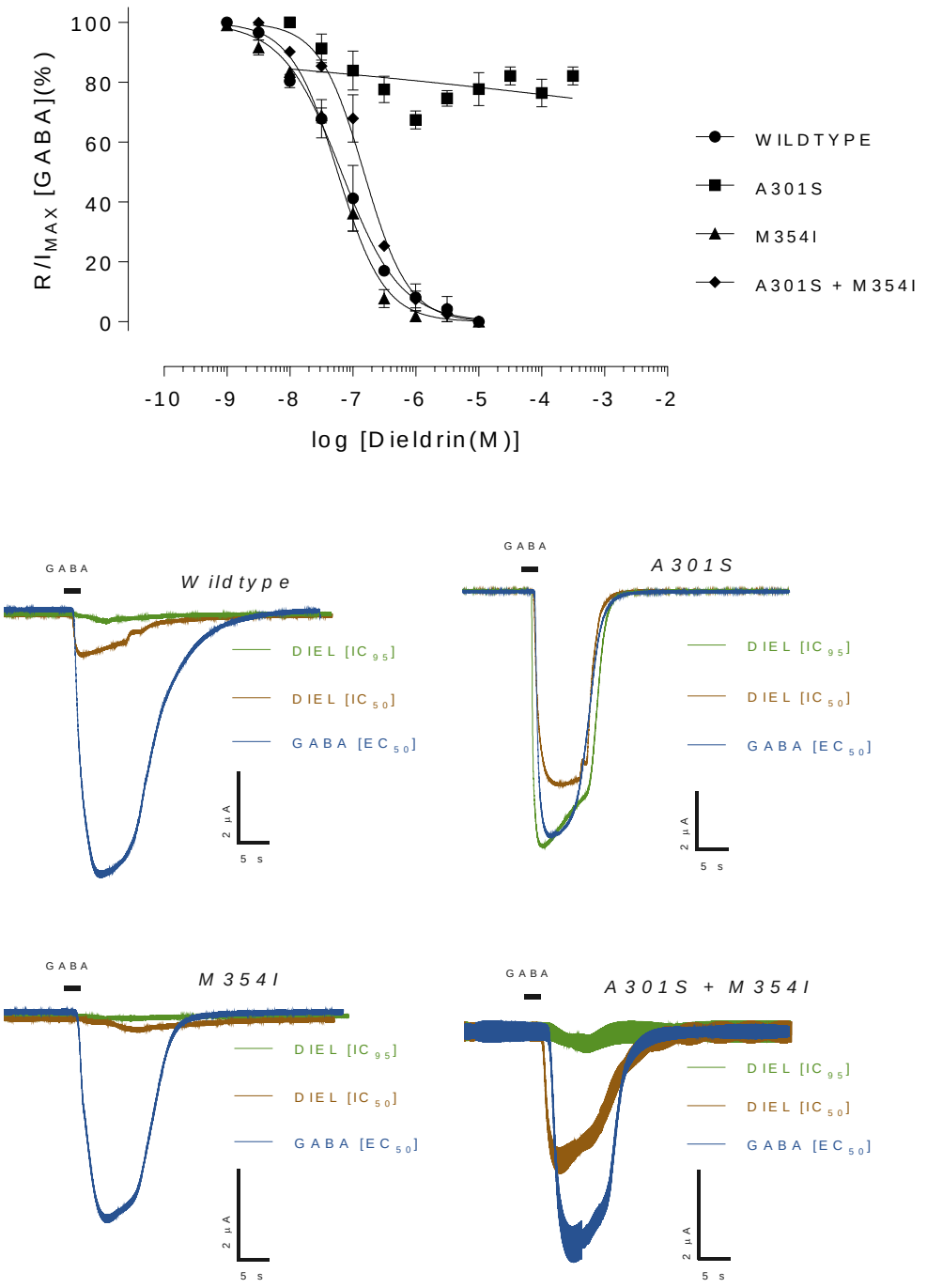


Figure 4.12. Above: Dieldrin (DIEL) concentration-inhibition curves for WT and mutated *C. felis* GABAR. R= response, I_{MAX} = maximal response to 1 mM GABA. Below: TEVC traces show GABA EC_{50} current and the inhibited DIEL IC_{50} and IC_{95} response. Points are mean % of I_{MAX} ± SEM.

4.3.5. Characterisation of the interactions of phenylpyrazoles with the *C. felis* GABARbd with the A301S and M354I Substitutions

TEVC experiments showed that both fipronil (FIP) and ethiprole (ETH) inhibited the WT *C. felis* GABARbd expressed in oocytes (Figure 4.13, Figure 4.14), which might be expected given that they are structurally similar. However, there was a factor of 200 difference in potency between the two compounds with the FIP IC_{50} values in the nM range and the ETH IC_{50}s in the µM range (Table 4.6). TEVC studies of the effect of fipronil on the *C. felis* GABARbd have not been published, however, the values here are in a similar nm range to the stem borer *Chilo suppressalis* (Sheng et al., 2018b). However, the WT receptor tested here was more sensitive to fipronil than N. *lugens* and *Anopheles gambiae* GABA channels which had IC_{50} values of 1.8 µM and 410 nM respectively (Taylor-Wells et al., 2018, Garrood et al., 2017).

For both FIP and ETH, the M354I GABAR had a similar IC_{50} to the WT, with only a slight hypersensitivity to both compounds (~1.5-2 fold). For the A301S channel there was a significantly higher IC_{50} value for both compounds compared to the WT, with a ~50-fold difference for FIP and a ~200-fold difference for ETH. The channel was completely `inhibited by 1 mM FIP, however, concentrations higher than 0.1 mM for ETH had no effect on the channel. The currents in response to GABA, after pre-treatment with FIP also showed that higher concentrations led to a longer wash time to return to the baseline after removal of GABA on the channel with the A301S substitution and the traces were consistently shaky and unstable (Figure 4.13, below). The A301S.M354I channel showed restored susceptibility to FIP with much lower resistance ratios (RR=8.2) and ETH (RR= 2.7).

Table 4.6. Parameters derived from fipronil and dieldrin concentration-inhibition curves for WT, A301S, M354I and A301S.M354I *C. felis* GABARs.

Fipronil	**IC_{50} (nM)**	**95% CI (nM)**	**Slope (± SD)**	**n**
WT	21.44	3.72-39.75	-0.6 ± 0.15	9
A301S	1243^{+}	681-1434	-0.1 ± 0.07	10
M354I	14.81^{+}	8.51-20.42	-0.6 ± 0.30	9
A301S.M354I	176.2^{+}	131.1-226.8	-1.3 ± 0.20	8
Ethiprole	**IC_{50} (µM)**	**95% CI (nM)**	**Slope (± SD)**	**n**
WT	4.084	2.17-8.07	-0.5 ± 0.09	10
A301S	744.9^{+}	426.6-1505	-0.3 ± 0.03	11
M354I	2.298^{+}	0.99-7.04	-0.4 ± 0.10	8
A301S.M354I	11.14*	11.42-41.42	-0.6 ± 0.22	8

**=significantly different to WT where P<0.05 in a two-sided F-test.*

+=significantly different to WT where P<0.0001 in a two-sided F-test.

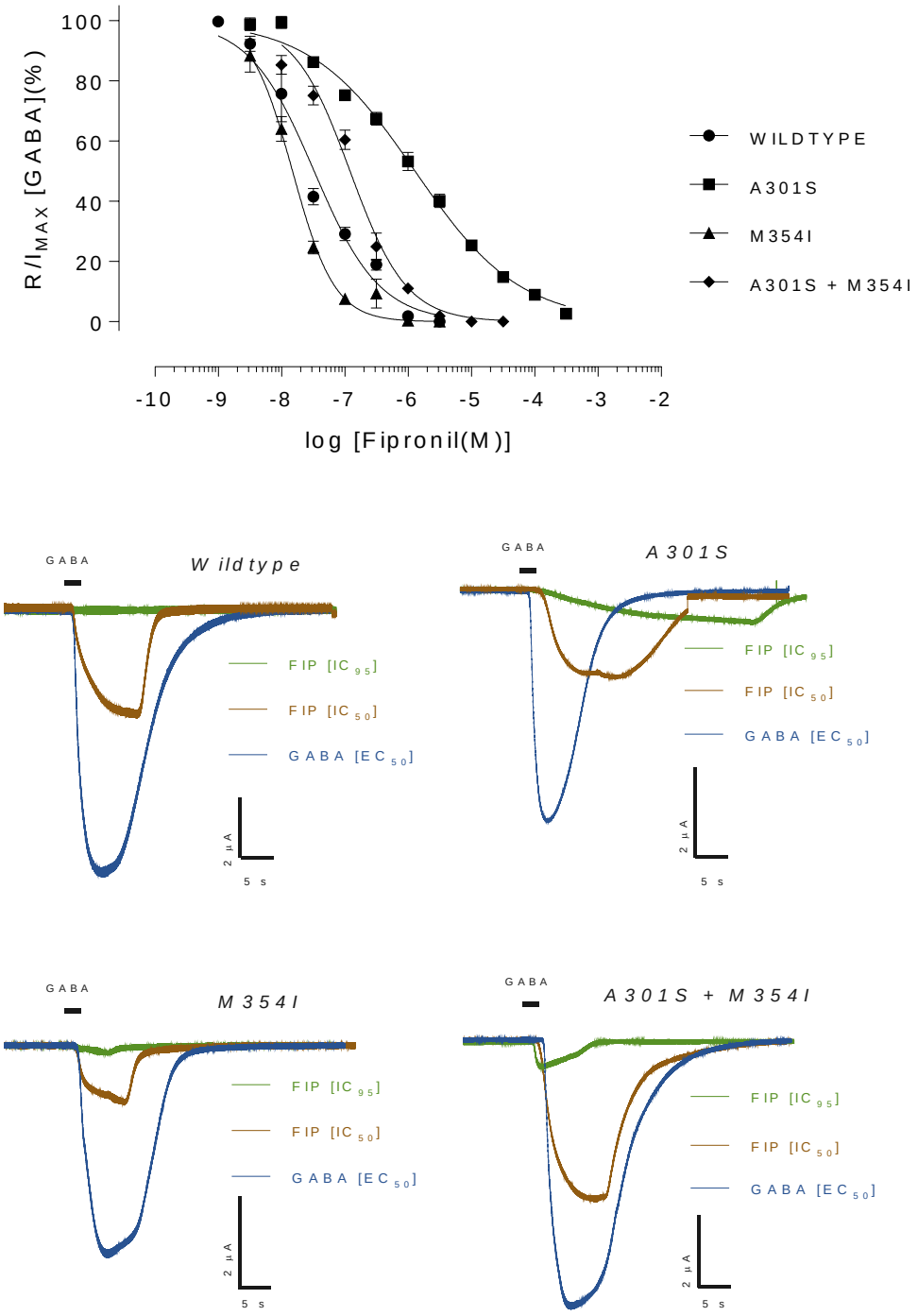


Figure 4.13. Above: Fipronil (FIP) concentration-inhibition curves for WT and mutated *C. felis* GABAR. R= response, I_{MAX} = maximal response to 1 mM GABA. Below: TEVC traces show GABA EC_{50} current and the inhibited PTX IC_{50} and IC_{95} response. Points are mean % of I_{MAX} ± SEM.

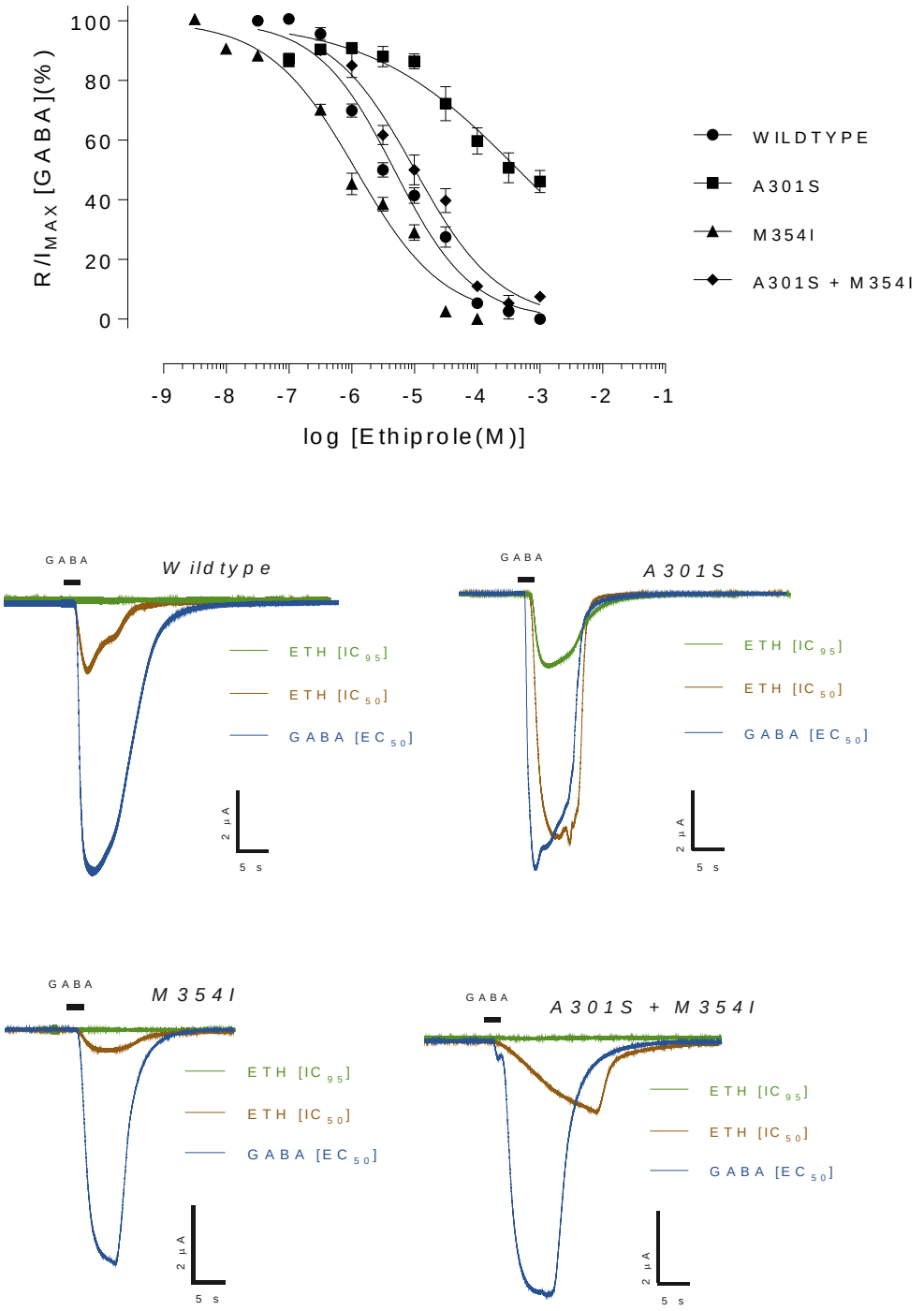


Figure 4.14. Ethiprole (ETH) concentration-inhibition curves for WT and mutated *C. felis* GABAR. R= response, I_{MAX} = maximal response to 1 mM GABA. Below: TEVC traces show GABA EC_{50} current and the inhibited PTX IC_{50} and IC_{95} response. Points are mean % of I_{MAX} ± SEM.

4.3.6. Recovery of *C. felis* GABARbd after removal of antagonists

An area under the curve (AUC) analysis was used to determine the recovery of the receptor, as this also incorporated the time taken to return to a baseline value, after the removal of GABA, which is not accounted for in a peak response analysis. The results showed that for the WT, M354I and A301S.M354I channels, recovery from all the antagonists was uniform. For the A301S channel recovery was faster after treatment with DIEL or ETH but the traces were much shallower and recovery was slower in response to FIP as shown in the current traces in Figure 4.12, Figure 4.13 and Figure 4.14.

Further analysis of the recovery rates of the A301S GABAR receptor compared to the WT GABAR was done by applying the antagonists to the cell and recording the percentage recovery over time (Figure 4.15). In comparison to the WT, the A301S receptor showed accelerated attenuation of inhibition for FIP, DIEL and ETH with a clear increase in dissociation from the receptor in response to DIEL and ETH.

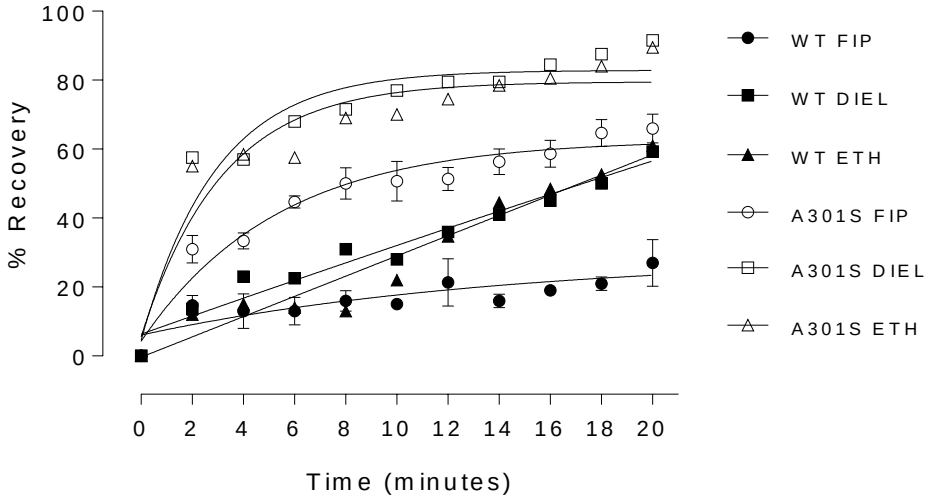


Figure 4.15. WT and A301S *C. felis* GABAR recovery after FIP, DIEL and ETH inhibition. Cells were pre-incubated with 300 nM FIP/DIEL or 3 µM ETH for 2 minutes, then washed with Ringer's solution. 1 mM GABA pulses were applied to the cell every 2 minutes up to 20 minutes. n=3/curve. % recovery compared to 1 mM GABA in the absence of antagonists. Points are mean % of I_{MAX} ± SEM.

4.3.7. Characterisation of the A301S and M354I *C. felis* GABARbds receptors with isoxazolines

The *C. felis* receptors A301S, M354I and A301S.M354I were tested with three isoxazolines, afoxolaner, fluralaner and sarolaner (Table 4.7, Figure 4.16, Figure 4.17 and Figure 4.18). The WT receptor was susceptible to all three compounds in the nM range, with sarolaner being the least effective. The introduction of the A301S substitution gave slightly decreased sensitivity (RR<5) but no cross-resistance and the M354I channel was ~10-fold hypersensitive to the compounds. The A301S.M354I channel had an IC_{50} similar to the WT for afoxolaner, but was ~3-fold more sensitive to fluralaner and ~6-fold more sensitive to sarolaner.

Table 4.7. Parameters derived from isoxazoline concentration-inhibition curves for WT, A301S, M354I and A301S.M354I *C. felis* GABARs.

Afoxolaner	**IC_{50} (nM)**	**95% CI (nM)**	**Slope (± SD)**	**n**
WT	72.04	22.05-109.7	-0.8 ± 0.24	4
A301S	246.6*	142.7-333.8	-0.7 ± 0.13	3
M354I	8.167^{+}	5.62-11.05	-1.0 ± 0.12	4
A301S + M354I	71.84*	55.15-88.57	-1.5 ± 0.18	5
Fluralaner	**IC_{50} (nM)**	**95% CI (nM)**	**Slope (± SD)**	**n**
WT	99.59	72.41-133	-1.1 ± 0.15	4
A301S	164.5^{+}	77.43-272.8	-0.8 ± 0.16	3
M354I	8.967^{+}	7.51-10.59	-1.3 ± 0.12	5
A301S + M354I	30.09^{+}	17.53-43.61	-0.7 ± 0.11	4
Sarolaner	**IC_{50} (nM)**	**95% CI (nM)**	**Slope (± SD)**	**n**
WT	366.8	261.8-516.6	-1.1 ± 0.17	3
A301S	445.1*	318-609.9	-1.1 ± 0.16	4
M354I	24.94^{+}	21.05-29.23.	-1.7 ± 0.19	3
A301S + M354I	54.93^{+}	36.57-76.32	-1.0 ± 0.15	5

**=significantly different to WT where P<0.05 in a two-sided F-test.*

$^{+}$=significantly different to WT where P<0.0001 in a two-sided F-test.

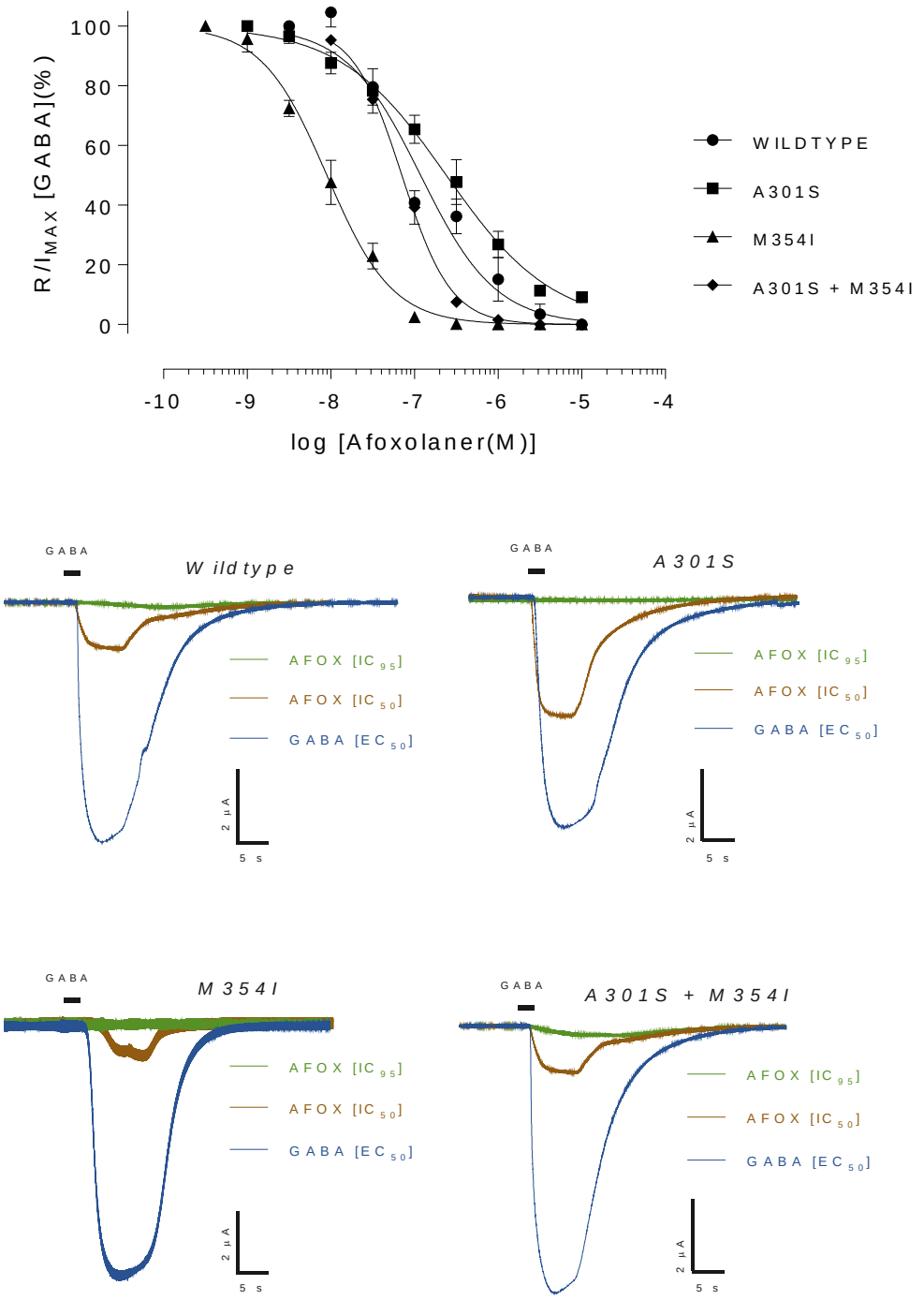


Figure 4.16. Above: Afoxolaner (AFOX) concentration-inhibition curves for WT and mutated *C. felis* GABARs. R= response, I_{MAX} = maximal response to 1 mM GABA. Below: TEVC traces show GABA EC_{50} current and the inhibited AFOX IC_{50} and IC_{95} response. Points are mean % of I_{MAX} ± SEM.

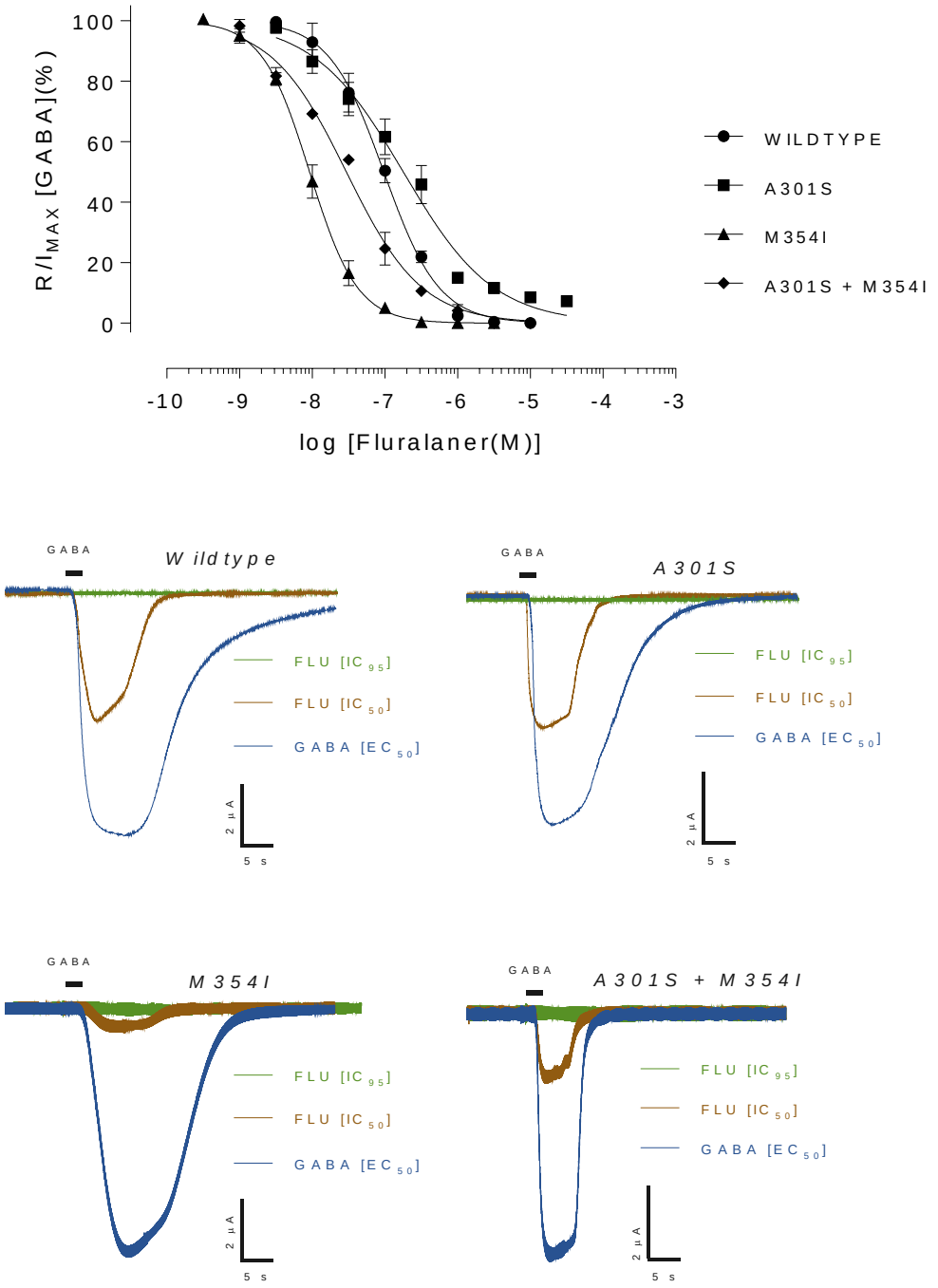


Figure 4.17. Above: Fluralaner (FLU) concentration-inhibition curves for WT and mutated *C. felis* GABARs. R= response, I_{MAX} = maximal response to 0.3 mM GABA. Below: TEVC traces show GABA EC_{50} current and the inhibited FLU IC_{50} and IC_{95} response. Points are mean % of I_{MAX} ± SEM.

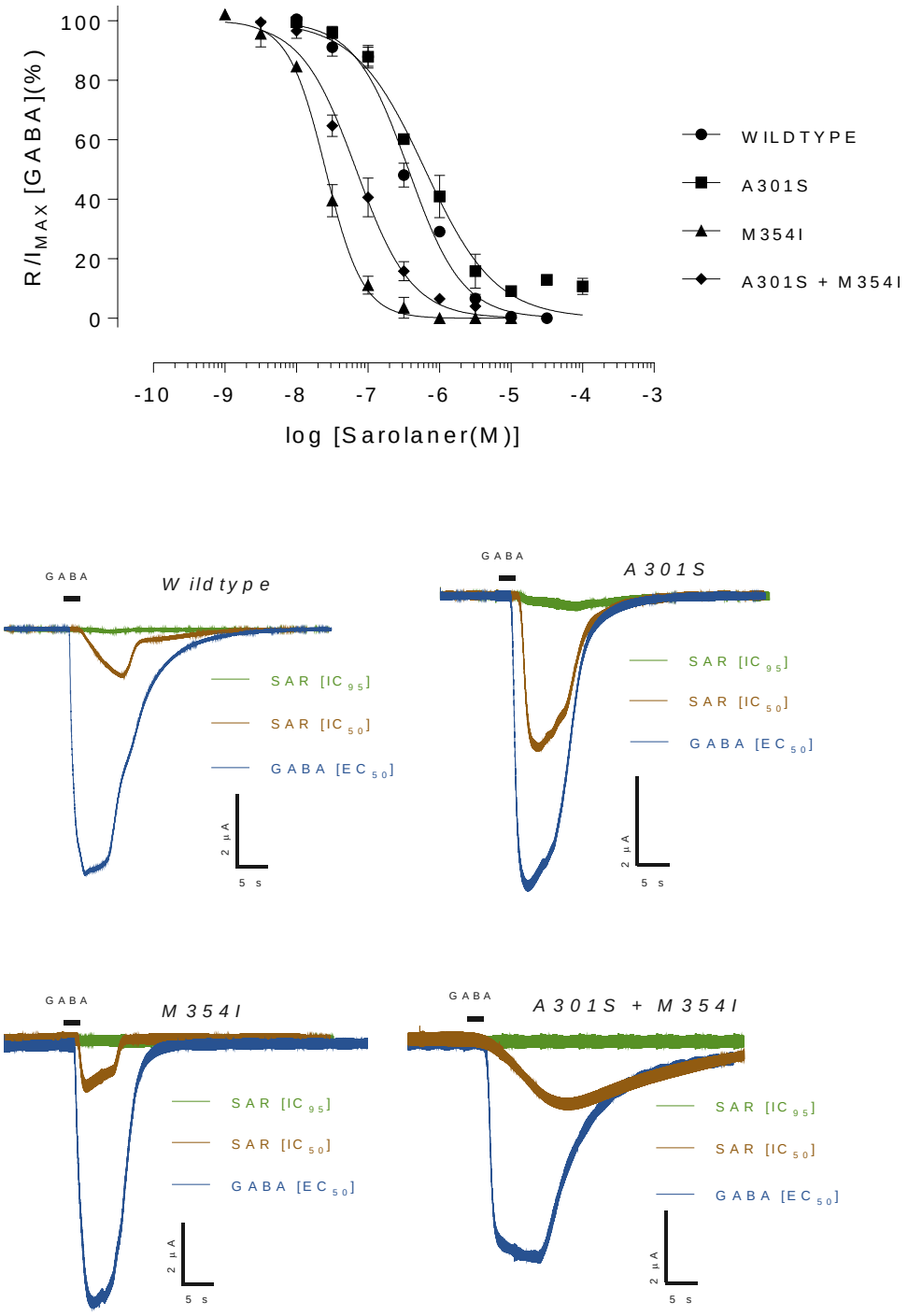


Figure 4.18. Above: Sarolaner (SAR) concentration-inhibition curves for WT and mutated *C. felis* GABARs. R= response, I_{MAX} = maximal response to 1 mM GABA. Below: TEVC traces show GABA EC_{50} current and the inhibited SAR IC_{50} and IC_{95} response. Points are mean % of I_{MAX} ± SEM.

4.4. Discussion

In this chapter, the amino acid substitutions which have been associated with resistance to phenylpyrazoles in lab strains of *C. felis* were introduced into the *C. felis* GABARbd receptor and TEVC functional studies used to determine their effect on interactions with several GABAergic antagonists.

The point mutation causing the A301S substitution was first shown to cause resistance to cyclodienes in *D. melanogaster* (Ffrench-Constant et al., 1993) and subsequently found in a range of other species. Dieldrin resistance in the *C. felis* GABAR has been shown to be attributable to the presence of a A301S substitution both *in vivo* (Bass et al., 2004, Daborn et al., 2004) and *in vitro* (Gassel et al., 2014), however, the link has never been clearly established in the *C. felis* GABAR as cyclodienes were not used for flea control unlike many of the insects and acari that carry the mutation. The experiments reported here confirmed this link. However, the cross-resistance to ethiprole found in the present study is a novel finding, and is consistent with a similar situation in the *N. lugens* and *Laodelphax striatellus* GABAR with the A301S mutation (Garrood et al., 2017, Sheng et al., 2018a). Although structurally similar to fipronil, ethiprole was a factor of 200 less potent on the *C. felis* GABAR, although this was not seen in planthoppers (Garrood et al., 2017, Sheng et al., 2018a). These findings can explain why ethiprole is not marketed as a flea control product but is used for the control of planthoppers. Further comparative sequence analyses of the two channels could highlight residues that are key for ethiprole binding to different insect GABARs.

The A301S substitution in GABARs has been shown to confer some low-level cross-resistance to fipronil and ethiprole in certain insect species, including ~14-fold (Cole et al., 1995) and ~73-fold (Cole et al., 1995, Remnant et al., 2014) in *D. melanogaster*. TEVC has also shown that the *D. melanogaster* GABAR with the A301S substitution had an IC_{50} ~5-fold higher than the WT for fipronil (Hosie et al., 1995), and cell line mutagenesis and membrane potential assays on the *Sogatella*

furcifera GABAR showed high levels of fipronil resistance in cell lines associated with the A301S substitution (Nakao et al., 2012). In contrast, other studies on *N. lugens*, *D. melanogaster* and *Heliothis virescens* GABARs found no difference in fipronil potency from the WT (Wolff and Wingate, 1998, Garrood et al., 2017). More recently, the WT and A301S *C. felis* GABARs have been expressed in HEK cells, showing that the substitution gave a ~20-fold reduction in the effectiveness of fipronil (Gassel et al., 2014). Thus, attempts to determine the relative effects of fipronil and ethiprole on insect GABARs and whether there is cross-resistance have been inconsistent. For TEVC studies this could be attributed to differing application protocols as well as the use of different isoforms of the GABAR. In the TEVC experiments reported here, a ~60-fold difference in fipronil efficacy between the *C. felis* WT and A301S GABARbds was seen, but it is important to note that there was full inhibition of the channel with the A301S substitution at 1 mM, which is inconsistent with the resistance shown in the *in vivo* bioassays where an increase in concentration did not increase toxicity. This implies there could be additional mechanisms of resistance.

This highlights the caution needed when trying to extrapolate between *in vitro* mutagenesis/electrophysiology experiments and *in vivo* whole insect effects shown in bioassays and in the field. However, mutagenesis/TEVC does allow detailed studies on the pharmacology of receptors which can be used to hypothesise how a mutation might affect function. For example, previously proposed mechanisms of resistance to cyclodienes and PTX, associated with the GABAR A301S substitution include structural alteration of the binding site and allosteric modulation (Zhang et al., 1994), or the favoured and accelerated recovery from antagonist application in response to convulsant compounds (Le Goff et al., 2005), which was tested and confirmed in the present study.

It has been suggested that convulsant compounds such as DIEL, PTX and FIP bind preferentially to agonist-bound receptors and stabilise the open state conformation (Dillon et al., 1995, Inoue and Akaike, 1988,

Yamamoto et al., 2012). This is supported by the experiments reported here, where there was a negligible reduction of GABA responses on the WT *C. felis* GABARbd with a co-application protocol of the antagonist and GABA. Le Goff et al. (2005) reported that repeated applications of GABA, in the presence of FIP, on the WT *Drosophila simulans* GABAR increased inhibition of the channel 23-fold. In the same channel with the A301G substitution, there was a limited effect, suggesting that the change reduces the accumulated potency of the insecticide. Repeated application and prolonged exposure to GABA drives the receptor into a desensitised state and the A301S (and A301G) substitution is hypothesised to destabilise the desensitised GABAR (Chang et al., 2002) causing a change to the antagonist's preferred open conformation of the receptor leading to reduced inhibition and hence resistance. This has been supported by patch-clamp electrophysiology, where it was found A301S causes net destabilisation of the receptor and prevents inhibition (Zhang et al., 1994). Although the current study did not look at prolonged GABA exposure, the Hill slope for the *C. felis* A301S curve was particularly shallow for FIP implying negative cooperativity and impeded binding, leading to reduced inhibition of the channel with additional GABA applications. This shallow curve was also seen for the DIEL and ETH resistant A301S GABAR.

In the present study the M354I *C. felis* GABAR had significant levels of hypersensitivity compared to the WT receptor; ~2-fold for the phenylpyrazoles and ~10-fold for the isoxazolines. This is the opposite effect to that seen for the A301S receptor and could be altering the binding site to encourage docking of antagonists. It could also be that it stabilises the desensitised closed-state receptor, encourages convulsant binding to a preferred GABAR conformation and slows down recovery of the receptor, this might be resolved by doing a dissociation analysis. There is little evidence of increased sensitivity in the GABAR associated with an amino acid substitution and this is probably because any mutation that did this would incur a fitness cost and not be subject to selection. There is one example where the binding site of the *V.*

destructor GABAR had a ~4-fold increased sensitivity to PTX with the introduction of an A210Q substitution in the M2 region of the receptor (Price and Lummis, 2014). For *C. felis*, the M354I substitution is only found in combination with A301S in the GABAR, where it restores sensitivity in channels where the A301S on its own reduces sensitivity to compounds. The presence of resistance-associated mutations co-existing with A301S is a key finding and has been reported in a number of other insect GABARs including V327I in *Anopheles funestas* (Wondji et al., 2011), T350M in *D. simulans* (Le Goff et al., 2005), R300Q in *N. lugens (Zhang et al., 2016)* and R340Q in *S. furcifera* (Nakao et al., 2012). However, for these pairs of substitutions, there is usually an additive effect on fipronil insensitivity rather than the reversal of sensitivity seen in *C. felis*.

So how does M354I act in *C. felis*? The substitution may be caused by a random SNP with no functional role in resistance or insensitivity, however, the presence of the amino acid change in resistant populations and that two separate codons were found makes this unlikely. Therefore, there could be a number of other reasons explaining the unexpected results here. Firstly, it could compensate for fitness costs of the A301S alone. However, A301S alone has been shown to persist in populations at high frequency without chemical selection indicating there is little, if any, fitness cost (Ffrench-Constant et al., 1993). Secondly, the increased frequency of M354I could result from physical linkage and genomic hitchhiking to the A301S. However, this seems unlikely given that the TEVC studies show a reversal of the adaptive advantage that A301S provides to the insect. Lastly, there could be metabolic resistance also present in *C. felis*, that complicates the effects of the target site changes. Much of the target-site resistance testing associated with A301S is inconsistent, with contradictory results suggesting there are other mechanisms at play. The interaction of detoxification and the A301S GABAR has been tested in *N. lugens*, where the use of synergists has implicated a metabolic component (Zhang et al., 2016). Therefore,

the up-regulation of P450's could play a role in the fipronil resistance seen in lab strains of *C. felis* containing target site changes.

Since their launch in 2013, the isoxazolines have proved to be effective both *in vivo* and *in vitro*, and this is further endorsed by the results presented here. There is no record of cross-resistance associated with this group of chemicals. In addition to this, these chemicals target both fleas, ticks and mites as well as having a highly effective systemic mode of action and an excellent safety profile. The lucrative nature of companion animal veterinary products dictates that there is continuous development and advancement of treatment, however, with the addition of so many new compounds, the monitoring of flea populations is key. A single resistance mechanism to any of the isoxazolines used in rotation could lead to cross-resistance across the entire chemistry.

4.5. Conclusions

A301S and M354I substitutions in the GABAR were identified in fipronil-resistant *C. felis* and the effect on the functionality of the receptor in response to antagonists was tested. The presence of A301S was found to confer ethiprole and dieldrin resistance as well as reduced susceptibility to fipronil and picrotoxin. The M354I substitution was found to confer increased sensitivity to fipronil, ethiprole and the isoxazolines. When found together there was a reversal of resistance and susceptibility to all compounds was restored to WT levels. The results strongly suggest that M354I does not play a significant role in conferring resistance to fipronil or any of the antagonists tested here. It is likely there are other unknown resistance mechanisms present and the most likely is some form of increased metabolism.

5. *In vivo* study of *C. felis* GABAR mutations introduced into *D. melanogaster*

5.1. Introduction

In the previous chapter, candidate resistance mutations, responsible for A301S and M354I substitutions were introduced into the *C. felis* GABAR and tested *in vitro* to determine whether they changed the conformation of the ion channel and altered their sensitivity to phenylpyrazoles. However, the two mutations in combination did not cause a recordable difference in the electrophysiological experiments described in Chapter 4. Since they are found at high frequency in certain *C. felis* populations, it was decided to test them in an alternative system by using transgenic methods to introduce them into the *D. melanogaster* GABAR and test the resulting phenotype.

5.1.1. φC31 integration and the GAL4/UAS systems

The *P*-element-mediated germ-line transformation system in *D. melanogaster* has been used to generate mutations and deletions in germline cellular DNA by utilising transposable elements (Rubin and Spradling, 1982). This method was further optimised by Bischof et al. (2007), with the φC31 integrase-mediated system, where precisely mapped *attP* sites act as the site for integration of exogenous DNA sequences. In this system, the φC31 integrase mediates recombination between *attP* docking sites and an *attB*-containing plasmid (pUAST), leading to the integration of the whole plasmid. An endogenous source of the φC31 integrase, introduced using the P-element transposable system, circumvents the need for co-injecting a φC31 plasmid and increases the percentage of successful integration (Bischof et al., 2007). In addition, stable transformation success rates can also be increased by using a germline-specific promoter such as *vasa* to drive the expression of the *φC31* gene. Genes cloned into the pUAST are expressed under the

control of the GAL4/UAS system. Stable lines carrying the pUAST plasmid with the gene of interest are crossed with GAL4 lines, which express this transcriptional activator under the control of endogenous regulatory sequences. In the progeny of these crosses, GAL4 will bind to the upstream activation sequence (UAS) and induce expression of the gene of interest. This binary system can be used to spatio-temporally control gene expression as thousands of GAL4 lines have been generated and are now publicly available (Jenett et al., 2012). The pUAST plasmid utilises the hsp70 promotor downstream of the UAS, the expression of which is induced under elevated temperatures and plays a role in regulation of heat shock (Petersen and Lindquist, 1989).

This chapter reports the use of φC31 integrase-mediated transgenesis and the GAL4/UAS systems to introduce the mutations of interest into the *GABAR* gene of *D. melanogaster* to assess the effects of the substitutions on the toxicity of phenylpyrazoles in bioassays.

5.2. Methods

5.2.1. Sub-cloning of the *D. melanogaster* GABAR

The DNA sequence encoding the *D. melanogaster* GABAR (bd splice variant- 1821 bp) was codon optimised for improved protein expression and synthesised by GeneArt (Invitrogen) in pMK vector (2393 bp) with a kanamycin resistance marker and an added Kozak consensus sequence (GCCACC) immediately upstream of the start codon to improve translational efficacy. The full sequence can be found in Appendix 5.

The lyophilised DNA (5 µg) was centrifuged, resuspended in 50 µL of nuclease-free water to give a 100 ng/µL solution. 10 µL was used in a restriction digest using *Bgl*II FastDigest Enzyme and run on a gel. The GABARbd insert was cut out of the gel and purified.

The GABARbd DNA was then sub-cloned into the UAS/GAL4 expression vector, pUASTattB (8904 bp) with an attB φ31 integrase-mediated transgenesis landing site and an ampicillin resistance marker. 1 µg of each of the GABARbd DNA and the pUAST vector were digested and linearised with *Bgl*II and *Xbal*I and run on a gel and the GABARbd and pUAST vector bands were cut out of the gel and purified. A T4 ligation reaction contained ~25 ng of ligated GABARbd DNA and ~75 ng of ligated pUAST and was incubated overnight. Ligation was confirmed by gel electrophoresis (~11 Kb band). The ligated plasmid DNA was transformed into Agilent Technologies XL10-Gold Ultracompetent Cells and plated onto an ampicillin plate incubated at 30°C. A colony PCR was carried out with pUAST forward (GAATAGGGAATTGGGAATTCG) and reverse (CTGTAGGTAGTTTGTCCAATTA) primers and run on a gel. Colonies with the GABARbd insert were propagated in liquid culture and the resulting samples were purified with the QIAGEN QIAprep Spin Miniprep Kit.

5.2.2. Site-directed mutagenesis and transformation

Primers for site directed mutagenesis of the *D. melanogaster* GABARbd were designed according to Agilent QuikChange II XL Site-Directed Mutagenesis guidelines and purchased from Sigma-Aldrich. This introduced the A301S, M354I and the double A301S and M354I (A301S.M354I) substitutions into the *D. melanogaster* GABARbd. (Table 5.1).

Table 5.1. Oligonucleotide primers used for site-directed mutagenesis of *D. melanogaster* GABARbd to introduce A301S and M354I substitutions and primers used for sequencing to verify the mutation of the DNA.

	Forward Primer (5'-> 3')	**Reverse Primer (5'-> 3')**
A301S primer	CCGGCGCGTGTG*TCG*CTCGG TGTGACA	TGTCACACCGAG*CGA*CACA CGCGCCGG
M354I primer	GCCACGGTCGGCTAC*ATT*GC AAAACGAATT	AATTCGTTTTGC*AAT*GTAGC CGACCGTGGC
Sequencing primers	GCCTGCGAAATTCAGTTCGT GC	TCCAACGCCCACTCCTCCGG GT
	Red italicised bases deviate from WT sequence	

The mutagenesis was carried out using the *D. melanogaster* GABARbd gene in the pMK vector. The reactions and PCRs were done according to the manufacturers protocol, transformed with Agilent Technologies XL10-Gold Ultracompetent Cells and plated out on ampicillin agar plates and incubated overnight at 37°C. Colonies were picked and a PCR carried out using the sequencing primers (Table 5.1). The PCR products were sequenced with the same primers to confirm the introduction of the mutations. Positive samples were propagated in liquid culture and the resulting samples were purified with the QIAGEN QIAprep Spin Miniprep Kit. The samples were then subcloned into the pUAST vector as described above in 5.2.1. All four plasmid constructs were precipitated using ethanol, dried and resuspended in sterile water to a 600 ng/ µL concentration. The mix for injections for germline

transformation was prepared from 5 µL of plasmid, 2.5 µL of phosphate buffer and 2.5 µL of 200 mg/L fluorescein sodium salt to aid injection.

5.2.3. *D. melanogaster* rearing

D. melanogaster strains were maintained in Dutscher Scientific narrow vials with 7 mL of Bloomington NutriFly fly food (with Nipagin and propionic acid). Stocks were stored at 17 °C, and maintained by anaesthetising flies with $C0_2$ and transferring ~15 adults to new vials every 2 weeks. Virgin female *D. melanogaster* for crosses were collected within 8 hours of emergence.

5.2.4. Crossing strategy for *D. melanogaster* injection line

An integration stock purchased from the University of Cambridge Fly Facility had the φC31 integrase under the *vasa* promotor marked with *RFP* (red fluorescence protein) on chromosome X, the attP landing site on chromosome 2 marked with *yellow+* eye colour marker and was *Wild Type* (+) on chromosome 3 (#1320 genotype: *RFP:vas:int/RFP:vas:int; attp40/attp40; +/+*). The GABAR knockout line was purchased from Bloomington Drosophila Stock Centre and had a GABA knockout over *Stubble* (*Sb*- short blunt bristles) on chromosome 3 (#1687 genotype: *+/+; +/+; GABAR⁻/Sb*). A double balancer line was supplied by D. Finnegan (University of Edinburgh) and had the markers *Sternum plural* (*Sp*- multiple bristles on the sternum near the leg) over *Curly* (*Cy*- curled-up wings) on chromosome 2, and *Sb* over *Tubby-humeral* (*Tb-Hu*- short larvae and adults, and increased number of humeral bristles) on chromosome 3 (#91 genotype: *+/+; Sp/Cy; Sb/Tb-Hu*). To create a *D. melanogaster* stock for φ31 integrase-mediated transgenesis, a GABAR knockout strain with an attp40 integration site and integrase was made using the crossing strategy outlined in Figure 5.1.

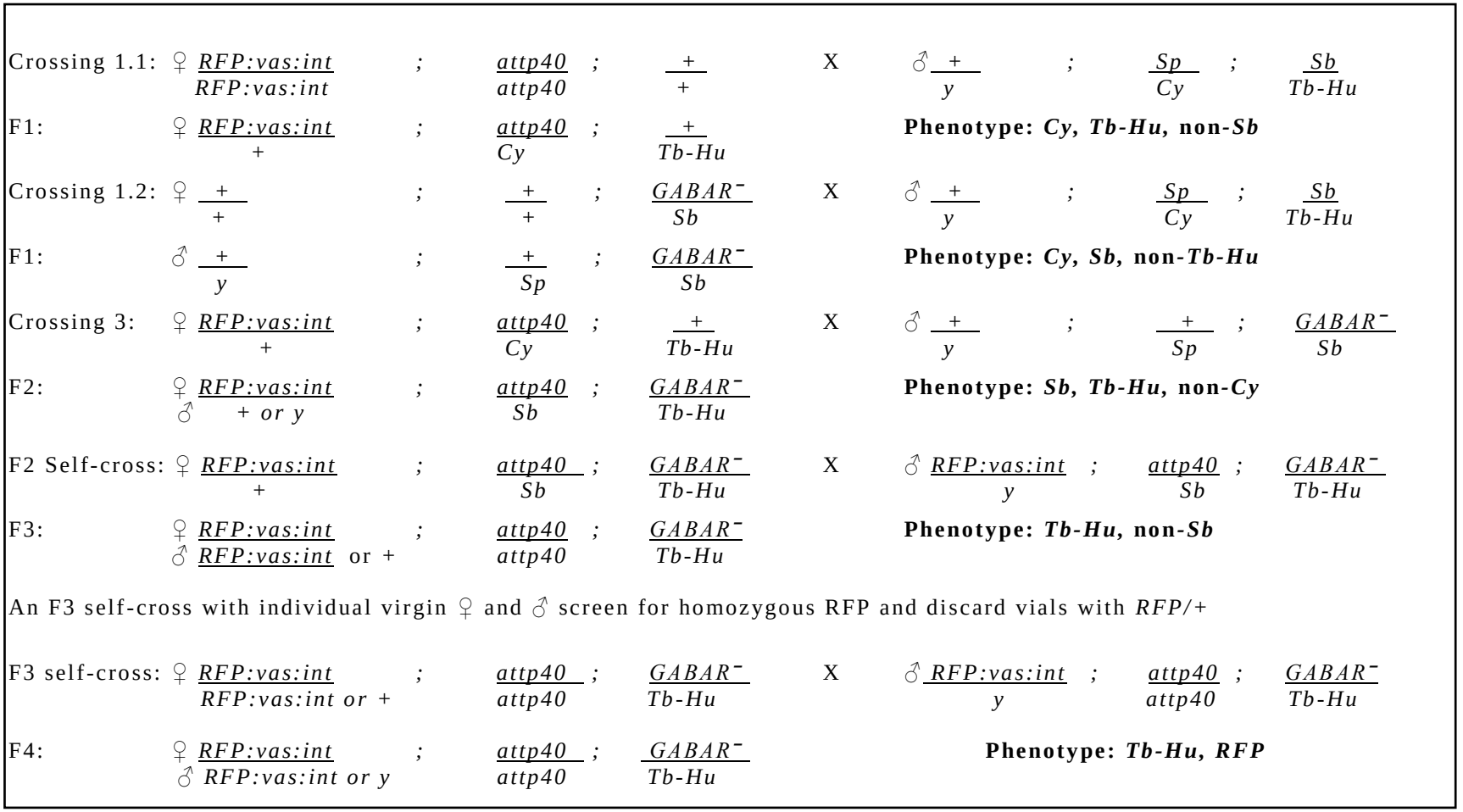


Figure 5.1. Crossing strategy to generate GABAR knockout lines with an integration site and integrase enzyme for φ31 integrase-mediated transgenesis. *RFP*=red fluorescence protein, *vas*=vasa promoter, *int*=integrase, +=Wild Type, *Sp*=Sternum plural, *Cy*=Curly, *Sb*=Stubble, *Tb-Hu*=Tubby humeral.

5.2.5. Germline transformation

The P-element based transgenesis protocol for germline transformation of *D. melanogaster* was developed by N. Gompel, (Faculty of Biology, LMU Munich), and modified and optimised for this experiment by C. Zimmer (Rothamsted Research) (http://carroll.molbio.wisc.edu/methods/Miscellaneous/injection.pdf).

~150 female and ~150 male flies from the strain prepared for injection (Figure 5.1) were transferred to a cage with an egg-laying plate made using FlyStuff grape agar mix streaked with a yeast paste. The flies were added to the cage 2 days before injection and left at 25°C to allow the flies to acclimate, and the food was change 2-3 times a day. On the day of injection, the grape plate was changed at 2 hours, 1 hour and 30 minutes before egg collection to empty females of old embryos. The embryos were rinsed off the grape plate into a mesh basket and washed with water, with an egg collection every 30 minutes to ensure injection was carried out using embryos where the blastoderm cells had not formed. Embryos were transferred to a 2 x 2 cm square glass cover slip, placed on a glass slide using a thin paintbrush and aligned with the dorsal side face up and the posterior end of the embryo ~2 mm from the edge of the coverslip in a line. The embryos were left to dry and attach to the coverslip for 3-5 minutes at 70% humidity. The coverslip was then coated with a thin layer of olive oil and left for 5 minutes to allow the oil to penetrate between the chorion and vitelline membrane. This facilitated injection and aided in successful staging of the embryos.

World Precision Instruments 1.0 mm Quartz capillaries with filament were prepared for injection by Rafael Homem (Rothamsted Research) using the Sutter Instruments Micropipette Puller. The slide was placed underneath the Ti-U Nikon Inverted Microscope, connected to the Eppendorf TransferMan micromanipulator and the Eppendorf FemtoJet air-pressure injection device. The injection needle was back-filled with 1 µL of the injection mix, aligned to the posterior of the first embryo in the line and gently injected ensuring that the needle did not penetrate

further than the first fifth of the embryo. A small droplet of the injection mix was injected into each embryo in quick succession, identified by a brief pulse of fluorescence made visible by the Nikon IntensiLight Illuminator. Any over-developed embryos were over-injected until the cells leaked out, ensuring no further development.

Once the embryos were injected, the coverslip was prepared for incubation by draining the oil, rinsing with 70% ethanol, rinsing with water and gently drying. The coverslip was then placed in a wide vial with 7 ml of Nutri-Flyfood, ensuring the embryos were above the food and not immersed and stored at 25°C. G0 virgin females and males were collected as they emerged and were later crossed to flies of the same genotype.

F1 individuals (males and virgin females) positive for the expression of the mini-white marker (orange eyed – Figure 5.2, middle fly) were selected and inter-crossed to generate homozygous stocks (red eyed - Figure 5.2, left fly).



Figure 5.2. From left to right: *D. melanogaster* with homozygous integration of the GABARbd gene at the attp40 landing site, flies with, heterozygous integration and flies with no integration.

5.2.6. Larval bioassays

A UAS/GAL4 expression line homozygous for *C747-GAL4* with *red+* eye marker on Chromosome 2 was purchased from the Bloomington Drosophila Stock Centre (#6494 genotype: *+/+; c747-GAL4/ c747-GAL4: +/+*). The crossing strategy outlined in Figure 5.3 details how larvae were generated for the larval bioassays. The homozygous larvae (genotype: *RFP:vas:int/+; attp40{GABARbd^{WT}}/ c747-GAL4; GABAR¯/ GABAR¯*) were selected based on the non-Tb-Hu phenotype and the heterozygous larvae (genotype: *RFP:vas:int/+; attp40{GABARbd^{WT}}/ c747-GAL4; GABAR¯/Tb-Hu*) based on the Tb-Hu phenotype. These two lines were generated for each of the WT, A301S, M354I and A301S.M354I GABARbd.

The protocol for larvae collection was modified from Nichols et al. (2012). ~20 *D. melanogaster* of the UAS-GABARbd lines were crossed with ~20 from the C747-GAL4 expression line in reciprocal crosses. The flies were removed from the bottles at 24 hours and incubated for a further 3 days to ensure a population of 3rd instar larvae only. The bottles were stored at 20°C. On the day of the bioassay, 75 mL of a 20% sucrose solution was placed in the bottles for 20 minutes. The larvae floated to the top and were removed with a wide-bore pipette, placed in a mesh basket and rinsed with water twice. The larvae were then placed on a grape agar plate and sorted according to the Tb-Hu phenotype. Narrow FlyStuff Vials with 3 mL of Nutri-Flyfood were prepared one day prior to the bioassays by placing 200 µL of the desired concentration of pesticide into the vial and left overnight for the compound to soak into the food and dry. 100% acetone 10,000 ppm stock solutions for fipronil, ethiprole and dieldrin (all from Sigma Aldrich) were used for 1 in 10 or 1 in 5 serial dilutions, prepared in 50% acetone.

The larval bioassays were done in triplicate at 20°C, with a fly-food only control and a food plus acetone-only control. 10 larvae were transferred into the centre of the food in each individual vial and scored for pupation for the homozygous larva and eclosion for the heterozygous

larvae every day for 2 weeks. Successful pupation was when the larvae were of normal size and had pupated on the side of the vial. Eclosion was when fully emerging *D.* adults were visible in the vial. The data were analysed using the Probit model of regression as per the methods in Chapter 3, section 3.2.6.

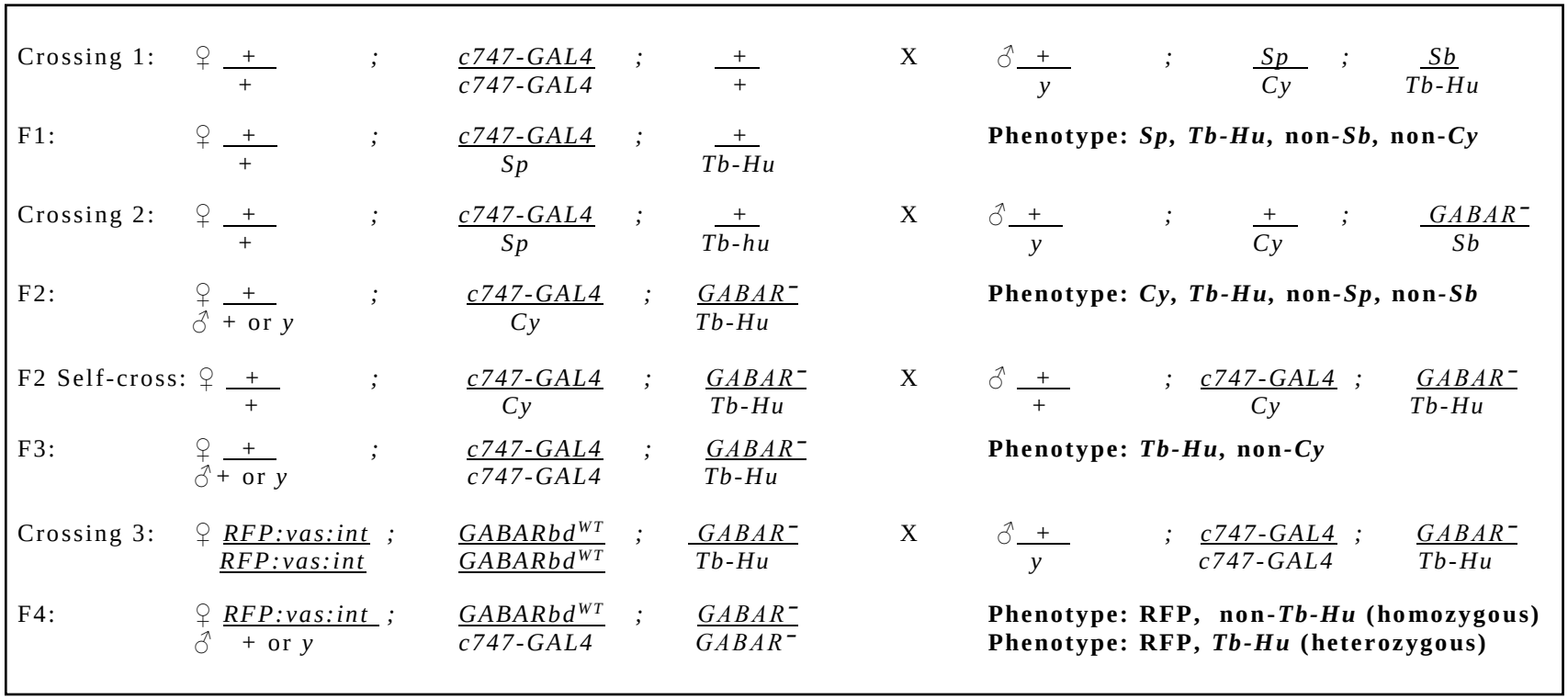


Figure 5.3. Crossing strategy to generate GABAR knockout *D. melanogaster* with positive integration of the *GABARbd* (WT, A301S, M354I and A301S.M354I) and the *c747-GAL4* driver, for larval bioassays. *RFP*=red fluorescence protein, *vas*=vasa promoter, *int*=integrase, +=Wild Type, *Sp*=Sternum plural, *Cy*=Curly, *Sb*=Stubble, *Tb-Hu*=Tubby humeral.

5.3. Results

The following transgenic strains were successfully generated:

'Homozygous' strains

RFP:vas:int/+;attp40{GABARbd^{WT}}/c747GAL4;GABAR^{-}/GABAR^{-}
RFP:vas:int/+;attp40{GABARbd^{A301S}}/c747GAL4;GABAR^{-}/GABAR^{-}
RFP:vas:int/+;attp40{GABARb^{M354I}}/c747GAL4;GABAR^{-}/GABAR^{-}
RFP:vas:int/+;attp40{GABARbd$^{A301S.M354I}$}/c747GAL4;GABAR^{-}/GABAR

'Heterozygous' strains.

RFP:vas:int/+;attp40{GABARbd^{WT}}/c747GAL4;GABAR^{-}/Tb-Hu
RFP:vas:int/+;attp40{GABARbd^{A301S}}/c747GAL4;GABAR^{-}/Tb-Hu
RFP:vas:int/+;attp40{GABARb^{M354I}}/c747GAL4;GABAR^{-}/Tb-Hu
RFP:vas:int/+;attp40{GABARbd$^{A301S.M354I}$}/c747GAL4;GABAR^{-}/Tb-Hu

The GABAR regions containing the mutations were sequenced using the sequencing primers (Table 5.1) from successfully-integrated homozygous populations of *D. melanogaster* prior to the bioassays to ensure the presence of the mutations. The recovery of positive transgenic flies was affected by temperature due to the mutated alleles present in the construct. Thus, the WT GABARbd construct was highly efficient in generating positive F1 adult flies (>30% of the survival G0s produced positive F1 flies), at 25°C but all the other constructs failed to do so. Pupal dissections revealed that these flies were unable to eclose from their pupal casing. Successful crossing was achieved at 18°C These phenotypes suggest that there is a leakage in expression from the pUAST, perhaps caused by the Hsp70 basal promoter cloned downstream of the UAS. Furthermore, they suggest that the mutations have a functional implication in the receptor's activity in *D. melanogaster*.

Next, the GAL4/UAS system was used to express the integrated alleles and try to rescue the lethality caused by GABAR^{-} homozygosity. This used standard genetic crosses to recombine the third chromosome of the GABAR^{-} with the second chromosome of the c747-GAL4 strain, which express GAL4 in the mushroom body, thoracic ganglion and wing

and leg discs (Schwaerzel et al., 2007). Unfortunately, none of these strains generated GABAR$^-$ rescued adult flies when crossed with the UAS-GABAR strains. However, the c747-GAL4 driver strain produced larvae of the expected phenotype. These results suggest that the expression of the UAS- GABAR driven by the c747-GAL4 driver can partially rescue GABAR$^-$ homozygous lethality at least in the larval stage.

A further cross was done to attempt to rescue the GABAR$^-$ adult flies. The Rdl-GAL4 line from the Bloomington Drosophila Stock Centre (#65421) was purchased which expresses GAL4 under the control of the GABAR endogenous regulatory region and has been shown to drive the expression of the GABAR primarily in the adult brain, but also in the mushroom body, ellipsoid body and antennal lobes (Diao et al., 2015). The Diao et al. (2015) study also showed the elimination of larval lethality in animal mutants for GABAR. However, in the current study the crossing of this line with GABAR$^-$ did not rescue the phenotype.

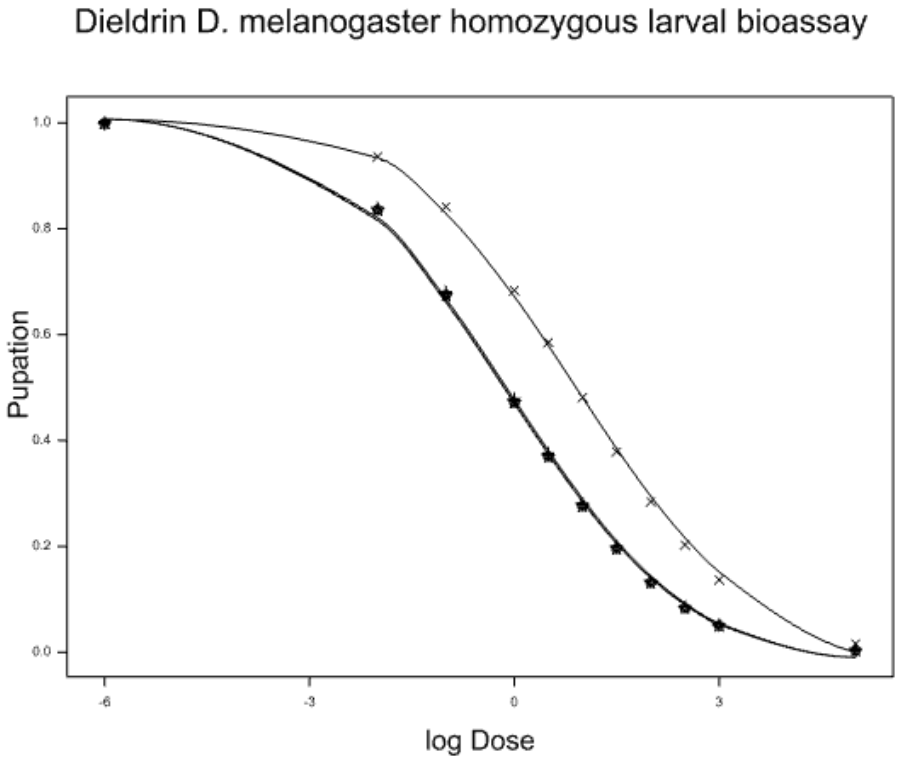
Larval bioassays were therefore carried out to determine the role of the mutation in insecticide resistance. This was done by scoring the percentage of larvae pupating after exposure to insecticides. An alternative bioassay was set up to determine the effect of the mutations on pesticide activity using heterozygous larvae with one copy of the endogenous gene and one copy of the GABARbd (WT and mutated), which was scored by measuring eclosion.

5.3.1. Range-finding trials

Range finding trials for the *D. melanogaster* larval bioassay were done with dieldrin, fipronil and ethiprole using 10-fold serial dilutions starting from 1000 ppm (1000, 100, 10, 1, 0.1, 0.01, 0.001, 0.0001, 0.00001, 0.000001 ppm) (data in Appendix 6). From these trials, it was determined that 1 in 10 dilutions starting from 10,000 ppm would be used for bioassays with dieldrin and 1 in 5 dilutions for ethiprole and fipronil starting from 1000 ppm and 10 ppm respectively.

5.3.2. *D. melanogaster* larval bioassays

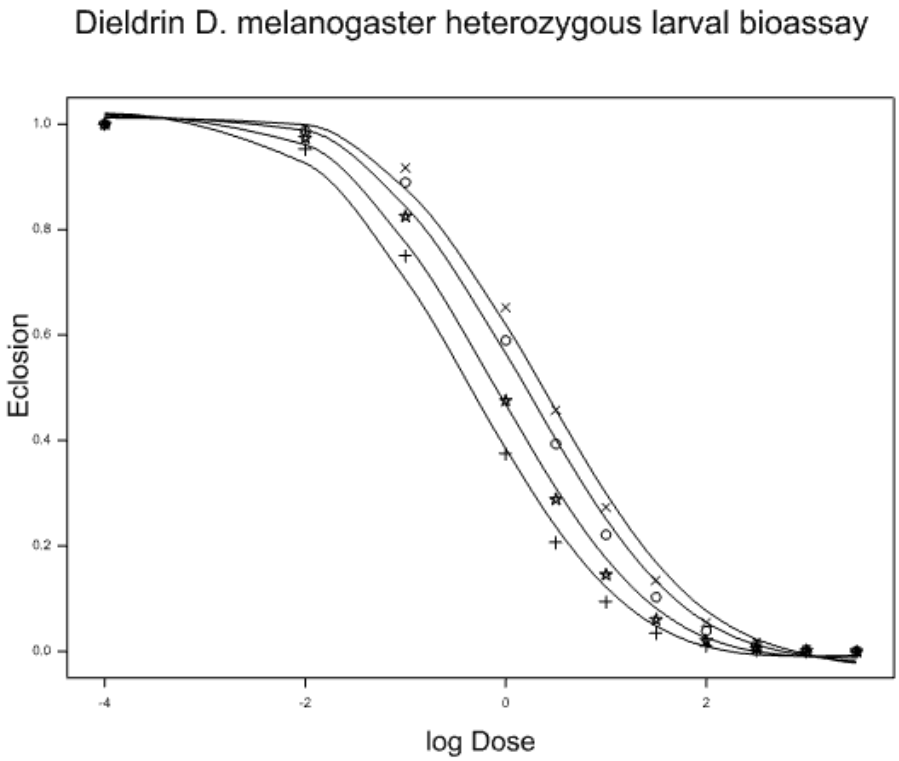
The results of the bioassays done with dieldrin on larvae homozygous and heterozygous for the GABAR substitutions, as measured by pupation and eclosion respectively, are shown in Figure 5.4 and Figure 5.5.



Genotype	LC_{50} (mg/L)	95%CI (mg/L)
WT	0.728	0.02-0.13
A301S	8.175*	0.03-0.17
M354I	0.792	0.03-0.11
A301S + M354I	0.728	0.42-1.57

Figure 5.4. Log dose response curves for *D. melanogaster* larvae homozygous for GABAR substitutions, treated with dieldrin. Scored by numbers pupating. *=significantly different to WT LC_{50} where P<0.05 in a two-sided t-test.

The bioassays show there was no significant difference between the dieldrin LC_{50} of ~1 mg/L for the homozygous WT *D. melanogaster* in comparison to the M354I and A301S.M254I flies However, there was a clear and significant ~11-fold reduction in the potency of dieldrin on the pupation of *D. melanogaster* larvae with the GABAR A301S substitution.

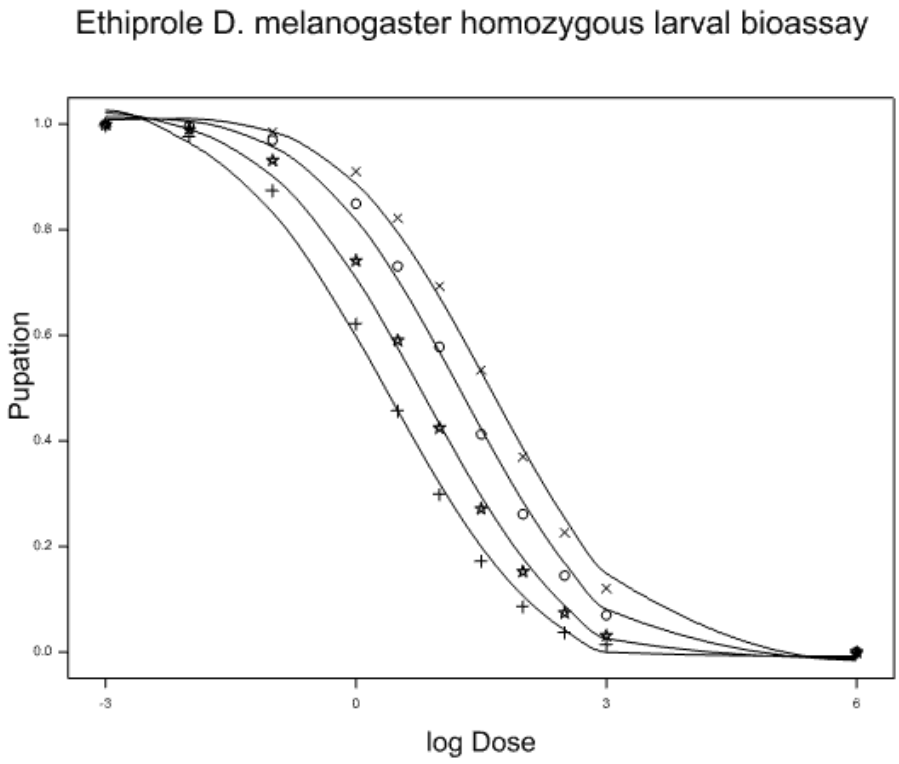


Genotype	LC_{50} (mg/L)	95%CI (mg/L)
WT	0.868	0.43-1.69
A301S	2.478*	1.28-4.76
M354I	0.478*	0.23-0.95
A301S + M354I	1.692*	0.87-3.27

Figure 5.5. Log dose response curves for *D. melanogaster* larvae heterozygous for GABAR substitutions, treated with dieldrin. Scored by numbers eclosing. *=significantly different to WT LC_{50} where P<0.05 in a two-sided t-test.

Experiments testing the effect of dieldrin with larvae heterozygous for the substitutions were in a similar range of mg/L but here there was a significant difference between all four of the genotypes tested, with the M354I larvae being marginally more susceptible to dieldrin, A301S larvae being ~3-fold less susceptible and the A301S.M254I larvae being 2-fold less sensitive.

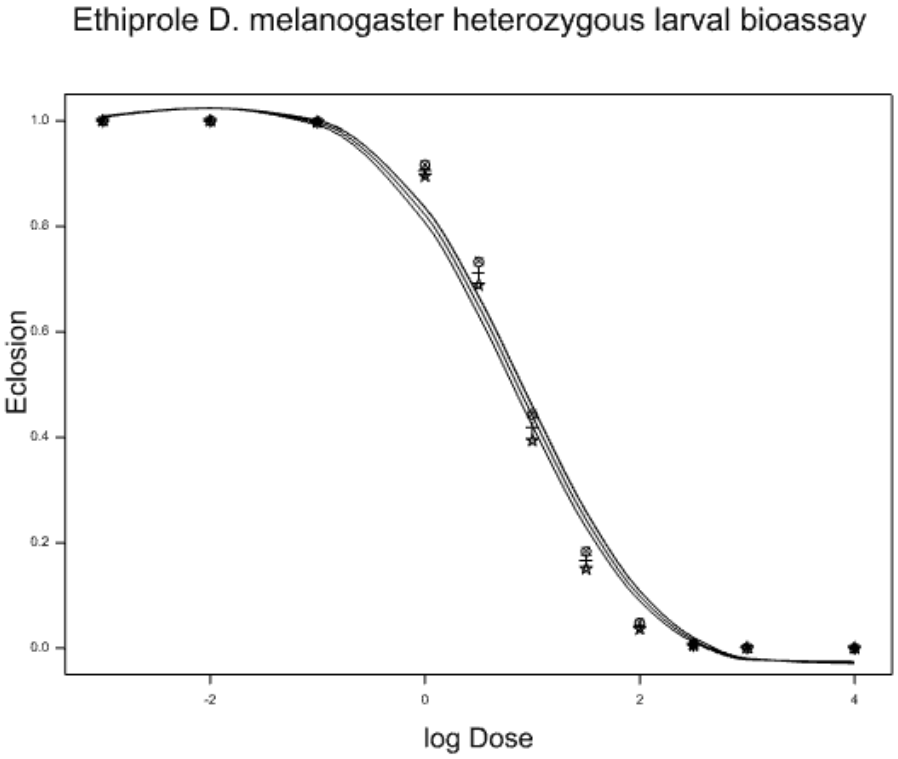
The results of the bioassays done with ethiprole on larvae homozygous and heterozygous for the GABAR substitutions as measured by pupation and eclosion respectively, are shown in Figure 5.6 and Figure 5.7.



Genotype	LC_{50} (mg/L)	95%CI (mg/L)
WT	5.921	3.16-10.5
A301S	40.11*	18.7-86.1
M354I	2.350	0.91-5.57
A301S + M354I	17.19*	9.78-29.5

Figure 5.6. Log dose response curves for *D. melanogaster* larvae homozygous for GABAR substitutions, treated with ethiprole. Scored by numbers pupating. *=significantly different to WT LC_{50} where P<0.05 in a two-sided t-test.

The bioassays show that there was no significant difference between the ethiprole LC_{50} of the homozygous WT *D. melanogaster* larvae and the M354I. The larvae with the A301S substitution were ~7-fold less susceptible than the WT and the double mutant with the A301S.M254I was ~3-fold less susceptible.

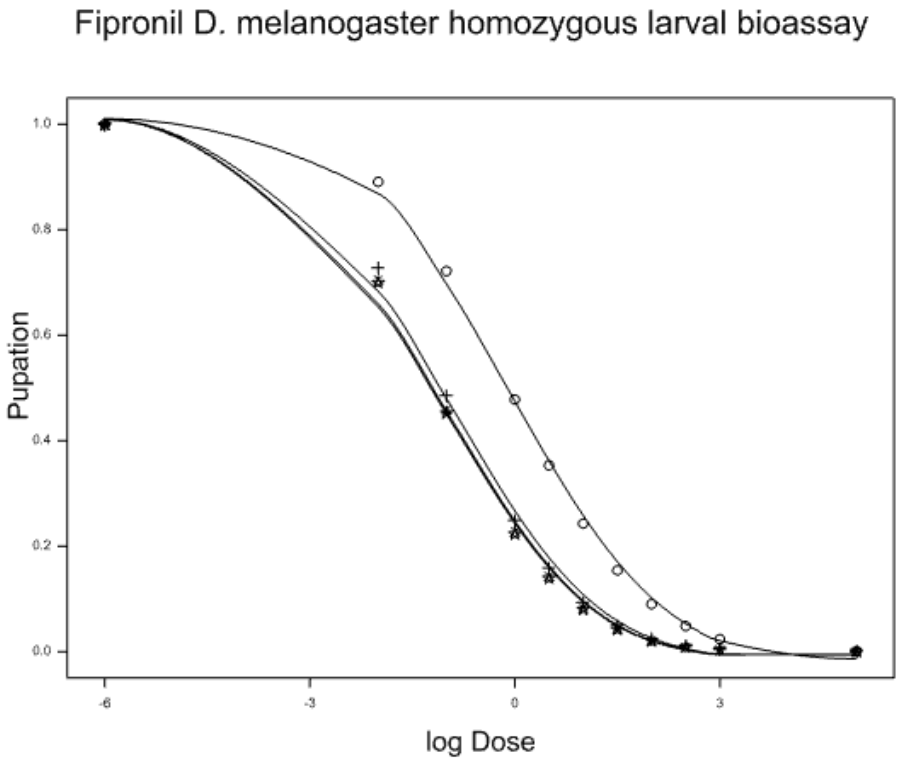


Genotype	LC_{50} (mg/L)	95%CI (mg/L)
WT	6.644	4.14-10.5
A301S	8.130	5.11-12.7
M354I	7.329	4.59-11.6
A301S + M354I	8.061	5.11-12.8

Figure 5.7. Log dose response curves for *D. melanogaster* larvae heterozygous for GABAR substitutions, treated with ethiprole. Scored by numbers eclosing. *=significantly different to WT LC_{50} where P<0.05 in a two-sided t-test.

The bioassays with ethiprole with for heterozygous larvae showed a similar LC_{50} to the homozygous larvae (7 mg/L and 6 mg/L respectively). There was no significant difference between the four genotypes of homozygous larvae tested in response to ethiprole.

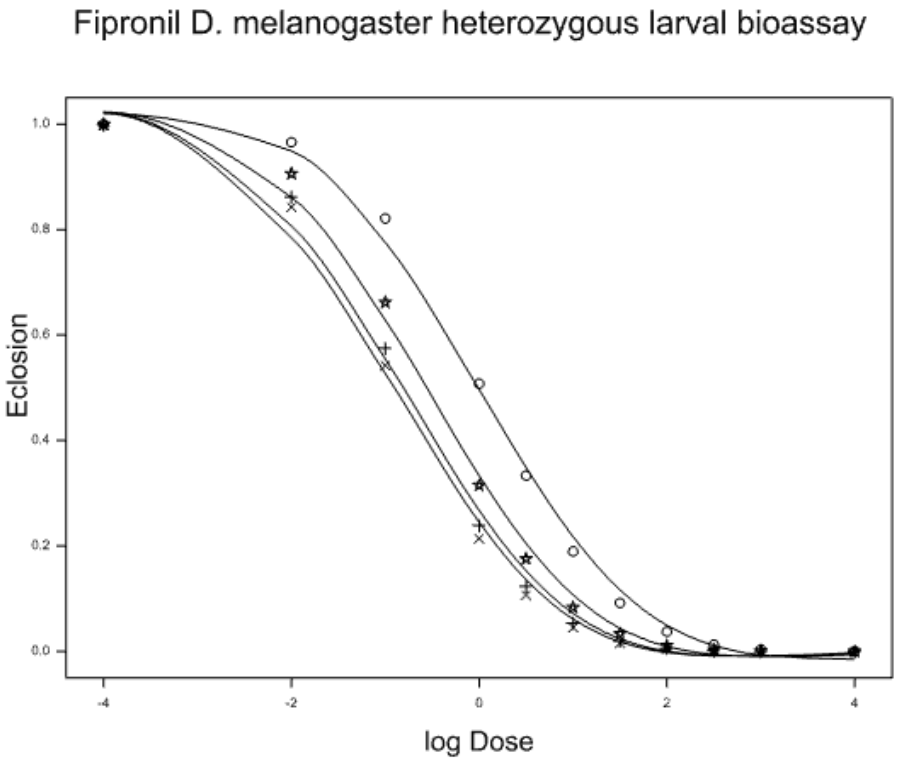
The results of the bioassays done with ethiprole on larvae homozygous and heterozygous for the GABAR substitutions as measured by pupation and eclosion respectively, are shown in Figure 5.8 and Figure 5.9.



Genotype	LC_{50} (mg/L)	95%CI (mg/L)
WT	0.065	0.02-0.13
A301S	0.069	0.03-0.17
M354I	0.082	0.03-0.11
A301S. M354I	0.822*	0.42-1.57

Figure 5.8. Log dose response curves for *D. melanogaster* larvae homozygous for GABAR substitutions, treated with fipronil. Scored by numbers pupating. *=significantly different to WT LC_{50} where P<0.05 in a two-sided t-test.

The fipronil bioassays with the homozygous larvae showed that there was no significant difference between the LC_{50} of the homozygous WT *D. melanogaster* larvae compared to the A301S and M354I. The larvae with the A301S.M354I double substitution were ~13-fold significantly less sensitive to fipronil compared to the WT.



Genotype	LC_{50} (mg/L)	95%CI (mg/L)
WT	0.101	0.08-0.43
A301S	0.131	0.06-0.29
M354I	0.093	0.07-0.15
A301S + M354I	1.051*	0.58-1.91

Figure 5.9. Log dose response curves for *D. melanogaster* larvae heterozygous for GABAR substitutions, treated with fipronil. Scored by numbers eclosing. *=significantly different to WT LC_{50} where P<0.05 in a two-sided t-test.

The fipronil bioassays with the heterozygous larvae results are similar to those with the homozygous larvae, once again showing that the larvae with the A301S.M354I substitutions are ~10-fold less susceptible to fipronil. There was no significant difference between larvae with the single A301S and M354I substitutions compared to the WT.

5.4. Discussion

Bioassays with dieldrin, ethiprole and fipronil were done for transgenic *D. melanogaster* larvae, homozygous and heterozygous for GABAR substitutions. The potency of these compounds on *D. melanogaster* pupation and eclosion varied across the chemistries. Fipronil was the most potent insecticide, with ethiprole a factor of two less effective and dieldrin a factor of one less effective.

The introduction of the A301S substitution into the *D. melanogaster* GABAR resulted in a ~11-fold reduced potency of dieldrin on the homozygous larvae, and was used as a positive control for resistance due to the long-established resistance conferred to cyclodienes by this substitution (Ffrench-Constant et al., 2016). This mutation when homozygous also caused a ~7-fold reduced susceptibility to ethiprole. In other work, the A301S mutation in its endogenous location (from the Bloomington Drosophila Stock Centre (#35492)) showed ~4000-fold resistance to ethiprole (Garrood et al., 2017), but this used adults and not larvae. Another study with transgenic *D. melanogaster*, selected for susceptible and resistant nAChR phenotypes in response to spinosad, found resistance ratios of 13-20-fold for larvae (Perry et al., 2015). It seems likely that *D. melanogaster* larvae are intrinsically more sensitive to chemical compounds than their adult counterparts. Overall, using the results from the dieldrin bioassay as a benchmark for resistance, it can be confirmed that the A301S substitution in the GABAR reduces susceptibility to ethiprole in *D. melanogaster* with a 'moderate' level of resistance (determined by a resistance ratio between 5-10).

The results with fipronil were unexpected. The bioassays with larvae, homozygous for GABAR substitutions showed a ~13-fold reduced susceptibility, and the bioassay with the A301S.M354I heterozygotes showed a ~10-fold reduced susceptibility to fipronil. Previous studies with adult *D. melanogaster* with the A301S substitution found a ~7-fold resistance to fipronil compared to the WT (Garrood et al., 2017) and a ~14-fold resistance compared to the WT (Remnant et al., 2014). In the

experiments here, there was no statistical significance in the response to fipronil with the A301S alone.

In the present study there were also key differences between the results of the bioassays with heterozygotes, compared to the homozygotes, which might result for the presence of the WT GABAR in its endogenous location. At the endogenous locus, one copy of the A301S GABAR allele has been found to confer intermediate resistance to dieldrin in cockroaches, whilst two copies are required for a highly resistant phenotype (Kristensen et al., 2005). In *D. melanogaster,* gene mapping studies of the A301S substitution have shown that the resistance allele is carried over a deficiency, where the second allelic copy is not expressed, and thus flies carry only one allele expressing insensitive receptors (Ffrench-Constant et al., 2000). This is not the case with the *D. melanogaster* tested here, as there is both a susceptible allele at the endogenous location and the mutated allele at the exogenous location. This fits in with the observed reduced resistance, from ~11-fold in the homozygous larvae to ~3-fold in the heterozygous larvae, suggesting that the presence of WT receptor proteins alongside the A301S GABAR receptors gives an increased sensitivity to dieldrin. This was also seen with ethiprole, where there was a reduction from ~7-fold resistance in homozygous A301S larvae to no significant difference to the WT in the heterozygous larvae. In addition to this, the resistance ratio of the A301S.M354I GABAR was reduced from ~13 to ~11 fold with the addition of the WT GABAR at the endogenous location.

Further work to determine if the GABAR is essential in larvae and the expression levels of the GABAR protein at each life-stage of *D. melanogaster* would help to determine the significance of the data presented here. A larval locomotion assay of *D. melanogaster* larvae with the A301S substitution found that picrotoxin had no effect on larvae with the mutation, even at the highest concentration of 3 mM, whereas the WT larvae exhibited a concentration-dependent decrease in activity (Graham et al., 2016). This implies that the GABAR is

necessary for function at the larval stage and beyond and that resistance caused by mutations can be quantified in larvae.

5.5. Conclusions

This chapter reports the introduction of A301S and M354I substitutions into the GABAR of *D. melanogaster*, both alone and in combination Bioassays on the transgenic flies, using numbers pupating confirmed a reduced susceptibility to dieldrin and ethiprole for the A301S substitution. The finding of moderate resistance to fipronil in transgenic *D. melanogaster* with both the A301S and M354I substitutions was novel and warrants further work.

6. Functional characterisation of the *R. microplus* nAChRα6 Spinosad binding site

6.1. Introduction

Control of the *Rhipicephalus microplus* cattle tick relies on the wide use of acaricides, and the selective pressure caused by this has resulted in resistance to most of the chemical classes used (Miller et al., 2011). Acaricides with different modes of action are key for the control of *R. microplus*, and spinosyns targeting the nicotinic acetylcholine receptor (nAChR) are widely used in pesticide rotations for resistance management programmes. Spinosad is a broad-spectrum pesticide made up of spinosyn A and spinosyn D (derived from the soil microorganism *Saccharopolyspora spinosa*) and is widely used for insect control. This compound causes paralysis in target pests by targeting the nervous system. Understanding the interactions of acaricides with their target receptors is a key component to effective management and can provide essential information for the discovery of selective molecules and for characterising resistance.

The homomeric expression of insect and acari nAChR subunits is particularly difficult, with a very limited number of studies assessing the pharmacological properties of arthropod nAChRs. However, functional studies of the *R. microplus* nAChRα6 and the human nAChRα7 using TEVC have been done previously and are further discussed in section 6.1.1. This chapter reports the characterisation of the two channels and mapping of the spinosad binding site using site-directed mutagenesis to alter key residues identified as important in spinosad binding.

6.1.1. Function expression of the *R. microplus* nAChRα6 and the human nAChRα7

The *R. microplus* nAChRα6 is patented as a nucleic acid molecule in the patent WO/2017/133938/A2 (Turberg, 2017). In summary, Mirel Puinean (Rothamsted Research) amplified and functional expressed the nAChRα6 gene from pools of *R. microplus* from Bayer Animal Health. Total RNA was extracted from the pools for cDNA sequencing and a transcriptome was assembled. Primers were designed and full-length sequences for the nAChRα6 were amplified. Sequencing determined alternative splicing at exon 3, giving the 3a and 3b splice variants of the nAChRα6 gene. These was functionally characterised and expressed in a journal article under review for publication in *The Journal of Neurochemistry*:

Puinean, A.M., Akkoese, M., Blockley, A., Field, L.M., Turberg, A. and Williamson M. (2019). Functional expression and characterisation of cattle tick, *Rhipicephalus microplus*, nAChR subunits.

Plasmid stocks of the Wild Type human nAChRα7 and the Wild Type *R. microplus* nAChRα6 channels used herein were provided by Mirel Puinean (Rothamsted Research). Mutagenesis and functional studies were done by the author.

6.1.2. Human nAChRα7 and the *R. microplus* nAChRα6 sequence alignment

Electrophysiological studies have shown that Spinosad binds effectively to the *R. microplus* nAChRα6 (Davey et al., 2001, Puinean et al., 2013b). A sequence analysis and protein modelling of the differences between the putative spinosad binding site of the *R. microplus* nAChRα6 and the human nAChRα7 was carried out by Andrias O'Reilly (University of Liverpool) and this was used to highlight candidate mutations responsible for the observed differences in response to spinosad, for TEVC studies reported here.

In summary, O'Reilly (personal communication) used a sequence alignment of the *R. microplus* nAChRα6 and the human nAChRα7 to highlight key non-conserved residues that could be responsible for the more successful binding of spinosad to the tick channel in comparison to the human. A docking model of spinosad with a refined structure of the nAChR (pdb ID: 2bg9) was then used to further analyse the interactions of key residues with spinosad. The non-conserved residues identified in the *R. microplus* nAChRα6 were a phenylalanine at position 265 in transmembrane region 1, a glycine at position 324 predicted to lie at the top of transmembrane region 3 and a cysteine at position 329 within transmembrane domain 3 (Figure 6.1). The glycine residue at position 324 here has previously been associated with resistance to spinosad in *Tuta absoluta*, *Thrips palmi* and *Frankliniella occidentalis* nAChRα6 (Silva et al., 2016, Puinean et al., 2013b, Bao et al., 2014). These three residues were found to interact and form bonds with spinosad in a ligand docking model and were therefore taken forward for the TEVC analyses (see Figure 6.1).

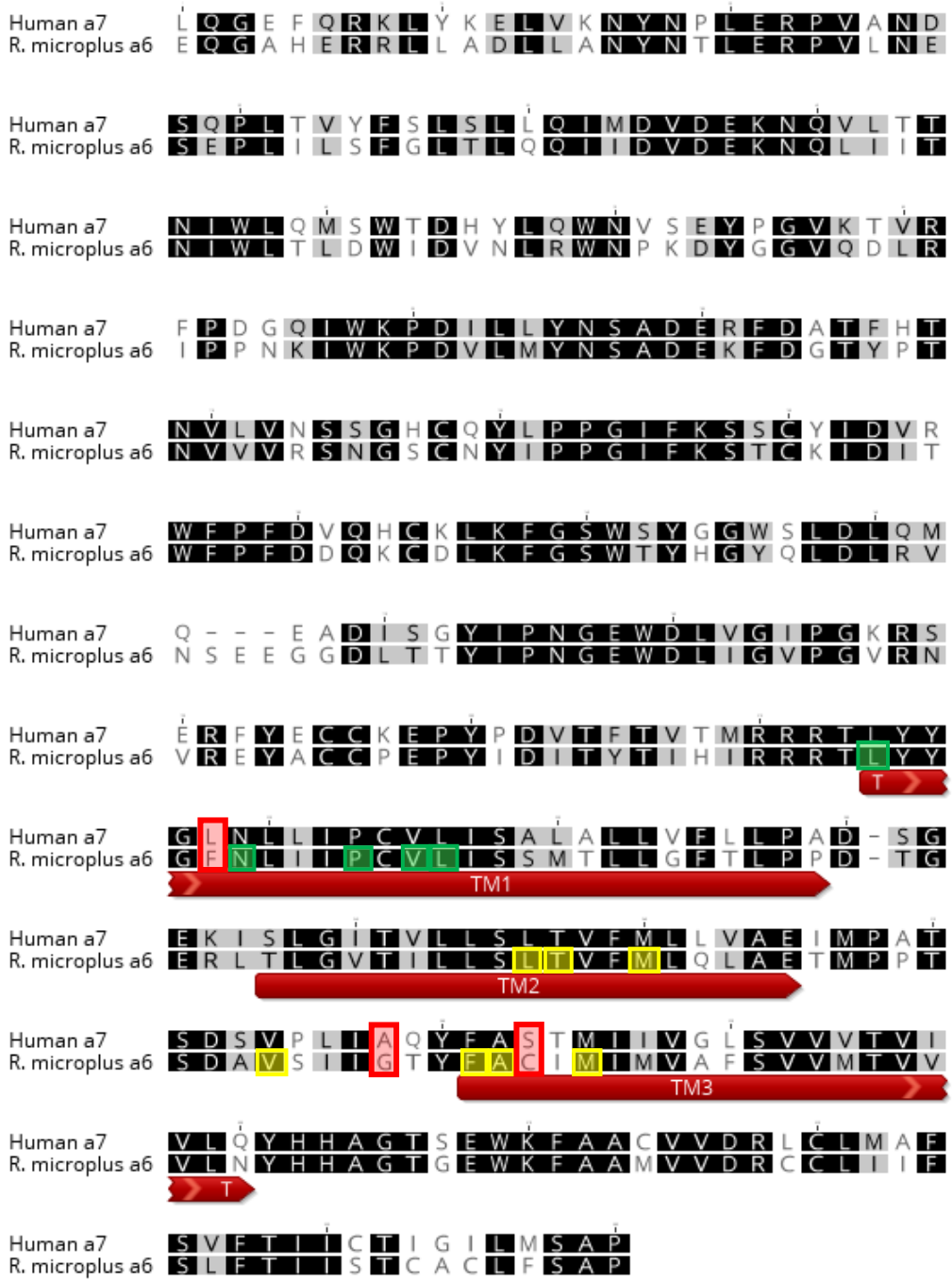


Figure 6.1. Partial sequence alignment of the human nAChRα7 and the R. microplus nAChRα6 (splice variant 3a). TM1, TM2 and TM3 of the R. microplus nAChRα6 are annotated. Residues on the principal subunit that form binding contacts with spinosad are highlighted in green. The equivalent residues on the complementary subunit that form binding contacts with spinosad are highlighted in yellow. The amino acids differences highlighted in red are not conserved and were taken forward for site-directed mutagenesis.

6.2. Methods

6.2.1. Source material

The human nAChRα7 cDNA cloned into the pSP64GL plasmid expression vector (containing the 5' and 3' untranslated *X. laevis* β-globin regions) was used for the mutagenesis and TEVC studies reported here. Sequence information is given in Appendix 7 (Couturier et al., 1990, Broadbent et al., 2006). The *R. microplus* nAChRα6 (splice variant 3a) cDNA was cloned into the PGEM-HE plasmid and expressed by A. M. Puinean, Rothamsted Research. Sequence information from patent WO/2017/133938/A2 is given in Appendix 8 (Turberg, 2017).

6.2.2. Site-directed mutagenesis

Primers for site-directed mutagenesis of the *R. microplus* nAChRα6 and the human nAChRα7 were manually designed by A. M. Puinean according to Agilent QuikChange II XL Site-Directed Mutagenesis guidelines and purchased from Sigma-Aldrich (Table 6.1 and Table 6.2).

Mutagenesis using the Agilent Site-Directed Mutagenesis QuikChange kit introduced the F265L, G324A and C329S substitutions individually into the *R. microplus* nAChRα6, and in 3 combinations F265L with G324A, F265L with C329S and G324A with C329S. Substitutions L299F, A358G and S363C were introduced in combination into the human nAChRα7 in one reaction giving a triple mutant. The sequences with the desired mutations were transformed using Life Technologies One Shot Top10 Competent *E. coli* cells and the resulting transformants plated out on ampicillin agar plates and incubated overnight at 37°C. 8-10 colonies were picked from each plate and used for a colony PCR using the sequencing primers (Table 6.1, Table 6.2). Using the same primers, DNA sequencing of the colony PCR products confirmed the introduction of the desired mutations into the sequences. Positive samples were propagated in liquid culture and purified using the QIAGEN QIAprep Spin Miniprep Kit.

Table 6.1. Oligonucleotide primers used for site-directed mutagenesis of the *R. microplus* nAChR to introduce F265L, G324A and C329S substitutions and primers used for sequencing to verify that the correct mutations were present.

	Forward Primer (5'-> 3')	**Reverse Primer (5'-> 3')**
F265L primers	CTCTACTACGGC*CTC*AA CCTCATCATTC	GAATGATGAGGTT*GAG*GCCG TAGTAGAG
G324A primers	GCTGTCTCCATAATA*GC A*ACTTATTTTGCCTGC	GCAGGCAAAATAAGT*TGC*TA TTATGGAGACAGC
C329S primers	GGAACTTATTTTGCC*TGC* ATCATGATCATGG	CCATGATCATGAT*GGA*GGCA AAATAAGTTCC
Sequencing primers	CAGGCCCACCACTCGCG GCG	CCGCGATGAGCGCTCCTTCA GCTCGAGC
	Red italicised bases deviate from WT sequence *Primers designed by A. M. Puinean*	

Table 6.2. Oligonucleotide primers used for site-directed mutagenesis of the human nAChR to introduce L299F, A358G and S363C substitutions and primers used for sequencing to verify that the correct mutations were present.

	Forward Primer (5'-> 3')	**Reverse Primer (5'-> 3')**
L299F primers	CTCTACTATGGC*TTC*AAC CTGCTGATCCC	GGGATCAGCAGGTT*GAA*GC CATAGTAGAG
A358G primers	CGGTACCATTGATA*GGC* CAGTACTTCGC	GCGAAGTACTG*GCC*TATCA ATGGTACCG
S363C primers	CAGTACTTCGCC*TGC*AC CATGATCATCG	CGATGATCATGGT*GCA*GGC GAAGTACTG
Sequencing primers	CCAGTGTCCCTGCAAGG CGAG	GCCATGCGGCCACACACTA CC
	Red italicised bases deviate from WT sequence *Primers designed by A. M. Puinean*	

6.2.3. *In vitro* cRNA synthesis

cRNA was synthesised according to section 2.6.1. The *R. microplus* nAChRα6 and human nAChRα7 DNAs were inserted into the plasmids downstream of the T7 and SP6 promoter respectively (A. M. Puinean, personal communication). The Ambion mMESSAGE mMACHINE T7 transcription kit was used to generate cRNA from the PGEM + *R. microplus* nAChRα6 plasmids (1. Wild Type, 2. F265L, 3. G324A and 4. C329S). For cRNA synthesis of pSP64GL + human nAChRα7 (1. Wild Type and 2. L299F.A358G.S363C), the Ambion mMESSAGE mMACHINE SP6 transcription kit was used. The DNA was linearised with *Bcul*I for *R. microplus* nAChRα6 and *Not*I for human nAChRα7, and gel electrophoresis was used to confirm complete cleavage and correct cRNA synthesis. A denatured sample was run on an agarose gel and confirmed the quality of the cRNA.

6.2.4. Electrophysiological recordings

X. laevis oocytes were prepared and injected as described in 2.6.2. The process was optimised for the best concentration and quantity of cRNA and the incubation time. For both the *R. microplus* nAChRα6 and the human nAChRα7, 50 nL of 500 ng/µL of cRNA (25 ng) was injected into the oocyte. The incubation time varied; the *R. microplus* was incubated for 3-4 days and the human nAChRα7 required 4-5 days at 17 ºC for robust expression. Acetylcholine (ACh) and spinosad were purchased from Sigma Aldrich and diluted in DMSO to 0.1 M stock solutions and stored at 4°C. Serial dilutions were carried out with fresh Ringer's solution on the day of testing.

ACh EC_{50} values were determined by applying the compound to the cells for ~3 seconds in increasing concentrations, with 2 minute washes with ringer solution between treatments. Spinosad is primarily an agonist of the nAChR, but has also been found to act as an allosteric modulator by keeping the channel open, slowing down the desensitisation rate of the

receptor and prolonging the ACh response (Nauen, 2002, Orr et al., 2009, Millar and Denholm, 2007). Therefore, in order to determine spinosad EC_{50} values, the oocytes were pre-treated with spinosad for 15 seconds, followed by a co-application of spinosad and 0.3 mM ACh (the EC_{95} of the nAChR WT) for ~3 seconds followed by a 2 minute wash. This protocol measured the spinosad agonist potential with the initial application, as well as any modulation of the subsequent ACh response (in comparison to ACh-only response). Control experiments were performed and the data analysed as per section 2.6.4 and 2.6.5 for concentration-response curves for ACh and spinosad.

6.2.5. Electrophysiological Data Analysis

Current traces were generated by exporting data acquired by LabScribe2 (with a reading every 0.005 seconds) into GraphPad. Percentage decay curves were calculated by taking the reading for the current at the peak response (R) and a second response 5 seconds later (R_2) in nA (Figure 6.2). R_2 was normalised to R and a 4PL logistic regression was performed on the data.

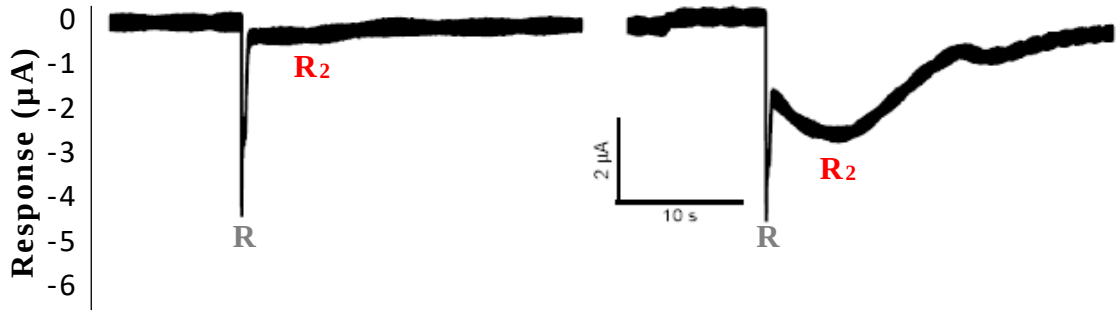


Figure 6.2. Illustration of the percentage decay analysis where R = the peak response in nA and R_2 is a second value taken 5 seconds after the removal of acetylcholine. Left: *R. microplus* nAChRα6 response to 0.3 mM achetylcholine. Right: *R. microplus* nAChRα6 response to 0.3 mM achetylcholine after 2 minute incubation with 30 µM spinosad.

Areas under the curves (AUC) were calculated by taking the Total AUC value generated by GraphPad and normalising the data to the control AUC of the maximal current in response to achetylcholine (AUC_{MAX}) (Figure 6.3). 4PL logistic regression was performed on the normalised data.

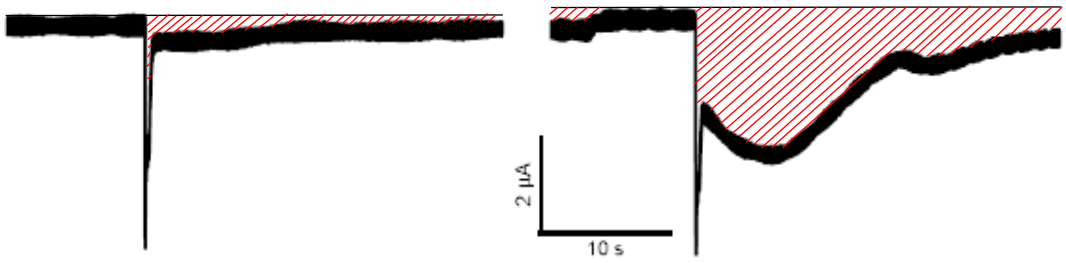


Figure 6.3. Illustration of the 'area under the curve' analysis where the total AUC of a test trace (right) is normalised to the response to acetylcholine-only (left) (AUC_{MAX}). The hatched red area indicates the total area used for calculations. Left: *R. microplus* nAChRα6 response to 0.3 mM achetylcholine. Right: *R. microplus* nAChRα6 response to 0.3 mM achetylcholine after 2 minute incubation with 30 µM spinosad.

6.3. Results

6.3.1. Responses of *R. microplus* nAChRα6 and human nAChRα7 expressed in oocytes to acetylcholine

The *R. microplus* nAChRα6 WT, F265L, G324A, C329S and human nAChRα7 WT and A955G.S960C.L1235F all formed functional receptors with robust concentration-dependent inward currents in response to Ach similar to the example traces in Figure 6.4. The *R. microplus* double mutants (F265L.G324A, F265L.C329S and G324A.C329S) gave small (<100 nA) to ACh indicating that these combinations of changes compromise functionality of the receptor.

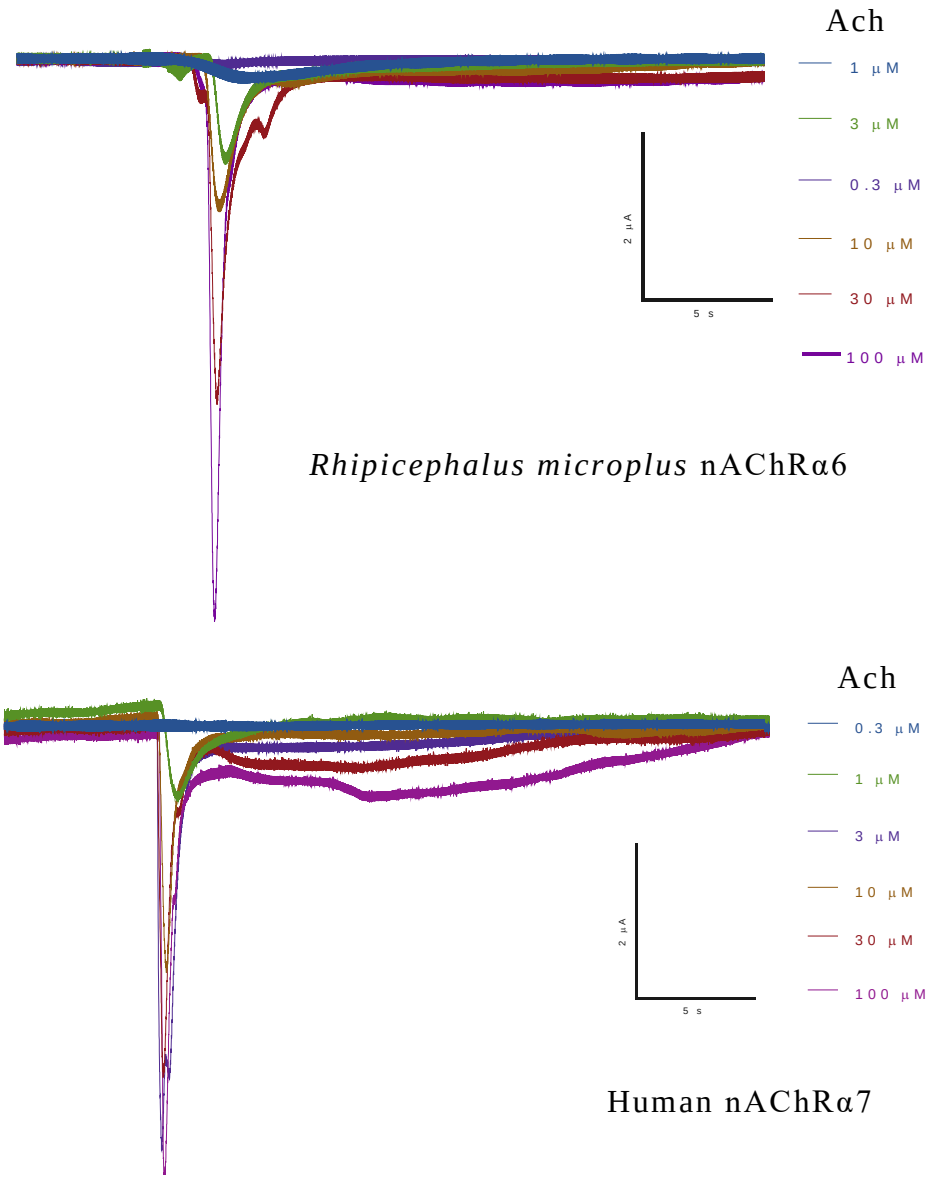


Figure 6.4. Representative traces of the concentration-dependent inward currents in response to acetylcholine in *X. laevis* receptors expressing the Wild Type *R. microplus* nAChRα6 (above) and human nAChRα7 (below).

Using increasing concentrations of acetycholine, the EC_{50} values of the *R. microplus* nAChRα6 WT, F265L, G324A, C329S and human nAChRα7 WT and A955G.S960C.L1235F were determined (Figure 6.5 and Table 6.3). The EC_{50} of the human L299F.A358G.S363C channel of 91.56 µM was slightly lower than the WT at 143.2 µM but the difference was not significant. Both of the human nAChRs tested were ~10-fold significantly less sensitive to ACh than was the *R. microplus* nAChRα6 WT.

There was no significant change to the *R. microplus* nAChRα6 WT EC_{50} value of 18.52 µM when the G324A and C329S substitutions were introduced into the channel. Interestingly, the F265L substitution made the channel ~2-fold ($P<0.0001$) more sensitive to ACh.

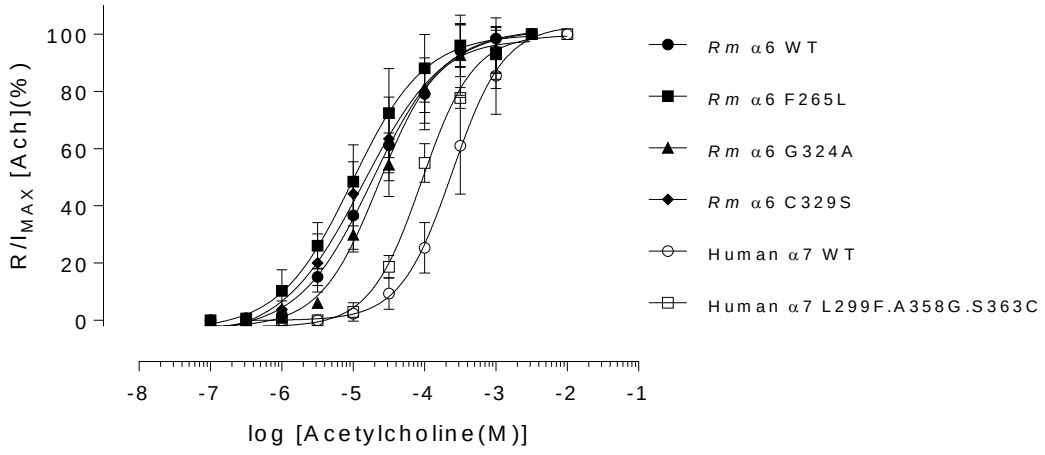


Figure 6.5. Acetylcholine concentration-response curves for WT and mutated *R. microplus* nAChrα6 and human nAChrα7 expressed in *X. laevis* oocytes. R= response, I_{MAX} = maximal response to 0.3 mM ACh.

Table 6.3. Parameters derived from acetylcholine concentration-response curves for *R. microplus* nAChRα6 (*Rm* α6) WT, F265L, G324A, C329S and human nAChRα7 (human α7) WT and L299F.A358G.S363C.

	EC_{50} (µM)	95% CI (µM)	Slope (± SD)	n
***Rm* α6 WT**	18.52	13.68-25.06	0.8 ± 0.11	8
***Rm* α6 F265L**	9.651*	6.551-14.22	0.9 ± 0.15	8
***Rm* α6 G324A**	22.92	18.03-29.14	1.1 ± 0.13	8
***Rm* α6 C329S**	13.85	9.008-21.28	0.8 ± 0.19	8
Human α7 WT	143.2*	76.8-234.6	1.2 ± 0.12	7
Human α7 L299F.A358G.S363C	91.56*	74.61-112.3	1.2 ± 0.13	7
***=significantly different to R. microplus WT where P<0.0001 in a two-sided F-test.**				

6.3.2. Characterisation of the *R. microplus* nAChRα6 spinosad binding site

Pre-application of spinosad followed by co-application with 0.3 mM ACh altered the *R. microplus* WT nAChRα6 desensitisation rate by reducing the response of subsequent ACh applications in a concentration-dependent fashion. Spinosad also acted as an agonist and activated the *R. microplus* nAChRα6 WT channels producing peak currents (although at a much lower level than ACh) as shown in the traces in Figure 6.6. The traces also show the nAChRα6 with F265L substitution was also modulated by spinosad, albeit with a slower rate of recovery, whilst the traces show very little effect of spinosad on the channel with G324A and C329S. The electrophysiological traces also show that spinosad has no visible effect on the human nAChRα7 WT and L299F.A358G.S363C.

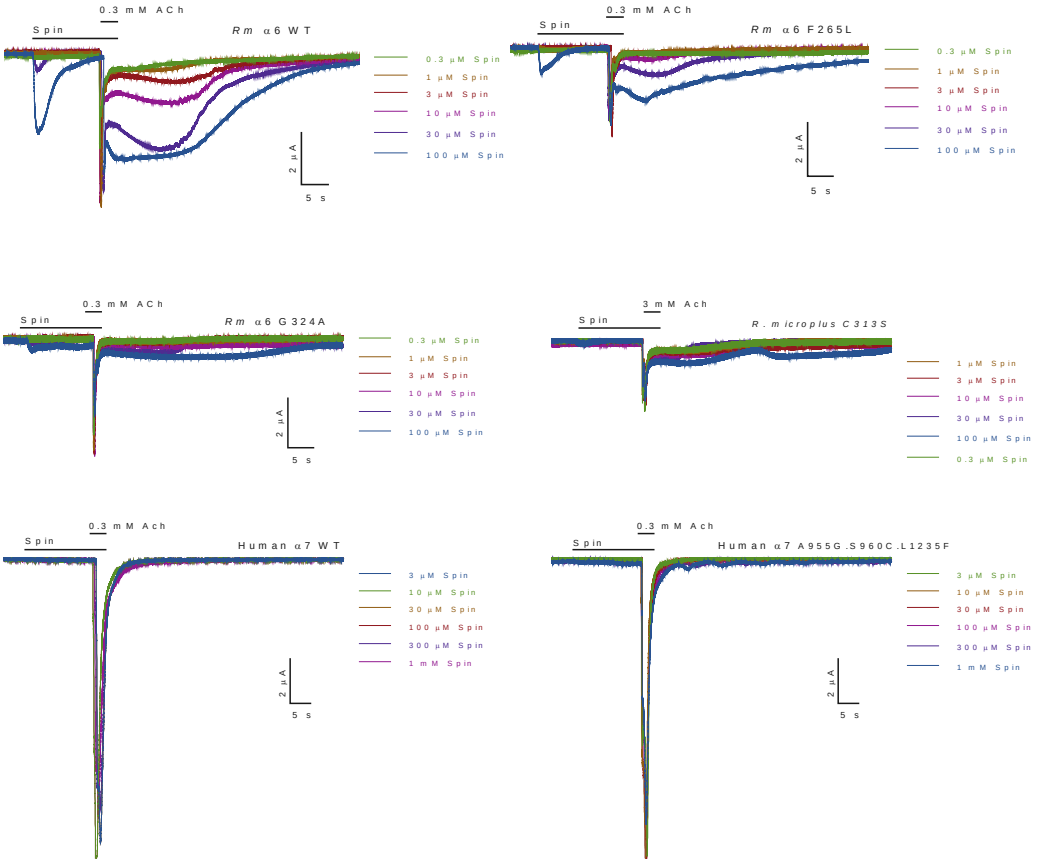


Figure 6.6. Sample electrophysiological trace from WT and mutated *R. microplus* nAChR*α*6 and human nAChR*α*7. For each current trace, spinosad was pre-applied for 15 seconds, then co-applied with 0.3 mM acetylcholine for a further ~3 seconds, with a 2 minute ringer wash in between increasing concentrations of spinosad.

Measuring the peak response of the *R. microplus* nAChRα6 channels to 0.3 mM spinosad, which was the highest concentration used, gave an average inward current of 1126 nA for the WT, 456.8 nA for F265L, 269.3 nA for G324A and 63.88 nA for C329S (n=9 for WT, n=8 per mutated channel) (Figure 6.7). No inward currents were measured in the human nAChRα7 receptors tested.

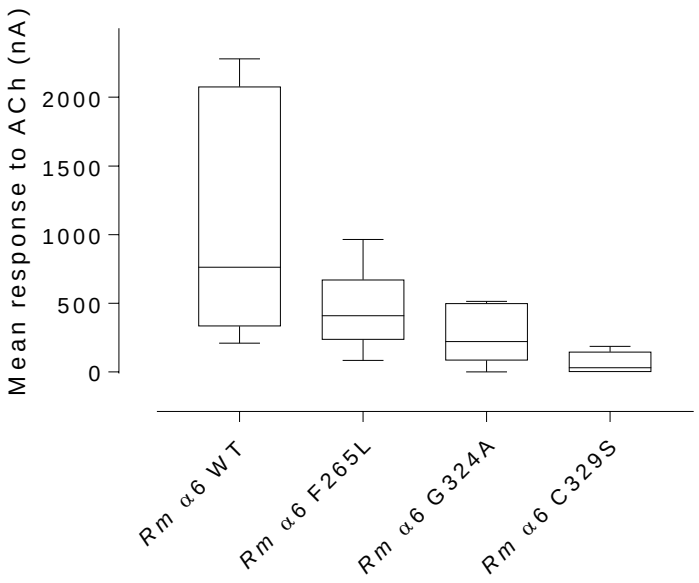


Figure 6.7. Boxplot of peak responses to 0.3 mM spinosad for *R. microplus* nAChrα6 (*Rmα*6) channels with an average inward current of 1126 nA for the WT, 456.8 nA for F265L, 269.3 nA for G324A and 63.88 nA for C329S (n=9 for WT, n=8 per mutated channel).

Peak responses were measured for a range of spinosad concentrations for the *R. microplus* nAChRα6 WT, however the F265L, G324A and C329S receptors did not produce sufficient responses to generate concentration-response curves. The analysis of the WT nAChRα6 gave an EC_{50} value of 31.05 µM (Figure 6.8).

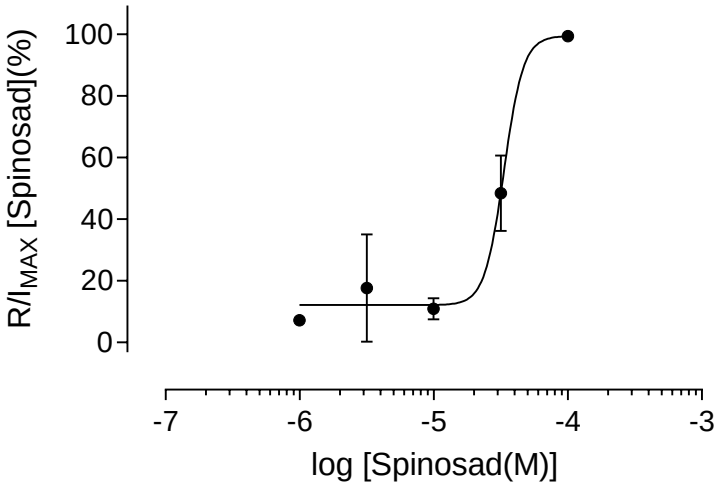


Figure 6.8. Spinosad agonist dose-response curve for *R. microplus* nAChRα6 Wild Type expressed in *X. laevis* oocytes. R=response, I_{MAX}=maximal response to spinosad. n=9. EC_{50}=31.05 µM (95% CI 25.78-37.39 µM), Hill Slope=4.2 ±11.3).

A percentage decay analysis of the data was done as per section 6.2.5. This analysis showed that the substitutions introduced into the WT *R. microplus* nAChRα6 had a significant effect on the modulation of the channel by spinosad (Figure 6.9). The WT channel ACh deactivation process was inhibited by spinosad with an EC_{50} of 3.62 µM, comparable to a previously determined value of 2.62 µM (A. M. Puinean *et al.*, under review). The F265L substitution caused a moderate 5-fold decrease in sensitivity to spinosad, whilst the G324A and C329S caused a dramatic decrease of 24-fold and 21-fold respectively (Table 6.4). The WT and mutated human nAChRα7 were 33-fold and 27-fold less sensitive to spinosad modulation than the WT *R. microplus* nAChRα6 respectively, with the introduction of the three substitutions into the

channel significantly increasing the sensitivity to spinosad. Interestingly, the introduction of G324A and C329S into the *R. microplus* channel led to an EC_{50} closer to the human channel rather than to the *R. microplus* WT.

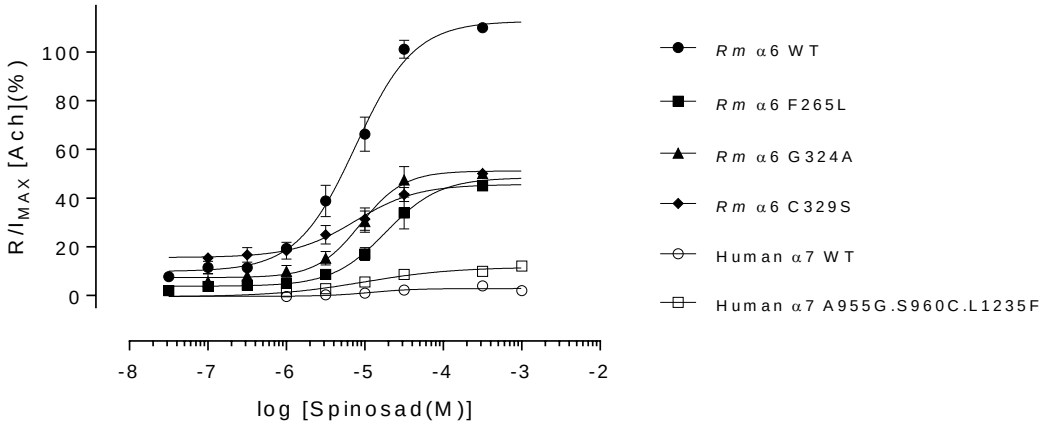


Figure 6.9. Spinosad percentage decay concentration-response curves for WT and mutated *R. microplus* nAChrα6 and human nAChrα7 expressed in *X. laevis* oocytes. R= peak response to 0.3 mM ACh, R_2 = response 5 seconds after removal of ACh.

Table 6.4. Parameters derived from spinosad percentage decay concentration-response curves for *R. microplus* nAChrα6 (*Rm*α6) WT, F265L, G324A, C329S and Human nAChrα7 WT and A955G.S960C.L1235F.

	EC_{50} (µM)	95% CI (µM)	Slope (± SD)	n
***Rm* α6 WT**	3.62	1.032- 5.62	1.2 ± 0.19	9
***Rm* α6 F265L**	18.67*	5.614 to 64.28	1.3 ± 0.28	7
***Rm* α6 G324A**	87.91*	12.09 to 120.6	1.6 ± 0.53	5
***Rm* α6 C329S**	76.03*	56.13 to 203.5	1.3 ± 0.47	5
Human α7 WT	119.3*	0.8275- 497.5	1.5 ± 1.43	5
Human α7 L299F.A358G.S363C	97.8*+	3.691- 572.5	0.8 ± 0.52	5

=significantly different to R. microplus WT where P<0.0001 in a two-sided F-test.
+=significantly different to Human WT where P<0.0001 in a two-sided F-test.

A more detailed 'Area Under the Curve' analysis as described in section 6.2.5 also demonstrated changes in spinosad modulation with the introduction of the substitutions into the *R. microplus* nAChRα6 (Figure 6.10, Table 6.5). The EC_{50} values derived from the curve are ~3-fold less than the percentage decay analysis, with all the channels producing lower values. Nonetheless, there was still a reduced effect of spinosad on the channel for F265L (11-fold less sensitive), G324A (16-fold less sensitive) and C329S (17-fold less sensitive). The difference between the WT *R. microplus* nAChRα6 with the WT human nAChRα7 was also higher with a 73-fold difference in spinosad effect, as was the mutated human nAChRα7 receptor (44-fold less sensitive). The difference between the WT and mutated human nAChRα7 was also more pronounced with a significant 1.6-fold decrease in sensitivity to spinosad. Although some of the spinosad EC_{50} values derived from the data differed, depending on the type of analysis done, the same conclusions can be drawn, with all three of the substitutions making the tick channel more human-like and significantly disrupting spinosad binding as hypothesised from the model. Introducing the inverse substitutions into the human channel had a smaller, but still significant, effect.

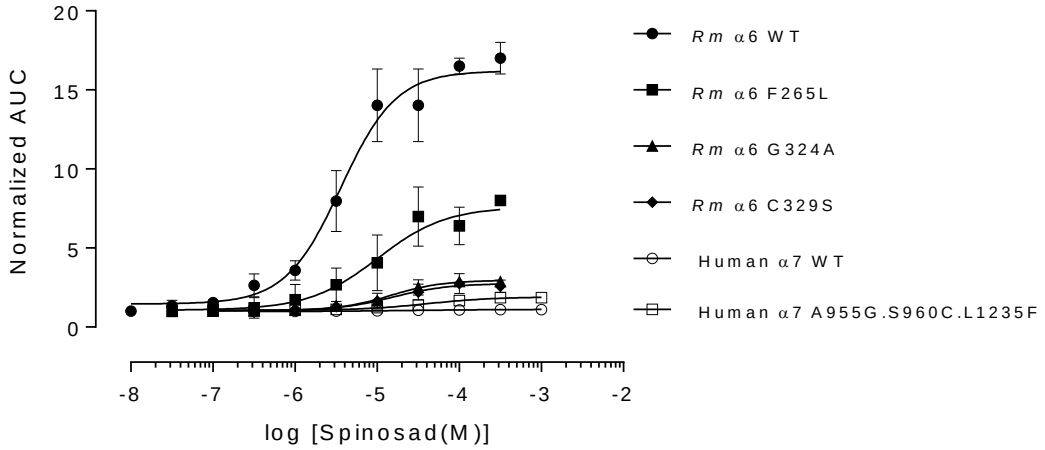


Figure 6.10. Spinosad 'Area Under the Curve' (AUC) concentration-response curves for WT and mutated *R. microplus* nAChrα6 and human nAChrα7 expressed in *X. laevis* oocytes. AUC of the spinosad-treated current normalised against the AUC of the 0.3 mM achetylcholine only current.

Table 6.5. Parameters derived from spinosad 'Area Under the Curve' concentration-response curves for *R. microplus* nAChrα6 (*Rm*α6) WT, F265L, G324A, C329S and Human nAChrα7 WT and A955G.S960C.L1235F.

	IC_{50} (μM)	95% CI	Slope (± SD)	n
***Rm* α6 WT**	0.9148	0.608-1.551	1.3 ± 0.35	9
***Rm* α6 F265L**	10.1*	1.418-3.268	1 ± 0.34	8
***Rm* α6 G324A**	14.67*	5.893-11.90	1.4 ± 0.30	7
***Rm* α6 C329S**	15.35*	6.143-12.54	1.3 ± 0.52	8
Human α7 WT	66.98*	41.47-169.5	0.7 ± 1.01	6
Human α7 L299F.A358G.S363C	40.22*+	27.19-75.80	1.1 ± 0.42	6

=significantly different to R. microplus WT where P<0.0001 in a two-sided F-test.

+=significantly different to Human WT where P<0.0001 in a two-sided F-test.

6.4. Discussion

Key residues highlighted as conserved in a sequence alignment of the *R. microplus* nAChRα6 and the human nAChRα7 receptor were found to disrupt spinosad binding in models of docking. In the studies reported in this chapter, these amino acid differences between the two channels, were tested in functional TEVC assays, to characterise the spinosad binding site of the *R. microplus* nAChRα6. By making the tick channel more like the human nAChrα7, the efficacy of spinosad was reduced.

The human nAChRα7 WT channel had an ACh EC_{50} of 143.2 μM, which is comparable to previously published data, which has given values of 129.3 μM in the original patent (Sivilotti, 2004) and in subsequent studies, 104 μM (Puinean et al., 2013b) and ~100 μM (Smelt et al., 2018). The *R. microplus* nAChRα6 WT EC_{50} was slightly higher than the patent published value of 9.39 μM (Turberg, 2017) and 8.84 μM (A. M. Puinean *et al.*, under review). The value is still within a reasonable range expected for heterologous expression of insect and acari nAChR subunits, as judged from the only other example, the *R. sanguineus* nAChRα1 subunit co-expressed with the chicken nAChRβ2, with and EC_{50} of 10.74 μM for ACh) (Table 6.6).

Table 6.6. Acetylcholine EC_{50} values of insect and acari nAChR subunits cloned and expressed in *X. laevis* oocytes in combination with a vertebrate subunit, excluding the homo-oligomeric *Myzus persicae* nAChRα1. N.B. nAChR subunits co-expressed with vertebrate subunits in cultured cell lines have been omitted but include *Drosophila melanogaster* nAChRα4, nAChRα6, nAChRα7, nAChRβ1, nAChRβ2, *Ctenocephalides felis* nAChRα1 and nAChRα2, *Schistocera gregaria* nAChRα1.

Receptor	Ach EC_{50} (μM)	Reference
***R. microplus* nAChRα5**	108.1	(A. M. Puinean et al., under review)
***R. microplus* nAChRα6**	8.84	(A. M. Puinean et al., under review)
***R. sanguineus* nAChRα1 (+ chicken nAChrβ2)**	10.74	(Lees et al., 2014a)
***D. melanogaster* nAChRα1 (+ chicken nAChrβ2)**	0.18	(Bertrand et al., 1994, Lansdell et al., 1997)
***D. melanogaster* nAChRα2 (+ chicken nAChrβ2)**	30	(Schulz et al., 2000)
***D. melanogaster* nAChRα3 (+ chicken nAChrβ2)**	0.15	(Schulz et al., 1998)
***D. melanogaster* nAChRα5 (+ RIC-3)**	8.8	(Lansdell et al., 2012)
***D. melanogaster* nAChRα7 (+ RIC-3)**	6.7	(Lansdell et al., 2012)
***D. melanogaster* nAChRα5 + nAChRα6 + nAChRα7**	13.5	(Lansdell et al., 2012)
***Myzus persicae* nAChRα1**	40	(Sgard et al., 1998)
***Nilaparvata lugens* nAChRα1 (+ rat nAChrβ2)**	33	(Liu et al., 2006)
***Nilaparvata lugens* nAChRα2 (+ rat nAChrβ2)**	62	(Liu et al., 2009)

An interesting finding was the agonistic effect of spinosad on the *R. microplus* nAChRα6 WT. Although this effect has been noted in the *R. microplus* nAChRα5 (Salgado and Saar, 2004, Puinean et al., 2013a), the *R. microplus* nAChRα6 has been previously found to be non-responsive to spinosad (A. M. Puinean et al., under review). However co-expressed *D. melanogaster* nAChRα5 and nAChRα6 found inward currents in the receptor in response to spinosad and analogues of spinosyn (Watson et al., 2010). The opposite effect was recorded in the *R. sanguineus* nAChRα1 with no agonist effect of spinosad, however this study also showed no antagonist effect on the channel (Lees et al., 2014a). Spinosad has been found to bind to the nAChR at an allosteric site distinct from the ACh binding site, therefore using the competitive antagonist methyllycaconitine (which is known to block the orthosteric site) and applying spinosad would determine whether the compound also binds the receptor at the ACh binding site (Hansen et al., 2005, Salgado and Saar, 2004). This interaction could be further defined with a spinosad-only application protocol with higher concentrations than those used here.

When the F265L substitution was introduced into the *R. microplus* nAChRα6, the effect of spinosad on subsequent ACh applications was reduced, whilst the G324A and C329S substitutions dramatically reduced the compound's efficacy. The resulting EC_{50} values were more similar to the vertebrate channel than the *R. microplus* nAChRα6 WT. The lack of response to ACh when the mutations were introduced in pairs indicated a likely incorrect protein folding and hence disruption in receptor. These residues may play important structural roles as well as being directly involved in spinosad binding. Introducing *R. microplus* residues into the human nAChRα7 made the channel more sensitive to spinosad modulation, however this increase was only marginal which implies that whilst the native residues are vital in the tick channel, they play a less important role in spinosad binding of the human nAChRα7.

6.5. Conclusions

The *R. microplus* nAChRα6 tested here is the first functional acari homo-pentamer that has been shown to expressed well in *X. laevis* oocytes, without the need for a vertebrate subunit chaperone. Previous studies have relied on mutagenesis of the human nAChRα7 which is genetically closely related to insect and acari nAChRα6 subunits, however the further characterisation of this robust functional expression of an acari subunit could lead to a better understanding of ligand-receptor interactions in insects and acari.

7. General discussion

The aim of the studies reported in this thesis was to undertake functional studies of how pesticides act on target ligand-gated ion channels in ticks and fleas. Firstly, the effect of a wide range of compounds was assessed on three species of tick (*I. ricinus*, *R. sanguineus* and *R. microplus*) and the cat flea *C. felis*. This was followed by characterisation of the *in vitro* effects of selected compounds on the *C. felis* GABARbd. Changes in amino acid residues, known or thought to be involved in pesticide binding were introduced into the channel to analyse their effects on compound efficacy and ligand-receptor interactions. This was followed by *in vivo* analysis of the same mutations by introducing them into the GABAR of transgenic *D. melanogaster*. Lastly, the spinosad binding site of the *R. microplus* nAChRα6 was investigated by mutating key residues identified from modelling studies. This chapter summaries and discusses these findings and makes suggestions for future work arising from the results.

7.1. Cross-resistance between dieldrin and ethiprole or fipronil

Cross resistance within a pesticide class is well established and as a result, the Insecticide Resistance Action Committee (IRAC) suggest rotation of compounds with different modes of action is used to prevent resistance from developing (IRAC, 2018). Bioassays carried out on the 'Georgi' strain of dieldrin-resistant *C. felis* at Bayer Animal Health showed significant levels of cross resistance to ethiprole. This strain has previously been shown to have the GABAR A301S, and transgenic *D. melanogaster* carrying the A301S substitution were also found to be significantly less susceptible to ethiprole. The A301S substitution, associated with dieldrin resistance in *D. melanogaster*, greatly reduces the potency of cyclodienes in many arthropod pests (Ffrench-Constant et al., 2000), and studies in *N. lugens* have shown cross-resistance to ethiprole due to this amino acid change (Garrood et al., 2017). This

cross-resistance and insensitivity in response to ethiprole was further verified in the *in vitro* TEVC studies of the *C. felis* GABAR expressed in oocytes reported here, where mutations resulting in A301S being introduced into the receptor conferred high levels of resistance to ethiprole, and confirmed resistance to dieldrin.

It might be expected that cross-resistance to ethiprole in dieldrin-resistant arthropods could also confer some cross-resistance to fipronil. The chemical structures of the two phenylpyrazoles only differ in a single moiety, an ethylsulfinyl substituent for ethiprole or a trifluoromethylsulfinyl substituent for fipronil. However, in this study results were mixed. Firstly, the bioassay studies in chapter three showed high efficacy of fipronil, consistent with it being used as a positive control in routine monitoring experiments at Bayer Animal Health. The compound was highly effective on a range of tick species and there was no cross-resistance to fipronil in *C. felis* populations known to have the A301S substitution. The *D. melanogaster* transgenic studies confirmed this, with no difference in fipronil toxicity between WT flies and those heterozygous and homozygous for the A301S GABAR allele. However, in the TEVC experiments on the *C. felis* GABAR with A301S, a ~60-fold reduced efficacy of fipronil compared to the WT was seen. This inconsistency is also seen in other studies reported in the literature. Previous toxicity studies on German cockroaches with the single nucleotide polymorphism resulting in A301S found a ~15-fold reduced susceptibility to fipronil in the homozygous insects and ~4-fold reduced susceptibility to fipronil in the heterozygous insects (Kristensen et al., 2005). A further study in *D. melanogaster* also found a ~14-fold resistance to fipronil in dieldrin-resistant flies (Remnant et al., 2014). This difference in potency was also noted *in vitro* in TEVC studies on the *D. melanogaster* GABAR with A301S (Hosie et al., 1995) and in cell lines expressing *S. furcifera* GABAR with A301S (Nakao et al., 2012). However, there are also studies showing no cross-resistance to fipronil in dieldrin-resistant *D. melanogaster, N. lugens* and *H. virescens* (Wolff and Wingate, 1998, Garrood et al., 2017). It may be

that there are other unpublished experiments where cross-resistance to fipronil is not present, as studies with positive results are more likely to be published than those with negative results (Chan et al., 2014). Although there was evidence of some cross-resistance to fipronil in the TEVC studies of the A301S *C. felis* GABARbd reported here, the channel was fully inhibited at 1 mM fipronil and the IC_{50} was still lower than the WT IC_{50} for ethiprole. Thus, it can be concluded that *in vivo* and *in vitro* cross-resistance to fipronil was not found.

It is also interesting that there is a distinct difference in the efficacy of the two phenylpyrazole compounds, particularly for the *in vivo* and *in vitro C. felis* experiments. In the bioassays in chapter three, there was a ~3-4-fold lower toxicity for ethiprole compared to fipronil on all three tick species, with both compounds effective in a micromolar range. This difference was much greater in *C. felis* bioassays, although in this case the reduced efficacy of ethiprole was attributed to the presence of the A301S mutation in the 'Georgi' strain. In chapter five, the difference in toxicity on the transgenic homozygous WT *D. melanogaster* was ~91-fold. For these bioassays, a potential lack of penetration resulting from the reduced lipophilic properties of ethiprole (associated with the change in chemical structure) could be responsible for the reduced toxicity (Caboni et al., 2003). This is supported by the difference in resistance ratios for ethiprole between topical application of the compound in the *C. felis* coated glass vial contact bioassays (RR=7513) and the ingestion of ethiprole in the 'artificial dog' feeding bioassay (RR=10). In chapter four the *in vitro* electrophysiology experiments on the *C. felis* GABAR showed a significant ~190-fold reduced potency of ethiprole compared to fipronil on the WT. In another study comparing the effect of ethiprole and fipronil on the *Musca domestica* GABAR, it was found that the two compounds were equally potent with IC_{50} values in the nanomolar range (Caboni et al., 2003). Ethiprole is widely used as an insecticide targeting planthopper crop pests, and has been found to be equivalent to fipronil in toxicity in a micromolar range against *N. lugens* and *L. striatellus* (Garrood et al., 2017, Sheng et al., 2018a).

Putting this data together, it can be concluded that since both fipronil and ethiprole are successful pesticides on arthropods where the LC_{50} is in a micromolar range, rather than ethiprole being less effective than fipronil, it is a hypersensitivity by *C. felis* to fipronil that is occurring in the work reported here. This could result from particularly strong docking of fipronil at the *C. felis* GABAR with specific ligand-receptor binding associated with the trifluoromethylsulfinyl moiety, or an unknown metabolic process present in some arthropods and missing in *C. felis*.

7.2. Functional studies of a novel mutation in the *C. felis* GABAR

Part of the work reported in this thesis was based around the hypothesis that two mutations (ATG to ATA or ATT) causing the novel M354I substitution, found in combination with A301S could be responsible for resistance in fipronil-resistant populations of *C. felis*. This was tested both *in vitro* (chapter four) and *in vivo* (chapter five). TEVC testing of *X. laevis* oocytes expressing the *C. felis* GABARbd with A301S.M354I substitutions showed a WT level of susceptibility to fipronil, and against the hypothesis, the M354I restored susceptibility in A301S dieldrin and ethiprole-resistant channels expressed in oocytes. This result is contrary to the moderate resistance seen in transgenic *D. melanogaster* with the same A301S.M354I GABAR genotype; ~13-fold reduced susceptibility to fipronil in larvae homozygous for the mutations compared to the WT and ~10-fold in larvae heterozygous for the mutations. It must be noted that there were many complications involved in introducing the mutated GABARbd gene into *D. melanogaster* using the φC31 integrase-mediated transgenesis system, and inability to fully rescue the phenotype meant that the final bioassays were assessed by the pupation and eclosion of the larvae, rather than the more established contact/feeding bioassay with adult flies. The results may have been different for adults. Furthermore, studies have shown that whilst the GABAR is expressed at the larval stage in *D.*

melanogaster, different splice variants are expressed that modulate receptor potency, and RNA editing is developmentally regulated (Jones et al., 2009). The natural regulatory features were not accounted for in the studies presented here, and because the transposon-mediated transgenesis targeted an exogenous landing site, the *in vivo* interactions at each *D. melanogaster* life stage were circumvented.

Although fipronil treatment results in the mortality of *C. felis* larvae (McTier et al., 2003, Mehlhorn et al., 2001), many commercialised products for the control of *C. felis* have fipronil as the primary active ingredient but also contain insect growth regulators to disrupt arthropods from reaching maturity, such as methoprene in Frontline®. This suggests that fipronil alone is not sufficiently effective against the larval stage of the insect. Therefore, whilst moderate resistance was found in *D. melanogaster* larvae homozygous for the A301S.M354I GABAR allele, firm conclusions cannot be drawn until further experiments with transgenic adult flies are conducted to determine the difference between potencies at different life stages. If the results presented here are confirmed, further exploration of the molecular basis for this resistance would be required to determine if there are metabolic processes involved, as the TEVC experiments suggest target-site resistance is not the cause.

7.3. Isoxazolines: the next generation of GABAergic compounds

The isoxazoline group of pesticides introduced onto the market in 2015 are inhibitors of both the arthropod GABAR and GluCl, with binding sites distinct from the phenylpyrazoles (Sojka, 2018). In the present study the toxicity of four members of this group, afoxolaner, fluralaner, sarolaner and lotilaner was tested on three tick species and *C. felis*. All four compounds were found to be highly effective with LC_{50} values close to those of fipronil. The efficacy of afoxolaner, fluralaner, sarolaner was further tested in TEVC studies of the *C. felis* GABAR

where they were all effective at blocking receptor response at nanomolar quantities. In combination with the excellent efficacy of these compounds, they are also very safe to use and have been found to have little environmental contamination (Sojka, 2018). These chemistries will no doubt increase in use and compounds from this class have been commercialised by a number of companies including Merck Animal Health, Zoetis, Merial and Elanco in the animal health sector and patented for agrochemical use by Du Pont, Bayer, BASF and Syngenta. In this thesis, it has been demonstrated that there is no cross-resistance to these products conferred by the ubiquitous A301S amino acid substitution in the receptor.

7.4. Spinosad binding to the *R. microplus* nicotinic acetylcholine receptor

Chapter six of this thesis reports studies of spinosad binding to the *R. microplus* nAChRα6 subunit. This is the first functioning homomeric nAChR to be expressed without the need for a chaperone. By mutating the channel to make it more like the human nAChRα7, key residues of the binding site were confirmed from modelling studies. The functionality of this channel is important as it could be used in a wide range of arthropod studies to inform more selective pesticide use and to predict and characterise resistance to compounds targeting the nAChRα6.

7.5. Future work

Some areas for potential further studies based on this thesis are:

1. The *C. felis* GABARbd could be integrated into the *D. melanogaster* genome using the φC31-mediated integration system and the resulting flies used to test the hypothesis that the difference in efficacy between ethiprole and fipronil is due to a hypersensitivity to fipronil on the *C. felis* GABAR. Whether this hypersensitivity is in fact due to metabolic processes could also be analysed by co-expressing P450s, CCEs and GSTs to see if this results in a more expected micromolar sensitivity.

2. The *D. melanogaster* GABARbd could be functionally expressed in oocytes and tested with both ethiprole and fipronil to examine any difference in efficacy of the compounds on the channel. Site-directed mutagenesis of this channel could also further clarify whether cross-resistance to fipronil is seen when the A301S substitution is present. These experiments could also confirm whether the introduction of M354I can restore susceptibility in dieldrin and ethiprole resistant A301S GABAR channels

3. The presence of resistance to fipronil in *D. melanogaster* carrying the A301S.M354I GABAR could be further explored by creating more stable transgenic lines using CRISPR/*cas9* and mutating the endogenous gene under the expression of the natural GABAR promotor. Using these lines, bioassays with fipronil and ethiprole could be done on adults as well as with the larvae. Metabolic processes involved in any resistance could be tested with the co-expression of enzymes such as P450s, CCEs and GSTs.

4. GABA receptor gene isoforms, and their expression levels at different life stages of *C. felis* could be investigated to determine a stage-specific expression profile for the GABAR. A further

analysis of the isoforms could be carried out by functionally expressing artificially synthesised GABAR isoforms in oocytes and analysing how the differences in genotype can lead to altered ligand binding of the channel. This might identify the best life-stages to target with pesticide applications

5. TEVC experiments analysing the agonistic role of spinosad on the *R. microplus* nAChRα6 could help and further define the compounds interactions with this receptor. Using an agonist application protocol and applying the compound for ~3 seconds to the receptor would yield the date required for a concentration-response curve. The system could also be used for additional characterisation of the receptor with other compounds targeting the arthropod nAChRα6.

8. Appendices

8.1. Appendix 1

GenStat code to produce dose response graphs for Probit analysis of bioassay data.

```
"_____________________________________________________"
"Model WITHOUT control mortality fitted"
"_____________________________________________________"

"save parameter estimates from the most recently fitted model"
rkeep estimates=e
getatt [nval] e; save=len_e
calc nchem=len_e[]-1

"get labels for the key"
getatt [labels] Chemical; chemlabs
text chems;chemlabs[]


"Choose a set of doses for the x values of the plot"
vari [valu=-3,-2.5,-2,-1.5,-1,-0.5,0,0.5,1,1.5,2] xs

"calculation of y values"
FOR chem=!(1...nchem)
calc ys[#chem]=normal(e$[#chem]+(e$[len_e[]]*xs))
ENDFOR

"produce plot"
pen 1,2,3,4,5,6,7,8; colour='black'; symbol=1,2,3,4,5,6,7,8
trellis [xtitle='log Dose';ytitle='KD/Mortality'; usepens=yes]
x=xs; y=ys[]; method=spline; desc=#chems


"save parameter estimates from the most recently fitted model"
rkeep estimates=e
getatt [nval] e; save=len_e
calc nchem=len_e[]-1

"get labels for the key"
getatt [labels] Chemical; chemlabs
text chems;chemlabs[]


"_____________________________________________________"
"Model WITH control mortality included"
"_____________________________________________________"

"save parameter estimates from the most recently fitted model"
rkeep estimates=e
getatt [nval] e; save=len_e
calc nchem=len_e[]-1

"get labels for the key"
getatt [labels] chemical; chemlabs
text chems;chemlabs[]


"Choose a set of doses for the x values of the plot"
vari [valu=-3,-2.5,-2,-1.5,-1,-0.5,0,0.5,1,1.5,2] xs

"calculation of y values"
FOR chem=!(2...nchem)
calc ys[#chem]=e$[1] + (1-e$[1])*normal(e$[#chem]+(e$[len_e[]]*xs))
ENDFOR

"produce plot- replace writing in red with relevant titles"
pen 1,2,3,4,5,6,7,8; colour='black'; symbol=1,2,3,4,5,6,7,8
trellis trellis [xtitle='log Dose';ytitle='KD/Mortality'; title='C.
felis Artificial Dog Biossay'; usepens=yes] x=xs; y=ys[];
method=spline; desc=#chems
```

GenStat code for Students t-test analysis of Probit data to determine statistical significance of a compounds effect in a bioassay in comparison to the positive control, fipronil.

```
"_____________________________________________________________"
"To calculate p values for statistical significance in comparison
to positive control fipronil"
"_____________________________________________________________"

"Run the relevant probit analysis first"

"calculation of relative potency and its approximate standard
error"
"Replace 'Chemical B' with relevant chemical name as written under
'Estimates of paramters' section"
expression [value=relpot=10**(('Chemical Fipronil'-'Chemical
B')/'logExpnVar')]relpot_calc
rfunction [print=esti,se; calc=relpot_calc; se=serelpot] relpot

"calculation of test statistic"
calc relpotstat=relpot/serelpot
print relpotstat

"Students t test to calculate t value and find p value for test"
rkeep df=resdf
calc tpvalue=1 - (CLT((abs(relpotstat) - 0)/1;resdf)-CLT((-
abs(relpotstat) - 0)/1;resdf))
print tpvalue
```

8.2. Appendix 2

LC_{50} and LC_{95} probit mortality data for *C. felis* coated glass vial bioassay.

Treatment (time)	LC	Estimate (ppm)	lower 95%CI	upper 95%CI
Afoxolaner 24	50	631	4.28E+02	9.33E+02
Afoxolaner 24	95	3042	2.03E+03	4.68E+03
Afoxolaner 48	50	54.1	3.70E+01	7.81E+01
Afoxolaner 48	95	261	1.79E+02	3.89E+02
Bifenazate 24	50	3108	1.64E+03	6.00E+03
Bifenazate 24	95	3108	7.72E+03	3.03E+04
Bifenazate 48	50	2075	1.23E+03	3.55E+03
Bifenazate 48	95	10009	5.78E+03	1.79E+04
Dieldrin 24	50	3108	1.64E+03	6.00E+03
Dieldrin 24	95	14992	7.72E+03	3.03E+04
Dieldrin 48	50	885	5.88E+02	1.34E+03
Dieldrin 48	95	4268	2.78E+03	6.73E+03
Endosulfan 24	50	18.2	1.01E+01	2.73E+01
Endosulfan 24	95	91.1	6.30E+01	1.36E+02
Endosulfan 48	50	10.2	7.00E+00	1.41E+01
Endosulfan 48	95	47.2	3.20E+01	7.03E+01
Ethiprole 24	50	37568	8.00E+00	1.78E+08
Ethiprole 24	95	181217	4.10E+01	8.71E+08
Ethiprole 48	50	37568	7.92E+03	1.78E+08
Ethiprole 48	95	181217	4.10E+06	8.71E+08
Fipronil 24	50	30	2.10E+01	4.27E+01
Fipronil 24	95	143	9.80E+01	2.13E+02
Fipronil 48	50	5.01	4.00E+00	7.40E+00
Fipronil 48	95	25	1.70E+01	3.69E+01
Fluralaner 24	50	19	1.30E+01	2.71E+01
Fluralaner 24	95	90	6.20E+01	1.35E+02
Fluralaner 48	50	3.67	2.00E+00	4.65E+00
Fluralaner 48	95	16	1.10E+01	2.32E+01
GABA 24	50	56931	0.00E+00	1.74E+13
GABA 24	95	274618	0.00E+00	8.49E+13
GABA 48	50	56931	0.00E+00	1.74E+13
GABA 48	95	274618	0.00E+00	8.49E+13
Glutamate 24	50	3108	1.64E+03	6.00E+03
Glutamate 24	95	14992	7.72E+03	3.03E+04
Glutamate 48	50	1391	8.82E+02	2.21E+03
Glutamate 48	95	6707	4.16E+03	1.12E+04
Glycine 24	50	56931	0.00E+00	1.74E+13
Glycine 24	95	274618	0.00E+00	8.49E+13
Glycine 48	50	3108	1.64E+03	6.00E+03
Glycine 48	95	14992	7.72E+03	3.03E+04

Heptachlor 24	50	138	9.50E+01	1.99E+02
Heptachlor 24	95	664	4.54E+02	9.92E+02
Heptachlor 48	50	111	7.70E+01	1.60E+02
Heptachlor 48	95	533	3.65E+02	7.96E+02
Isoguvacine 24	50	56931	0.00E+00	1.74E+13
Isoguvacine 24	95	274618	0.00E+00	8.49E+13
Isoguvacine 48	50	3108	1.64E+03	6.00E+03
Isoguvacine 48	95	14992	7.72E+03	3.03E+04
Ivermectin 24	50	2075	1.23E+03	3.55E+03
Ivermectin 24	95	10009	5.78E+03	1.79E+04
Ivermectin 48	50	885	5.88E+02	1.34E+03
Ivermectin 48	95	4268	2.78E+03	6.73E+03
Lindane 24	50	19.1	1.30E+01	2.72E+01
Lindane 24	95	90.1	6.20E+01	1.35E+02
Lindane 48	50	13.4	9.00E+00	1.92E+01
Lindane 48	95	63.0	4.30E+01	9.52E+01
Lotilaner 24	50	51	3.50E+01	7.30E+01
Lotilaner 24	95	244	1.67E+02	3.64E+02
Lotilaner 48	50	14.5	9.00E+00	1.95E+01
Lotilaner 48	95	65	4.50E+01	9.72E+01
Moxidectin 24	50	3108	1.64E+03	6.00E+03
Moxidectin 24	95	14992	7.72E+03	3.03E+04
Moxidectin 48	50	167	1.15E+02	2.41E+02
Moxidectin 48	95	803	5.49E+02	1.20E+03
Picrotoxin 24	50	2075	1.23E+03	3.55E+03
Picrotoxin 24	95	10009	5.78E+03	1.79E+04
Picrotoxin 48	50	2075	1.23E+03	3.55E+03
Picrotoxin 48	95	10009	5.78E+03	1.79E+04
Sarolaner 24	50	39	2.70E+01	5.68E+01
Sarolaner 24	95	190	1.30E+02	2.83E+02
Sarolaner 48	50	11.4	8.00E+00	1.65E+01
Sarolaner 48	95	55	3.80E+01	8.24E+01

LC_{50} and LC_{95} probit mortality data for *I. ricinus* coated glass vial bioassay.

Treatment (time)	LC	Estimate (ppm)	lower 95%CI	upper 95%CI
Afoxolaner 24	50	87.4	3.95E+01	1.97E+02
Afoxolaner 24	95	4574.4	1.76E+03	1.49E+04
Afoxolaner 48	50	1.81	7.00E-01	5.00E+00
Afoxolaner 48	95	95.8	3.75E+01	2.77E+02
Bifenazate 24	50	7092539	0.00E+00	3.95E+18
Bifenazate 24	95	3E+08	0.00E+00	1.76E+20
Bifenazate 48	50	7092539	0.00E+00	3.95E+18
Bifenazate 48	95	3E+08	0.00E+00	1.76E+20
Dieldrin 24	50	5.8	2.56E+00	1.20E+01
Dieldrin 24	95	78.34	3.71E+01	1.85E+02
Dieldrin 48	50	0.01	0.00E+00	2.82E+06
Dieldrin 48	95	0.19	0.00E+00	4.09E+07
Endosulfan 24	50	7.86	4.19E+00	1.40E+01
Endosulfan 24	95	106.15	5.37E+01	2.50E+02
Endosulfan 48	50	7.86	4.19E+00	1.40E+01
Endosulfan 48	95	106.15	5.37E+01	2.50E+02
Ethiprole 24	50	11.79	4.71E+00	2.82E+01
Ethiprole 24	95	356.54	1.32E+02	1.38E+03
Ethiprole 48	50	3.54	1.25E+00	8.90E+00
Ethiprole 48	95	106.47	3.93E+01	3.91E+02
Fipronil 24	50	4.72	1.95E+00	1.11E+01
Fipronil 24	95	142.78	5.32E+01	5.62E+02
Fipronil 48	50	1.21	4.70E-01	3.00E+00
Fipronil 48	95	37.6	1.41E+01	1.40E+02
Fluralaner 24	50	1.6	7.00E-01	4.00E+00
Fluralaner 24	95	83.1	3.45E+01	2.35E+02
Fluralaner 48	50	0.47	1.00E-01	1.00E+00
Fluralaner 48	95	19.1	7.50E+00	5.50E+01
GABA 24	50	10271772	0.00E+00	9.98E+22
GABA 24	95	4.34E+08	0.00E+00	4.42E+24
GABA 48	50	18228	3.43E+03	1.04E+05
GABA 48	95	769923	1.34E+05	5.13E+06
Glutamate 24	50	4050	1.25E+03	1.38E+04
Glutamate 24	95	171055	4.82E+04	6.85E+05
Glutamate 48	50	18228	3.43E+03	1.04E+05
Glutamate 48	95	769923	1.34E+05	5.13E+06
Glycine 24	50	10183	2.43E+03	4.55E+04
Glycine 24	95	430090	9.41E+04	2.25E+06
Glycine 48	50	10183	2.43E+03	4.55E+04
Glycine 48	95	430090	9.41E+04	2.25E+06

Heptachlor 24	50	29.01	1.53E+01	5.40E+01
Heptachlor 24	95	391.69	1.97E+02	9.20E+02
Heptachlor 48	50	24.25	1.26E+01	4.50E+01
Heptachlor 48	95	327.36	1.65E+02	7.66E+02
Isoguvacine 24	50	2617	8.79E+02	8.12E+03
Isoguvacine 24	95	110539	3.40E+04	4.03E+05
Isoguvacine 48	50	10271772	0.00E+00	9.98E+22
Isoguvacine 48	95	4.34E+08	0.00E+00	4.42E+24
Ivermectin 24	50	113493	1.05E+04	6.81E+06
Ivermectin 24	95	26776670	8.37E+05	2.34E+10
Ivermectin 48	50	2167	6.40E+02	1.58E+04
Ivermectin 48	95	511345	4.95E+04	5.63E+07
Lindane 24	50	3.26	1.27E+00	7.00E+00
Lindane 24	95	43.99	1.93E+01	1.09E+02
Lindane 48	50	4.32	1.80E+00	9.00E+00
Lindane 48	95	58.31	2.67E+01	1.41E+02
Lotilaner 24	50	39.3	1.78E+01	8.70E+01
Lotilaner 24	95	2057.2	8.20E+02	6.34E+03
Lotilaner 48	50	1.11	4.00E-01	3.00E+00
Lotilaner 48	95	59.8	2.26E+01	1.77E+02
Moxidectin 24	50	1.4E+09	0.00E+00	7.77E+39
Moxidectin 24	95	3.31E+11	0.00E+00	5.13E+42
Moxidectin 48	50	1.4E+09	0.00E+00	7.77E+39
Moxidectin 48	95	3.31E+11	0.00E+00	5.13E+42
Picrotoxin 24	50	1893	5.73E+02	1.30E+04
Picrotoxin 24	95	446570	4.46E+04	4.62E+07
Picrotoxin 48	50	458	1.67E+02	1.88E+03
Picrotoxin 48	95	107950	1.46E+04	5.90E+06
Sarolaner 24	50	24.4	1.10E+01	5.40E+01
Sarolaner 24	95	1278	5.17E+02	3.83E+03
Sarolaner 48	50	2.91	1.10E+00	7.00E+00
Sarolaner 48	95	149.4	5.99E+01	4.28E+02

LC_{50} and LC_{95} probit mortality data for *R. sanguineus* coated glass vial bioassay.

Treatment (time)	LC	Estimate (ppm)	lower 95%CI	upper 95%CI
Afoxolaner 24	50	718	5.82E+02	8.90E+02
Afoxolaner 24	95	13569	1.05E+04	1.77E+04
Afoxolaner 48	50	71.1	5.90E+01	8.50E+01
Afoxolaner 48	95	1334	1.08E+03	1.66E+03
Bifenazate 24	50	523320	0.00E+00	2.46E+12
Bifenazate 24	95	9415490	2.00E+00	4.64E+13
Bifenazate 48	50	523320	0.00E+00	2.46E+12
Bifenazate 48	95	9415490	2.00E+00	4.64E+13
Dieldrin 24	50	219.1	9.74E+01	5.01E+02
Dieldrin 24	95	1969.5	8.33E+02	5.80E+03
Dieldrin 48	50	88.	3.95E+01	1.96E+02
Dieldrin 48	95	791.1	3.43E+02	2.24E+03
Endosulfan 24	50	30.8	1.39E+01	6.81E+01
Endosulfan 24	95	276.8	1.21E+02	7.76E+02
Endosulfan 48	50	22.4	1.01E+01	4.96E+01
Endosulfan 48	95	201.3	8.79E+01	5.64E+02
Ethiprole 24	50	31.04	2.20E+01	4.38E+01
Ethiprole 24	95	110.38	7.55E+01	1.79E+02
Ethiprole 48	50	22.82	1.62E+01	3.22E+01
Ethiprole 48	95	81.14	5.55E+01	1.32E+02
Fipronil 24	50	25.67	1.82E+01	3.62E+01
Fipronil 24	95	91.28	6.24E+01	1.48E+02
Fipronil 48	50	5.18	3.60E+00	7.17E+00
Fipronil 48	95	18.07	1.24E+01	2.93E+01
Fluralaner 24	50	21	1.70E+01	2.50E+01
Fluralaner 24	95	394	3.21E+02	4.88E+02
Fluralaner 48	50	2.17	2.00E+00	3.00E+00
Fluralaner 48	95	42	3.50E+01	5.30E+01
GABA 24	50	7814	1.51E+03	4.26E+04
GABA 24	95	140588	2.61E+04	8.51E+05
GABA 48	50	7814	1.51E+03	4.26E+04
GABA 48	95	140588	2.61E+04	8.51E+05
Glutamate 24	50	7814	1.51E+03	4.26E+04
Glutamate 24	95	140588	2.61E+04	8.51E+05
Glutamate 48	50	7814	1.51E+03	4.26E+04
Glutamate 48	95	140588	2.61E+04	8.51E+05
Glycine 24	50	732839	0.00E+00	1.40E+15
Glycine 24	95	13185119	0.00E+00	2.63E+16
Glycine 48	50	732839	0.00E+00	1.40E+15

Glycine 48	95	13185119	0.00E+00	2.63E+16
Heptachlor 24	50	68.2	3.06E+01	1.52E+02
Heptachlor 24	95	613.5	2.67E+02	1.72E+03
Heptachlor 48	50	80.5	3.61E+01	1.79E+02
Heptachlor 48	95	723.8	3.14E+02	2.04E+03
Isoguvacine 24	50	732839	0.00E+00	1.40E+15
Isoguvacine 24	95	13185119	0.00E+00	2.63E+16
Isoguvacine 48	50	732839	0.00E+00	1.40E+15
Isoguvacine 48	95	13185119	0.00E+00	2.63E+16
Ivermectin 24	50	2832	5.58E+02	4.00E+04
Ivermectin 24	95	279797	2.35E+04	5.67E+07
Ivermectin 48	50	41.7	9.00E+00	1.53E+02
Ivermectin 48	95	4089	8.09E+02	1.05E+05
Lindane 24	50	17.7	7.50E+00	4.06E+01
Lindane 24	95	159.1	6.79E+01	4.43E+02
Lindane 48	50	12.7	4.80E+00	2.82E+01
Lindane 48	95	107.5	4.49E+01	3.01E+02
Lotilaner 24	50	195	1.62E+02	2.35E+02
Lotilaner 24	95	3679	2.95E+03	4.64E+03
Lotilaner 48	50	9	7.00E+00	1.10E+01
Lotilaner 48	95	169	1.38E+02	2.09E+02
Moxidectin 24	50	469	1.24E+02	2.92E+03
Moxidectin 24	95	46342	6.02E+03	3.61E+06
Moxidectin 48	50	30.4	6.00E+00	1.09E+02
Moxidectin 48	95	2928	6.02E+02	6.56E+04
Picrotoxin 24	50	148	6.30E+01	3.47E+02
Picrotoxin 24	95	2654	1.10E+03	6.83E+03
Picrotoxin 48	50	29.2	1.20E+01	6.94E+01
Picrotoxin 48	95	526	2.18E+02	1.33E+03
Sarolaner 24	50	98	8.20E+01	1.17E+02
Sarolaner 24	95	1849	1.49E+03	2.31E+03
Sarolaner 48	50	8.06	6.00E+00	9.00E+00
Sarolaner 48	95	147	1.19E+02	1.81E+02

LC_{50} and LC_{95} *C. felis* probit mortality data for the 'artificial dog' bioassay.

Treatment (time)	LC	Estimate (ppm)	lower 95%CI	upper 95%CI
Dieldrin 24	50	31.84	1.93E+01	5.28E+01
Dieldrin 24	95	138.91	8.25E+01	2.52E+02
Dieldrin 48	50	25.13	1.52E+01	4.16E+01
Dieldrin 48	95	109.62	6.52E+01	1.99E+02
Endosulfan 24	50	33.46	2.02E+01	5.55E+01
Endosulfan 24	95	145.95	8.66E+01	2.65E+02
Endosulfan 48	50	20.7	1.21E+01	3.31E+01
Endosulfan 48	95	87.3	5.20E+01	1.58E+02
Ethiprole 24	50	1.09	6.60E-01	1.81E+00
Ethiprole 24	95	4.77	2.85E+00	8.62E+00
Ethiprole 48	50	0.48	2.90E-01	7.90E-01
Ethiprole 48	95	2.09	1.25E+00	3.78E+00
Fipronil 24	50	0.05	4.00E-02	8.00E-02
Fipronil 24	95	0.24	1.60E-01	3.90E-01
Fipronil 48	50	0.05	3.00E-02	7.00E-02
Fipronil 48	95	0.21	1.40E-01	3.40E-01
Lindane 24	50	2.11	1.28E+00	3.47E+00
Lindane 24	95	9.19	5.48E+00	1.66E+01
Lindane 48	50	0.98	5.90E-01	1.61E+00
Lindane 48	95	4.26	2.54E+00	7.70E+00
Heptachlor 24	50	3324	6.60E-01	1.77E+07
Heptachlor 24	95	14903	2.97E+00	8.08E+07
Heptachlor 48	50	3324	6.60E-01	1.77E+07
Heptachlor 48	95	14903	2.97E+00	8.08E+07
GABA 24	50	27835	0.00E+00	3.43E+15
GABA 24	95	124801	0.00E+00	1.56E+16
GABA 48	50	27835	0.00E+00	3.43E+15
GABA 48	95	124801	0.00E+00	1.56E+16
Glutamate 24	50	27835	0.00E+00	3.43E+15
Glutamate 24	95	124801	0.00E+00	1.56E+16
Glutamate 48	50	27835	0.00E+00	3.43E+15
Glutamate 48	95	124801	0.00E+00	1.56E+16
Glycine 24	50	27835	0.00E+00	3.43E+15
Glycine 24	95	124801	0.00E+00	1.56E+16
Glycine 48	50	27835	0.00E+00	3.43E+15
Glycine 48	95	124801	0.00E+00	1.56E+16
Isoguvacine 24	50	27835	0.00E+00	3.43E+15
Isoguvacine 24	95	124801	0.00E+00	1.56E+16
Isoguvacine 48	50	27835	0.00E+00	3.43E+15
Isoguvacine 48	95	124801	0.00E+00	1.56E+16

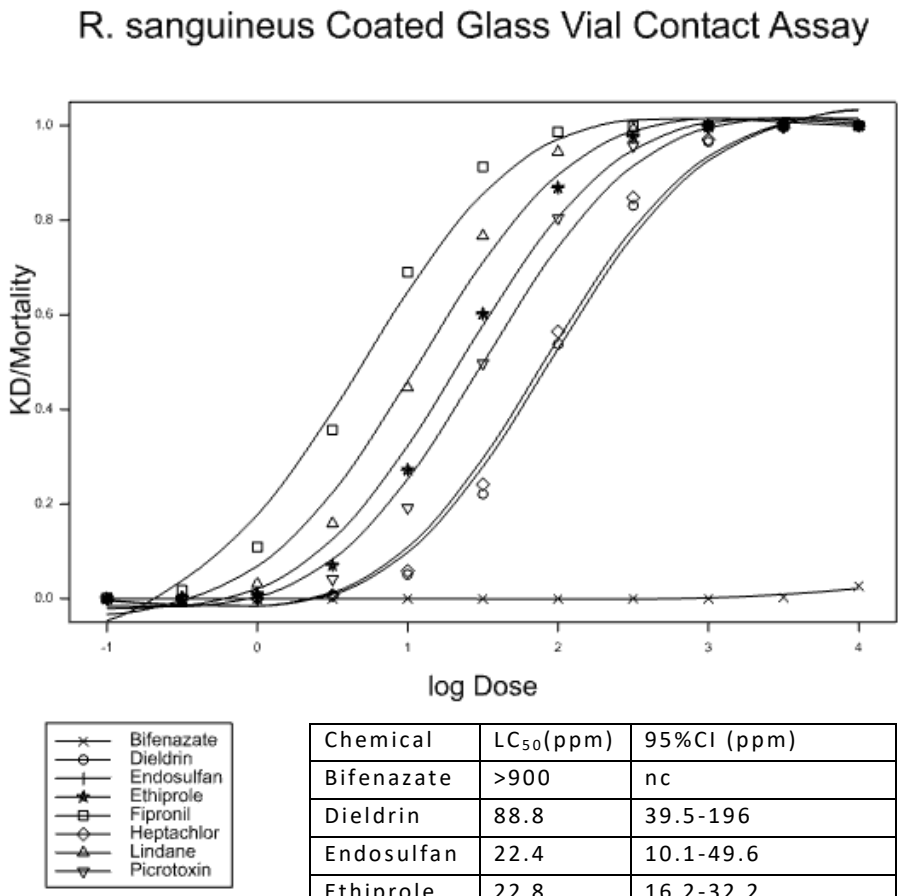
Afoxolaner 24	50	0.0896	4.93E-02	1.64E-01
Afoxolaner 24	95	0.5225	2.74E-01	1.25E+00
Afoxolaner 48	50	0.0314	1.53E-02	6.00E-02
Afoxolaner 48	95	0.1831	9.53E-02	4.06E-01
Fluralaner 24	50	0.0477	2.51E-02	8.70E-02
Fluralaner 24	95	0.2785	1.48E-01	6.27E-01
Fluralaner 48	50	0.0113	3.80E-03	2.80E-02
Fluralaner 48	95	0.0658	2.64E-02	1.72E-01
Lotilaner 24	50	0.582	2.94E-01	1.18E+00
Lotilaner 24	95	3.3946	1.63E+00	9.03E+00
Lotilaner 48	50	0.582	2.94E-01	1.18E+00
Lotilaner 48	95	3.3946	1.63E+00	9.03E+00
Sarolaner 24	50	0.0896	4.93E-02	1.64E-01
Sarolaner 24	95	0.5225	2.74E-01	1.25E+00
Sarolaner 48	50	0.0896	4.93E-02	1.64E-01
Sarolaner 48	95	0.5225	2.74E-01	1.25E+00
Ivermectin 24	50	3.49	2.87E+00	4.24E+00
Ivermectin 24	95	13.39	1.05E+01	1.80E+01
Ivermectin 48	50	2.11	1.73E+00	2.56E+00
Ivermectin 48	95	8.09	6.33E+00	1.09E+01
Moxidectin 24	50	28.29	2.24E+01	3.64E+01
Moxidectin 24	95	108.67	7.96E+01	1.59E+02
Moxidectin 48	50	25.63	2.05E+01	3.26E+01
Moxidectin 48	95	98.44	7.28E+01	1.42E+02
Bifenazate 24	50	44.77	3.42E+01	5.86E+01
Bifenazate 24	95	140.83	1.04E+02	2.05E+02
Bifenazate 48	50	18.6	1.42E+01	2.43E+01
Bifenazate 48	95	58.52	4.33E+01	8.50E+01
Picrotoxin 24	50	29.81	2.28E+01	3.90E+01
Picrotoxin 24	95	93.78	6.91E+01	1.37E+02
Picrotoxin 48	50	20.1	1.53E+01	2.61E+01
Picrotoxin 48	95	62.92	4.65E+01	9.15E+01

LC_{50} and LC_{95} probit mortality data for the *R. microplus* Oviposition bioassay

Treatment (time)	LC	Estimate (ppm)	lower 95%CI	upper 95%CI
Afoxolaner	50	13.01	7.24E+00	2.26E+01
Afoxolaner	95	90.5	4.97E+01	2.00E+02
Bifenazate	50	199676	7.51E+03	5.64E+06
Bifenazate	95	1341157	5.11E+04	4.07E+07
Dieldrin	50	1462	9.54E+02	2.21E+03
Dieldrin	95	5082	3.25E+03	9.42E+03
Endosulfan	50	1367	9.42E+02	1.91E+03
Endosulfan	95	4752	3.28E+03	7.95E+03
Ethiprole	50	71.2	3.66E+01	1.21E+02
Ethiprole	95	574.8	3.08E+02	1.64E+03
Fipronil	50	16.5	7.80E+00	3.13E+01
Fipronil	95	133.1	6.49E+01	4.30E+02
Fluralaner	50	12.3	7.32E+00	1.93E+01
Fluralaner	95	85.4	5.22E+01	1.65E+02
GABA	50	50685	2.91E+04	8.80E+04
GABA	95	340434	1.91E+05	6.57E+05
Glycine	50	378022	1.24E+05	1.21E+06
Glycine	95	2539054	8.04E+05	9.15E+06
Heptachlor	50	3748	2.47E+03	5.56E+03
Heptachlor	95	13029	8.51E+03	2.34E+04
Isoguvacine	50	105475	5.57E+04	2.02E+05
Isoguvacine	95	708440	3.61E+05	1.53E+06
Ivermectin	50	5.71	4.18E+00	7.80E+00
Ivermectin	95	9.27	6.83E+00	1.27E+01
Lindane	50	1732	1.10E+03	2.69E+03
Lindane	95	6021	3.79E+03	1.13E+04
Lotilaner	50	141.8	8.02E+01	2.43E+02
Lotilaner	95	984.8	5.44E+02	2.18E+03
Moxidectin	50	196.65	1.15E+02	3.53E+02
Moxidectin	95	319.06	1.83E+02	5.92E+02
Picrotoxin	50	820	4.89E+02	1.35E+03
Picrotoxin	95	5510	3.30E+03	9.80E+03
Sarolaner	50	9.12	4.99E+00	1.59E+01
Sarolaner	95	62.8	3.38E+01	1.43E+02

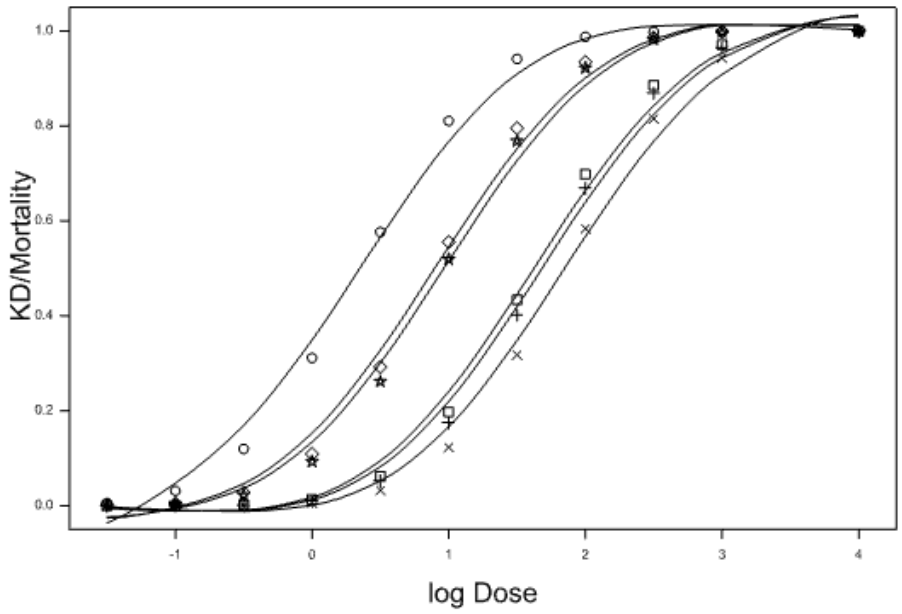
8.3. Appendix 3

The results of contact bioassays on *R. sanguineus*, using organochlorines (dieldrin, endosulfan, heptachlor and lindane), phenylpyrazoles (fipronil and ethiprole), bifenazate, picrotoxin, isoxazolines (afoxolaner, fluralaner, lotilaner and sarolaner) and macrocyclic lactones (ivermectin and moxidectin).



Chemical	LC_{50}(ppm)	95%CI (ppm)
Bifenazate	>900	nc
Dieldrin	88.8	39.5-196
Endosulfan	22.4	10.1-49.6
Ethiprole	22.8	16.2-32.2
Fipronil	5.18	3.6-7.17
Heptachlor	80.5	36.1-179
Lindane	12.7	4.8-28.2
Picrotoxin	29.2	12-69.4

R. sanguineus Coated Glass Vial Contact Assay



Chemical	LC_{50}(ppm)	95%CI(ppm)
Afoxolaner	71.1	59-85
Fluralaner	2.17	2-3
Ivermectin	41.2	9-153
Lotilaner	9.46	7-11
Moxidectin	30.4	6-109
Sarolaner	8.06	6-9

8.4. Appendix 4

DNA sequence for *C. felis* GABAR synthesised by Invitrogen GeneArt optimised for *X. laevis* expression

[1]GAATTGGCGGAAGGCCGTCAAGGCCACGTGTCTTGTCCGCGGTACCCATCGGCGGC
CGCAAGAAGAATCCGGGCCGTCGGTGAGATGCGCCAGGGGCGGCTGGTGTAGCGGG
GGCATGGCTGCTCTGACAAGAGCTACAATGGGAGCACTGCTGCTGGCTCTGTCTCCA
GCTCTGCTGCTGATTTGGCTGCCATACGCTGATGCTGCTACAGGCGGAGGATCTATGT
ACGGGGATGTGAACATTAGCGCCATCCTGGATAACTTCAGCGTGTCCTACGATAAGA
GAGTTAGGCCAAATTACGGCGGACCACCAGTGGAAGTGGGAGTGACTATGTACGTGC
TGTCTATCTCTAGCCTGAGCGAAGTGAAGATGGACTTCACCCTGGACTTCTACTTTAG
GCAGTTCTGGACAGATCCAAGGCTGGCTTACAGAAAAAGACCAGGCGTGGAAACAC
TGAGCGTGGGATCTGAGTTTATCAAGAACATCTGGGTGCCCGACACCTTCTTTGTGA
ACGAGAAGCAGAGCTACTTCCACATTGCCACAACCAGCAACGAGTTCATCAGAATCC
ACCACAGCGGATCCATCACAAGATCCATCAGACTGACAATCACAGCCAGCTGCCCAA
TGAACCTGCAGTACTTTCCAATGGATAGGCAGCTGTGCCACATCGAGATCGAGAGCT
TTGGATACACCATGAGGGACATCAGATACAAGTGGAACGAGGGACCAAACAGCGTG
GGAGTGTCTAATGAAGTGTCTCTGCCACAGTTTAAGGTGCTGGGACACAGACAGAGA
GCTATGGAAATTAGCCTGACCACCGGAAACTACTCTAGACTGGCTTGCGAGATCCAG
TTCGTTAGATCTATGGGCTACTACCTGATCCAGATCTACATCCCATCTGGCCTGATCG
TGATTATCAGCTGGGTGTCCTTTTGGCTGAACAGACACGCAACACCAGCTAGAGTGG
CTCTGGGAGTGACAACAGTGCTGACAATGACAACACTGATGAGCAGCACAAACGCT
GCTCTGCCAAAGATCAGCTACGTGAAGTCTATCGATGTGTACCTGGGAACCTGCTTT
GTGATGGTGTTTGCTTCTCTGCTGGAATACGCTACAGTGGGCTACATGGCTAAGAGG
ATCCAGATGAGAAAGCAGAGATTCATGGCCATCCAGAAGATCGCTGAACAGAAAAA
ACTGCAGGCTGAAGGCGGAGGACCAGGCGGACCTGGCGATCACTCTCACGCTCCAA
AACAGACCGAAGTTAGATTCAAAGTTAGAGATCCCAAGGCCCACTCTAAGGGCGGA
ACACTGGAAAACACAATCAATGGCGGAAGAGGCGGAGCTGCTGCAGATGAAGAATC
TGCTGCTCCAGCTCCACAGCACCTGATTCATCCTGGAAAGGATATCAACAAGCTGCT
GGGAATCACACCAAGCGGAATCGATAAGTACAGCAGGATCGTGTTTCCAGTGTGCTT
TGTGTGCTTCAACCTGATGTACTGGATCATGTACCTGCACGTGTCCGATGTGGTGGCT
GATGATCTGGTGCTGCTGGGAGAAGATAAGTGAAGGCGGCCGCCAGTATGCACTCCC
GAGCTCGGAGCACAAGACTGGCCTCATGGGCCTTCCGCTCACTGCC[1545]

8.5. Appendix 5

Codon optimised DNA sequence for *D. melanogaster* GABARbd synthesised by Invitrogen GeneArt

[1]ATGAGTGATTCAAAAATGGACAAGCTGGCCCGGATGGCGCCCCTGCCCCGCACACC
GCTGCTAACCATCTGGCTGGCCATCAACATGGCCCTGATTGCACAGGAAACGGGCCA
CAAACGGATCCATACAGTGCAAGCGGCGACTGGCGGTGGCAGCATGCTGGGTGACG
TAAACATATCCGCTATTCTCGACTCCTTTAGTGTTAGTTACGACAAAAGAGTAAGAC
CCAATTACGGTGGACCTCCTGTCGAAGTCGGAGTCACCATGTATGTGCTATCGATCA
GCTCGCTCTCAGAAGTGAAAATGGACTTCACATTGGATTTTTACTTTCGTCAATTTTG
GACCGATCCTCGTTTAGCGTATAGAAAACGACCTGGTGTAGAAACACTATCGGTTGG
ATCAGAGTTCATTAAGAATATTTGGGTACCTGACACCTTTTTTGTAAATGAAAAACA
ATCATATTTTCACATTGCAACAACCAGTAATGAATTCATACGTGTGCATCATTCTGGA
TCGATAACAAGAAGTATTAGATTGACTATAACCGCATCGTGTCCGATGAATCTACAA
TATTTCCCCATGGATCGCCAGCTGTGCCACATTGAAATCGAAAGCTTCGGCTACACG
ATGCGTGACATCCGCTATAAATGGAACGAAGGCCCCAACTCGGTCGGTGTCTCGAGT
GAGGTTTCGCTGCCCCAATTTAAGGTCTTGGGTCATCGGCAAAGAGCTATGGAAATC
AGTCTTACCACAGGCAACTATTCGCGTTTAGCCTGCGAAATTCAGTTCGTGCGTTCGA
TGGGCTACTACCTTATACAAATCTACATACCCTCTGGACTGATCGTTATTATATCATG
GGTATCATTTTGGCTCAATCGCAATGCAACGCCGGCGCGTGTGGCGCTCGGTGTGAC
AACCGTGTTGACAATGACCACTTTGATGTCGTCAACAAATGCAGCGCTGCCAAAGAT
TTCGTACGTCAAATCGATTGACGTCTATCTGGGAACATGCTTCGTTATGGTCTTTGCC
AGTCTACTGGAATACGCCACGGTCGGCTACATGGCAAAACGAATTCAAATGCGAAAA
CAAAGATTTATGGCGATCCAAAAGATAGCCGAACAGAAAAAGCAACAGCTCGACGG
AGCGAACCAACAGCAGGCGAATCCCAATCCCAATGCAAATGTGGGCGGACCCGGAG
GAGTGGGCGTTGGACCCGGCGGACCCGGAGGACCCGGTGGCGGGGTCAATGTGGGC
GTCGGTATGGGCATGGGACCGGAACATGGCCACGGGCATGGACACCACGCCCACAG
CCATGGACATCCGCATGCGCCCAAGCAAACAGTGAGTAACCGCCCAATCGGCTTTTC
CAATATCCAACAAAACGTTGGTACGCGCGGTTGCTCGATAGTGGGACCCTTGTTCCA
GGAGGTGAGATTCAAGGTCCACGACCCGAAGGCCCACTCCAAGGGCGGAACGCTGG
AGAATACGGTGAATGGCGGACGCGGTGGTCCGCAATCGCATGGACCGGGTCCGGGC
CAAGGCGGCGGACCGCCCGGCGGTGGCGGAGGCGGTGGAGGCGGGGGCGGACCGCC
CGAGGGCGGTGGCGATCCGGAGGCAGCGGTTCCAGCCCATCTTCTGCATCCGGGAAA
AGTAAAAAAGGACATCAACAAGCTGCTGGGCATCACGCCCTCCGACATCGACAAGT
ACTCACGCATCGTGTTCCCCGTGTGCTTCGTGTGCTTCAACCTGATGTACTGGATCAT
TTACCTGCATGTCAGCGACGTGGTCGCCGATGATCTGGTGCTCCTGGGCGAGGAGTA
G[1821]

8.6. Appendix 6

Raw data for dieldrin, ethiprole and fipronil range-finding *D. melanogaster* larval bioassays with the genotype

RFP:vas:int/+ ;attp40{GABARbd^{WT}}/c747GAL4; GABAR^{-}/GABAR^{-}.

Chemical	Concentration (mg/L)	Number of larvae	Number of pupae	Mortality (%)
Dieldrin	1000	20	1	95
	100	20	2	90
	10	20	10	50
	1	20	12	40
	0.1	20	15	25
	0.01	20	18	10
	0.001	20	19	5
	0.0001	20	20	0
	0.00001	20	18	10
	0.000001	20	19	5
Ethiprole	1000	10	0	100
	100	10	1	90
	10	10	8	20
	1	10	9	10
	0.1	10	9	10
	0.01	10	8	20
	0.001	10	10	0
	0.0001	10	9	10
	0.00001	10	9	10
	0.000001	10	9	10
Fipronil	1000	20	0	100
	100	20	0	100
	10	20	0	100
	1	20	8	60
	0.1	20	12	40
	0.01	20	19	5
	0.001	20	20	0
	0.0001	20	18	10
	0.00001	20	19	5
	0.000001	20	20	0
Control	-	20	19	95
Control	-	20	18	90
Acetone	-	20	17	85
Acetone	-	20	19	95

8.7. Appendix 7

DNA sequence for human nAChRα7 cloned into plasmid vector pSP64GL for *X. laevis* expression

[1]AAAGGCGCGCGAGCCGAGCGGCGAGGTGCCTCTGTGGCCGCAGGCGCAGGCCCGG
GCGACAGCCGAGACGTGGAGCGCGCCGGCTCGCTGCAGCTCCGGGACTCAACATGC
GCTGCTCGCCGGGAGGCGTCTGGCTGGCGCTGGCCGCGTCGCTCCTGCACGGTAAAG
CCACTGCCTCCCCGCCCTCCACTCCTCCGTGGGATCCCGGGCACATCCCGGGCGCCTC
TGTGCGCCCCGCGCCTGGGCCAGTGTCCCTGCAAGGCGAGTTCCAGAGGAAGCTTTA
CAAGGAGCTGGTCAAGAACTACAATCCCTTGGAGAGGCCCGTGGCCAATGACTCGCA
ACCACTCACCGTCTACTTCTCCCTGAGCCTCCTGCAGATCATGGACGTGGATGAGAA
GAACCAAGTTTTAACCACCAACATTTGGCTGCAAATGTCTTGGACAGATCACTATTT
ACAGTGGAATGTGTCAGAATATCCAGGGGTGAAGACTGTTCGTTTCCCAGATGGCCA
GATTTGGAAACCAGACATTCTTCTCTATAACAGTGCTGATGAGCGCTTTGACGCCAC
ATTCCACACTAACGTGTTGGTGAATTCTTCTGGGCATTGCCAGTACCTGCCTCCAGGC
ATATTCAAGAGTTCCTGCTACATCGATGTACGCTGGTTTCCCTTTGATGTGCAGCACT
GCAAACTGAAGTTTGGGTCCTGGTCTTACGGAGGCTGGTCCTTGGATCTGCAGATGC
AGGAGGCAGATATCAGTGGCTATATCCCCAATGGAGAATGGGACCTAGTGGGAATCC
CCGGCAAGAGGAGTGAAAGGTTCTATGAGTGCTGCAAAGAGCCCTACCCCGATGTCA
CCTTCACAGTGACCATGCGCCGCAGGACGCTCTACTATGGCCTCAACCTGCTGATCC
CCTGTGTGCTCATCTCCGCCCTCGCCCTGCTGGTGTTCCTGCTTCCTGCAGATTCCGG
GGAGAAGATTTCCCTGGGGATAACAGTCTTACTCTCTCTTACCGTCTTCATGCTGCTC
GTGGCTGAGATCATGCCCGCAACATCCGATTCGGTACCATTGATAGCCCAGTACTTC
GCCAGCACCATGATCATCGTGGGCCTCTCGGTGGTGGTGACAGTGATCGTGCTGCAG
TACCACCACCACGACCCCGACGGGGGCAAGATGCCCAAGTGGACCAGAGTCATCCTT
CTGAACTGGTGCGCGTGGTTCCTGCGAATGAAGAGGCCCGGGGAGGACAAGGTGCG
CCCGGCCTGCCAGCACAAGCAGCGGCGCTGCAGCCTGGCCAGTGTGGAGATGAGCG
CCGTGGCGCCGCCGCCCGCCAGCAACGGGAACCTGCTGTACATCGGCTTCCGCGGCC
TGGACGGCGTGCACTGTGTCCCGACCCCCGACTCTGGGGTAGTGTGTGGCCGCATGG
CCTGCTCCCCCACGCACGATGAGCACCTCCTGCACGGCGGGCAACCCCCCGAGGGGG
ACCCGGACTTGGCCAAGATCCTGGAGGAGGTCCGCTACATTGCCAACCGCTTCCGCT
GCCAGGACGAAAGCGAGGCGGTCTGCAGCGAGTGGAAGTTCGCCGCCTGTGTGGTG
GACCGCCTGTGCCTCATGGCCTTCTCGGTCTTCACCATCATCTGCACCATCGGCATCC
TGATGTCGGCTCCCAACTTCGTGGAGGCCGTGTCCAAAGACTTTGCGTAACCACGCC
TGGTTCTGTACATGTGGAAAACTCACAGATGGGCAAGGCCTTTGGCTTGGCGAGATT
TGGGGGTGCTAATCCAGGACAGCATTACACGCCACAACTCCAGTGTTCCCTTCTGGC
TGTCAGTCGTGTTGCTTACGGTTTCTTTGTTACTTTAGGTAGTAGAATCTCAGCACTT
TGTTTCATATTCTCAGATGGGCTGATAGATATCCTTGGCACATCCGTACCATCGGTCA
GCAGGGCCACTGAGTAGTCATTTTGCCCATTAGCCCACTGCCTGGAAAGCCCTTCGG
AGAGCTCCCCATGGCTCCTCACCACCGAGACAGTTGGTTTTGCATGTCTGCATGAAG
GTCTACCTGAAAATTCAACATTTGCTTTTTGCTTGTGTACAAACCCAGATTGAAGCTA
AAATAAACCAGACTCACTAAATCCTTTCCAATAATTGACTGGTGGAAGGAAAACAAA
AAACAAAAACTAAAAACCTCTTAGCTTTTCTGCAATTCAACTTTTTATTTTTATTTTT
ATTTCTATCAAAGACGGTAGAGAGAAACAGCTTGATGCTGTTTCTACATTAAAAAAA

AAAAAAAAAGACAGACTGTTGGTCTTACTAAGGATGTTTTTACCAGCCTGCCTGACT
TCTGCAAACCTACCCTGTCAAGGAGATCAAAGGGACGCAGGTTTCTGTTTATTCTGA
ACAAGGGCCAGGCCCCGCGGAGTGTCTTTGGTGGATCCCAGATAACTCCTAGGTGCT
GCTCTCAGACACTGAGGAGTTGAGCAAATCTGTTCTATTCTGCAGAACCCACAGGAC
AAATAAGAGTTCTACTAGAATTAACAGCCCAAAAGAATAGCTACAGCTAAGTGAAG
CCACTTACGTGGGCTTTAAAAAAATAATGTGTTAGCTGATTCACATGCACTGGAGTT
AATTAGTCTTAGAAATGTGTGCATCCATACAAATGCACAACATAAAGTGAACATATT
CCTAGGCCCTTTCTGCCTGTGTCAGGGCCAGGAAGTAGAGGCTGGGAACTCTTCTGG
TCCCCAGTATGGCAGGCGCCAGGGAGGGGATGGTGTGGCCCATCCCTTCTCTGGATA
CCTGGCCAGTGGCAGGCAGCAGGGAGGAGCTGGCCGACCCTCAGTGACTGACAAGC
CAGCAATTCTGAGTTCTGGCCTTTGGGAGTCTGCCTGCTCCAAGCCAGTCCACCCCA
GCTGCAGCCCCAAAAGCTGGCTCAAAGTCCTTGGGTGGATTCACTGGAGATGGGCAA
CTTAAAACAAGAGAAACTTTAATTTTTAAACCTAAGTGATGATACAGCTCTTCCCTTA
GATTATCGCCCAGGCTGGAGTGCAGTGGCATGATCTCAGCTCACTGCAAGCTCCACC
TCCTGGGTTCATGCCATTCTCCTGCCTCAGCCTCCCCCCGAGTAACTGGGAATACAGG
CGCCCGCCACCATGCCTGGCTAATTTTTTGTATTTTTAGTAGAGATAGGGTTTCATCA
TGTTAGCCAGGATGGTCTCATTCTTATTCTTTAATGAGATCAGAGGGTAATTCACCAA
GAAAGACCTCTCCTGTTCCATTGTGTCATCCAACAACTGCTCAGAGCTCAAAATTATA
GAAGGCTTCTGAGCCCCTAGAGATTTTTAATTTGCTTCTAATCCCTGAGGTGGGAACA
TCATGAGGGAAGATTTGATTTTCAGAGTTAAATAAATTGTATGTGCTTTTCCAGCCA[34]
[28]

8.8. Appendix 8

DNA sequence for *R. microplus* nAChRα6 cloned into a plasmid vector for *X. laevis* expression

[1]GAAGAGGCCCGCAGGCCCACCACTCGCGGCGTACCACGACGCGGACCATGCGCCCC
GGACGCCTGTCTGTGCCGCTGCAGCTAGGCTTCTGCGCCAACCTGCTGTGGATCGCC
GTGCTGCTCACCGCGCCTCAGGACTCTGAACAAGGCGCGCACGAGCGGCGGCTTCTG
GCAGACCTGCTGGCCAACTACAACACCCTGGAGCGGCCCGTGCTCAACGAGTCGGAG
CCGCTCATCCTCAGCTTCGGGCTCACACTGCAGCAGATCATAGACGTCGACGAAAAG
AATCAGCTAATTATTACAAATATCTGGTTAACATTGGATTGGATAGATGTGAATCTA
CGTTGGAACCCAAAAGACTACGGCGGAGTGCAGGACCTGCGTATTCCGCCAAACAA
AATTTGGAAGCCTGACGTGCTCATGTACAACAGCGCGGACGAAAAGTTCGACGGCAC
GTACCCGACCAACGTGGTCGTGCGGAGCAACGGCAGTTGCAACTACATCCCTCCTGG
CATCTTTAAGAGCACGTGCAAGATCGACATTACGTGGTTCCCTTTTGACGATCAGAA
GTGCGACCTGAAGTTCGGCTCCTGGACCTATCACGGTTATCAGCTGGACCTTCGTGTC
AACAGTGAGGAAGGCGGGGATCTGACTACCTACATTCCCAATGGCGAGTGGGACCTG
ATAGGCGTGCCGGGAGTGCGCAACGTTCGCGAGTATGCCTGCTGTCCGGAGCCGTAC
ATCGACATCACGTACACCATCCACATCCGGCGGCGCACGCTCTACTACGGCTTCAAC
CTCATCATTCCCTGCGTGCTCATCTCGTCCATGACTCTGCTCGGTTTCACGCTGCCCC
CCGACACCGGAGAGAGGCTCACCCTGGGTGTAACCATTTTGCTGTCCCTGACGGTAT
TCATGCTCCAGCTCGCCGAGACCATGCCTCCGACGTCCGATGCTGTCTCCATAATAG
GAACTTATTTTGCCTGCATCATGATCATGGTCGCCTTTTCGGTGGTCATGACCGTGGT

GGTCCTGAACTATCATCACAGAAATCAAGAGACGACCGAAATGCCTGCTTTGATTCG
CACGGTGTTCCTGGTGTGGCTCCCGTGGCTTCTGCGCATGGAGCCTCCGGGCCAGAA
GGCGAACAGGCGCAGCCTCTTCCTCAACAGCAAGATGAAAGAGCTCGAGCTGAAGG
AGCGCTCATCGCGGAGTCTGCTGGCCAACGTGCTGGACATCGACGACGACTTCCGCA
CGGCCAACAGCGCCGCCGCCGCCGACTGCCACGGGTCTCGGACCCCGTTCCTGGGCG
GTGGCGGCGGGGCGTCCACGGTGCACGCTTGCGTCCACTCGTCGCGTGAACTGAACT
TGATCTTGCGCGAGCTGCGCTTCATCACGAGCCGCATGCGCAAGGACGAGCAAGAGC
GGGAGGTCGTTGGCGAGTGGAAGTTCGCGGCCATGGTCGTCGACCGCTGCTGCCTCA
TCATCTTCTCCCTGTTCACCATCATCTCCACCTGCGCCTGCCTCTTCTCGGCRCCCCAT
CTGGTCGCCTAGCGCACCCTGCTYCTAGGACAGCACWTTAACCGCCACCAGCTTCCT
CCACCGGCGGCCTTCCTCTCGGAGAGCTTGTTCGCTACGTTCTTTTGCGCAAGCCCTG
CTTGTTAGAGCGCGGCTTCYGAGATTGATTGCTGGAGCCAATCTCGAAGGCCACAAT
CTCACAGCGCGGGCTCGTGTGCGAGAACGTGGCTCGTGAAGAGTTCCAGGTGACGCC
CTTGTTGCAACAYCCCGTGAAGTCCTGTCCACTTCCCCACGCCATCACGTGCGAAGA
GATGCAGCGCGAAACACGTAYGACGCGAAGACTTCGTACCGCACTGACCCTTACTGT
GGGGAGGAGGAAGACACGTGGAGGTCGCAGGAGCTAGTTTTTTTTTAAGTCTCAACT
CATGTGCCAATCATGAGCCGCCACTTGTGCGAAAGCGTTGGACCATCTCGGAGGATC
TGGTAGCACCGTCCGAAGCTGGTGCCTTGGCCGTCGCTTTCATTCTATATAGGATAAA
ATAACTTCATGTATGGCTGCCAAACTGTTTGAAGGGTCAAGCGGACTTATCAACCGA
GCCCAACGAAGGAAGTAAAGCACCGGGTCTTCCCTCTACGAGCTTCGTGATCGTGAG
ATGCCCGCCATGATGCGACGCCACTYGTTACTTGCTTGACCACCGTCATGGACGGCT
CGTCGGAGTAGGATAAGCCACGCRCGCAACGTCATCTTGCCAGTCCTTTCTTTCGTCG
GTGAATGGTGCGTATGAGTAAAAAAAAA[2329]

9. References

ALAO, O. R. & DECKER, C. F. 2012. Lyme Disease. *Dm Disease-a-Month,* 58**,** 335-345.

ARTHROPOD-PESTICIDE-RESISTANCE-DATABASE. 2018. https://www.pesticideresistance.org/ [Online]. [Accessed].

ASAHI, M., KOBAYASHI, M., MATSUI, H. & NAKAHIRA, K. 2015. Differential mechanisms of action of the novel gamma-aminobutyric acid receptor antagonist ectoparasiticides fluralaner (A1443) and fipronil. *Pest Manag Sci,* 71**,** 91-5.

AU, S., COHEN, S. & PANTE, N. 2010. Microinjection of Xenopus laevis oocytes as a system for studying nuclear transport of viruses. *Methods,* 51**,** 114-120.

BAKER, C., TIELEMANS, E., PRULLAGE, J. B., CHESTER, S. T., KNAUS, M., REHBEIN, S., FOURIE, J. J., YOUNG, D. R., EVERETT, W. R. & ROSENTEL, J. K. 2014. Efficacy of a novel topical combination of fipronil, (S)-methoprene, eprinomectin and praziquantel against adult and immature stages of the cat flea (Ctenocephalides felis) on cats. *Vet Parasitol,* 202**,** 54-8.

BANETH, G. 2014. Tick-borne infections of animals and humans: a common ground. *Int J Parasitol,* 44**,** 591-6.

BAO, W. X., NARAI, Y., NAKANO, A., KANEDA, T., MURAI, T. & SONODA, S. 2014. Spinosad resistance of melon thrips, Thrips palmi, is conferred by G275E mutation in alpha6 subunit of nicotinic acetylcholine receptor and cytochrome P450 detoxification. *Pestic Biochem Physiol,* 112**,** 51-5.

BASS, C., DENHOLM, I., WILLIAMSON, M. S. & NAUEN, R. 2015. The global status of insect resistance to neonicotinoid insecticides. *Pestic Biochem Physiol,* 121**,** 78-87.

BASS, C. & FIELD, L. M. 2011. Gene amplification and insecticide resistance. *Pest Management Science,* 67**,** 886-890.

BASS, C., PUINEAN, A. M., ZIMMER, C. T., DENHOLM, I., FIELD, L. M., FOSTER, S. P., GUTBROD, O., NAUEN, R., SLATER, R. & WILLIAMSON, M. S. 2014. The evolution of insecticide resistance in the peach potato aphid, Myzus persicae. *Insect Biochem Mol Biol,* 51**,** 41-51.

BASS, C., SCHROEDER, I., TURBERG, A., FIELD, L. M. & WILLIAMSON, M. S. 2004. Identification of the Rdl mutation in laboratory and field strains of the cat flea, Ctenocephalides felis (Siphonaptera: Pulicidae). *Pest Manag Sci,* 60**,** 1157-62.

BAXTER, S. W., CHEN, M., DAWSON, A., ZHAO, J. Z., VOGEL, H., SHELTON, A. M., HECKEL, D. G. & JIGGINS, C. D. 2010. Mis-Spliced Transcripts of Nicotinic Acetylcholine Receptor alpha 6 Are Associated with Field Evolved Spinosad Resistance in Plutella xylostella (L.). *Plos Genetics,* 6.

BECK, W. & PFISTER, K. 2004. Recent investigations on the population dynamics of cat fleas (Ctenocephalides felis) and the concept of an integrated flea control. *Praktische Tierarzt,* 85**,** 555-+.

BECSKEI, C., DE BOCK, F., ILLAMBAS, J., MAHABIR, S. P., FARKAS, R. & SIX, R. H. 2016. Efficacy and safety of a novel oral isoxazoline, sarolaner (Simparica (TM)) in the treatment of naturally occurring flea and tick infestations in dogs presented as veterinary patients in Europe. *Veterinary Parasitology,* 222**,** 49-55.

BELELLI, D., CALLACHAN, H., HILLVENNING, C., PETERS, J. A. & LAMBERT, J. J. 1996. Interaction of positive allosteric modulators with human and Drosophila recombinant GABA receptors expressed in Xenopus laevis oocytes. *British Journal of Pharmacology,* 118**,** 563-576.

BERTRAND, D., BALLIVET, M., GOMEZ, M., BERTRAND, S., PHANNAVONG, B. & GUNDELFINGER, E. D. 1994. Physiological-Properties of Neuronal Nicotinic Receptors Reconstituted from the Vertebrate Beta-2 Subunit and Drosophila Alpha-Subunits. *European Journal of Neuroscience,* 6**,** 869-875.

BEUGNET, F., DEVOS, C., LIEBENBERG, J., HALOS, L. & FOURIE, J. 2014. Afoxolaner against fleas: immediate efficacy and resultant mortality after short exposure on dogs. *Parasite,* 21.

BEUGNET, F. & MARIE, J. L. 2009. Emerging arthropod-borne diseases of companion animals in Europe. *Vet Parasitol,* 163**,** 298-305.

BISCHOF, J., MAEDA, R. K., HEDIGER, M., KARCH, F. & BASLER, K. 2007. An optimized transgenesis system for Drosophila using germ-line-specific phi C31 integrases. *Proceedings of the National Academy of Sciences of the United States of America,* 104**,** 3312-3317.

BITTENCOURT, V. R. E. P. 2000. Trials to control South American ticks with entomopathogenic fungi. *Tropical Veterinary Diseases,* 916**,** 555-558.

BLAGBURN, B. L. & DRYDEN, M. W. 2009. Biology, Treatment, and Control of Flea and Tick Infestations. *Veterinary Clinics of North America-Small Animal Practice,* 39**,** 1173-+.

BLANTON, L. S. & WALKER, D. H. 2017. Flea-Borne Rickettsioses and Rickettsiae. *Am J Trop Med Hyg,* 96**,** 53-56.

BLISS, C. I. 1934. The Method of Probits. *Science,* 79**,** 38-9.

BLOEMER, S. R., MOUNT, G. A., MORRIS, T. A., ZIMMERMAN, R. H., BARNARD, D. R. & SNODDY, E. L. 1990. Management of Lone Star Ticks (Acari, Ixodidae) in Recreational Areas with Acaricide Applications, Vegetative Management, and Exclusion of White-Tailed Deer. *Journal of Medical Entomology,* 27**,** 543-550.

BOOTH, T. F. 1989. Effects of Biogenic-Amines and Adrenergic-Drugs on Oviposition in the Cattle Tick Boophilus - Evidence for Octopaminergic Innervation of the Oviduct. *Experimental & Applied Acarology,* 7**,** 259-266.

BROADBENT, S., GROOT-KORMELINK, P. J., KRASHIA, P. A., HARKNESS, P. C., MILLAR, N. S., BEATO, M. & SIVILOTTI, L. G. 2006. Incorporation of the beta 3 subunit has a dominant-negative effect on the function of recombinant central-type neuronal nicotinic receptors. *Molecular Pharmacology,* 70**,** 1350-1357.

BUCKINGHAM, S. D., BIGGIN, P. C., SATTELLE, B. M., BROWN, L. A. & SATTELLE, D. B. 2005. Insect GABA receptors: Splicing, editing, and targeting by antiparasitics and insecticides. *Molecular Pharmacology,* 68**,** 942-951.

BUSVINE, J. R. 1963. The present status of insecticide resistance. *Bull World Health Organ,* 29 Suppl**,** 31-40.

CABONI, P., SAMMELSON, R. E. & CASIDA, J. E. 2003. Phenylpyrazole insecticide photochemistry, metabolism, and GABAergic action: Ethiprole compared with fipronil. *Journal of Agricultural and Food Chemistry,* 51**,** 7055-7061.

CAMPANHOLA, C. & PLAPP, F. W. 1989. Pyrethroid Resistance in the Tobacco Budworm (Lepidoptera, Noctuidae) - Insecticide Bioassays and Field Monitoring. *Journal of Economic Entomology,* 82**,** 22-28.

CASIDA, J. E. 2015. Golden age of RyR and GABA-R diamide and isoxazoline insecticides: common genesis, serendipity, surprises, selectivity, and safety. *Chem Res Toxicol,* 28**,** 560-6.

CASIDA, J. E. & DURKIN, K. A. 2013. Neuroactive insecticides: targets, selectivity, resistance, and secondary effects. *Annu Rev Entomol,* 58**,** 99-117.

CASIDA, J. E. & DURKIN, K. A. 2015. Novel GABA receptor pesticide targets. *Pestic Biochem Physiol,* 121**,** 22-30.

CDC 2018. https://www.cdc.gov/.

CHAN, A. W., SONG, F., VICKERS, A., JEFFERSON, T., DICKERSIN, K., GOTZSCHE, P. C., KRUMHOLZ, H. M., GHERSI, D. & VAN DER WORP, H. B. 2014. Increasing value and reducing waste: addressing inaccessible research. *Lancet,* 383**,** 257-66.

CHANG, Y., GHANSAH, E., CHEN, Y., YE, J. & WEISS, D. S. 2002. Desensitization mechanism of GABA receptors revealed by single oocyte binding and receptor function. *J Neurosci,* 22**,** 7982-90.

COLE, L. M., ROUSH, R. T. & CASIDA, J. E. 1995. Drosophila GABA-gated chloride channel: modified [3H]EBOB binding site associated with Ala-->Ser or Gly mutants of Rdl subunit. *Life Sci,* 56**,** 757-65.

COMITANI, F., COHEN, N., ASHBY, J., BOTTEN, D., LUMMIS, S. C. & MOLTENI, C. 2014. Insights into the binding of GABA to the insect RDL receptor from atomistic simulations: a comparison of models. *J Comput Aided Mol Des,* 28**,** 35-48.

COUTURIER, S., BERTRAND, D., MATTER, J. M., HERNANDEZ, M. C., BERTRAND, S., MILLAR, N., VALERA, S., BARKAS, T. & BALLIVET, M. 1990. A Neuronal Nicotinic Acetylcholine-Receptor Subunit (Alpha-7) Is Developmentally Regulated and Forms a

Homooligomeric Channel Blocked by Alpha-Btx. *Neuron,* 5**,** 847-856.

CRAMER, L. G., CARVALHO, L. A. F., BRIDI, A. A., AMARAL, N. K. & BARRICK, R. A. 1988. Efficacy of Topically Applied Ivermectin against Boophilus-Microplus (Canestrini, 1887) in Cattle. *Veterinary Parasitology,* 29**,** 341-349.

CROSSTHWAITE, A. J., RENDINE, S., STENTA, M. & SLATER, R. 2014. Target-site resistance to neonicotinoids. *J Chem Biol,* 7**,** 125-8.

DABORN, P., MCCART, C., WOODS, D. & FFRENCH-CONSTANT, R. H. 2004. Detection of insecticide resistance-associated mutations in cat flea Rdl by TaqMan-allele specific amplification. *Pesticide Biochemistry and Physiology,* 79**,** 25-30.

DAVEY, R. B., GEORGE, J. E. & SNYDER, D. E. 2001. Efficacy of a single whole-body spray treatment of spinosad, against Boophilus microplus (Acari : Ixodidae) on cattle. *Veterinary Parasitology,* 99**,** 41-52.

DERMAUW, W., ILIAS, A., RIGA, M., TSAGKARAKOU, A., GRBIC, M., TIRRY, L., VAN LEEUWEN, T. & VONTAS, J. 2012. The cys-loop ligand-gated ion channel gene family of Tetranychus urticae: implications for acaricide toxicology and a novel mutation associated with abamectin resistance. *Insect Biochem Mol Biol,* 42**,** 455-65.

DIAO, F. Q., IRONFIELD, H., LUAN, H. J., DIAO, F. C., SHROPSHIRE, W. C., EWER, J., MARR, E., POTTER, C. J., LANDGRAF, M. & WHITE, B. H. 2015. Plug-and-Play Genetic Access to Drosophila Cell Types using Exchangeable Exon Cassettes. *Cell Reports,* 10**,** 1410-1421.

DILLON, G. H., IM, W. B., CARTER, D. B. & MCKINLEY, D. D. 1995. Enhancement by Gaba of the Association Rate of Picrotoxin and Tert-Butylbicyclophosphorothionate to the Rat Cloned Alpha-1-Beta-2-Gamma-2 Gaba(a) Receptor Subtype. *British Journal of Pharmacology,* 115**,** 539-545.

DRYDEN, C. 2014. Insectide aracide resistance in fleas and ticks infesting dogs and cats.pdf>.

DUCE, I. R., BHANDAL, N. S., SCOTT, R. H. & NORRIS, T. M. 1995. Effects of Ivermectin on Gamma-Aminobutyric-Acid and Glutamate-Gated Chloride Conductance in Arthropod Skeletal-Muscle. *Molecular Action of Insecticides on Ion Channels,* 591**,** 251-263.

DUDEL, J., FRANKE, C., HATT, H. & USHERWOOD, P. N. R. 1989. Chloride Channels Gated by Extrajunctional Glutamate Receptors (H-Receptors) on Locust Leg Muscle. *Brain Research,* 481**,** 215-220.

DUFFY, D., DOWNER, R. & BRINKLEY, C. 1992. The effectiveness of helmeted guineafowl in the control of the deer tick, the vector of Lyme disease. *Wilson Bulletin,* 104**,** 342-345.

DUMONT, P., BLAIR, J., FOURIE, J. J., CHESTER, T. S. & LARSEN, D. L. 2014. Evaluation of the efficacy of afoxolaner against two European dog tick species: Dermacentor reticulatus and Ixodes ricinus. *Veterinary Parasitology,* 201**,** 216-219.

ECDPC. 2018. https://www.ecdc.europa.eu/en/disease-vectors/facts/tick-factsheets [Online]. [Accessed December 2018].

EISEN, R. J., BORCHERT, J. N., HOLMES, J. L., AMATRE, G., VAN WYK, K., ENSCORE, R. E., BABI, N., ATIKU, L. A., WILDER, A. P., VETTER, S. M., BEARDEN, S. W., MONTENIERI, J. A. & GAGE, K. L. 2008. Early-phase transmission of Yersinia pestis by cat fleas (Ctenocephalides felis) and their potential role as vectors in a plague-endemic region of Uganda. *Am J Trop Med Hyg,* 78**,** 949-56.

FFRENCH-CONSTANT, R. H. 1994. The molecular and population genetics of cyclodiene insecticide resistance. *Insect Biochem Mol Biol,* 24**,** 335-45.

FFRENCH-CONSTANT, R. H., ANTHONY, N., ARONSTEIN, K., ROCHELEAU, T. & STILWELL, G. 2000. Cyclodiene insecticide resistance: from molecular to population genetics. *Annu Rev Entomol,* 45**,** 449-66.

FFRENCH-CONSTANT, R. H., STEICHEN, J. C., ROCHELEAU, T. A., ARONSTEIN, K. & ROUSH, R. T. 1993. A single-amino acid substitution in a γ -aminobutyric acid subtype A receptor locus is associated with cyclodiene insecticide resistance in Drosophila populations. *Proceedings of the National Academy of Sciences of the United States of America,* 90.

FFRENCH-CONSTANT, R. H., WILLIAMSON, M. S., DAVIES, T. G. E. & BASS, C. 2016. Ion channels as insecticide targets. *Journal of Neurogenetics,* 30**,** 163-177.

FFRENCHCONSTANT, R. H. & ROCHELEAU, T. A. 1993. Drosophila Gamma-Aminobutyric-Acid Receptor Gene Rdl Shows Extensive Alternative Splicing. *Journal of Neurochemistry,* 60**,** 2323-2326.

FIVAZ, B., PETNEY, T. & HORAK, I. 2012. *Tick vector biology: medical and veterinary aspects*, Spinger Science & Business Media.

GARCIA-REYNAGA, P., ZHAO, C., SARPONG, R. & CASIDA, J. E. 2013. New GABA/glutamate receptor target for [(3)H]isoxazoline insecticide. *Chem Res Toxicol,* 26**,** 514-6.

GARROOD, W. T., ZIMMER, C. T., GORMAN, K. J., NAUEN, R., BASS, C. & DAVIES, T. G. 2015. Field-evolved resistance to imidacloprid and ethiprole in populations of brown planthopper Nilaparvata lugens collected from across South and East Asia. *Pest Manag Sci*.

GARROOD, W. T., ZIMMER, C. T., GUTBROD, O., LUKE, B., WILLIAMSON, M. S., BASS, C., NAUEN, R. & DAVIES, T. G. E. 2017. Influence of the RDL A301S mutation in the brown planthopper Nilaparvata lugens on the activity of phenylpyrazole insecticides. *Pesticide Biochemistry and Physiology,* 142**,** 1-8.

GASSEL, M., WOLF, C., NOACK, S., WILLIAMS, H. & ILG, T. 2014. The novel isoxazoline ectoparasiticide fluralaner: Selective inhibition of arthropod gamma-aminobutyric acid- and L-glutamate-gated

chloride channels and insecticidal/acaricidal activity. *Insect Biochemistry and Molecular Biology,* 45**,** 111-124.

GILL, B. S., BHATTACHARYULU, Y. & KAUR, D. 1977. Symptoms and pathology of experimental bovine tropical theileriosis (Theileria annulata infection). *Ann Parasitol Hum Comp,* 52**,** 597-608.

GRAHAM, S., ROGERS, R. P. & ALPER, R. H. 2016. An automated method to assay locomotor activity in third instar Drosophila melanogaster larvae. *J Pharmacol Toxicol Methods,* 77**,** 76-80.

GRATION, K. A., CLARK, R. B. & USHERWOOD, P. N. 1979. Three types of L-glutamate receptor on junctional membrane of locust muscle fibres. *Brain Res,* 171**,** 360-4.

GROFF, K. & BISHOP, P. 2017. Itching for change: Embracing modern flea and tick product development. *Regul Toxicol Pharmacol,* 88**,** 349-355.

GROSS, M. 2013. EU ban puts spotlight on complex effects of neonicotinoids. *Curr Biol,* 23**,** R462-4.

HANSEN, S. B., SULZENBACHER, G., HUXFORD, T., MARCHOT, P., TAYLOR, P. & BOURNE, Y. 2005. Structures of Aplysia AChBP complexes with nicotinic agonists and antagonists reveal distinctive binding interfaces and conformations. *Embo Journal,* 24**,** 3635-3646.

HANSON, M. S. & EDELMAN, R. 2003. Progress and controversy surrounding vaccines against Lyme disease. *Expert Rev Vaccines,* 2**,** 683-703.

HARRISON, J. B., CHEN, H. H., SATTELLE, E., BARKER, P. J., HUSKISSON, N. S., RAUH, J. J., BAI, D. & SATTELLE, D. B. 1996. Immunocytochemical mapping of a C-terminus anti-peptide antibody to the GABA receptor subunit, RDL in the nervous system of Drosophila melanogaster. *Cell and Tissue Research,* 284**,** 269-278.

HESKA CORPORATION, N. W., KEVIN. S. BRANDT. 2002. *FLEA GABA RECEPTOR SUBUNIT NUCLEIC ACID MOLECULES, PROTEINS AND USES THEREOF.* US patent application.

HIRATA, K., JOURAKU, A., KUWAZAKI, S., KANAZAW, J. & IWASA, T. 2017. The R81T mutation in the nicotinic acetylcholine receptor of Aphis gossypii is associated with neonicotinoid insecticide resistance with differential effects for cyano- and nitro-substituted neonicotinoids. *Pesticide Biochemistry and Physiology,* 143**,** 57-65.

HOPE, M., MENZIES, M. & KEMP, D. 2010. Identification of a dieldrin resistance-associated mutation in Rhipicephalus (Boophilus) microplus (Acari: Ixodidae). *J Econ Entomol,* 103**,** 1355-9.

HOSIE, A. M., ARONSTEIN, K., SATTELLE, D. B. & FFRENCHCONSTANT, R. H. 1997. Molecular biology of insect neuronal GABA receptors. *Trends in Neurosciences,* 20**,** 578-583.

HOSIE, A. M., BAYLIS, H. A., BUCKINGHAM, S. D. & SATTELLE, D. B. 1995. Actions of the Insecticide Fipronil, on Dieldrin-Sensitive and

Dieldrin-Resistant Gaba Receptors of Drosophila-Melanogaster. *British Journal of Pharmacology,* 115**,** 909-912.

HOSIE, A. M., BUCKINGHAM, S. D., PRESNAIL, J. K. & SATTELLE, D. B. 2001. Alternative splicing of a Drosophila GABA receptor subunit gene identifies determinants of agonist potency. *Neuroscience,* 102**,** 709-714.

HOSIE, A. M. & SATTELLE, D. B. 1996. Agonist pharmacology of two Drosophila GABA receptor splice variants. *British Journal of Pharmacology,* 119**,** 1577-1585.

IANNINO, F., SULLI, N., MAITINO, A., PASCUCCI, I., PAMPIGLIONE, G. & SALUCCI, S. 2017. Fleas of dog and cat: species, biology and flea-borne diseases. *Vet Ital,* 53**,** 277-288.

INOUE, M. & AKAIKE, N. 1988. Blockade of gamma-aminobutyric acid-gated chloride current in frog sensory neurons by picrotoxin. *Neurosci Res,* 5**,** 380-94.

IRAC. 2018. *IRAC MoA Classification Scheme* [Online]. [Accessed].

JENETT, A., RUBIN, G. M., NGO, T. T., SHEPHERD, D., MURPHY, C., DIONNE, H., PFEIFFER, B. D., CAVALLARO, A., HALL, D., JETER, J., IYER, N., FETTER, D., HAUSENFLUCK, J. H., PENG, H., TRAUTMAN, E. T., SVIRSKAS, R. R., MYERS, E. W., IWINSKI, Z. R., ASO, Y., DEPASQUALE, G. M., ENOS, A., HULAMM, P., LAM, S. C., LI, H. H., LAVERTY, T. R., LONG, F., QU, L., MURPHY, S. D., ROKICKI, K., SAFFORD, T., SHAW, K., SIMPSON, J. H., SOWELL, A., TAE, S., YU, Y. & ZUGATES, C. T. 2012. A GAL4-driver line resource for Drosophila neurobiology. *Cell Rep,* 2**,** 991-1001.

JONES, A. K., BUCKINGHAM, S. D., PAPADAKI, M., YOKOTA, M., SATTELLE, B. M., MATSUDA, K. & SATTELLE, D. B. 2009. Splice-variant- and stage-specific RNA editing of the Drosophila GABA receptor modulates agonist potency. *J Neurosci,* 29**,** 4287-92.

KAJI, M. D., KWAKA, A., CALLANAN, M. K., NUSRAT, H., DESAULNIERS, J. P. & FORRESTER, S. G. 2015. A molecular characterization of the agonist binding site of a nematode cys-loop GABA receptor. *Br J Pharmacol,* 172**,** 3737-47.

KARADZOVSKA, D., CHAPPELL, K., COBLE, S., MURPHY, M., CAVALLERI, D., WISEMAN, S., DRAKE, J. & NANCHEN, S. 2017. A randomized, controlled field study to assess the efficacy and safety of lotilaner flavored chewable tablets (Credelio (TM)) in eliminating fleas in client-owned dogs in the USA. *Parasites & Vectors,* 10.

KIBBE, W. A. 2007. OligoCalc: an online oligonucleotide properties calculator. *Nucleic Acids Research,* 35**,** W43-W46.

KISS, T., CADAR, D. & SPINU, M. 2012. Tick prevention at a crossroad: New and renewed solutions. *Veterinary Parasitology,* 187**,** 357-366.

KLAFKE, G. M., DE ALBUQUERQUE, T. A., MILLER, R. J. & SCHUMAKER, T. T. S. 2010. Selection of an ivermectin-resistant strain of Rhipicephalus microplus (Acari: Ixodidae) in Brazil. *Veterinary Parasitology,* 168**,** 97-104.

KRISTENSEN, M., HANSEN, K. K. & JENSEN, K. M. V. 2005. Cross-resistance between dieldrin and fipronil in German cockroach (Dictyoptera : Blattellidae). *Journal of Economic Entomology,* 98**,** 1305-1310.

KROBER, T. & GUERIN, P. M. 2007. An in vitro feeding assay to test acaricides for control of hard ticks. *Pest Management Science,* 63**,** 17-22.

LANSDELL, S. J., COLLINS, T., GOODCHILD, J. & MILLAR, N. S. 2012. The Drosophila nicotinic acetylcholine receptor subunits D alpha 5 and D alpha 7 form functional homomeric and heteromeric ion channels. *Bmc Neuroscience,* 13.

LANSDELL, S. J., SCHMITT, B., BETZ, H., SATTELLE, D. B. & MILLAR, N. S. 1997. Temperature-sensitive expression of Drosophila neuronal nicotinic acetylcholine receptors. *Journal of Neurochemistry,* 68**,** 1812-1819.

LANUSSE, C., LIFSCHITZ, A., VIRKEL, G., ALVAREZ, L., SANCHEZ, S., SUTRA, J. F., GALTIER, P. & ALVINERIE, M. 1997. Comparative plasma disposition kinetics of ivermectin, moxidectin and doramectin in cattle. *J Vet Pharmacol Ther,* 20**,** 91-9.

LAPPIN, M. R. 2005. General concepts in zoonotic disease control. *Vet Clin North Am Small Anim Pract,* 35**,** 1-20.

LE GOFF, G., HAMON, A., BERGE, J. B. & AMICHOT, M. 2005. Resistance to fipronil in Drosophila simulans: influence of two point mutations in the RDL GABA receptor subunit. *Journal of Neurochemistry,* 92**,** 1295-1305.

LEE, R. & OPDEBEECK, J. P. 1999. Arthropod vaccines. *Infect Dis Clin North Am,* 13**,** 209-26.

LEES, K., JONES, A. K., MATSUDA, K., AKAMATSU, M., SATTELLE, D. B., WOODS, D. J. & BOWMAN, A. S. 2014a. Functional characterisation of a nicotinic acetylcholine receptor alpha subunit from the brown dog tick, Rhipicephalus sanguineus. *International Journal for Parasitology,* 44**,** 75-81.

LEES, K., MUSGAARD, M., SUWANMANEE, S., BUCKINGHAM, S. D., BIGGIN, P. & SATTELLE, D. 2014b. Actions of agonists, fipronil and ivermectin on the predominant in vivo splice and edit variant (RDLbd, I/V) of the Drosophila GABA receptor expressed in Xenopus laevis oocytes. *PLoS One,* 9**,** e97468.

LI, X., SCHULER, M. A. & BERENBAUM, M. R. 2007. Molecular mechanisms of metabolic resistance to synthetic and natural xenobiotics. *Annu Rev Entomol,* 52**,** 231-53.

LINDQUIST, L. & VAPALAHTI, O. 2008. Tick-borne encephalitis. *Lancet,* 371**,** 1861-1871.

LIU, Z., WILLIAMSON, M. S., LANSDELL, S. J., DENHOLM, I., HAN, Z. & MILLAR, N. S. 2005. A nicotinic acetylcholine receptor mutation conferring target-site resistance to imidacloprid in Nilaparvata lugens (brown planthopper). *Proc Natl Acad Sci U S A,* 102**,** 8420-5.

LIU, Z. W., HAN, Z. J., ZHANG, Y. X., SONG, F., YAO, X. M., LIU, S. H., GU, J. H. & MILLAR, N. S. 2009. Heteromeric co-assembly of two insect nicotinic acetylcholine receptor alpha subunits: influence on sensitivity to neonicotinoid insecticides. *Journal of Neurochemistry,* 108**,** 498-506.

LIU, Z. W., WILLIAMSON, M. S., LANSDELL, S. J., HAN, Z. J., DENHOLM, I. & MILLAR, N. S. 2006. A nicotinic acetylcholine receptor mutation (Y151S) causes reduced agonist potency to a range of neonicotinoid insecticides. *Journal of Neurochemistry,* 99**,** 1273-1281.

LONGHURST, C., BABCOCK, J. M., DENHOLM, I., GORMAN, K., THOMAS, J. D. & SPARKS, T. C. 2013. Cross-resistance relationships of the sulfoximine insecticide sulfoxaflor with neonicotinoids and other insecticides in the whiteflies Bemisia tabaci and Trialeurodes vaporariorum. *Pest Manag Sci,* 69**,** 809-13.

MAGALHAES, V. S., CID, Y. P., FERREIRA, T. P., MEDEIROS, D. M. V., BATISTA, L. C. D. O., CORREIA, T. R., ALBERT, A. L. M. & SCOTT, F. B. 2016. Evaluation of pharmacokinetics and efficacy of ivermectin following oral administration in dogs against experimental infection of Ctenocephalides felis felis and Rhipicephalus sanguineus. *Veterinary Parasitology,* 228**,** 167-171.

MARANGA, R. O., KAAYA, G. P., MUEKE, J. M. & HASSANALI, A. 2005. Effects of combining the fungi Beauveria bassiana and Metarhizium anisopliae on the mortality of the tick Amblyomma variegatum (ixodidae) in relation to seasonal changes. *Mycopathologia,* 159**,** 527-532.

MARCELINO, I., DE ALMEIDA, A. M., VENTOSA, M., PRUNEAU, L., MEYER, D. F., MARTINEZ, D., LEFRANCOIS, T., VACHIERY, N. & COELHO, A. V. 2012. Tick-borne diseases in cattle: applications of proteomics to develop new generation vaccines. *J Proteomics,* 75**,** 4232-50.

MARTINS, J. R. & FURLONG, J. 2001. Avermectin resistance of the cattle tick Boophilus microplus in Brazil. *Veterinary Record,* 149**,** 64-64.

MCTIER, T. L., EVANS, N. A., MARTIN-SHORT, M. & GRATION, K. 2003. Comparison of the activity of selamectin, fipronil, and imidacloprid against flea larvae (Ctenocephalides felis felis) in vitro. *Vet Parasitol,* 116**,** 45-50.

MEHLHORN, H. 2001. *Encyclopedic reference of parasitology: Biology, structure, function,* Berlin, DE, Springer-Verlag.

MEHLHORN, H., HANSEN, O. & MENCKE, N. 2001. Comparative study on the effects of three insecticides (fipronil, imidacloprid, selamectin) on developmental stages of the cat flea (Ctenocephalides felis Bouche 1835): a light and electron microscopic analysis of in vivo and in vitro experiments. *Parasitol Res,* 87**,** 198-207.

MERINO, O., ALBERDI, P., PEREZ DE LA LASTRA, J. M. & DE LA FUENTE, J. 2013. Tick vaccines and the control of tick-borne pathogens. *Front Cell Infect Microbiol,* 3**,** 30.

METZGER, M. E. & RUST, M. K. 1997. Effect of temperature on cat flea (Siphonaptera:Pulicidae) development and overwintering. *J Med Entomol,* 34**,** 173-8.

MIGLIANICO, M., ELDERING, M., SLATER, H., FERGUSON, N., AMBROSE, P., LEES, R. S., KOOLEN, K. M. J., PRUZINOVA, K., JANCAROVA, M., VOLF, P., KOENRAADT, C. J. M., DUERR, H. P., TREVITT, G., YANG, B., CHATTERJEE, A. K., WISLER, J., STURM, A., BOUSEMA, T., SAUERWEIN, R. W., SCHULTZ, P. G., TREMBLAY, M. S. & DECHERING, K. J. 2018. Repurposing isoxazoline veterinary drugs for control of vector-borne human diseases. *Proc Natl Acad Sci U S A,* 115**,** E6920-E6926.

MILLAR, N. S. & DENHOLM, I. 2007. Nicotinic acetylcholine receptors: targets for commercially important insecticides. *Invert Neurosci,* 7**,** 53-66.

MILLER, R. J., WHITE, W. H., DAVEY, R. B., GEORGE, J. E. & PEREZ DE LEON, A. 2011. Efficacy of spinosad against acaricide-resistant and -susceptible Rhipicephalus (Boophilus) microplus and acaricide-susceptible Amblyomma americanum and Dermacentor variabilis. *J Med Entomol,* 48**,** 358-65.

MOULTON, J. K., PEPPER, D. A. & DENNEHY, T. J. 2000. Beet armyworm (Spodoptera exigua) resistance to spinosad. *Pest Management Science,* 56**,** 842-848.

MURPHY, M., CAVALLERI, D., SEEWALD, W., DRAKE, J. & NANCHEN, S. 2017. Laboratory evaluation of the speed of kill of lotilaner (Credelio (TM)) against Ixodes ricinus ticks on dogs. *Parasites & Vectors,* 10.

NAKAO, T., HAMA, M., KAWAHARA, N. & HIRASE, K. 2012. Fipronil resistance in Sogatella furcifera: Molecular cloning and functional expression of wild-type and mutant RDL GABA receptor subunits. *Journal of Pesticide Science,* 37**,** 37-44.

NAKAO, T., KAWASE, A., KINOSHITA, A., ABE, R., HAMA, M., KAWAHARA, N. & HIRASE, K. 2011. The A2'N mutation of the RDL gamma-aminobutyric acid receptor conferring fipronil resistance in Laodelphax striatellus (Hemiptera: Delphacidae). *J Econ Entomol,* 104**,** 646-52.

NARAHASHI, T., ZHAO, X. L., IKEDA, T., SALGADO, V. L. & YEH, J. Z. 2010. Glutamate-activated chloride channels: Unique fipronil targets present in insects but not in mammals. *Pesticide Biochemistry and Physiology,* 97**,** 149-152.

NAUEN, R. B., T. 2002. New modes of action of insecticides. *Pesticide Outlook,* 13**,** 241-245.

NAVA, S., GUGLIELMONE, A. A. & MANGOLD, A. J. 2009. An overview of systematics and evolution of ticks. *Front Biosci (Landmark Ed),* 14**,** 2857-77.

NICHOLS, C. D., BECNEL, J. & PANDEY, U. B. 2012. Methods to assay Drosophila behavior. *J Vis Exp*.

OLSEN, R. W. 2006. Picrotoxin-like channel blockers of GABAA receptors. *Proc Natl Acad Sci U S A,* 103**,** 6081-2.

ORR, N., SHAFFNER, A. J., RICHEY, K. & CROUSE, G. D. 2009. Novel mode of action of spinosad: Receptor binding studies demonstrating lack of interaction with known insecticidal target sites. *Pesticide Biochemistry and Physiology,* 95**,** 1-5.

OSTFELD, R. S., PRICE, A., HORNBOSTEL, V. L., BENJAMIN, M. A. & KEESING, F. 2006. Controlling ticks and tick-borne zoonoses with biological and chemical agents. *Bioscience,* 56**,** 383-394.

OTRANTO, D. 2018. Arthropod-borne pathogens of dogs and cats: From pathways and times of transmission to disease control. *Vet Parasitol,* 251**,** 68-77.

OTRANTO, D. & WALL, R. 2008. New strategies for the control of arthropod vectors of disease in dogs and cats. *Med Vet Entomol,* 22**,** 291-302.

OZOE, Y. 2013. gamma-Aminobutyrate- and Glutamate-gated Chloride Channels as Targets of Insecticides. *Target Receptors in the Control of Insect Pests: Pt I,* 44**,** 211-286.

PAYNE, P. A., DRYDEN, M. W., SMITH, V. & RIDLEY, R. K. 2001. Effect of 0.29% w/w fipronil spray on adult flea mortality and egg production of three different cat flea, Ctenocephalides felis (Bouche), strains infesting cats. *Vet Parasitol,* 102**,** 331-40.

PEGRAM, R. G. & LEMCHE, J. 1985. Observations on the efficacy of ivermectin in the control of cattle ticks in Zambia. *Vet Rec,* 117**,** 551-4.

PEREZ-COGOLLO, L. C., RODRIGUEZ-VIVAS, R. I., RAMIREZ-CRUZ, G. T. & MILLER, R. J. 2010. First report of the cattle tick Rhipicephalus microplus resistant to ivermectin in Mexico. *Veterinary Parasitology,* 168**,** 165-169.

PERRY, T., BATTERHAM, P. & DABORN, P. J. 2011. The biology of insecticidal activity and resistance. *Insect Biochemistry and Molecular Biology,* 41**,** 411-422.

PERRY, T., MCKENZIE, J. A. & BATTERHAM, P. 2007. A D alpha 6 knockout strain of Drosophila melahogaster confers a high level of resistance to spinosad. *Insect Biochemistry and Molecular Biology,* 37**,** 184-188.

PERRY, T., SOMERS, J., YANG, Y. T. & BATTERHAM, P. 2015. Expression of insect alpha6-like nicotinic acetylcholine receptors in Drosophila melanogaster highlights a high level of conservation of the receptor:spinosyn interaction. *Insect Biochem Mol Biol*.

PETERSEN, R. B. & LINDQUIST, S. 1989. Regulation of Hsp70 Synthesis by Messenger-Rna Degradation. *Cell Regulation,* 1**,** 135-149.

PETNEY, T. N. 1997. Ecological implications of control strategies: arthropods of domestic and production animals. *Int J Parasitol,* 27**,** 155-65.

PFISTER, K. & ARMSTRONG, R. 2016. Systemically and cutaneously distributed ectoparasiticides: a review of the efficacy against ticks and fleas on dogs. *Parasit Vectors,* 9**,** 436.

POSTAL, J. M. R., JEANNIN, P. C. & CONSALVI, P. J. 1995. Field Efficacy of a Mechanical Pump Spray Formulation Containing 0.25-Percent Fipronil in the Treatment and Control of Flea Infestation and Associated Dermatological Signs in Dogs and Cats. *Veterinary Dermatology,* 6**,** 153-158.

PRICE, K. L. & LUMMIS, S. C. R. 2014. An atypical residue in the pore of Varroa destructor GABA-activated RDL receptors affects picrotoxin block and thymol modulation. *Insect Biochemistry and Molecular Biology,* 55**,** 19-25.

PRICHARD, R., MENEZ, C. & LESPINE, A. 2012. Moxidectin and the avermectins: Consanguinity but not identity. *Int J Parasitol Drugs Drug Resist,* 2**,** 134-53.

PUINEAN, A. M., ELIAS, J., SLATER, R., WARREN, A., FIELD, L. M., WILLIAMSON, M. S. & BASS, C. 2013a. Development of a high-throughput real-time PCR assay for the detection of the R81T mutation in the nicotinic acetylcholine receptor of neonicotinoid-resistant Myzus persicae. *Pest Manag Sci,* 69**,** 195-9.

PUINEAN, A. M., LANSDELL, S. J., COLLINS, T., BIELZA, P. & MILLAR, N. S. 2013b. A nicotinic acetylcholine receptor transmembrane point mutation (G275E) associated with resistance to spinosad in Frankliniella occidentalis. *J Neurochem,* 124**,** 590-601.

RAHLENBECK, S., FINGERLE, V. & DOGGETT, S. 2016. Prevention of tick-borne diseases: an overview. *Br J Gen Pract,* 66**,** 492-4.

REMNANT, E. J., MORTON, C. J., DABORN, P. J., LUMB, C., YANGA, Y. T., NG, H. L., PARKER, M. W. & BATTERHAMA, P. 2014. The role of the rdl in resistance to phenylpyrazole in Drosophila melanogaster. *Insect Biochemistry and Molecular Biology,* 54**,** 11-21.

ROSARIO-CRUZ, R., ALMAZAN, C., MILLER, R. J., DOMINGUEZ-GARCIA, D. I., HERNANDEZ-ORTIZ, R. & DE LA FUENTE, J. 2009. Genetic basis and impact of tick acaricide resistance. *Frontiers in Bioscience-Landmark,* 14**,** 2657-2665.

RUBIN, G. M. & SPRADLING, A. C. 1982. Genetic transformation of Drosophila with transposable element vectors. *Science,* 218**,** 348-53.

RUST, M. K. 2017. The Biology and Ecology of Cat Fleas and Advancements in Their Pest Management: A Review. *Insects,* 8.

RUST, M. K., VETTER, R., DENHOLM, I., BLAGBURN, B., WILLIAMSON, M. S., KOPP, S., COLEMAN, G., HOSTETLER, J., DAVIS, W., MENCKE, N., REES, R., FOIT, S., BOHM, C. & TETZNER, K. 2015. Susceptibility of Adult Cat Fleas (Siphonaptera: Pulicidae) to Insecticides and Status of Insecticide Resistance Mutations at

the Rdl and Knockdown Resistance Loci. *Parasitol Res,* 114 Suppl 1**,** 7-18.

SALGADO, V. L. & SAAR, R. 2004. Desensitizing and non-desensitizing subtypes of alpha-bungarotoxin-sensitive nicotinic acetylcholine receptors in cockroach neurons. *J Insect Physiol,* 50**,** 867-79.

SCHULZ, R., BERTRAND, S., CHAMAON, K., SMALLA, K. H., GUNDELFINGER, E. D. & BERTRAND, D. 2000. Neuronal nicotinic acetylcholine receptors from Drosophila: Two different types of alpha subunits coassemble within the same receptor complex. *Journal of Neurochemistry,* 74**,** 2537-2546.

SCHULZ, R., SAWRUK, E., MULHARDT, C., BERTRAND, S., BAUMANN, A., PHANNAVONG, B., BETZ, H., BERTRAND, D., GUNDELFINGER, E. D. & SCHMITT, B. 1998. D alpha 3, a new functional alpha subunit of nicotinic acetylcholine receptors from Drosophila. *Journal of Neurochemistry,* 71**,** 853-862.

SCHWAERZEL, M., JAECKEL, A. & MUELLER, U. 2007. Signaling at A-kinase anchoring proteins organizes anesthesia-sensitive memory in Drosophila. *Journal of Neuroscience,* 27**,** 1229-1233.

SGARD, F., FRASER, S. P., KATKOWSKA, M. J., DJAMGOZ, M. B. A., DUNBAR, S. J. & WINDASS, J. D. 1998. Cloning and functional characterisation of two novel nicotinic acetylcholine receptor alpha subunits from the insect pest Myzus persicae. *Journal of Neurochemistry,* 71**,** 903-912.

SHENG, C. W., CASIDA, J. E., DURKIN, K. A., CHEN, F., HAN, Z. J. & ZHAO, C. Q. 2018a. Fiprole insecticide resistance of Laodelphax striatellus: electrophysiological and molecular docking characterization of A2 ' N RDL GABA receptors. *Pest Management Science,* 74**,** 2645-2651.

SHENG, C. W., JIA, Z. Q., OZOE, Y., HUANG, Q. T., HAN, Z. J. & ZHAO, C. Q. 2018b. Molecular cloning, spatiotemporal and functional expression of GABA receptor subunits RDL1 and RDL2 of the rice stem borer Chilo suppressalis. *Insect Biochemistry and Molecular Biology,* 94**,** 18-27.

SHIMOMURA, M., YOKOTA, M., IHARA, M., AKAMATSU, M., SATTELLE, D. B. & MATSUDA, K. 2006. Role in the selectivity of neonicotinoids of insect-specific basic residues in loop D of the nicotinic acetylcholine receptor agonist binding site. *Mol Pharmacol,* 70**,** 1255-63.

SIBSON, G. J. 1994. The Effects of Moxidectin against Natural Infestations of the Cattle Tick (Boophilus-Microplus). *Australian Veterinary Journal,* 71**,** 381-382.

SILVA, W. M., BERGER, M., BASS, C., WILLIAMSON, M., MOURA, D. M., RIBEIRO, L. M. & SIQUEIRA, H. A. 2016. Mutation (G275E) of the nicotinic acetylcholine receptor alpha6 subunit is associated with high levels of resistance to spinosyns in Tuta absoluta (Meyrick) (Lepidoptera: Gelechiidae). *Pestic Biochem Physiol,* 131**,** 1-8.

SIVILOTTI, L., GROOT-KORMELINK, P. . 2004. *NOVEL TOOL FOR TESTING PHARMACOLOGICAL ACTIVITIES*. United Kingdom patent application.

SIX, R. H., BECSKEI, C., MAZALESKI, M. M., FOURIE, J. J., MAHABIR, S. P., MYERS, M. R. & SLOOTMANS, N. 2016a. Efficacy of sarolaner, a novel oral isoxazoline, against two common mite infestations in dogs: Demodex spp. and Otodectes cynotis. *Vet Parasitol,* 222**,** 62-6.

SIX, R. H., GEURDEN, T., CARTER, L., EVERETT, W. R., MCLOUGHLIN, A., MAHABIR, S. P., MYERS, M. R. & SLOOTMANS, N. 2016b. Evaluation of the speed of kill of sarolaner (Simparica (TM)) against induced infestations of three species of ticks (Amblyomma maculatum, Ixodes scapularis, Ixodes ricinus) on dogs. *Veterinary Parasitology,* 222**,** 37-42.

SMELT, C. L. C., SANDERS, V. R., NEWCOMBE, J., BURT, R. P., SHEPPARD, T. D., TOPF, M. & MILLAR, N. S. 2018. Identification by virtual screening and functional characterisation of novel positive and negative allosteric modulators of the alpha 7 nicotinic acetylcholine receptor. *Neuropharmacology,* 139**,** 194-204.

SMIT, R. 2012. Cost-effectiveness of tick-borne encephalitis vaccination in Slovenian adults. *Vaccine,* 30**,** 6301-6.

SOJKA, P. A. 2018. Isoxazolines. *Journal of Exotic Pet Medicine,* 27**,** 118-122.

SPARKS, T. C., DRIPPS, J. E., WATSON, G. B. & PAROONAGIAN, D. 2012. Resistance and cross-resistance to the spinosyns - A review and analysis. *Pesticide Biochemistry and Physiology,* 102**,** 1-10.

SPARKS, T. C. & NAUEN, R. 2015. IRAC: Mode of action classification and insecticide resistance management. *Pestic Biochem Physiol,* 121**,** 122-8.

STAFFORD, K. C., WILLIAMS, S. C. & MOLAEI, G. 2017. Integrated Pest Management in Controlling Ticks and Tick-Associated Diseases. *Journal of Integrated Pest Management,* 8.

STALEY, K. J., SOLDO, B. L. & PROCTOR, W. R. 1995. Ionic mechanisms of neuronal excitation by inhibitory GABAA receptors. *Science,* 269**,** 977-81.

STENSETH, N. C., ATSHABAR, B. B., BEGON, M., BELMAIN, S. R., BERTHERAT, E., CARNIEL, E., GAGE, K. L., LEIRS, H. & RAHALISON, L. 2008. Plague: past, present, and future. *PLoS Med,* 5**,** e3.

TAYLOR-WELLS, J., BROOKE, B. D., BERMUDEZ, I. & JONES, A. K. 2015. The neonicotinoid imidacloprid, and the pyrethroid deltamethrin, are antagonists of the insect Rdl GABA receptor. *Journal of Neurochemistry,* 135**,** 705-713.

TAYLOR-WELLS, J., SENAN, A., BERMUDEZ, I. & JONES, A. K. 2018. Species specific RNA A-to-I editing of mosquito RDL modulates GABA potency and influences agonistic, potentiating and antagonistic actions of ivermectin. *Insect Biochemistry and Molecular Biology,* 93**,** 1-11.

TAYLOR, S. M. & KENNY, J. 1990. An Ivermectin Sustained-Release Bolus in Cattle - Its Effects on the Tick Ixodes-Ricinus. *Medical and Veterinary Entomology,* 4**,** 147-150.

TIAGO, P. V., DE OLIVEIRA, N. T. & LIMA, E. A. D. A. 2014. Biological insect control using Metarhizium anisopliae: morphological, molecular, and ecological aspects. *Ciencia Rural,* 44**,** 645-651.

TOZON, N., PETROVEC, M. & AVSIC-ZUPANC, T. 2003. Clinical and laboratory features of the first detected cases of A-phagocytophila infections in dogs from Slovenia. *Rickettsiology: Present and Future Directions,* 990**,** 424-428.

TRAYNELIS, S. F., WOLLMUTH, L. P., MCBAIN, C. J., MENNITI, F. S., VANCE, K. M., OGDEN, K. K., HANSEN, K. B., YUAN, H., MYERS, S. J. & DINGLEDINE, R. 2010. Glutamate receptor ion channels: structure, regulation, and function. *Pharmacol Rev,* 62**,** 405-96.

TURBERG, A., AKKOSE, MELANIA., PUINEAN, MIREL., WILLIAMSON, MARTIN. 2017. *RHIPICEPHALUS NICOTINIC ACETYLCHOLINE RECEPTOR AND PEST CONTROL ACTING THEREON*. Germany patent application.

VAN LEEUWEN, T., VONTAS, J., TSAGKARAKOU, A., DERMAUW, W. & TIRRY, L. 2010. Acaricide resistance mechanisms in the two-spotted spider mite Tetranychus urticae and other important Acari: A review. *Insect Biochemistry and Molecular Biology,* 40**,** 563-572.

WADE, S. E. & GEORGI, J. R. 1988. Survival and Reproduction of Artificially Fed Cat Fleas, Ctenocephalides-Felis Bouche (Siphonaptera, Pulicidae). *Journal of Medical Entomology,* 25**,** 186-190.

WALTHER, F. M., ALLAN, M. J., ROEPKE, R. K. A. & NUERNBERGER, M. C. 2014. The effect of food on the pharmacokinetics of oral fluralaner in dogs. *Parasites & Vectors,* 7.

WATSON, G. B., CHOUINARD, S. W., COOK, K. R., GENG, C. X., GIFFORD, J. M., GUSTAFSON, G. D., HASLER, J. M., LARRINUA, I. M., LETHERER, T. J., MITCHELL, J. C., PAK, W. L., SALGADO, V. L., SPARKS, T. C. & STILWELL, G. E. 2010. A spinosyn-sensitive Drosophila melanogaster nicotinic acetylcholine receptor identified through chemically induced target site resistance, resistance gene identification, and heterologous expression. *Insect Biochemistry and Molecular Biology,* 40**,** 376-384.

WENGENMAYER, C., WILLIAMS, H., ZSCHIESCHE, E., MORITZ, A., LANGENSTEIN, J., ROEPKE, R. K. & HECKEROTH, A. R. 2014. The speed of kill of fluralaner (Bravecto (TM)) against Ixodes ricinus ticks on dogs. *Parasites & Vectors,* 7.

WICHER, D., WALTHER, C. & WICHER, C. 2001. Non-synaptic ion channels in insects - basic properties of currents and their modulation in neurons and skeletal muscles. *Progress in Neurobiology,* 64**,** 431-525.

WOLFF, M. A. & WINGATE, V. P. 1998. Characterization and comparative pharmacological studies of a functional gamma-aminobutyric acid (GABA) receptor cloned from the tobacco budworm, Heliothis virescens (Noctuidae:Lepidoptera). *Invert Neurosci,* 3**,** 305-15.

WOLSTENHOLME, A. J. 2012. Glutamate-gated chloride channels. *J Biol Chem,* 287**,** 40232-8.

WONDJI, C. S., DABIRE, R. K., TUKUR, Z., IRVING, H., DJOUAKA, R. & MORGAN, J. C. 2011. Identification and distribution of a GABA receptor mutation conferring dieldrin resistance in the malaria vector Anopheles funestus in Africa. *Insect Biochem Mol Biol,* 41**,** 484-91.

YAMAMOTO, I., CARLAND, J. E., LOCOCK, K., GAVANDE, N., ABSALOM, N., HANRAHAN, J. R., ALLAN, R. D., JOHNSTON, G. A. & CHEBIB, M. 2012. Structurally diverse GABA antagonists interact differently with open and closed conformational states of the rho1 receptor. *ACS Chem Neurosci,* 3**,** 293-301.

ZAKSON-AIKEN, M., GREGORY, L. M., MEINKE, P. T. & SHOOP, W. L. 2001. Systemic activity of the avermectins against the cat flea (Siphonaptera: Pulicidae). *J Med Entomol,* 38**,** 576-80.

ZHANG, H. G., FFRENCH-CONSTANT, R. H. & JACKSON, M. B. 1994. A unique amino acid of the Drosophila GABA receptor with influence on drug sensitivity by two mechanisms. *J Physiol,* 479 (Pt 1)**,** 65-75.

ZHANG, H. G., LEE, H. J., ROCHELEAU, T., FFRENCHCONSTANT, R. H. & JACKSON, M. B. 1995. Subunit Composition Determines Picrotoxin and Bicuculline Sensitivity of Drosophila Gamma-Aminobutyric-Acid Receptors. *Molecular Pharmacology,* 48**,** 835-840.

ZHANG, Y. X., MENG, X. K., YANG, Y. X., LI, H., WANG, X., YANG, B. J., ZHANG, J. H., LI, C. R., MILLAR, N. S. & LIU, Z. W. 2016. Synergistic and compensatory effects of two point mutations conferring target-site resistance to fipronil in the insect GABA receptor RDL. *Scientific Reports,* 6.

ZHAO, J. Z., LI, Y. X., COLLINS, H. L., GUSUKUMA-MINUTO, L., MAU, R. F., THOMPSON, G. D. & SHELTO, A. M. 2002. Monitoring and characterization of diamondback moth (Lepidoptera: Plutellidae) resistance to spinosad. *J Econ Entomol,* 95**,** 430-6.